DESIGN AND OPTIMIZATION OF METAL STRUCTURES

József Farkas • Károly Jármai

DESIGN AND OPTIMIZATION OF METAL STRUCTURES

ABOUT THE AUTHORS

Dr József Farkas is Professor Emeritus of metal structures at the University of Miskolc, Hungary. He graduated from the Faculty of Civil Engineering at the Technical University of Budapest and moved to the University of Miskolc where he became an assistant professor in 1950, an associate professor in 1966 and a university professor in 1975. He obtained degrees as a Candidate of Technical Science in 1966 and Doctor of Technical Science in 1978. Dr. Farkas's research field is the optimum design of metal structures, residual welding stresses and distortions, tubular structures, stiffened plates, vibration damping of sandwich structures. He has written expert opinions for many industrial problems, especially on storage tanks, cranes, welded press frames and other metal structures. He is the author of a Hungarian university textbook on metal structures, a book in English *Optimum Design of Metal Structures* (Ellis Horwood Ltd, Chichester 1984), the first author of two books in English *Analysis and Optimum Design of Metal Structures* (Balkema, Rotterdam-Brookfield 1997), *Economic Design of Metal Structures* (Millpress, Rotterdam 2003) and about 260 scientific articles in journals and conference proceedings. He is a Hungarian delegate of the International Institute of Welding (IIW), member of the International Society for Structural and Multidisciplinary Optimization (ISSMO) and honorary member of the Hungarian Scientific Society of Mechanical Engineers (GTE). The University of Miskolc has also honoured him as doctor honoris causa.

Dr Károly Jármai is a professor at the Faculty of Mechanical Engineering at the University of Miskolc, where he graduated as a mechanical engineer and received his doctorate (dr.univ.) in 1979. He teaches design of steel structures, welded structures, composite structures and optimization in Hungarian and in the English language for foreign students. His research interests include structural optimization, mathematical programming techniques and expert systems. Dr. Jármai wrote his C.Sc. (Ph.D.) dissertation at the Hungarian Academy of Science in 1988, became a European Engineer (Eur. Ing. FEANI, Paris) in 1990 and did his habilitation (dr.habil.) at Miskolc in 1995. Having successfully defended his doctor of technical science thesis (D.Sc.) in 1995, he subsequently received awards from the Engineering for Peace Foundation in 1997 and a scholarship as Széchenyi professor between the years 1997-2000 He is the co-author (with Farkas) of two books in English *Analysis and Optimum Design of Metal Structures*, *Economic Design of Metal Structures* and one in Hungarian, and has published over 300 professional papers, lecture notes, textbook chapters and conference papers. He is a founding member of ISSMO, a Hungarian delegate, vice chairman of commission XV and a sub-commission chairman XV-F of IIW. He has held several leading positions in GTE and has been the president of this society at the University of Miskolc since 1991. He was a visiting researcher at Chalmers University of Technology in Sweden in 1991, visiting professor at Osaka University in 1996-97, at the National University of Singapore in 1998 and at the University of Pretoria several times between 2000-2005.

DESIGN AND OPTIMIZATION OF METAL STRUCTURES

Dr. József Farkas
Professor Emeritus of Metal Structures
University of Miskolc, Hungary

Dr. Károly Jármai
Professor of Mechanical Engineering
University of Miskolc, Hungary

Horwood Publishing
Chichester, UK

HORWOOD PUBLISHING LIMITED
International Publishers in Science and Technology
Coll House, Westergate, Chichester, West Sussex, PO20 3QL, England

First published in 2008.

British Library Cataloguing in Publication Data
A catalogue record of this book is available from the British Library

ISBN: 978-1-904275-29-9

Cover design by Jim Wilkie.
Printed and bound in the UK by Antony Rowe Limited.

Table of Contents

About the authors

Dr József Farkas is a professor emeritus of metal structures at the University of Miskolc, Hungary. He graduated in 1950 at the Faculty of Civil Engineering of the Technical University of Budapest. He has been an assistant professor of the University of Miskolc since 1950, an associate professor since 1966, a university professor since 1975. His scientific degrees are candidate of technical science 1966, doctor of technical science 1978. His research field is the optimum design of metal structures, residual welding stresses and distortions, tubular structures, stiffened plates, vibration damping of sandwich structures. He has written expert opinions for many industrial problems, especially on storage tanks, cranes, welded press frames and other metal structures. He is the author of a university textbook about metal structures, a book in English "Optimum Design of Metal Structures" (Ellis Horwood, Chichester 1984), the first author of two books in English "Analysis and Optimum Design of Metal Structures" (Balkema, Rotterdam-Brookfield 1997), "Economic Design of Metal Structures" (Millpress, Rotterdam 2003) and about 260 scientific articles in journals and conference proceedings. He is a Hungarian delegate of the International Institute of Welding (IIW), member of the International Society for Structural and Multidisciplinary Optimization (ISSMO) and honorary member of the Hungarian Scientific Society of Mechanical Engineers (GTE). He is doctor honoris causa of the University of Miskolc.

Dr Károly Jármai is a professor at the Faculty of Mechanical Engineering at the University of Miskolc. He graduated as a mechanical engineer and received his doctorate (dr.univ.) in 1979 at the University of Miskolc. He teaches design of steel structures, welded structures, composite structures and optimization in Hungarian and in the English language for foreign students. His research interests include structural optimization, mathematical programming techniques and expert systems. He wrote his C.Sc. (Ph.D.) dissertation at the Hungarian Academy of Science in 1988. He became a European Engineer (Eur.Ing. FEANI, Paris) in 1990. He did his habilitation (dr.habil.) at the University of Miskolc in 1995. He defended his doctor of technical science thesis (D.Sc.) in 1995. He was awarded a Széchenyi professor scholarship in the years 1997-2000 and an award of the Engineering for Peace Foundation in 1997. He is the co-author of two books in English "Analysis and Optimum Design of Metal Structures" (Balkema, Rotterdam-Brookfield 1997), "Economic Design of Metal Structures" (Millpress, Rotterdam 2003) and one in Hungarian (Műegyetemi Kiadó 2001). He has published over 300 professional papers, lecture notes, textbook chapters and conference papers. He is a founding member of ISSMO, a Hungarian delegate, vice chairman of commission XV and a subcommission chairman XV-F of IIW. He has held several leading positions in GTE and has been the president of this society at the University of Miskolc since 1991. He was a visiting researcher at Chalmers University of Technology in Sweden in 1991, visiting professor at Osaka University in 1996-97, at the National University of Singapore in 1998 and at University of Pretoria in several times between 2000-2005.

List of Symbols

a	Spacing of ribs [mm]
a_g	Ground acceleration
a_W	Weld dimension [mm]
A	Cross-sectional area [mm^2]
A_m	Surface area of a member per unit length [mm^2]
A_p	Area of the inner surface of the fire protection material per unit length of the member [mm^2]
A_p/V	Section factor for steel members insulated by fire protection material [1/mm]
A_r	Cross-sectional area of a ring-stiffener [mm^2]
A_T	Thermal impulse due to welding [mm]
b	Side length, plate width, beams spacing [mm]
B	Bending stiffness
B_x, B_y	Bending stiffnesses [Nmm^2]
c	Specific heat
c	Coefficient (Eq.5.5)
c_a	Temperature dependant specific heat of steel [J/kgK]
c_p	Temperature independent specific heat of the fire protection material [J/kgK]
c_x, c_y,c_{fx},c_{fy},c_w	factors for bent stiffened plates
C	Curvature [1/mm]
C	Factor (Eq.8.101)
C	Parameter (Eq. 10.8)
C_W	Welding time parameter
d	Diameter [mm]
d_r	Interstorey drift
D	Diameter [mm]
D	Plate bending stiffness (Eq. 7.15)

d_p	Thickness of fire protection material
e	Truss joint eccentricity [mm]
E	Modulus of elasticity [GPa]
E_a	Modulus of elasticity of steel on normal temperature [GPa]
$E_{a,\theta}$	Modulus of elasticity of steel on elevated temperature θ_a [GPa]
$E_{d,fi}$	Design effect of actions in the fire situation;
f	Eigenfrequency [Hz]
f_{max}	Maximum deflection [mm]
$f_{p,\theta}$	Proportional limit for steel at elevated temperature θ_a
$f_{f,\theta}$	Effective yield strength of steel at elevated temperature θ_a
f_y	Yield stress [MPa]
F	Force [N]
g	Truss joint gap [mm]
G	Shear modulus [GPa]
h	Truss height [mm]
$\dot{h}_{net,d}$	Net heat flux per unit area [ ]
H	Plate torsional stiffness [Nmm^2]
H	Horizontal component force (Eq.5.7)
H_F	Horizontal force
I_x, I_y	Moments of inertia [mm^4]
I_W	Arc current [A]
I_t	Torsional constant [mm^4]
I_ω	Warping constant [mm6]
k	Cost factor
k_θ	Relative value of a strength or deformation property of steel at elevated temperature θ_a
K	Effective length factor
K	Cost [$]
l	Length at 20 °C [mm]
L	Length, span length [mm]
m	Mass [kg]
M	Bending moment [Nmm]
n	Number of ribs
n	Parameter (Eq.8.28)
N	Normal force [N]
p, q	Distributed load intensity [N/mm]
q	Seismic behaviour factor
q_x, q_y	Specific shear forces
Q	Shear force [N]
Q_T	Heat input of welding [J/mm]
r	Radius of gyration [mm]
R	Shell radius [mm]
s	Normal force due to X=1 (Eq.9.56)
s_e	Effective plate width

S	Surface [mm^2]
S	Tubular member force
S_x, S_y	Static moments [mm^3]
S_j	Rotational stiffness of a beam-to-column connection
S_d	Seismic design spectrum
t	Thickness [mm]
t	Time in fire exposure [sec]
T	Time [s]
T	Axial force (Eq.5.10)
U	Arc voltage [V]
v_W	Welding speed of travel [mm/s]
V	Volume [mm^3]
w	Deflection [mm]
w_i	Weighting coefficients
W_x, W_y	Section moduli [mm^3]
X	Unknown force
Z	Factor (Eq.8.102)
α	Angle of inclination
α	Factor for buckling strength
α	Parameter (Eq. 5.12)
α	Eigenfrequency (Eq.9.29)
α_0	Thermal expansion coefficient
β	Web slenderness ratio
β	Seismic low bound factor
β	Parameter (Eq.7.62)
$\gamma=d/2t$	Tubular truss parameter
γ_{M1}	Partial safety factor
γ_{Mf}	Fatigue safety factor
δ	Local buckling factor
Δt	The time interval at fire calculation [sec]
$\varepsilon = \sqrt{235/f_y}$	Modifying factors for steels
$\varepsilon_x, \varepsilon_y$	Specific strains
η	Loss factor
η	Heat efficiency of a welding technology
η	Column imperfection factor
η	Parameter (Eq.7.206)
η_{fi}	Reduction factor for design load level in the fire situation;
η_G	Distance of gravity center [mm]
κ	Number of assembled structural elements
κ	Adaptation factor at fire resistance
Θ_d	Fabrication difficulty factor
λ	Seismic correction factor
λ	Slenderness

λ	Thermal conductivity
λ_p	Thermal conductivity of the fire protection system [W/mK]
$\overline{\lambda}$	Reduced slenderness
μ	Penalty parameter
μ_0	Degree of utilisation at time $t = 0$
ν	Poisson ratio
ρ	Material density [kg/m^3]
ρ_a	Unit mass of steel [kg/m^3]
ρ_p	Unit mass of the fire protection material [kg/m^3]
θ	Angle of inclination
θ	Temperature [°C]
$\theta_{a,t}$	Steel temperature at time t [°C]
$\theta_{g,t}$	Ambient gas temperature at time t [°C]
Θ_B	Parameter (Eq. 7.162)
σ	Normal stress [MPa]
σ_{cr}	Critical buckling stress
σ_{adm}	Admissible stress [MPa]
τ	Shear stress [MPa]
τ_{adm}	Admissible shear stress [MPa]
φ	Number of rib spacings
φ	Angle of inclination
Φ	Buckling parameter
χ	Flexural buckling factor
ψ	Stress ratio (Eq.3.1)
$\omega = H/a$	Geometric characteristic of a parallel-chord truss
ΔF	Pulsating force range [N]
$\Delta\theta_{g,t}$	Increase of the ambient gas temperature during the time interval Δt [K]
$\Delta\sigma, \Delta\tau$	Stress range [MPa]

Abbreviations

CHS	Circular hollow section
DE	Differential evolution
EC3	Eurocode 3
EC8	Eurocode 8
ECCS	European Convention for Constructional Steelwork
FCAW	Flux Cored Arc Welding
FCAW-MC	Metal Cored Arc Welding
FRP	Fiber reinforced plastic
GA	Genetic algorithm
GMAW-C	Gas Metal Arc Welding with CO_2
GMAW-M	Gas Metal Arc Welding with Mixed Gas
GTAW	Gas Tungsten Arc Welding
IIW	International Institute of Welding

PSO	Particle swarm optimization
RHS	Rectangular hollow section
SHS	Square hollow section
SAW	Submerged Arc Welding
SMAW	Shielded Metal Arc Welding
SMAW HR	Shielded Metal Arc Welding High Recovery
SSFCAW (ISW)	Self Shielded Flux Cored Arc Welding

Preface

Structural optimization is a design system for searching better solutions, which better fulfil engineering requirements. The main requirements of a modern load-carrying structure are the safety, fitness for production and economy. The safety and producibility are guaranteed by design and fabrication constraints, and economy can be achieved by minimization of a cost function.

The main aim of this book is to give designers and fabricators aspects for selection of the best structural solution. A lot of structural versions fulfil the design and fabrication constraints and designers should select from these possibilities the best ones. A suitable cost function helps this selection, since a modern structure should be not only safe and fit for production but also economic.

A simple numerical example illustrates this aspect. In Table 1 three cross-sections of a bent box beam are shown. Their bending moment capacity (or section modulus) is nearly equal, but their cross-sectional areas (or mass) and costs (for a beam length of 20 m) are different.

Furthermore, their safeties against plate buckling (or plate slendernesses) are also near equal. The limiting plate slenderness in the case of a steel of yield stress 235 MPa for webs is 69 and for compression flange is 42. The cost includes material cost and welding cost of four longitudinal fillet welds. It can be seen that, to select the most suitable version, the beam of the minimum mass or cost should be selected, since this structural version is safe and economic.

This simple calculation is made by varying only few parameters. In most cases, treated in this book, much more unknowns should be varied to find the best solution. In these cases one needs special mathematical methods, some of them are treated in this book as well.

Table 1 Characteristics of three different bent box beam cross-sections

	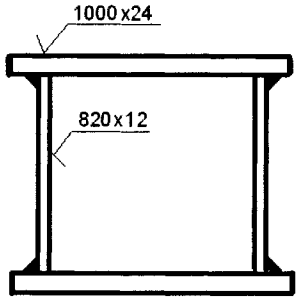	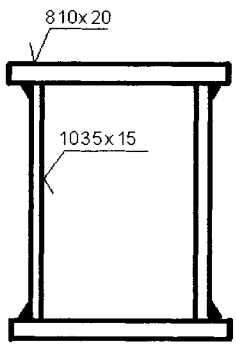	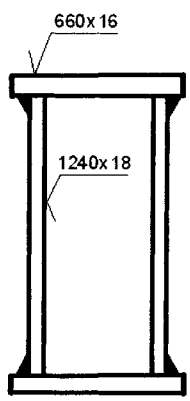
cross-sectional area mm^2	67680	63450	65760
section modulus mm^3	$22.3696x10^6$	$22.1231x10^6$	$22.3200x10^6$
web slenderness	820/12 = 68.3	1035/15 = 69	1240/18 = 68.9
flange slenderness	1000/24 = 41.7	810/20 = 40.5	660/16 = 41.2
cost $	11916	11734	12709

The optimum design procedure can be formulated mathematically as follows:
the objective function should be minimized

$$f(x) \rightarrow min,\ x = (x_1,...,x_n)$$

subject to constraints

$$g_j(x) \leq 0,\ j = 1...p$$

where n is the number of unknowns and p is the number of constraints.

The solution of this constrained function minimization problem needs effective mathematical methods.
The above description shows that the structural optimization has four main components:

(1) *design constraints* relate to stress, stability, deformation, eigenfrequency, damping,

(2) *fabrication constraints* formulate the limitation of residual welding distortions, requirements for welding technology, limitations of plate thicknesses and main structural dimensions, definition of available profile series,

(3) *a cost function* is formulated according to the fabrication sequence and contains the cost of materials, assembly, welding, cutting and painting,

(4) *mathematical methods.*

In our systematic research we have developed suitable means for these main components. Design constraints are formulated according to relevant Eurocodes or design rules of American Petroleum Institute (API), Det Norske Veritas (DNV) and European Convention for Constructional Steelwork (ECCS).

We have worked out a calculation method for residual welding stresses and distortions, for the cost function we have created a calculation method mainly for welded structures and we use several effective mathematical algorithms.

We have solved a lot of structural optimization problems for various structural models. Since these models are the main components of industrial structures, designers can use them in their work. The cost estimation in design stage is a good basis for the comparison of candidate structural versions.

Our structural models of welded I- and box-beams, tubular trusses, steel frames, stiffened plates and shells can be used in all industrial applications i.e. in bridges, buildings, roofs, columns, towers, ships, cranes, offshore structures, belt-conveyor bridges, machine structures, vehicles, etc.

Some special structural models are involved as follows: cellular plates, suspended beams for roofs, wind turbine towers, a tubular member of a truss tower of a fixed offshore platform.

Since the functions are highly nonlinear only numerical problems can be treated. Therefore, the conclusions are not completely general. In spite of this the solutions give valuable aspects for optimum design, because the numerical data are selected realistically.

The first step of the optimization procedure is the selection of variables. For this selection we need to know the main characteristics of a typical structure as follows: materials, loads, geometry, topology, profiles, fabrication technology, joints, costs. The better solutions can be obtained by changing these characteristics.

The new design aspects of our book to be emphasized are as follows. Seismic- and fire-resistant design methods are treated in special chapters and their applications are worked out in the chapter for frames. In the case of welded stiffened plates and cylindrical shells the problem of economy of stiffening is systematically investigated.

A question arises whether a thicker unstiffened or a thinner stiffened plate or shell is cheaper. The studies in the relevant chapters show that the economy of stiffening depends on loads (axial compression, bending, external pressure or combined) and on stiffening type (ring-, longitudinal- or orthogonal).

Summarizing: the general aspect of our book is the cost comparison, which is an effective means to select the most suitable structural versions.

We participate continuously in the following conference series: Annual Assemblies International Institute of Welding (IIW), World Congresses of ISSMO (International Society of Structural and Multidisciplinary Optimization), Eurosteel European Conferences of Steel Structures, Tubular Structures Symposia (organized by the IIW subcommission XV-E).

Beside the Conference Proceedings, we publish our studies also in well-known international engineering journals i.e. Structural and Multidisciplinary Optimization, Welding in the World, Computers and Structures, Engineering Optimization, Engineering Structures, Thin-walled Structures, Journal of Constructional Steel Research etc.

Some of our studies have been worked out with a very valuable cooperation of our scientific partner professors from Japan, South-Africa, Portugal, Slovakia and Poland.

This book is a continuation of our previous book "Economic design of metal structures". This new book contains our studies worked out in the last 5 years and published in the above mentioned journals and conference proceedings.

We hope that this book can help designers, students, researchers, manufacturers with the aspects shown in realistic models to find better, optimal, competitive structural solutions.

Acknowledgements

The research work was supported by the *József Öveges scholarship* OMFB 01385/2006, given by the National Office of Research and Technology (NKTH) and the Agency for Research Fund Management and Research Exploitation (KPI).

The project was also supported by the *Hungarian-South African* Intergovernmental S&T Co-operation program DAK 2/99 and 7/02. The Hungarian partner was the Ministry of Education, R&D Deputy Undersecretary of State, the South African partner was the Foundation for Research Development. Many thanks to Prof. Jan Snyman from the University of Pretoria for the Snyman-Fatti algorithm, Prof. Albert Groenwold for the Particle Swarm Optimization algorithm and Dr. Petronella Visser-Uys for some cost calculations.

The project was also supported by the *Hungarian-Japanese* Intergovernmental S&T co-operation program JAP 23/00. The Hungarian partner is the Ministry of Education, R&D Deputy Undersecretary of State, the Japanese partner is the Science and Technology Agency. Special thanks for Prof. Yoshiaki Kurobane and Yuji Makino from the Kumamoto University, Dr. Koji Azuma and Mr. Hideaki Shinde from the Sojo University for their contributions and suggestions in the research.

The project was also supported by the *Hungarian-Portuguese* Intergovernmental S&T Co-operation program P 6/99. The Hungarian partner was the Ministry of Education, R&D Deputy Undersecretary of State, the Portuguese partner was the Portuguese Institute for Scientific and Technological Cooperation ICCTI and Oriente Foundation. Thanks to Prof. Luis C. Simões, Dr. João Negrão and Dr. Paulo Rodrigues for their contribution.

The project was also supported by the *Hungarian-Slovakian* Intergovernmental S&T co-operation program SK 9/2004. The Hungarian partner is the Research and Technological Innovation Fund. This work is a part of the research project No. 13

MR, partially founded by the Department of International Scientific-technical Co-operation of the Ministry of Education of Slovak. Many thanks for Prof. Stanislav Kmeť and Dr. Jan Kanócz from the Technical University of Košice for the suspended beam calculations.

The project was also supported by the *Hungarian-Polish* Intergovernmental S&T co-operation program PL 4/2005. The Hungarian partner is the Research and Technological Innovation Fund, the Polish partner is the Polish Ministry of Science and Informatics. The research work was also supported by the Poznan University of Technology Grand DS 11-957/2007. Many thanks to Dr. Katarzyna Rzeszut for the finite element calculations.

Thanks for the calculation work and help of Dr. György Kovács, Mr. Zoltán Virág and Mr. László Kota, former PhD. students and Dr. Ferenc Orbán professor for the finite element calculations from the University of Pécs.

Last but not least many-many thanks for our family members, who helped a lot everyday.

1

Newer Mathematical Optimization Methods

1.1 INTRODUCTION

In the structural optimization process for an engineer it is important to know the behaviour of the structure well, the stresses, deformations, stability, eigenfrequency, damping, etc. It is as important to have a reliable optimization technique to find the optimum. The question is always the same: which is the best, which is the most reliable technique? The answer is that for the user always that kind of method is the best, which he knows the best. Non of the algorithm is superior. All of them can have benefits and disadvantages.

In our practice on structural optimization we have used several techniques in the last decades. We have published them in our books and gave several examples as engineering applications (Farkas 1984, Farkas & Jármai 1997, 2003). Most of the techniques were modified to be a good engineering tool in this work.

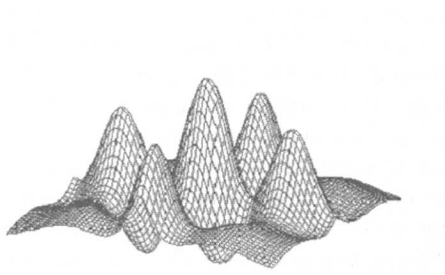

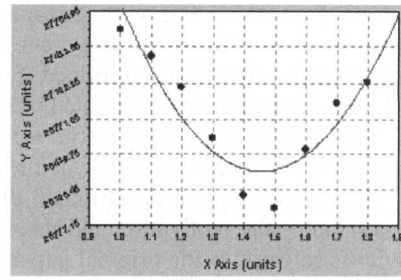

There are a great number of methods available for single objective optimization as it was described in Farkas & Jármai (1997). Methods without derivatives like: Complex (Box 1965), Flexible Tolerance (Himmelblau 1971) and Hillclimb (Rosenbrock 1960). Methods with first derivatives such as: Sequential Unconstrained Minimization Technique (*SUMT*) (Fiacco & McCormick 1968), Davidon-Fletcher-Powell (Rao 1984), etc. Methods with second derivatives such as:

Newton (Mordecai 2003), Sequential Quadratic Programming, *SQP* (Fan et al. 1988), the *Feasible SQP* (Zhou & Tits 1996). There are also other classes of techniques like Optimality Criteria methods (*OC*) (Rozvany 1997), or the discrete methods like Backtrack (Golomb & Baumert (1965), Annamalai 1970), the entropy-based method (Simões & Negrão 2000) (Farkas et al. 2005).

Multicriteria optimization is used when more objectives are important to find the compromise solution (Osyczka 1984, 1992, Koski 1994).

The general formulation of a single-criterion non-linear programming problem is the following:

$$\text{minimize} \quad f(x) \quad x_1, x_2, \ldots, x_N \,, \tag{1.1}$$

$$\text{subject to} \quad g_j(x) \leq 0, \quad j = 1,2,\ldots,P \,, \tag{1.2}$$

$$h_i(x) = 0 \quad i = P+1,\ldots,P+M \,, \tag{1.3}$$

$f(x)$ is a multivariable non-linear function, $g_j(x)$ and $h_i(x)$ are non-linear inequality and equality constraints, respectively.

In the last two decades some new techniques appeared e.g. the evolutionary techniques, like Genetic Algorithm, *GA* by Goldberg (1989), the Differential Evolution, *DE* method of Storn & Price (1995), the Ant Colony Technique (Dorigo et al. 1999), the Particle Swarm Optimization, *PSO* by Kennedy & Eberhart (1995), Millonas (1994) and the Artificial Immune System, *AIS* (Farmer et al. (1986), de Castro & Timmis (2001), Dasgupta (1999). Some other high performance techniques such as leap-frog with the analogue of potential energy minimum (Snyman 1983, 2005), similar to the FEM technique, have also been developed.

1.2 THE SNYMAN-FATTI METHOD

The global method described here, namely the Snyman-Fatti (*SF*) multi-start global minimization algorithm with dynamic search trajectories for global continuous unconstrained optimization (Snyman & Fatti 1987, Groenwold & Snyman 2002), was recently reassessed and refined (Snyman & Kok 2007) to improve its efficiency and to be applicable to constrained problems. The resultant improved computer code has been shown to be competitive with of the best evolutionary global optimization algorithms currently available when tested on standard test problems. Here we wish to apply it to the practical stiffened plate problem. For a detailed presentation and discussion of the motivation and theorems on which the *SF* algorithm is based, the reader is referred to the original paper of Snyman and Fatti (1987). Here we restrict ourselves to a summary giving the essentials of the multi-start global optimization methodology using dynamic search trajectories.
Consider the general inequality constrained problem:

$$\underset{w.r.t.\ \boldsymbol{x}}{\text{minimize}} \quad f(\boldsymbol{x}), \ \boldsymbol{x} = [x_1, x_2, \ldots x_n]^T \in R^n \,, \tag{1.4}$$

subject to inequality constraints:

$$g_j(\boldsymbol{x}) \leq 0, \quad j = 1,2,\ldots,m.$$

The optimum solution to this problem is denoted by $\boldsymbol{x}^*$ with associate optimum function value $f(\boldsymbol{x}^*)$.

We address the constrained problem (1.4) by transforming it to an unconstrained problem via the formulation of the penalty function $F(\boldsymbol{x})$, to which the unconstrained global *SF* optimization algorithm is applied. The penalty function $F(\boldsymbol{x})$ is defined as

$$F(\boldsymbol{x}) = f(\boldsymbol{x}) + \sum_{j=1}^{m} \rho_j \{g(\boldsymbol{x})\}^2, \tag{1.5}$$

where $\rho_j = 0$ if $g_j(\boldsymbol{x}) \leq 0$, else $\rho_j = \mu$ (a large number).
Thus we consider the unconstrained global optimization problem that can be stated: for a continuously differentiable objective function $F(\boldsymbol{x})$: find a point $\boldsymbol{x}^*(\mu)$ in the set $X \subset R^n$ such that

$$F^* = F(\boldsymbol{x}^*(\mu)) = \text{minimum of } F(\boldsymbol{x}) \text{ over } \boldsymbol{x} \in X. \tag{1.6}$$

The *SF* algorithm applied to this problem, is basically a multi-start technique in which several starting points are sampled in the domain of interest X (usually defined by a box in R^n), and a local search procedure is applied to each sample point. The method is heuristic in essence with the lowest minimum found after a finite number of searches being taken as an estimate of F^*.

In the local search the *SF* algorithm explores the variable space X using search trajectories derived from the differential equation:

$$\ddot{\boldsymbol{x}} = -\nabla F(\boldsymbol{x}(t)), \tag{1.7}$$

where ∇F is the gradient vector of $F(\boldsymbol{x})$.

Equation (1.4) describes the motion of a particle of unit mass in an n-dimensional conservative force field, where $F(\boldsymbol{x}(t))$ represents the potential energy of the particle at position $\boldsymbol{x}(t)$. The search trajectories generated here are similar to those used in Snyman's dynamic method for local minimization (Snyman 1982, 1983). In the *SF* global method, however, the trajectories are modified in a manner that ensures, in the case of multiple local minima, a higher probability of convergence to a lower local minimum than would have been achieved had conventional gradient local search methods been used.

The specific modifications employed result in an increase in the *regions of convergence* of the lower minima including, in particular, that of the global minimum. A stopping rule, derived from a Bayesian probability argument, is used to decide when to end the global sampling and accept the current overall minimum value of F, taken over all sampling points to date, as the global minimum F^*.

For initial conditions, position $\boldsymbol{x}(0) = \boldsymbol{x}^0$ and velocity $\dot{\boldsymbol{x}}(0) = \boldsymbol{v}(0) = \boldsymbol{v}^0 = 0$, integrating (1,7) from time 0 to t, implies the energy conservation relationship:

$$\tfrac{1}{2}\|\boldsymbol{v}(t)\|^2 + F(\boldsymbol{x}(t)) = \tfrac{1}{2}\|\boldsymbol{v}(0)\|^2 + F(\boldsymbol{x}(0)) = F(\boldsymbol{x}(0)). \tag{1.8}$$

The first term on the left-hand side of (1.8) represents the kinetic energy, whereas the second term represents the potential energy of the particle of unit mass, at any instant t. Obviously the particle will start moving in the direction of steepest descent and its kinetic energy will increase and thus F will decrease, as long as it moves downhill, i.e. as long as $-\nabla F \cdot \boldsymbol{v} > 0$, where $\cdot$ denotes the scalar product.

If descent is not met along the generated path then the magnitude of the velocity $\boldsymbol{v}$ decreases as it moves uphill and its direction changes towards a local minimizer. If the possibility of more than one local minimizer exists and we are interested in finding the global minimum, a realistic global strategy is to monitor the trajectory and record the point $\boldsymbol{x}^m$ and corresponding velocity $\boldsymbol{v}^m = \dot{\boldsymbol{x}}^m$ and function value F^m at which the minimum along the path occurs, letting the particle continue uninterrupted along its path with conserved energy. This is done in the hope that it may surmount a ridge of height F^r, $F^m < F^r < F(\boldsymbol{x}(0))$, continuing further along a path that may lead to an even lower value of F beyond the ridge.

On the other hand it is necessary to terminate the trajectory before it retraces itself or approximately retraces itself in indefinite periodic or ergodic (space-filling) motion. A proper termination condition, and that employed in the *SF* algorithm, is to stop the first trajectory once it reaches a point with a function value close to its starting value $F^s = F(\boldsymbol{x}(0))$ while still moving uphill, i.e. while $\nabla F \cdot \boldsymbol{v} > 0$. At this point, once termination has occurred and after setting the best point $\boldsymbol{x}^b := \boldsymbol{x}^m$ with corresponding function value $F^b := F^m$, it is proposed that a further auxiliary or inner trajectory be started from a new inner starting point $\boldsymbol{x}^s := \tfrac{1}{2}(\boldsymbol{x}^0 + \boldsymbol{x}^b)$ with initial velocity $\tfrac{1}{2}\boldsymbol{v}^m$ and associated starting function value $F^s = F(\boldsymbol{x}^s)$. Again for this new auxiliary or inner trajectory the function value is monitored and for this new trajectory $\boldsymbol{x}^m$ and associated $\boldsymbol{v}^m$ are recorded anew.

On its termination, again once the function value approaches F^s sufficiently closely while moving uphill, the starting point for the next inner trajectory is taken as $\boldsymbol{x}^s = \tfrac{1}{2}(\boldsymbol{x}^s + \boldsymbol{x}^b)$ with initial velocity $\tfrac{1}{2}\boldsymbol{v}^m$, where $\boldsymbol{x}^b$ again corresponds to the overall best point for the current sampling point. This generation of successive inner trajectories is continued until $\boldsymbol{x}^b$ converges or $\nabla F(\boldsymbol{x}^b)$ is effectively zero.

Of course, the above strategy assumes that the trajectory obtained from the solution of differential equation (1.4) is exactly known at all time instances. In practice this is not possible, and the generation of the trajectories is done numerically by means of the leap-frog scheme (Snyman 1982): Given initial position $\boldsymbol{x}^0 = \boldsymbol{x}(0)$ and initial velocity $\boldsymbol{v}^0 = \boldsymbol{v}(0) = \dot{\boldsymbol{x}}(0)$ and a time step Δt, compute for $k = 0,1,2,\ldots$

$$\boldsymbol{x}^{k+1} = \boldsymbol{x}^k + \boldsymbol{v}^k \Delta t, \tag{1.9}$$

$$\boldsymbol{v}^{k+1} = \boldsymbol{v}^k - \nabla F(\boldsymbol{x}^{k+1}) \Delta t. \tag{1.10}$$

For the first step $\boldsymbol{v}^0 := \tilde{=} \tfrac{1}{2}\nabla F(\boldsymbol{x}^0)\Delta t$. A heuristic procedure is used to select an appropriate time step Δt (Snyman, Kok 2007). Once the sequence of inner

(auxiliary) trajectories for the current iteration (i.e. current random starting point) is terminated the local minimum $\boldsymbol{x}^{k+1}$ with function value F^{k+1} obtained at that iteration, is evaluated for its probability of being the global minimum. This global component of the algorithm involves a stochastic criterion that reports the probability of the lowest obtained minimum to be the global one (Snyman, Fatti 1987).

To this end, let R_j denote the region of convergence of a local minimum $\hat{F}_j$ in the search space, and α_j denote the probability that a randomly selected point falls within R_j. Let R^* and α^* denote the corresponding quantities for the global minimum F^*. Snyman & Fatti (1987) then argue that, because of its special characteristic of seeking a low local minimum that for the local search methodology described above one may, for a large class of problems of practical and scientific importance, make the assumption that

$$\alpha^* = \text{maximum}_j\{\alpha_j\}. \tag{1.11}$$

Accordingly, they made use of the following theorem to terminate the multi-start algorithm.

Theorem: Let *ir* be the number of sample (starting) points falling within the region of convergence of the current overall minimum F^{opt} after *it* points have been sampled. Then, under the assumption given in (1.6) and a non-informative prior distribution, the probability that F^{opt} be equal to F^* , $Pr[F^{opt} = F^*]$, satisfies the following relationship:

$$Pr \geq q(it,ir) = 1-(it+1)!(2\times it-ir)!/[(2\times it+1)!(it-ir)!]. \tag{1.12}$$

In practice a tolerance ε_F is prescribed in order to determine whether a newly obtained local minimum also corresponds to the current overall minimum F^{opt}. Thus, if at the end of the final inner trajectory, $|F^{k+1} - F^{opt}| < \varepsilon_F$, then the number of successes *ir* is stepped up by one. Also a prescribed target value q^* is set for $q(it,ir)$ so that once $q(it,ir) > q^*$ the global procedure terminates with $F^* := F^{opt}$.

Once $\boldsymbol{x}^*(\mu)$, the global minimizer of the penalty function defined in equation (1.5) is found, it is a straightforward matter to determine the active constraints of the original constrained problem (1.4). The exact solution $\boldsymbol{x}^*$ to the constrained problem is then found by the one-time application of the trajectory method to the minimization of the sum of the squares of the residues of the active constraints, using $\boldsymbol{x}^*(\mu)$ as starting point.

The *SF* algorithm was successfully applied at several structural optimization, such as at stiffened plates Farkas et al. (2007a), Snyman, Kok (2007).

1.3 THE PARTICLE SWARM OPTIMIZATION ALGORITHM

Programs that work very well in optimizing convex functions very often perform poorly when the problem has multiple local minima or maxima. They are often caught or trapped in the local minima/maxima. Several methods have been developed to escape from being caught in such local optima. The Particle Swarm

Method of global optimization is one of such methods. A swarm of birds or insects or a school of fish searches for food, protection, etc. in a very typical manner. If one of the members of the swarm sees a desirable path to go, the rest of the swarm will follow quickly. Every member of the swarm searches for the best in its locality - learns from its own experience.

Additionally, each member learns from the others, typically from the best performer among them. Even human beings show a tendency to learn from their own experience, their immediate neighbours and the ideal performers. The Particle Swarm method of optimization mimics this behaviour. Every individual of the swarm is considered as a particle in a multidimensional space that has a position and a velocity. These particles fly through hyperspace and remember the best position that they have seen. Members of a swarm communicate good positions to each other and adjust their own position and velocity based on these good positions. The Particle Swarm method of optimization testifies the success of bounded rationality and decentralized decisionmaking in reaching at the global optima. It has been used successfully to optimize extremely difficult multimodal functions.

Particle swarm optimization (*PSO*) is a population based stochastic optimization technique developed by Eberhart and Kennedy (1995), inspired by social behaviour of bird flocking or fish schooling.

PSO shares many similarities with evolutionary computation techniques such as Genetic Algorithms (*GA*). The system is initialized with a population of random solutions and searches for optima by updating generations. However, unlike *GA*, PSO has no evolution operators such as crossover and mutation. In *PSO*, the potential solutions, called particles, fly through the problem space by following the current optimum particles.

Each particle keeps track of its coordinates in the problem space which are associated with the best solution (fitness) it has achieved so far. (The fitness value is also stored.) This value is called *pbest*. Another "best" value that is tracked by the particle swarm optimizer is the best value, obtained so far by any particle in the neighbours of the particle. This location is called *lbest*. when a particle takes all the population as its topological neighbours, the best value is a global best and is called *gbest*.

The particle swarm optimization concept consists of, at each time step, changing the velocity of (accelerating) each particle toward its p*best* and *lbest* locations (local version of *PSO*). Acceleration is weighted by a random term, with separate random numbers being generated for acceleration toward *pbest* and *lbest* locations.

In past several years, *PSO* has been successfully applied in many research and application areas. It is demonstrated that *PSO* gets better results in a faster, cheaper way compared with other methods.

Another reason that *PSO* is attractive is that there are few parameters to adjust. One version, with slight variations, works well in a wide variety of applications. Particle swarm optimization has been used for approaches that can be used across a wide

range of applications, as well as for specific applications focused on a specific requirement.

The method is derivative free, and by its very nature the method is able to locate the global optimum of an objective function. Constrained problems can simply be accommodated using penalty methods.

Lately, the *PSO* was successfully applied to the optimum shape and size design of structures by Fourie and Groenwold (2000). An operator, namely craziness, was re-introduced, together with the use of dynamic varying maximum velocities and inertia.

The pseudo code of the procedure can be written as follows:

I) *For* each particle:
Initialize particle

II) *Do*:

a) *For* each particle:
1) Calculate fitness value
2) If the fitness value is better than the best fitness value (*pbest*) in history
3) Set current value as the new *pbest*
End

b) *For* each particle:
1) Find in the particle neighbourhood, the particle with the best fitness
2) Calculate particle velocity according to the velocity equation (1.13)
3) Apply the velocity constriction
4) Update particle position according to the position equation (1.14)
5) Apply the position constriction
End

While maximum iterations or minimum error criteria is not attained.

A more precise and detailed description of the particular *PSO* algorithm, as applied to penalty function formulation and used in this study now follows.

Basic *PSO* Algorithm

Given M, k_{max}, N_{max}. Set (time) instant k=0, $F_i^b = F^g = F_{before}^g = \infty$. Initialise a random population (swarm) of M particles (swarm members), by assigning an initial random position $\boldsymbol{x}_i^0$ (candidate solution), as well as a random initial velocity $\boldsymbol{v}_i^0$, to each particle i, i=1,2,...,M. Then compute simultaneous trajectories, one for each particle, by performing the following steps.

1) At instant k, compute the fitness of each individual particle i at discrete point $\boldsymbol{x}_i^k$, by evaluating $F(\boldsymbol{x}_i^k)$. With reference to the minimization of (1.4), the lower the value of $F(\boldsymbol{x}_i^k)$, the greater the particle's fitness.

2) For i=1,2,…,M:

   if $F(\boldsymbol{x}_i^k) \le F_i^b$ then set $F_i^b = F(\boldsymbol{x}_i^k)$ and $\boldsymbol{p}_i^b = \boldsymbol{x}_i^k$ {best point on trajectory i}

   if $F(\boldsymbol{x}_i^k) \le F^g$ then set $F^g = F(\boldsymbol{x}_i^k)$ and $\boldsymbol{g}^b = \boldsymbol{x}_i^k$ {best global point}

3) If $F^g < F_{before}^g$ then set $N = 1$, else set $N = N + 1$.

4) If $N > N_{max}$ or $k > k_{\max}$ then STOP and set $\boldsymbol{x}^* = \boldsymbol{g}^b$; else continue.

5) Compute new velocities and positions for instant k+1, using the rule:

   for i=1,2,…,M:

$$\boldsymbol{v}_i^{k+1} := \boldsymbol{v}_i^k + c_1 r_1 (\boldsymbol{p}_i^b - \boldsymbol{x}_i^k) + c_2 r_2 (\boldsymbol{g}^b - \boldsymbol{x}_i^k), \tag{1.13}$$

$$\boldsymbol{x}_i^{k+1} := \boldsymbol{x}_i^k + \boldsymbol{v}_i^{k+1}, \tag{1.14}$$

where r_1 and r_2 are independently generated random numbers in the interval [0,1], and c_1, c_2 are parameters with appropriately chosen values.

6) Set $k = k + 1$ *and* $F_{before}^g = F^g$; go to step 2.

The technique is modified in order to be efficient in technical applications. It uses dynamic inertia reduction and craziness for some particles (Fourie & Groenwold 2000).

PSO was applied at several structural optimization problems cost minimization of an orthogonally stiffened welded steel plate (Farkas et al. 2007a), ring-stiffened conical shell (Farkas et al. 2007b), optimization of a wind turbine tower structure (Uys et al. 2007), optimization of a stiffened shell (Farkas et al. 2007c).

One can find much information from the internet.

http://www.swarmintelligence.org
http://www.particleswarm.info/

Lot of information about Particle Swarms and particularly on Particle Swarm Optimization is available. Many Particle Swarm Links are also available.

1.4 MULTIOBJECTIVE OPTIMIZATION

Multiobjective Optimization (*MO*) problems are defined as those problems where two or more, sometimes competing and/or incommensurable, objective functions have to be minimized simultaneously (Pareto 1875).

In a general case, the solution to the *MO* problem is a set of points that represent the best trade-offs between the objective functions. These points are called *Pareto*

Optimal points. The set of all the Pareto Optimal points is called the *Pareto Optimal Set*. A point in the search space is Pareto Optimal if it is not pareto-dominated by any other point.

To determine if a point in the search is dominates another, a vector whose components are the values of the objective functions in the point is defined. A vector $\boldsymbol{A}$ dominates another vector $\boldsymbol{B}$ if the values for each of the components of $\boldsymbol{A}$ are at least equal to the values of $\boldsymbol{B}$, and at least a value from $\boldsymbol{A}$ is strictly greater than the corresponding value from $\boldsymbol{B}$.

A multicriteria optimization problem can be formulated as follows:

Find $\boldsymbol{x}$ such that

$$\boldsymbol{f(x^*)} = opt\, \boldsymbol{f(x)}, \tag{1.15}$$

such that

$$g_j(\boldsymbol{x}) \geq 0 \qquad j = 1,....,P, \tag{1.16}$$

$$h_i(\boldsymbol{x}) = 0 \qquad i = P,....,P+Q,$$

where x is the vector of decision variables defined in n-dimensional Euclidean space and $f_k(x)$ is a vector function defined in r-dimensional Euclidean space. $g_j(x)$ and $h_i(x)$ are inequality and equality constraints.

The solutions of this problem are the Pareto Optimal Set (or part of it). The definition of these optima is based upon the intuitive conviction that the point x^* is chosen as the optimal, if no objective can be improved without worsening at least one other objective. As a result, the algorithms used to resolve these problems have to be able to provide more than one solution.

One way is to use a Weights approach technique; a global objective function is defined as a weighted sum of the values of the competing objective functions in the problems. Weights can either be fixed or not. Alternatively, population-based algorithms, such as Evolutionary Algorithms (*EA*) or the *PSO* can be used without defining a combined function.

Finding the Pareto Optimal set can be performed by several runs of the algorithm providing a single Pareto Optimal point each time. As an alternative, in several algorithms, including the *PSO* variations, a repository stores the points that are potentially part of the Pareto Optimal Set (Koski 1994). This repository is updated whenever a non dominated point while the execution of the algorithm continues.

1.4.1 Weighting objectives method

The pure weighting method means to add all the objective functions together using different weighting coefficients for each. It means that we transform our multicriteria optimization problem to a scalar one by creating one function of the form:

$$f(\mathbf{x}) = \sum_{i=1}^{r} w_i \, f_i(x) \quad \text{where } w_i \geq 0 \text{ and } \sum_{i=1}^{r} w_i = 1. \tag{1.17}$$

If we change the weighting coefficients, results of this model can vary significantly, and depend greatly from the nominal values of the different objective functions.

1.4.2 Normalized objectives method

The normalized objectives method solves the problem of the pure weighting method e.g. at the pure weighting method, the weighting coefficients do not reflect proportionally the relative importance of the objective, because of the great difference on the nominal value of the objective functions. At the normalized weighting method w_i reflect closely the importance of objectives.

$$f(\mathbf{x}) = \sum_{i=1}^{r} \frac{w_i \, f_i(x)}{f_i^0}, \qquad \text{where } w_i \geq 0 \text{ and } \sum_{i=1}^{r} w_i = 1. \tag{1.18}$$

The condition $f_i^0 \neq 0$ is assumed.

1.4.3 Global criterion method type I

Let f^0 be the ideal solution that simultaneously yields minimum values for all criteria. Such a solution does not exist but is introduced in compromise programming as a target or a goal to approach, although impossible to reach (perfection is impossible).

Global criterion method means that a function which describes a global criterion is a measure of closeness the solution to the ideal vector of f^0. The common form of this function is:

$$f(x) = \sum_{i=1}^{r} \left[\frac{f_i^0 - f_i(x)}{f_i^0} \right]^P, \qquad P = 1,2,3,... \tag{1.19}$$

It is suggested to use P=2, but other values of P such as 1,3,4, etc. can be used. Naturally, the solution obtained will differ greatly according to the value of P chosen, P=1 means a linear correlation, $P = 2$ a quadratic one, etc.

1.4.4 Global criterion method type II

This family of L_p metrics indicates how close the satisfying solution is to the ideal solution, and represents the feasible set. In this paper, the satisfying solutions are determined for two particular values of P, namely, $P = 2$ and $P = \infty$ (which correspond to the minimization of the Euclidean and maximum distances, respectively), and are given below. For the case $P = \infty$, the largest deviation is the criterion of comparison and is referred to as min-max criterion.

The deviations in the absolute sense are as follows:

$$L_P(f) = \left[\sum_{i=1}^{k} \left| f^0{}_i - f_i(x) \right|^P \right]^{1/P}, \qquad 1 \le P \le \infty, \tag{1.20}$$

if P=1 $$L_P(f) = \sum_{i=1}^{k} \left| f_i^0 - f_i(x) \right|, \tag{1.21}$$

if P=2 $$L_P(f) = \left[\sum_{i=1}^{k} \left| f_i^0 - f_i(x) \right|^2 \right]^{1/2}, \qquad \text{Euclidean metric.} \tag{1.22}$$

1.4.5 Global criterion method type III

Instead deviations in the absolute sense it is recommended to use relative deviations such as

$$L_P(f) = \left[\sum_{i=1}^{r} \left| \frac{f_i^0 - f_i(x)}{f_i^0} \right|^P \right]^{1/P}, \qquad 1 \le P \le \infty. \tag{1.23}$$

In this case the P has a larger set.

1.4.6 Weighting global criterion method

The weighting global criterion method is made, by introducing weighting parameters, one could get a great number of Pareto optima with (1.24) (Jármai 1989). If we choose P = 2, which means the Euclidean distance between Pareto optimum and ideal solution Jármai (1989a). The coordinates of this distance are weighted by the parameters as follows:

$$L_P(f) = \left[\sum_{i=1}^{r} w_i \left| \frac{f_i^0 - f_i(x)}{f_i^0} \right|^2 \right]^{1/2}, \tag{1.24}$$

where P is the dimension of the function space, x indicates the design variables and X the constraint set, r is the number of objective functions, f^0 is the optimum of the i^{th} objective function, and w_i are the weighting factors.

The solution obtained by minimizing Eq. (1.24) differs greatly depending on the value of P chosen.

1.4.7 Min-max method

At the min-max method the maximum loss of the collective objective will be minimized. The min-max optimum compares relative deviations from the separately reached minima. The relative deviation can be calculated from

$$z_i'(x) = \frac{\left|f_i(x) - f_i^0\right|}{\left|f_i^0\right|} \quad \text{or} \quad z_i''(x) = \frac{\left|f_i(x) - f_i^0\right|}{\left|f_i(x)\right|}. \tag{1.25}$$

If we know the extremes of the objective functions which can be obtained by solving the optimization problems for each criterion separately, the desirable solution is the one which gives the smallest values of the increments of all the objective functions.

The point x^* may be called the best compromise solution considering all the objective functions simultaneously and on equal terms of importance.

$$z_i(x) = \max \{ z_i'(x), z_i''(x) \}, \qquad i \in I, \tag{1.26}$$

$$\mu(x^*) = \min \max \{ z_i(x) \}, \qquad x \in X \; i \in I, \tag{1.27}$$

where X is the feasible region.

1.4.8 Weighting min-max method

The weighting min-max method is the combination of the min-max approach with the weighting method, a desired representation of Pareto optimal solutions can be obtained

$$z_i(x) = \max \{ w_i z_i'(x), w_i z_i''(x) \} \quad i \in I. \tag{1.28}$$

The weighting coefficients w_i reflect exactly the priority of the criteria, the relative importance of it. We can get a distributed subset of Pareto optimal solutions.

1.4.9 Programsystem for single- and multiobjective optimization

The Particle Swarm Optimizer has been built into this interactive decision support program system (Jármai 1989a), which contains the following single objective optimization methods

Complex method of Box (1965)

Flexible Tolerance (*FT*) method of Himmelblau (1971),

Direct Random Search (*DRS*) method (Siddal 1982),

Hillclimb method (*HILL*) of Rosenbrock (1960),

Davidon-Flecher-Powell (*DFP*) method of Rao (1984),

Particle Swarm Optimization (*PSO*), (Jármai 2005).

The efficiencies of these methods are different. All of them use the same objective, constraints subroutines. For a problem, which is highly non-linear, several local minima exist. They find different ones. The advantage of Particle Swarm Optimization is that it can find optimum for a nonconvex problem.

The interactive decision support programsystem contains several multiobjective optimization methods. They are the following:

Min-max method,

Global criterion method: type - I,

Global criterion method: type - II,

Weighted min-max method,

Weighted global criterion method,

Pure weighting method,

Normalized weighting method.

Once a subset of Pareto optima has been generated, the designer has to make an important decision concerning the selection of the best solution from this subset. The selection is not obvious when several conflicting criteria are considered but may be made subjectively by giving preference to one criterion over the others.

The programsystem was used to optimize sandwich beams (Jármai 1989b) and stiffened shells with stringer stiffeners (Jármai 2005) and was found to be very efficient finding the Pareto optima.

2

Cost Calculations

2.1 INTRODUCTION

When we consider the interaction of design and technology, we should not forget the cost of the structure as the third leg of the system. These three together help us to find the best solution. These cost calculations are founded on material costs and those fabrication costs, which have direct effect on the sizes, dimensions or shape of the structure. Other costs, like amortization, investment, transportation, maintenance are not considered here. Sometimes we can predict the cost of design and inspection, but usually they are proportional to the weight of the structure. Cost and production time data come form different companies from all over the world. When we compare the same design at different countries, we should consider the differences between labour costs. It has the most impact on the structure, if the technology is the same.

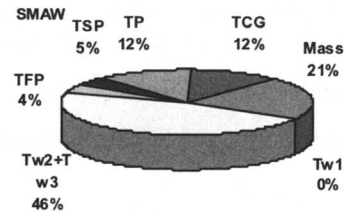

2.2 THE COST FUNCTION

The cost function includes the cost of material, assembly, welding as well as surface preparation, painting and cutting, edge grinding, forming the shell and is formulated according to the fabrication sequence. Not too much research has been done in this field, but we have to refer to the work of Klansek & Kravanja (2006ab), Jalkanen (2007), Tímár et al. (2003).

2.2.1 The cost of material

$$K_M = k_M \rho V; k_M = 1.0 \text{ \$/kg} . \tag{2.1}$$

where K_M [kg] is the fabrication cost, k_M [\$/kg] is the corresponding material cost factor, V [mm^3] is the volume of the structure, ρ is the density of the material. For steel it is 7.85x10^{-6} kg/mm^3. If several different materials are used, then it is possible to use different material cost factors simultaneously in Equation (2.1).

2.2.2 The fabrication cost in general

$$K_f = k_f \sum_i T_i , \tag{2.2}$$

where K_f [\$] is the fabrication cost, k_f [\$/min] is the corresponding fabrication cost factor, T_i [min] are production times. It is assumed that the value of k_f is constant for a given manufacturer. If not, it is possible to apply different fabrication cost factors simultaneously in Equation (2.2).

a.) Fabrication times for welding

The most important times related to welding are as follows: preparation, assembly, tacking, time of welding, changing the electrode, deslagging and chipping.

b.) Calculation of the times of preparation, assembly and tacking

The times of preparation, assembly and tacking can be calculated with an approximation formula as follows

$$T_{w1} = C_1 \Theta_{dw} \sqrt{\kappa \rho V} , \tag{2.3}$$

where C_1 is a parameter depending on the welding technology (usually equal to 1), Θ_{dw} is a difficulty factor, κ is the number of structural elements to be assembled. The difficulty factor expresses the complexity of the structure. Difficulty factor values depend on the kind of structure (planar, spatial), the kind of members (flat, tubular). The range of values proposed is between 1-4 (Farkas & Jármai 1997).

c.) Calculation of real welding time

Real welding time can be calculated on the following way

$$T_{w2} = \sum_i C_{2i} a_{wi}^2 L_{wi} , \tag{2.4}$$

where a_{wi} is weld size, L_{wi} is weld length, C_{2i} is constant for different welding technologies. C_2 contains not only the differences between welding technologies but the time differences between positional (vertical, overhead) and normal welding in downhand position as well. The whole equation list and tables can be found in the Appendix D1-8.

d.) Calculation of additional fabrication actions time

There are some additional fabrication actions to be considered such as changing the electrode, deslagging and chipping. The time of these is as follows

$$T_{w3} = \sqrt{\Theta_{dw}} \sum_i C_{3i} a_{wi}^2 L_{wi} . \tag{2.5}$$

Formulae (2.3, 2.4, 2.5) were proposed by Pahl & Beelich (1982) and used in (Farkas & Jármai 1999, Jármai & Farkas 2003).
Ott & Hubka (1985) proposed that C_3 = (0.2-0.4) C_2 on average $C_3 = 0.3C_2$. Thus, the modified formula for T_{w3} neglecting $\sqrt{\Theta_{dw}}$, is

$$T_{w3} = 0.3 \sum C_{2i} a_{wi}^2 L_{wi} . \tag{2.6}$$

In the negligence of $\sqrt{\Theta_{dw}}$ it is assumed that the difficulty factor should be considered only for T_{w1}.

The Netherlands Institute of Welding has developed the software COSTCOMP (2002). It gives welding times and costs for different welding technologies (Bodt 1990) on the basis of theoretical and experimental investigations. Considering the times given by companies all over the world and the times calculated by COSTCOMP here Equation (2.3) is used for T_{w1} and the other times are calculated with a generalized formula, where the power of a_w is n, which is some cases equal to 2, or close to it.

$$T_{w2} + T_{w3} = 1.3 \sum C_{2i} a_{wi}^n L_{wi} . \tag{2.7}$$

e.) Calculation of the times of arc-spot welding

$$T_{w4} = n_S T_S , \tag{2.8}$$

where n_S is the number of spots, T_S is the time of welding one spot weld and of transferring the electrode to the next spot. T_S depends on the welding equipment and the degree of automation. For example, the time of arc-spot welding of a cellular plate for ship deck panel is T_S = 0.3 min.

f.) Fabrication times of post-welding treatments

$$T_{PWT} = T_0 L_t , \tag{2.9}$$

where T_0 is the specific time (min/mm), L_t is the treated weld length (mm). Table D9 shows the specific times for the given *PWT* in the Appendix D.

g.) Time for flattening plates

$$T_{FP} = \Theta_{df} \left(a_e + b_e t^3 + \frac{1}{a_e t^4} \right) A_p , \tag{2.10}$$

where a_e=9.2x10^{-4} min/mm^2, b_e= 4.15x10^{-7} min/mm^5, Θ_{df} is the difficulty parameter (Θ_{df} = 1,2 or 3). The difficulty parameter depends on the form of the plate.

h.) Surface preparation time

The surface preparation means the surface cleaning, sand spraying, etc. The surface cleaning time can be defined in the function of the surface area (A_s [mm^2]) as follows:

$$T_{SP} = \Theta_{ds} a_{sp} A_s \,, \tag{2.11}$$

where a_{sp} = 3x10^{-6} min/mm^2, Θ_{ds} is a difficulty parameter.

i.) Painting time

The painting means making the ground- and the topcoat. The painting time can be given in the function of the surface area (A_s [mm^2]) as follows:

$$T_P = \Theta_{dp}(a_{gc} + a_{tc})A_s \,, \tag{2.12}$$

where a_{gc} = 3x10^{-6} min/mm^2 , a_{tc} = 4.15x10^{-6} min/mm^2, Θ_{dp} is a difficulty factor, Θ_{dp}=1,2 or 3 for horizontal, vertical or overhead painting. Tizani et al. (1996) proposed a value for painting 14.4 x10^{-6} \$/mm^2. For more complicated structures we use k_P = 2x14.4x10^{-6} \$/mm^2.

j.) Plate cutting and edge grinding times

The cutting and edge grinding can be made by different technologies, like Acetylene, Stabilized gasmix and Propane with normal and high speed.
The cutting cost function can be formulated using Tables D10 and D11 in the function of the thickness (t [mm]) and cutting length (L_c [mm]):

$$T_{CP} = \sum_i C_{CPi} t_i^n L_{ci} \,, \tag{2.13}$$

where t_i the thickness in [mm], L_{ci} is the cutting length in [mm]. The value of n comes from curve fitting calculations.

k.) Times of hand cutting and machine grinding of strut ends

At tubular structures a main part of the total cost is the cost of hand cutting and machine grinding of strut ends. We use the following formula (Farkas & Jármai 1997)

$$T_{CG} = \Theta_{dc} \sum_i \frac{2\pi d_i}{\sin\varphi}\left(4.54 + 0.4229 t_i^2\right), \tag{2.14}$$

where the fabrication cost factor is taken on the basis of Tizani et al. (1996) as 40 \$/h = 0.6667 \$/min, and the difficulty factor is considered as $\Theta_{dc} = 3$. The diameter of the brace is d_i in m, thickness is t_i in mm. φ is the angle between the two members (chord and brace) connected. Note that Glijnis (1999) proposed a formula for one strut end in the case of oxyfuel cutting on CNC machine as follows:

$$K_{CG}(\$) = \frac{2.5\pi d_i}{(350 - 2t_i)0.3 \sin\varphi_i}, \tag{2.15}$$

where 350 mm/min is the cutting speed, 0.3 is the efficiency factor, d_i and t_i are in mm.

l.) Forming of plate elements into shell segments

Forming of plate elements into shell segments depends on the shape of shell. If it is a cylindrical one, than the forming time is more simple, as it is written in (2.16).

$$T_{F0i} = \Theta e^{\mu}, \tag{2.16}$$

$$\mu = 6.8582513 - 4.527217 t_i^{-0.5} + 0.009541996(2R_i)^{0.5}. \tag{2.17}$$

where t_i is the shell segment thickness, R_i is the radius, the factor of fabrication difficulty is taken as $\Theta = 3$. The approximation is valid till $R_{\max}$ = 1500 and t = 30 mm.

If the shell is a slightly conical one, than each segment has different curvature, so the final time is a sum of the single segment production time

$$K_{F0} = \sum_{i=1}^{n} k_f T_{F0i}. \tag{2.18}$$

m.) Material cost of bolts

The cost of bolts depends on several parameters, like the material, the steel grade, the diameter, the length of the bolt and the length of the screw-cut. In our example in Section 6.2 (Jármai et al. 2004) it is

K_b = 0.54 \$, 8.8 grade M20 bolts.

n.) Drilling cost of bolts

Drilling of bolts depend on the diameter of the bolt, the steel grade of the plate and its thickness. In our example in Section 6.2, drilling of M20 holes it is

K_d = 0.38 \$.

2.2.3 Total cost function

The total cost function can be formulated by adding the previous cost functions together (depending on the structure some can be zero).

$$\frac{K}{k_m} = \rho V + \frac{k_f}{k_m}\left(T_{w1} + T_{w2} + T_{w3} + T_{w4} + T_{PWT} + T_{FP} + T_{SP} + T_P + T_{CP} + T_{CG} + T_{F0} + \ldots\right) \tag{2.19}$$

Taking k_m = 0.5-1.5 \$/kg, k_f =0 -1 \$/min. The k_f/k_m ratio varies between 0 - 2 kg/min. If k_f/k_m = 0, then we get the mass minimum. If k_f/k_m = 2.0 it means a very high labour cost (Japan, USA), k_f/k_m = 1.5 and 1.0 means a West European labour cost, k_f/k_m = 0.5 means the labour cost of developing countries. Even if the production rate is similar for these cases, the difference between costs due to the different labour costs is significant.

3

Seismic Resistant Design

3.1 INTRODUCTION

Earthquakes, can cause catastrophic damage, thus, steel structures should be designed to be seismic resistant. In Chapter 6 problems of seismic resistant design of steel frames are worked out (Farkas & Jármai 2006, Jármai et al. 2006). The aim of the present chapter is to give some design rules from Eurocode 8 (EC8) (1998, 2004), which have been used in these problems. Only buildings of steel unbraced frames are treated here. On the theoretical basis, rules for base isolation and National Annexes are not introduced. It should be mentioned that in Design (1995) one can find worked examples for seismic design of building frames.

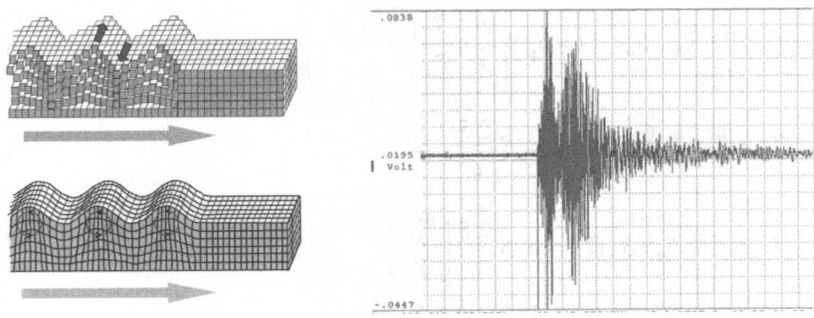

3.2 GROUND CONDITIONS AND SEISMIC ACTION

3.2.1 Ground types

The following ground categories are used:
A – rocks, including at most 5 m of weaker material at the surface

B – very dense sand, gravel or very stiff clay, at least several tens of metres in thickness

C – deep deposits of dense or medium dense sand, gravel or stiff clay

D – deposits of loose-to-medium cohesionless soil or of predominantly soft-to-firm cohesive soil

E – a soil profile consisting of a surface alluvium layer

3.2.2 Cases of very low seismicity

Cases of very low seismicity, for which the EC8 provisions need not be observed are as follows: the design ground acceleration a_g is not greater than 0.04 g (0.39 m/s^2), or the product $a_g S$ is not greater than 0.05 g (0.49 m/s^2)(S is the soil factor given in Table 3.1.

3.2.3 Parameters of elastic response spectra

Table 3.1 Values of parameters of elastic response spectra

Ground type	S	T_B [s]	T_C [s]	T_D [s]
A	1.0	0.15	0.4	2.0
B	1.2	0.15	0.5	2.0
C	1.15	0.20	0.6	2.0
D	1.35	0.20	0.8	2.0
E	1.4	0.15	0.5	2.0

3.2.4 Design spectrum for elastic analysis

The design spectrum $S_d(T)$ for the horizontal components of the seismic action is defined by the following expressions:

$$0 \le T \le T_B : S_d(T) = a_g S\left[\frac{2}{3} + \frac{T}{T_B}\left(\frac{2.5}{q} - \frac{2}{3}\right)\right], \tag{3.1}$$

$$T_B \le T \le T_C : S_d(T) = a_g S \frac{2.5}{q}, \tag{3.2}$$

$$T_C \le T \le T_D : S_d(T) = a_g S \frac{2.5}{q}\left(\frac{T_C}{T}\right) \quad \text{and} \quad S_d(T) \ge \beta a_g, \tag{3.3}$$

$$T_D \le T : S_d(T) = a_g S \frac{2.5}{q}\left(\frac{T_C T_D}{T^2}\right) \quad \text{and} \quad S_d(T) \ge \beta a_g, \tag{3.4}$$

where

a_g is the ground acceleration given by the National Annex, e.g. the larger value of 0.40 is prescribed in Japan,

q is the behaviour factor,

β is the lower bound factor for the horizontal design spectrum, given by the National Annex, the recommended value is 0.2.

3.3 DESIGN OF BUILDINGS

3.3.1 Combination coefficients for variable actions

Combination of actions for seismic design situations

$$\sum G_{k,j} + \gamma_1 A_E + \sum \psi_{E,i} Q_{k,i} \,, \tag{3.5}$$

where

G_k is the characteristic value of a permanent action
A_E is the characteristic value of seismic action
Q_k is the characteristic value of variable action

$$\psi_E = \varphi \psi_2 \,, \tag{3.6}$$

is the factor of permanent action.

For roof $\varphi = 1$, for other storeys $\varphi = 0.5$.

Values of the factor ψ_2 are given in Table 3.2.

Table 3.2 Recommended values of ψ_2 factors for buildings

Building	ψ_2
domestic, residential	0.3
office	0.3
congregation	0.6
shopping	0.6
storage	0.8
traffic, vehicle weight <30 kN	0.6
traffic, 30 kN < vehicle weight < 160 kN	0.3

3.3.2 Importance classes and importance factors

Important classes for buildings and importance factors are as follows:

I – Buildings of minor importance, e.g. agricultural buildings, etc., $\gamma_1 = 0.8$,

II – Ordinary buildings, $\gamma_1 = 1.0$,

III – Buildings whose seismic resistance is of importance, e.g. schools, assembly halls, cultural institutions, etc., $\gamma_1 = 1.2$,

IV – Buildings whose integrity during earthquakes is of vital importance, e.g. hospitals, fire stations, power plants, etc., $\gamma_1 = 1.4$.

3.3.3 Base shear force

$$F_b = S_d(T_1)m\lambda\,, \tag{3.7}$$

where

T_1 is the fundamental period of vibration of the building for lateral motion,
$S_d(T_1)$ is the ordinate of the design spectrum at period T_1,
m is the total mass of the building,
λ is the correction factor, $\lambda = 0.85$ if $T_1 \leq 2T_C$ and the building has more than two storeys, or $\lambda = 1.0$ otherwise.

For buildings with heights of up to 40 m T_1 (in s) may be approximated by

$$T_1 = C_1 H^{3/4}, \tag{3.8}$$

where

$C_1 = 0.085$ for moment resistant steel frames,
$C_1 = 0.075$ for eccentrically braced steel frames,
$C_1 = 0.050$ for other structures,

H is the height of the building in m.

3.3.4 Distribution of the horizontal seismic forces

The seismic action shall be determined by horizontal forces F_i to all storeys:

$$F_i = F_b \frac{s_i m_i}{\sum s_j m_j}\,, \tag{3.9}$$

where

F_i is the horizontal force acting on storey I,
s_i, s_j are the displacements of masses m_i, m_j,
m_i, m_j are the storey masses.

When the fundamental mode shape is approximated by horizontal displacements increasing linearly along the height

$$F_i = F_b \frac{z_i m_i}{\sum z_j m_j}\,, \tag{3.10}$$

where

z_i, z_j are the heights of the masses m_i, m_j above the level of application of the seismic action.

3.3.5 Displacement calculation

If linear analysis is performed the displacements induced by the design seismic action can be calculated on the basis of the elastic deformations of the structural system

$$d_s = q d_e, \tag{3.11}$$

where d_e is the displacement determined by a linear analysis, q is the behaviour factor.

3.3.6 Limitation of interstorey drift

For buildings having non-structural elements of brittle materials attached to the structure

$$d_r \nu \leq 0.005 h, \tag{3.12}$$

where d_r is the interstorey drift calculated according to Sec. 3.3.5, ν is a reduction factor, for importance classes I and II $\nu = 0.5$, for importance classes III and IV $\nu = 0.4$, h is the storey height,

for buildings having ductile non-structural elements

$$d_r \nu \leq 0.0075 h, \tag{3.13}$$

for buildings having non-structural elements fixed in a way so as not to interfere with structural deformations or with non-structural elements

$$d_r \nu \leq 0.010 h. \tag{3.14}$$

3.3.6 Second-order effects

Second-order effects (P - Δ effects) need not be taken into account if the following condition is fulfilled in all storeys:

$$\theta = \frac{P_{tot} d_r}{V_{tot} h} \leq 0.10, \tag{3.15}$$

where

P_{tot} is the total gravity load at and above the storey considered in the seismic design situation,
d_r is the interstorey drift,
V_{tot} is the total seismic storey shear,
h is the interstorey height.

If $0.1 < \theta \leq 0.2$, the second-order effects may approximately be taken into account by multiplying the relevant seismic action effects by a factor of $1/(1-\theta)$. The value of θ shall not exceed 0.3.

3.4 SPECIFIC RULES FOR STEEL BUILDINGS

3.4.1 Behaviour factors for moment resisting frames

For unbraced frames, where the dissipative zones are in beams and at bottom of columns:

One storey one bay frames $q = 5.5$,
multi-storey one bay frames $q = 6.0$,
multi-storey multi-bay frames $q = 6.5$.

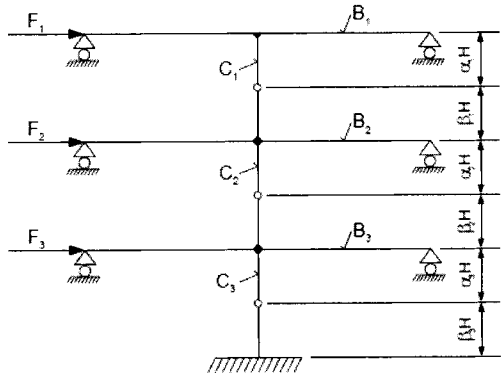

Figure 3.1 Horizontal seismic forces. The frame is divided to 4 parts by considering inflection points on the column parts

For $q > 4$ the required cross-sectional class is 1 (plastic).

Since the frames are statically indeterminate, in order to determine the inner forces due to these horizontal forces, an approximate method of Ifrim (1984) can be used based on the localization of inflection points. For the top floor $\alpha_1 = 0.65$, for the middle floors $\alpha_2 = 0.5$ and for bottom part of the column $\alpha_3 = 0.4$ (Figure 3.1).

4

Fire Resistant Design

4.1 INTRODUCTION

Fire protection is the prevention and reduction of the hazards associated with fires. A fire-resistance rating typically means the duration for which a passive fire protection system can withstand a standard fire resistance test. The aim for passive fire protection systems is typically to demonstrate in fire testing the ability to maintain the item or the side to be protected at or below either 140°C (for walls, floors and electrical circuits required to have a fire-resistance rating) or ca. 540°C, which is considered the critical temperature for structural steel, above which, there is a risk of losing its strength, leading to collapse. Fire testing involves live fire exposures upwards of 1100°C, depending on the fire-resistance rating and duration one is after. More items than just fire exposures are typically required to be tested to ensure the survivability of the system under realistic conditions.

Fire design of steel structures is usually based on the thermal conductivity of the protective material. Design values of thermal conductivity can be determined by full-scale fire tests. These tests also show whether the protective material stays attached to the steel structure and protects it against fire as long as required.

The steel can be protected by materials such as mineral fibres, gypsum boards, concrete, intumescent paints and water-filled structures.

Fire resistance of load-bearing structures can be evaluated by both full-scale fire tests and calculations. Computational determination of fire resistance requires that cross-sectional temperature distribution is known.

Fire research has tended to lag behind other fields of scientific and technological endeavour. This is due, no doubt, partly to its extreme complexity but also due to the relatively low perceived importance of the topic in man's progress towards industrial development. Safety in general and fire safety in particular, after several major disasters, has become a subject of increasing importance in recent years. A general definition for the fire resistance of construction elements can be the following: the time after which an element, when submitted to the action of a fire, ceases to fulfil the functions for which it has been designed (Kay et al. 1996, Cox 1999, Rodrigues et al. 2000).

The beams and column parts are subject to bending and compression, thus, stress constraints should be formulated for beam and column profiles according to Eurocode 3 (2005) ($EC3_1$)

4.2 CALCULATION OF THE STEEL MECHANICAL PROPERTIES AT ELEVATED TEMPERATURES

The calculation of the yield stress and Young's modulus on elevated temperatures is according to EC 3_2. Figure 4.1 and Table 4.1 show the reduction factors in the function of temperature between 20 and 1200 C°.

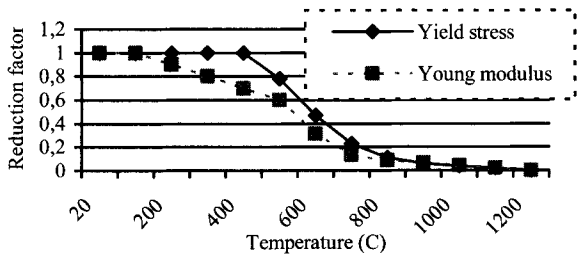

Figure 4.1 The yield stress and the Young's modulus reduction factors in the function of temperature

4.2.1 Calculation of yield strength

The yield strength at a given temperature can be calculated by $k_{y,\theta}$ reduction factor

$$f_{y,\theta} = k_{y,\theta} f_y \,. \tag{4.1}$$

4.2.2 Calculation of Young's modulus

The yield strength at a given temperature can be calculated by $k_{E,\theta}$ reduction factor

$$E_{a,\theta} = k_{E,\theta} E_a \,. \tag{4.2}$$

Values of $k_{y\theta}$ and $k_{E,\theta}$ can be calculated according to Table 4.1 and Figure 4.1.

Table 4.1 The yield stress and the Young's modulus reduction factors in the function of temperature

Temperature	$k_{y,\theta}$ reduction factor (relative to f_y)	$k_{E,\theta}$ reduction factor (relative to E_a)
20	1,000	1,000
100	1,000	1,000
200	1,000	0,900
300	1,000	0,800
400	1,000	0,700
500	0,780	0,600
600	0,470	0,310
700	0,230	0,130
800	0,110	0,090
900	0,060	0,0675
1000	0,040	0,0450
1100	0,020	0,0225
1200	0,000	0,0000

4.2.3 Thermal conductivity

The thermal conductivity of steel λ_a should be determined from the following:

If 20 [°C] $\leq \theta_a <$ 800 [°C] then

$$\lambda_a = 54 - 3{,}33 \times 10^{-2}\ \theta_a \ \text{[W/mK]} \,. \tag{4.3}$$

If 800 [°C] $\leq \theta_a \leq$ 1200 [°C] then

$$\lambda_a = 27.3 \ \text{[W/mK]} \,, \tag{4.4}$$

where: θ_a is the steel temperature.

4.2.4 The specific heat

The specific heat of steel can be calculated as a function of temperature as follows:

If $0 < \theta_a \leq$ 600 [°C] then

$$c_a = 425 + 7.73x10^{-1}\theta_a - 1.69x10^{-3}\theta_a^2 + 2.22x10^{-6}\theta_a^3 \ \text{[J/kgK]}. \tag{4.5}$$

If $600 < \theta_a \leq$ 735 [°C] then

$$c_a = 666 + 13002/(738 - \theta_a) \ \text{[J/kgK]}. \tag{4.6}$$

If $735 < \theta_a \leq 900$ [°C] then

$$c_a = 545 + 17820/(\theta_a - 731) \text{ [J/kgK]}. \tag{4.7}$$

If $900 < \theta_a \leq 1200$ [°C] then $c_a = 650$ [J/kgK]. (4.8)

The value of specific heat in the function of temperature can be seen on Figure 4.2.

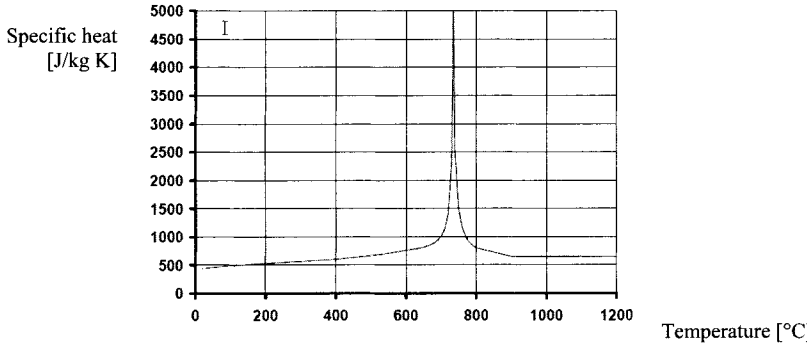

Figure 4.2 The value of specific heat in the function of temperature

4.3 CALCULATION OF THE ACTIONS FOR THE FIRE SITUATION

A general definition for the *fire resistance* of construction elements can be as follows: *the time after which an element, when submitted to the action of a fire, ceases to fulfil the functions for which it has been designed.* For the time being, the fire resistance required in most national fire safety regulations for the construction elements, does not refer to the fire that could happen with a given probability under the real conditions in a building. It is referred to the standard fire (ISO 834). Therefore, since structural elements have a load carrying function, their standard fire resistance represents the time after which, when subjected to the standard fire, they can no longer resist the effects of the accidental load combination, according to EC1[2].

$$\sum \gamma_{GA} \cdot G_k + \psi_{1,1} \cdot Q_{k,1} + \sum \psi_{2,i} \cdot Q_{k,i} + \sum A_d(t), \tag{4.9}$$

where:

G_k Characteristic values of permanent actions,

$Q_{k,1}$ Characteristic value of the main variable action,

$Q_{k,i}$ Characteristic value of the other variable actions,

$A_d(t)$ Design values of actions from fire exposure, or indirect fire actions,

γ_{GA} Partial safety factor for permanent actions in the accidental situation,

$\psi_{1,1}, \psi_{2,i}$ Combination coefficients for buildings according to EC 1_2.

The last term of this load combination represents the interaction between the heated element and the cold structure from which it is a part. The first terms represent the mechanical action on the heated element at the beginning of the fire, that is, the design effect of actions in fire situation at time $t = 0$, $E_{\mathrm{fi,d,t=0}}$. For the analysis of the fire resistance of a single member, the Eurocodes state that "the internal forces and moments at supports and ends of members applicable at time $t = 0$, may be assumed to remain unchanged throughout the fire exposure", that is, $E_{fi,d,t} = E_{fi,d,t=0}$. For member analysis a reduction factor for load combination should be taken according to Rodrigues (2000). In our case, when we have applied the calculation of the frame, which is for supporting pressure vessels, no variable loading can be considered, so $Q_{\mathrm{k},1}/G_{\mathrm{k}}$ according to Figure 4.1 of EC 3_2 is $\eta_{fi} = 0.74$, the maximum.

$$E_{fi,d} = \eta_{fi} E_d \,. \tag{4.10}$$

4.3.1 Simple calculation models

The load-bearing function of a steel member shall be assumed to be maintained after a time t in a given fire if:

$$E_{fi,d} \leq R_{fi,d,t}\,, \tag{4.11}$$

where

$E_{fi,d}$ is the design effect of actions for the fire design situation, according to EN 1991-1-2;

$R_{fi,d,t}$ is the corresponding design resistance of the steel member, for the fire design situation, at time t.

The design resistance $R_{fi,d,t}$ at time t shall be determined, usually in the hypothesis of a uniform temperature in the cross-section, by modifying the design resistance for normal temperature design to EN 1993-1-1, to take account of the mechanical properties of steel at elevated temperatures.

4.3.2 Member analysis

The effect of actions should be determined for time t=0 using combination factors $\psi_{1,1}$ or $\psi_{2,1}$.

As a simplification to this, the effect of actions $E_{fi,d}$ may be obtained from a structural analysis for normal temperature design as:

$$E_{fi,d} = \eta_{fi}\ E_d\,, \tag{4.12}$$

where:

E_d is the design value of the corresponding force or moment for normal temperature design, for a fundamental combination of actions,

η_{fi} is the reduction factor for the design load level for the fire situation.

The reduction factor η_{fi} for load combination (6.10) in EN 1990 should be taken as:

$$\eta_{fi} = \frac{G_k + \psi_{fi} Q_{k,1}}{\gamma_G G_k + \gamma_{Q,1} Q_{k,1}}. \tag{4.13}$$

The value of $\psi_{fi,1}$ is according to Figure 4.3.

The cross-sections may be classified as for normal temperature design with a reduced value for ε as given in (4.14).

$$\varepsilon = 0.85 \sqrt{\frac{235}{f_y}}, \tag{4.14}$$

where: f_y is the yield strength at 20 °C.

The reduction factor 0.85 considers influences due to increasing temperature.

4.3.3 Resistance of tension members

The design resistance $N_{fi,\theta,Rd}$ of a tension member with a uniform temperature θ_a should be determined from:

$$N_{fi,\theta,Rd} = k_{y,\theta} N_{Rd} [\gamma_{M,1} / \gamma_{M,fi}], \tag{4.15}$$

where:

$k_{y,\theta}$ is the reduction factor for the yield strength of steel at temperature θ_a, reached at time t;

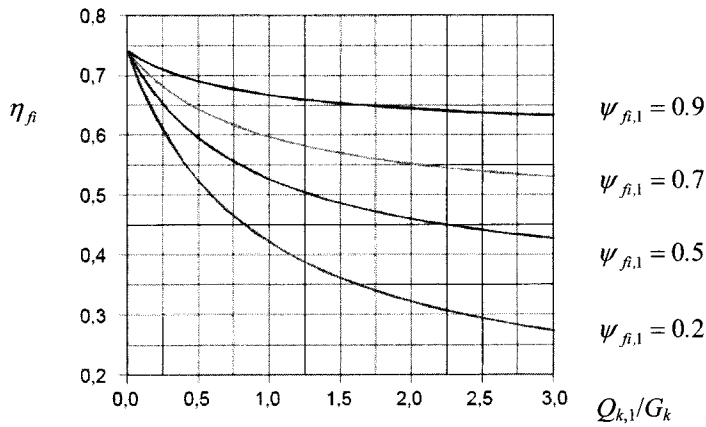

Figure 4.3 The value of the combination factor

N_{Rd} is the design resistance of the cross-section $N_{pl,Rd}$ for normal temperature design, according to EN 1993-1-1.

4.3.4 Compression members with Class 3 cross-sections

The design buckling resistance $N_{b,fi,t,Rd}$ at time t of a compression member with a Class 3 cross-section with a uniform temperature θ_a should be determined from:

$$N_{b,fi,t,Rd} = \chi_{fi} A k_{y,\theta} f_y / \gamma_{M,fi}, \tag{4.16}$$

where: χ_{fi} is the reduction factor for flexural buckling in the fire design situation;

$k_{y,\theta}$ is the reduction factor from Section 4.2 for the yield strength of steel at the steel temperature θ_a reached at time t.

The value of χ_{fi} should be taken as the lesser of the values of $\chi_{y,fi}$ and $\chi_{x,fi}$ determined according to:

$$\chi_{fi} = \frac{1}{\varphi_\theta + \sqrt{\varphi_\theta^2 - \bar{\lambda}_\theta^2}}, \tag{4.17}$$

with $$\varphi_\theta = \frac{1}{2}\left(1 + \alpha\bar{\lambda}_\theta + \bar{\lambda}_\theta^{\,2}\right). \tag{4.18}$$

The non-dimensional slenderness for the temperature θ_a, is given by:

$$\bar{\lambda}_\theta = \bar{\lambda}\left(\frac{k_{y,\theta}}{k_{E,\theta}}\right)^{0.5}, \bar{\lambda} = \frac{KL}{r\lambda_E}; \quad \lambda_E = \pi\sqrt{\frac{E}{f_y}}; \quad r = \sqrt{\frac{I}{A}}, \tag{4.19}$$

where KL is the buckling length, r radius of gyration, I the section moment of inertia, A is the cross-section area.

$$\alpha = 0.65\sqrt{\frac{235}{f_y}}. \tag{4.20}$$

4.3.5 Beams with Class 3 cross-sections

The design moment resistance $M_{fi,t,Rd}$ at time t of a Class 3 cross-section with a uniform temperature should be determined from:

$$M_{fi,t,Rd} = k_{y,\theta} M_{Rd} [\gamma_{M,1}/\gamma_{M,fi}] \tag{4.21}$$

where: M_{Rd} is the elastic moment resistance of the gross cross-section $M_{el,Rd}$ for normal temperature design, or the reduced moment resistance allowing for the effects of shear if necessary;

$k_{y,\theta}$ is the reduction factor for the yield strength of steel at the steel temperature θ_a.
The design moment resistance $M_{fi,t,Rd}$ at time t of a Class 3 cross-section with a non-uniform temperature distribution may be determined from:

$$M_{fi,t,Rd} = k_{y,\theta,max} M_{Rd} [\gamma_{M,1}/\gamma_{M,fi}]/\kappa_1\kappa_2, \tag{4.22}$$

where:

M_{Rd} is the elastic moment resistance of the gross cross-section $M_{el,Rd}$ for normal temperature design or the reduced moment resistance allowing for the effects of shear if necessary according to EN 1993-1-1;

$k_{y,\theta,max}$ is the reduction factor for the yield strength of steel at the maximum steel temperature $\theta_{a,max}$ reached at time t;

κ_1 is an adaptation factor for non-uniform temperature in a cross-section;

κ_2 is an adaptation factor for non-uniform temperature along the beam

The design lateral torsional buckling resistance moment $M_{b,fi,t,Rd}$ at time t of a laterally unrestrained beam with a Class 3 cross-section should be determined from:

$$M_{b,fi,t,Rd} = \chi_{LT,fi} W_{el,y} k_{y,\theta,com} f_y / \gamma_{M,fi} \ . \tag{4.23}$$

Conservatively $\theta_{a,com}$ can be assumed to be equal to the maximum temperature $\theta_{a,max}$.

The design shear resistance $V_{fi,t,Rd}$ at time t of a Class 3 cross-section should be determined from:

$$V_{fi,t,Rd} = k_{y,\theta,web} V_{Rd} [\gamma_{M,1}/\gamma_{M,fi}] \ , \tag{4.24}$$

where: V_{Rd} is the shear resistance of the gross cross-section for normal temperature design, according to EN 1993-1-1.

4.3.6 Members with Class 3 cross-sections, subject to combined bending and axial compression

The design buckling resistance $R_{fi,t,d}$ at time t of a member subject to combined bending and axial compression should be verified by satisfying expressions for a member with a Class 3 cross-section.

$$\frac{N_{fi,Ed}}{\chi_{min,fi} A k_{y,\theta} \dfrac{f_y}{\gamma_{M,fi}}} + \frac{k_y M_{y,fi,Ed}}{W_{el,y} k_{y,\theta} \dfrac{f_y}{\gamma_{M,fi}}} + \frac{k_z M_{z,fi,Ed}}{W_{el,z} k_{y,\theta} \dfrac{f_y}{\gamma_{M,fi}}} \le 1 , \tag{4.25a}$$

$$\frac{N_{fi,Ed}}{\chi_{z,fi} A k_{y,\theta} \dfrac{f_y}{\gamma_{M,fi}}} + \frac{k_{LT} M_{y,fi,Ed}}{\chi_{Lt,fi} W_{el,y} k_{y,\theta} \dfrac{f_y}{\gamma_{M,fi}}} + \frac{k_z M_{z,fi,Ed}}{W_{el,z} k_{y,\theta} \dfrac{f_y}{\gamma_{M,fi}}} \le 1 , \tag{4.25b}$$

where:

$$\chi_{LT,fi} = \frac{1}{\Phi_{LT,\theta,com} + \sqrt{\left(\Phi_{LT,\theta,com}\right)^2 - \left(\bar{\lambda}_{LT,\theta,com}\right)^2}} \ , \tag{4.26}$$

$$\Phi_{LT,\theta,com} = \frac{1}{2}\left[1 + \alpha \bar{\lambda}_{LT,\theta,com} + \left(\bar{\lambda}_{LT,\theta,com}\right)^2\right] , \tag{4.27}$$

$$\alpha = 0.65\sqrt{235 / f_y}\ , \tag{4.28}$$

$$\bar{\lambda}_{LT,\theta,com} = \bar{\lambda}_{LT}\sqrt{k_{y,\theta,com} / k_{E,\theta,com}}\ , \tag{4.29}$$

where:

$k_{E,\theta,com}$ is the reduction factor from Section 4.2 for the slope of the linear elastic range at the maximum steel temperature in the compression flange $\theta_{a,com}$ reached at time t.

$$k_{LT} = 1 - \frac{\mu_{LT} N_{fi,Ed}}{\chi_{z,fi} A k_{y,\theta} \dfrac{f_y}{\gamma_{M,fi}}} \le 1, \tag{4.30}$$

where $\mu_{LT} = 0.15\bar{\lambda}_{z,\theta}\beta_{M,LT} - 0.15 \le 0.9$, (4.31)

$$k_y = 1 - \frac{\mu_y N_{fi,Ed}}{\chi_{y,fi} A k_{y,\theta} \dfrac{f_y}{\gamma_{M,fi}}} \le 3, \tag{4.32}$$

where $\mu_y = (1.2\beta_{M,y} - 3)\bar{\lambda}_{y,\theta} + 0.44\beta_{M,y} - 0.29 \le 0.8$, (4.33)

$$k_z = 1 - \frac{\mu_z N_{fi,Ed}}{\chi_{z,fi} A k_{y,\theta} \dfrac{f_y}{\gamma_{M,fi}}} \le 3, \tag{4.34}$$

where $\mu_z = (2\beta_{M,z} - 5)\bar{\lambda}_{z,\theta} + 0.44\beta_{M,z} - 0.29 \le 0.8$. (4.35)

4.4 STEEL TEMPERATURE DEVELOPMENT

4.4.1 Unprotected internal steelwork

For an equivalent uniform temperature distribution in the cross-section, the increase of temperature $\Delta\theta_{a,t}$ in an unprotected steel member during a time interval Δt should be determined from:

$$\Delta\theta_{a,t} = k_{sh} \frac{A_m / V}{c_a \rho_a} \dot{h}_{net,d} \Delta t\ , \tag{4.36}$$

where: k_{sh} is correction factor for the shadow effect, from 5.2.5.1(2) in EC 3;

A_m/V is the section factor for unprotected steel members;

A_m is the surface area of the member per unit length [m^2];

V is the volume of the member per unit length [m^3];

c_a is the specific heat of steel, from section 4.2.4 [J/kgK];

$\dot{h}_{net,d}$ is the design value of the net heat flux per unit area [W/m^2];

Δt is the time interval [seconds];

ρ_a is the unit mass of steel [kg/m^3].

For I-sections under nominal fire actions, the correction factor for the shadow effect may be determined from:

$$k_{sh} = 0.9\frac{[A_m/V]_b}{[A_m/V]}, \tag{4.37}$$

where: $[A_m/V]_b$ is box value of the section factor. In all other cases, the value of k_{sh} shall be taken as:

$$k_{sh} = \frac{[A_m/V]_b}{[A_m/V]}. \tag{4.38}$$

For cross sections with a convex shape (e.g. rectangular or circular hollow sections) fully embedded in fire, the shadow effect does not play a role and consequently the correction factor k_{sh} equals unity. Ignoring the shadow effect (i.e. k_{sh} = 1), leads to conservative solutions.

The value of Δt should not be taken as more than 5 seconds. The value of the section factor A_m/V should not be taken as less than 10 m^{-1}. The calculation the design values of the section factor A_m/V for unprotected steel members are as in Table 4.2.

Table 4.2 Value of the section factor A_m/V for different cross sections and fire effects.

Description	A_m/V
Open section exposed to fire on all sides	*perimeter/cross-section area*
Tube exposed to fire on all sides	$1/t$
Open section exposed to fire on three sides	*surface exposed to fire/cross-section area*
Hollow section (or welded box section of uniform thickness) on all sides	$1/t$ if $t \ll b$
I-section flange exposed to fire on three sides	$(b + 2t_f)/(bt_f)$ if $t \ll b$
Welded box section exposed to fire on all sides	$2(b+ h)$/*cross-section,* if $t \ll b$ than $A_m/V \approx 1/t$

4.4.2 Internal steelwork insulated by fire protection material

Traditional fireproofing materials include concrete encasement, gypsum wallboard, and coatings categorized as Spray-Applied Fire-Resistive Materials (SFRMs) that are typically composed of ingredients such as mineral wool, cement, and gypsum, and can vary in density. Intumescent fire-resistive coatings are newer fireproofing

materials. They are paint-like coatings that are applied to structural steel members at a final thickness up to 15 mm.

All of these fireproofing materials are designed to provide an insulating barrier between the heat from a fire and the structural steel. The barrier prevents the high temperatures within a fire from affecting the structural performance of the steel members. Because the intumescent coatings have paint-like properties, they are receiving increasing attention from architects and designers.

There are actually two types of "fire" coatings on the market. They are designed for use on different substrates and respond very differently when exposed to fire.
Fire-retardant paints are applied to combustible materials (wood, plastic, foam) and are designed to reduce the rate of flame spread. Typically, they are based on vinyl or vinyl acrylic resins. They look like paints and are formulated to be applied like paints (brush, roller, or spray). They do burn, can generate smoke, and do not have high temperature resistance.

Many fire-retardant coatings are only rated for the ability to "not contribute" to a fire, i.e. they will not become a fuel source. Some do provide resistance in keeping the fire from getting to the substrate.

Fire-resistant coatings provide insulation to the substrate. Intumescent fire-resistant coatings work by expanding their volume from 10 to 75 times and generating an ash-like char. The extent of char will be dependent upon the material contained in the coating. The shape of the structural steel will affect expansion and char formation. These coatings provide fire ratings (1, 2, 3, and 4 hours) depending on the coating thickness, steel shape, and steel mass.

For a uniform temperature distribution in a cross-section, the temperature increase $\Delta\theta_{a,t}$ of an insulated steel member during a time interval Δt should be obtained from:

$$\Delta\theta_{a,t} = \frac{\lambda_p A_p / V\left(\theta_{g,t} - \theta_{a,t}\right)}{d_p c_a \rho_a \left(1 + \Phi/3\right)} \Delta t - \left(e^{\Phi/10} - 1\right)\Delta\theta_{g,t} \ , \tag{4.39}$$

but $\Delta\theta_{a,t} \geq 0$ if $\Delta\theta_{g,t} > 0$,

$$\Phi = \frac{c_p \rho_p}{c_a \rho_a} d_p A_p / V \ , \tag{4.40}$$

where:

A_p/V is the section factor for steel members insulated by fire protection material;

A_p is the appropriate area of fire protection material per unit length of the member [m²];

V is the volume of the member per unit length [m³];

c_a is the temperature dependant specific heat of steel, from section 4.2.4 [J/kgK];

c_p is the temperature independent specific heat of the fire protection material [J/kgK];

d_p is the thickness of the fire protection material [m];

Δt is the time interval [seconds];

$\theta_{a,t}$ is the steel temperature at time t [°C];

$\theta_{g,t}$ is the ambient gas temperature at time t [°C];

$\Delta\theta_{g,t}$ is the increase of the ambient gas temperature during the time interval Δt [K];

λ_p is the thermal conductivity of the fire protection system [W/mK];

ρ_a is the unit mass of steel [kg/m^3];

ρ_p is the unit mass of the fire protection material [kg/m^3].

The value of Δt should not be taken as more than 30 seconds.

Section factor A_p/V for steel members insulated by fire protection material for in Table 4.3.

Table 4.3 Section factor A_p/V for steel members insulated by fire protection material

Description	A_p/V
I-beam with contour encasement of uniform thickness on all surfaces	steel perimeter/steel cross-section area
I-beam with hollow encasement of uniform thickness on all surfaces	$2(b+h)$/steel cross-section area
I-beam exposed to fire on three sides with contour encasement of uniform thickness	steel perimeter-b /steel cross-section area
I-beam exposed to fire on three sides with hollow encasement of uniform thickness on all surfaces	$(2h+b)$/steel cross-section area

4.4.3 The calculation of the evolution of steel temperature

For unprotected steel structure the calculation of the evolution of the steel temperature is as follows with an iteration process (EC3$_2$, ISO 1975):

The time at the beginning of the fire is

$t_i = 0$, and every time period: $\Delta t_i = 5$ we calculate it $t_{i+1} = t_i + \Delta t_i$ [sec]. (4.41)

Changing the time from $0 \le t_i \le t_{max}$ [sec], (4.42)

where t_{max} can be ½, 1, 1 ½, 2 , 4 hours, means 1800, 3600, 5400, 7200, 14400 [sec].

The temperature of the steel can be between

$$20\ [^\circ\text{C}] \le \theta_a \le 1200\ [^\circ\text{C}]. \quad (4.43)$$

The starting values are as follows:

$$\theta_a = 20\ ^\circ\text{C},\ \Delta\theta_a\ [^\circ\text{C}],\ \rho_a = 7850\ \text{kg/m}^3. \tag{4.44}$$

The gas temperature in the vicinity of the fire exposed member (standard temperature-time curve):

$$\theta_g = 20 + 345\log\left(8\frac{t_i}{60} + 1\right)\ [^\circ\text{C}]. \tag{4.45}$$

The net convection heat flux:

$$\dot{h}_{netc} = \alpha_c\left(\theta_g - \theta_a\right), \tag{4.46}$$

where the coefficient of heat transfer by convection $\alpha_c = 25\ \text{W/m}^2\text{K}$. (4.47)

The net radiative heat flux

$$\dot{h}_{netr} = \Phi\varepsilon_m\varepsilon_f\sigma\left[\left(\theta_g + 273\right)^4 - \left(\theta_a + 273\right)^4\right]\ [\text{W/m}^2], \tag{4.48}$$

where:

the configuration factor $\Phi = 1$,

the surface emissivity of the member $\varepsilon_{\text{m}} = 0.8$,

the emissivity of the fire $\varepsilon_{\text{f}} = 1.0$,

the Stephan Boltzmann constant $\sigma = 5.67x10^{-8}\ \text{W/m}^2\text{K}^4$. (4.49)

The total net heat flux can be calculated as the sum of convection and radiative heat fluxes:

$$\dot{h}_{netd} = \dot{h}_{netc} + \dot{h}_{netr}\,. \tag{4.50}$$

For a tube exposed to fire on all sides:

$$\frac{A_m}{V} = \frac{1}{10^{-3}t_0}\text{, where } t_0 \text{ is the cross section thickness.} \tag{4.51}$$

The temperature changing:

$$\Delta\theta_a = k_{sh}\frac{\frac{A_m}{V_m}\dot{h}_{netd}\Delta t_i}{c_a\rho_a}, \tag{4.52}$$

where $k_{sh} = 1$. (4.53)

The surface temperature of the steel member in every iteration step is the following:

$$\theta_a^n = \theta_a^{n-1} + \Delta\theta_a^{n-1} \tag{4.54}$$

The iteration is stopped, when either the time, or the temperature limit is reached.

4.4.4 Advanced calculation models

Advanced calculation methods are based on fundamental physical behaviour in such a way as to lead to a reliable approximation of the expected behaviour of the relevant structural component under fire conditions. Advanced calculation methods should include separate calculation models for the determination of: the development and distribution of the temperature within structural members (thermal response model) and the mechanical behaviour of the structure or of any part of it (mechanical response model).

Advanced calculation methods for thermal response based on the acknowledged principles and assumptions of the theory of heat transfer, the relevant thermal actions, the variation of the thermal properties of the material with the temperature, the effects of non-uniform thermal exposure and of heat transfer to adjacent building components, the influence of any moisture content and of any migration of the moisture within the fire protection material may conservatively be neglected.

Advanced calculation methods for mechanical response shall be based on the acknowledged principles and assumptions of the theory of structural mechanics, taking into account the changes of mechanical properties with temperature. The effects of thermally induced strains and stresses both due to temperature rise and due to temperature differentials, shall be considered. The model for mechanical response shall also take into account of the combined effects of mechanical actions, geometrical imperfections and thermal actions and the temperature dependent mechanical properties of the material, the geometrical non-linear effects, the effects of non-linear material properties, including the unfavourable effects of loading and unloading on the structural stiffness.

5

Large-span Suspended Roof Members

5.1 INTRODUCTION

Suspended steel and/or timber members subjected to tension and bending offer an economical and efficient alternative for many structural problems (Figure 5.1). They can be widely used in bridge and structural engineering and building practice as bearing suspended systems of pedestrian and pipeline bridges as well as of large-span roofs and floors in buildings.

Some research results and analytical studies on non-linear solutions of suspension members of finite flexible stiffness with parabolic or similar shape have been published (Kachurin 1962, Telojan & Vedenikov 1977, Moskalev 1980). These theories provide simple methods for finding the static response of a hinge-suspended member to applied vertical loads in the elastic range.

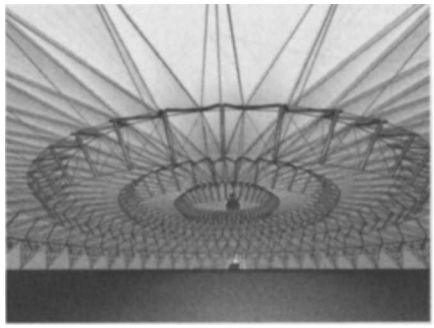

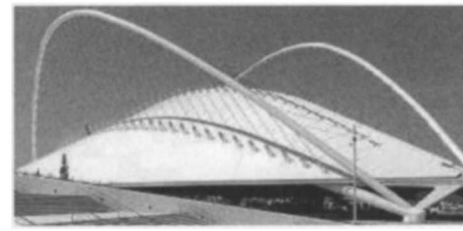

The growth of the plastic deformations provokes the redistribution of the forces, i.e. the axial tensions and the bending moments in the suspended structures, that often leads to increasing of their bearing capacity and more effective behaviour under the

load. Comprehensive analytical treatments on the behaviour of suspension members of finite bending stiffness in elastic-plastic range have been given by Skladnev & Shimanovsky (1992). Because of the mathematical derivation difficulties that can arise in a geometrically and parametrically non-linear analytical solution, numerical methods are by far the most popular. Most of the recent methods of non-linear analysis of suspension structures are based on the discretization of the equilibrium equations using FEM and solving the resulting non-linear algebraic equations by numerical methods (Kmet' and Bin 2002).

Some results of the experimental and theoretical behaviour investigation of the geometrically and physically non-linear suspension steel members of bending stiffness working in the field of elastic and plastic deformations of material are in (Bin 2003) (Figure 5.1a). Results confirmed the sensitivity of such structures to local and asymmetrical actions. The behaviour of structure and resulting stresses (tension or compression at cross-section) in the elastic range depends on the interaction of axial tension forces and bending moments. After, the structural member reaches the phase of full plasticity of material (formation and development of plastic zones) its behaviour becomes similar to the behaviour of a suspension cable with the dominant tension stiffness.

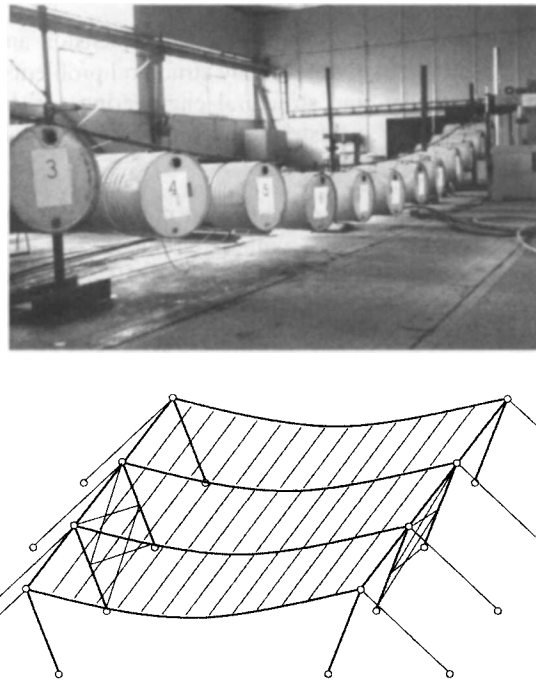

Figure 5.1(a) (b) Test of the suspended member of bending stiffness (a) and suspended structure (b)

Suspension members of finite flexible stiffness usually have a parabolic shape, but new information about behaviour of members of rectilinear shape was published recently by Kvedaras & Sharashkinas (2003). However, a little attention is paid to

the optimization and probabilistic reliability analysis of suspension parabolic members of finite flexible stiffness with random properties. That is why the authors focus on these problems, and elaborating them they start with the work of Telojan & Vedenikov (1977), which is further complemented.

5.2 THE SUSPENDED ROOF MEMBERS

In this chapter a non-linear closed-form static solution and elastic-plastic design method of a large-span suspended member of bending stiffness subjected to a uniformly distributed symmetric and asymmetric load are presented and used for its optimization procedure as well as for its simulation-based reliability assessment. Transformation analytical model serves for determining the response, *i.e.* horizontal component of member axial tension force, bending moment and deflection of the geometrically non-linear suspension member due to the applied permanent and variable action, considering effects of elastic deformations, temperature changes and elastic supports. The results of the optimization and reliability analyses of a large-span suspension member under symmetric and asymmetric load (as the bearing member of a suspension roof structure) in the form of steel rolled I-section as an example are briefly presented. Its geometry and loads are shown in Figure 5.2.

5.3 DESCRIPTION OF ANALYTICAL MODEL

Basic scheme for the static solution of suspended members of bending stiffness with parabolic sag profile defined as $z_0(x) = 4d_0 x/l^2(l-x)$ is shown in Figure 5.3.

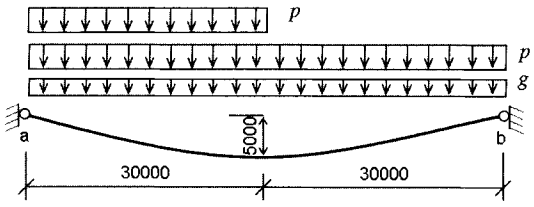

Figure 5.2 Geometry and loading of the investigated suspended member

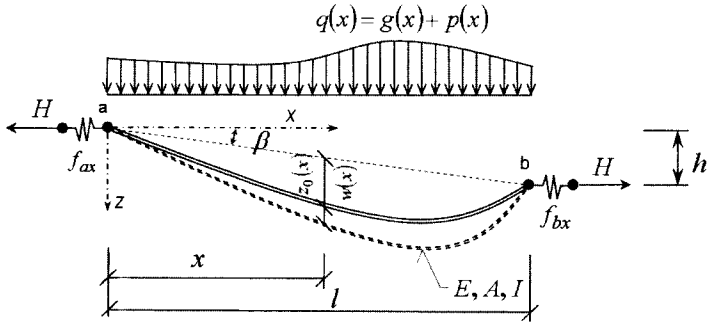

Figure 5.3 Basic scheme, geometry and loading of suspended member of bending stiffness

5.3.1 Symmetric loading

The following cubic equation for vertical deflection w at the middle of the span l of suspended member under a uniformly distributed load $q = g + p$ applied over the entire span of member (symmetric loading) can be used

$$C_1 w^3 + C_2 w^2 + C_3 w - C_4 = 0, \tag{5.1}$$

where

$$C_1 = \frac{4}{15}\frac{cA}{c_L I}, \quad C_2 = \frac{4}{5}\frac{cA}{c_L I} d_0, \tag{5.2}$$

$$C_3 = \frac{8}{15}\frac{cA}{c_L I} d_0^2 + \frac{1}{80}\frac{gl^4}{EId_0} + 1, \tag{5.3}$$

$$C_4 = \frac{1}{80}\frac{pl^4}{EI}. \tag{5.4}$$

Coefficient of supports flexibilities and temperature change is given as

$$c = \frac{\cos^2 \beta}{1 \pm \frac{EA}{ml}\left(f_{ax} + f_{bx} + \frac{\alpha_0 \Delta T l}{H - H_0} \right)}, \tag{5.5}$$

where A is the cross-sectional area of the suspended member, β is the inclination of the connecting line of suspension points of the member with the axis x, f_{ax} and f_{bx} are elastic yieldings of the support a and b in horizontal direction x, respectively. $\alpha_0 \Delta T l = \alpha_0 (T - T_0) l$ is length change due to temperature difference $\Delta T = T - T_0$, where α_0 is the coefficient of expansion. For $\beta = f_{ax} = f_{bx} = \Delta T = 0$ coefficient $c = 1$. Sign plus corresponds to the supports displacements in the direction inside of the member span and to a uniform temperature rise of $\Delta T = T - T_0$. d_0 is the initial mid span sag of the suspended member at the cross section $x = l/2$ under self weight g. It is necessary to note that under this loading only very small bending moments occur and the member behaviour is similar to flexible suspended cable. $g = g_{roof} + A\rho$ and p are the initial permanent (g_{roof} represents weight of covering trapezoidal or membrane sheet, purlins and stiffening elements and $A\rho$ is self weight of suspended member per unit length, ρ is material density) and additional design values of variable action (as snow and wind), respectively.

Coefficient c_L of the member length is

$$c_L = 1 + \frac{16 d_0^2}{3 l^2} + tan^2 \beta \,. \tag{5.6}$$

The horizontal component of member force H is expressed as

$$H = \frac{8}{3} \frac{cEA}{c_L l^2} (2 d_0 + w) w + H_0 \,, \tag{5.7}$$

where the initial horizontal component H_0 of the member axial force under the load g is for $\beta = 0$, given as

$$H_0 = \frac{g l^2}{8 d_0} \,. \tag{5.8}$$

Bending moment M in the middle of the span of the suspended member is

$$M = M_0 - H(d_0 + w) = \frac{1}{8} q l^2 - H(d_0 + w) \,. \tag{5.9}$$

The axial force $T(x)$ in an arbitrary cross section x is given as

$$T(x) = H \sqrt{1 + \left(\frac{V(x)}{H} + tan \beta \right)^2} \,, \tag{5.10}$$

where $V(x)$ is the shear force in cross section x of horizontal simple beam of the same span and load as the suspended member.

5.3.2 Asymmetric loading

The following two equations can be used for the horizontal component of member force H for suspended member under a uniformly distributed variable load p applied over the left half of its span (asymmetric loading) and under a uniformly distributed permanent load g applied over the entire span l of the member.

$$H = \frac{cEA}{2 c_L l} \alpha (\alpha R_1 + R_3) + H_0 \,, \tag{5.11}$$

$$\alpha = \frac{1}{1 + \frac{EI}{H} \frac{R_1}{R_2}} \,. \tag{5.12}$$

where the individual terms are

$$R_1 = \frac{Q_1}{H^2} - \frac{2 S_1}{H} + \phi_1 \,, \tag{5.13}$$

$$R_2 = \frac{Q_2}{H^2} - \frac{2S_2}{H} + \phi_2, \tag{5.14}$$

$$R_3 = \frac{S_1}{H} - \phi_1, \tag{5.15}$$

$$\phi_1 = \int_0^l \left(\frac{dz_0(x)}{dx} \right)^2 dx = \frac{16d_0^2}{3l}, \tag{5.16}$$

$$\phi_2 = \int_0^l z_0^2(x)dx = \frac{8d_0^2}{15} l, \tag{5.17}$$

$$S_1 = \int_0^l q(x)z_0(x)dx = \frac{ld_0}{3}(2g + p), \tag{5.18}$$

$$S_2 = \int_0^l M(x)z_0(x)dx = \frac{l^3 d_0}{30}(2g + p), \tag{5.19}$$

$$Q_1 = \int_0^l V^2(x)dx = \frac{g^2 l^3}{12} \left(1 + \frac{p}{g} + \frac{5}{16} \left(\frac{p}{g} \right)^2 \right), \tag{5.20}$$

$$Q_2 = \int_0^l M^2(x)dx = \frac{g^2 l^5}{120} \left(1 + \frac{p}{g} + \frac{17}{64} \left(\frac{p}{g} \right)^2 \right). \tag{5.21}$$

Eqs. (5.11, 5.12) for H and α should be solved simultaneously by an iterative method. If the horizontal component of member force H is known, deflection $w(x)$ of suspended member is calculated from

$$w(x) = \alpha \left(\frac{M_b(x)}{H} - z_0(x) \right), \tag{5.22}$$

and resultant bending moment is

$$M(x) = M_b(x) - H(z_0(x) + w(x)), \tag{5.23}$$

where $M_b(x)$ is analogous to the bending moment at cross section x of a simple supported beam under the action of a uniformly distributed load $q = g + p$. Maximum values of the deflection $w(x)$ and of the bending moment $M(x)$ are reached in the quarter of the span, consequently at the cross section $x = l/4$ along the span l. For this point the following expressions hold true

$$w(x = l/4) = \alpha \left(\frac{l^2}{32.H} (3.g + 2.p) - \frac{3}{4} d_0 \right), \tag{5.24}$$

$$M(x=l/4)=\frac{l^2}{32}(3g+2p)-H\left(\frac{3}{4}d_0+\alpha\left(\frac{l^2}{32.H}(3.g+2.p)-\frac{3}{4}d_0\right)\right). \quad (5.25)$$

5.4 OPTIMIZATION

In the optimum design procedure a structural version is sought, which fulfils the design constraints and minimizes the objective function of Farkas and Jármai (2003). In the present case a rolled I-section beam is used with constant cross-section, thus, the objective function is the cross-sectional area. The optimum rolled I-section is selected from a series of available British Universal Beam (UB) profiles. The section characteristics are given in tables by Sales program (2007). The design constraints are formulated according to Eurocode3 (2002). Calculations show that the governing load is the asymmetric one, thus the design constraints relate to this load case (Kmet' et al. 2006).

The plastic stress constraint for the beam loaded by tension and bending is given by

$$\frac{H}{Af_{y1}}+\frac{M_{max}}{W_{pl,y}f_{y1}}\le 1, f_{y1}=\frac{f_y}{1.1}, \quad (5.26)$$

where a tension force H is given by Eqs (5.11-5.21 and 5.8), A – cross-sectional area, $W_{pl,y}$ - plastic section modulus, f_y - the yield stress, the maximum bending moment M_{max} can be calculated using Eq (5.25).

The elastic lateral torsional buckling constraint is formulated as

$$\frac{M_{max}}{W_y}-\frac{H}{A}\le \chi_{LT}f_{y1},\ \chi_{LT}=\frac{1}{\phi_{LT}+\sqrt{\phi_{LT}^2-\lambda_{LT}^2}}, \quad (5.27)$$

$$\phi_{LT}=0.5\left[1+0.49(\lambda_{LT}-0.2)+\lambda_{LT}^2\right]\ \lambda_{LT}=\sqrt{\frac{W_y f_y}{M_{cr}}}, \quad (5.28)$$

$$M_{cr}=C_1\frac{\pi^2 EI_y}{L_z^2}\sqrt{\frac{I_\omega}{I_z}+\frac{L_z^2 GI_t}{\pi^2 EI_z}}, C_1=1, \quad (5.29)$$

where W_y is the elastic section modulus, E – elastic modulus, G – shear modulus, I_y and I_z – moments of inertia, I_ω – warping constant, I_t – torsional constant, L_z – distance of lateral braces for the upper flange of the beam.

The deflection constraint is given by

$$w_{max}\le\frac{l}{250}, \quad (5.30)$$

where w_{max} is calculated using Eq (5.24).

5.5 NUMERICAL DATA (Figure 5.2)

$\beta = 0$, $l = 60$ m, $L_z = 3$ m, $d_0 = 5$ m, $f_y = 235$ MPa, $E = 2.1\text{x}10^5$ MPa, $G = 0.81\text{x}10^5$ MPa, intensity of variable load $p = 8.0$ N/mm, intensity of permanent load $g = g_{roof} + \rho A$, $\rho = 7.85\text{x}10^{-5}$ N/mm^3, $g_{roof} = 0.25\text{x}6.0 = 1.50$ N/mm including covering sheet, purlins and stiffening elements with 6 m loading width. The allowable deflection is given as $w_{allow} = 60000/250 = 240$ mm. Table 5.1 gives results for three rolled I-section beams.

Table 5.1 Results for UB457x152x60, 533x210x92 and 610x229x113

	UB457	UB533	UB610
A [mm^2]	7623	**11740**	14390
α	0.2183	**0.2270**	0.2331
$10^{-5}H$ [N]	5.3286	**5.7070**	5.9264
Eq.(5.26)	1.77>1	**0959<1**	0.702<1
Eq.(5.27) [MPa]	288>107	**129<172**	82.9<177
Eq.(5.30) [mm]	209<240	**190<240**	183<240

It can be seen that the profile UB 533x210x92 gives the optimum, since the smaller 457x152x60 does not fulfil the constraints on plastic stress and lateral torsional buckling. The profile of 610x229x113 fulfils all the constraints, but its cross-sectional area is larger.

5.6 PARAMETRIC EVALUATION

We have made several parametric evaluations. First, we changed the length of the suspension member l, up to 120 m (Kmet' et al. 2007).

Table 5.2 Results for UB610x229x113, 686x254x140, 762x267x173

$l = 80$ m	UB610	UB686	UB762
A [mm^2]	14390	**17840**	22040
α	0.38824	**0.29325**	0.22229
$10^{-5}H$ [N]	7.19757	**7.41061**	7.70123
Eq.(5.26)	0.870<1	**0.755<1**	0.606<1
Eq.(5.27) [MPa]	105.18<166.7	**95.27<173.49**	59.72<176.23
Eq.(5.30) [mm]	393.30>320	**305.42<320**	232.69<320

Table 5.3 Results for UB762x267x173, 838x292x194

$l = 100$ m	UB762	UB838
A [mm^2]	22040	**24680**
α	0.41351	**0.34567**
$10^{-5}H$ [N]	12.1351	**12.3894**
Eq.(5.26)	0.790<1	**0.738<1**
Eq.(5.27) [MPa]	75.83<176.27	**73.31<183.24**
Eq.(5.30) [mm]	409.67>400	**349.74<400**

Table 5.2, 5.3 and 5.4 show the results for different cross sections. Numerical data are similar to the previous one, only the value of l is changing from 60 to 80, 100 and 120 m and initial mid span sag $d_0 = 7.5$ m.

Table 5.2, 5.3 and 5.4 shows the optima for different span length, where in most cases the deflection constraint is active. The optimum cross section is signed bold. We have found, that increasing the span length up to 120 m, i.e. 100 % from 60 m, the cross section area has a 243 % increment, having the same initial mid span sag of the suspended member d_0 = 7.5 m. Figure 5.4 shows the effect of the span-length on the beam cross section.

Table 5.4 Results for UB838x292x194, 914x305x224

l = 120 m	UB838	UB914
A [mm^2]	24680	**28560**
α	0.52368	**0.45752**
$10^{-5}H$ [N]	17.9001	**18.5085**
Eq.(5.26)	0.857<1	**0.793<1**
Eq.(5.27) [MPa]	54.55<180.99	**55.45<180.05**
Eq.(5.30) [mm]	518.31>480	**453.57<480**

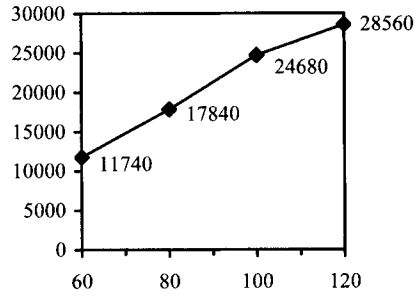

Figure 5.4 The cross section area of the beam (A in mm^2) in the function of span-length (l in m)

Secondly, we changed the value of d_0. d_0 is the initial mid span sag of the suspended member at the cross section $x = l/2$ under self weight g. The interval for the variable sag is as follows:

$$d_0 \in \left\langle \frac{L}{8} \div \frac{L}{12} \right\rangle. \tag{5.31}$$

Consequently, the following quantities for d_0 could be considered

$$d_0 = \frac{l}{8} = \frac{120}{8} = 15{,}0 \text{ m}$$

$$d_0 = \frac{l}{10} = \frac{120}{10} = 12{,}0 \text{ m}$$

$$d_0 = \frac{l}{12} = \frac{120}{12} = 10{,}0 \text{ m}.$$

Table 5.5 shows the results for three different d_0, at l = 120 m.

Table 5.5 shows, that a larger initial mid span sag causes larger deflection and stresses. For the cross section UB 914x305x224 the mid span sag cannot be larger than l /12 for l = 120. Figure 5.5 shows the effect of the mid span sag on the beam deflection.

Table 5.5 Results for UB 914x305x224

l = 120 m	d_0 = 10 m	d_0 = 12 m	d_0 = 15 m
A mm^2	**28560**	28560	28560
α	**0.39082**	0.34972	0.30138
$10^{-5}H$ (N)	**14.0431**	11.7394	9.40067
Eq.(5.26)	**0.743<1**	0.729<1	0.726<1
Eq.(5.27) MPa	**76.98<183.05**	90.97<183.05	107.83<183.05
Eq.(5.30) mm	**476.90<480**	500.62<480	534.20>480

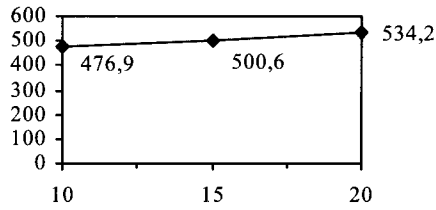

Figure 5.5 The midspan deflection of the beam (w in mm) in the function of mid span sag (d_0 in m)

Further investigations are needed to determine the effect of the β angle, i.e. the difference of the height at the two supports (see Figure 5.3) and to consider the cost of supports on the optimum structure.

5.7 CONCLUSIONS

Suspension members of bending stiffness offer an economical and efficient alternative for many structural problems. In this chapter a non-linear closed-form static solution and elastic-plastic design method (determination of internal forces in the elastic region and utilization of critical section in the plastic range) of a large-span suspended member of bending stiffness subjected to a uniformly distributed symmetric and asymmetric load are presented and used for its optimization procedure.

The transformation of the analytical model serves for determining the response, i.e. horizontal component of member axial tension force, bending moment and deflection of the geometrically non-linear suspension member due to the applied permanent and variable action, considering effects of elastic deformations, temperature changes and elastic supports.

In the optimization process the systematic search determines the optimal rolled I-section beam for a numerical problem, which fulfils the constraints on plastic stress, lateral torsional buckling and deflection for asymmetric load and its cross-sectional area is minimal. Parametric investigations show the effect of span length and the initial mid span sag on the optimum cross section values.

6

Frames

6.1 INTRODUCTION

Framing is mainly used at building industry as a technique based around structural members, which provide a stable frame to which interior and exterior wall coverings are attached, and covered by a roof. Frames are used also at vehicles and machines like punch presses, etc.

A space frame is a truss-like, lightweight rigid structure constructed from interlocking struts in a geometric pattern. Space frames usually utilize a multidirectional span, and are often used to accomplish long spans with few supports. They derive their strength from the inherent rigidity of the triangular frame; flexing loads (bending moments) are transmitted as tension and compression loads along the length of each strut.

Frames are used in automobile construction technology also. Mounting a separate body to a rigid frame which supports the drivetrain was the original method of building automobiles, and its use continues to this day. In the case of vehicles, the term chassis means the frame plus the "running gear" like engine, transmission, etc. A body, which is usually not necessary for integrity of the structure, is built on the chassis to complete the vehicle.

At frame design the calculations of the internal bending moments and forces are more complicated, due to the fact, that the frame is statically undetermined. That is why some finite element calculations are useful (Ross 1998). In our frame examples we show a building frame and a high pressure vessel supporting frame and consider their earthquake and fire resistant design and optimization.

6.2 SIMPLE FRAME WITH WELDED OR BOLTED CORNER JOINTS

Steel frames can be constructed using either welded or bolted connections. Welded joints are rigid, while the behaviour of bolted joints is semi-rigid, since the local displacements of joint components cause an additional angle deformation of corner connections. These angle deformations affect the bending moments, normal and shear forces in frame members and the frame stability. Thus, this effect should be taken into account in the frame optimization as well.

In a previous study (Farkas et al. 2002) we have shown how the economics of structures are influenced by the differences in bending moments and shear forces. The aim of the present study is to investigate these differences in the case of a simple planar sway frame and also to determine the optimum design of the frame in the case of welded as well as bolted connections. This is a relevant issue since single story sway frames constitute the basic buildings units of structures such as warehouses overhead cranes, car ports canopy structures and rollbars for vehicles

The optimum design of frames with semi-rigid joints has been dealt with by several authors e.g. Al-Salloum & Almusallam (1995), Simões (1996), Kameshki & Saka (2003). The difficulty of the optimization is that the additional angle deformation depends on many parameters (such as the type of bolted connection, elongation of bolts and local displacements of plate elements of connected profiles). Thus, the bending moments depend on unknown profile dimensions. To ease the optimization procedure the guess formula for the joint stiffness proposed by Steenhuis et al. (1998) is used here.

Another problem is that available rolled I-section rods have to be used. These present a discrete range of profiles which are listed by manufacturers in tabulated form, e.g. universal beams (UB) and columns (UC) (as given by Sales program 2007). The characteristics of these profiles (cross-sectional area, moments of inertia etc.) depend on main section dimensions and it is difficult to calculate them as simple functions which is what is required for optimisation purposes. For this reason approximate functions determined by curve-fitting selection using only one variable (profile height).

The optimization of a welded as well as a bolted frame is performed using the structural volume as objective function to be minimized, and the costs are calculated and compared to each other. British and South African cost data are used.

6.2.1 Forces and bending moments in the frame

We investigate a one-storey one-bay sway (unbraced) frame shown in Figure 6.1 loaded by a uniformly distributed vertical load of intensity p and a concentrated

horizontal force F. The corner bending moment M_p (Fig. 6.2) is derived from an angle deformation equation as follows.

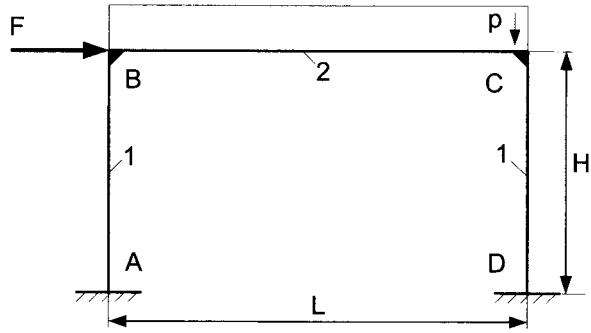

Figure 6.1 Unbraced planar frame

The angle deformation of the beam due to load p (Fig. 6.3) is

$$\varphi_0 = \frac{pL^3}{24EI_2}, \tag{6.1}$$

and due to the bending moments

$$\varphi_1 = \frac{M_p L}{2EI_2}, \tag{6.2}$$

where E is the elastic modulus and I_2 is the moment of inertia of the beam section.

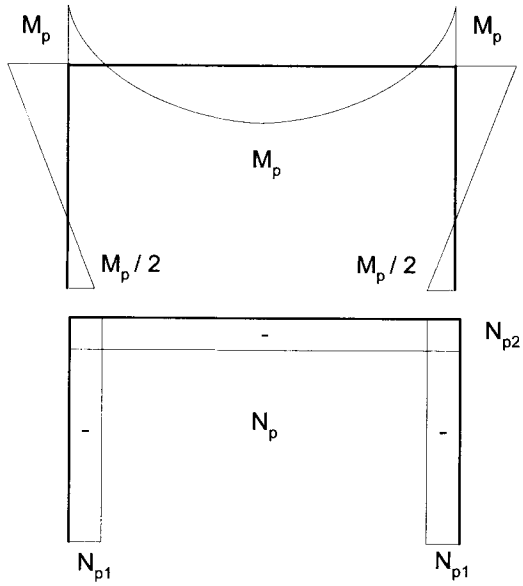

Figure 6.2 Diagrams of bending moments and axial forces

The angle deformation of the column end due to the bending moment M_p and reactive force $N_{p2} = 3M_p/(2H)$ is

$$\varphi_2 = \frac{M_p H}{4EI_1}, \tag{6.3}$$

where I_1 is the moment of inertia of the column section. The angle deformation equation, considering the angle difference caused by the semi-rigid connection of stiffness S_j, is

$$\varphi_0 - \varphi_1 - \varphi_2 = \theta = \frac{M_p}{S_j}. \tag{6.4}$$

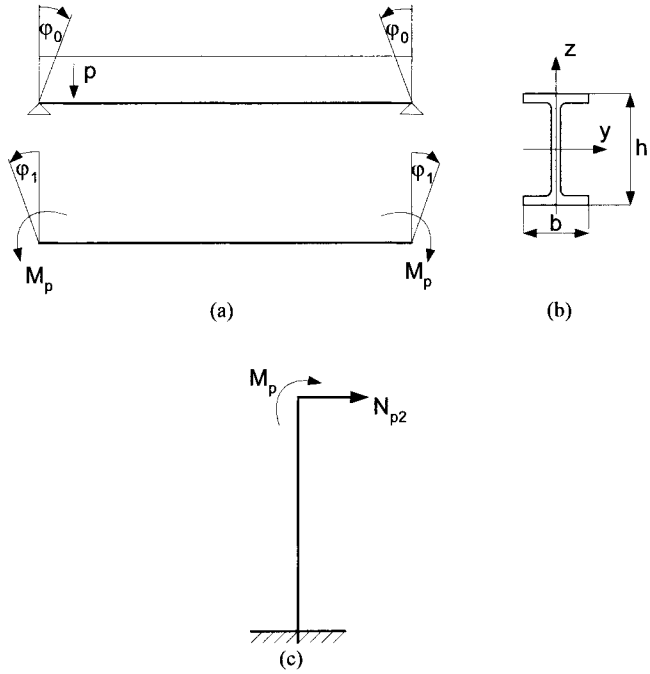

Figure 6.3 (a) Angle deformations of the beam due to uniform normal load. (b) The main dimensions of a rolled I-beam. (c) Bending moment and horizontal force acting on a column

From Eq.(6.4) one obtains

$$M_p = \frac{pL^2}{24} \cdot \frac{1}{\frac{1}{2} + \frac{HI_2}{4LI_1} + \frac{EI_2}{LS_j}}. \tag{6.5}$$

Note that for welded (rigid) joints $S_j \to \infty$ and the third member in the denominator becomes zero.

Similarly, the corner bending moments due to the horizontal force F (Fig. 6.4) can be calculated considering the following angle deformation in the beam due to M_F (Fig. 6.5):

$$\varphi_{MF} = \frac{M_F L}{6EI_2}, \tag{6.6}$$

and the angle deformations of the column top due to $F/2$ and M_F are

$$\frac{FH^2}{4EI_1} - \frac{M_F H}{EI_1}. \tag{6.7}$$

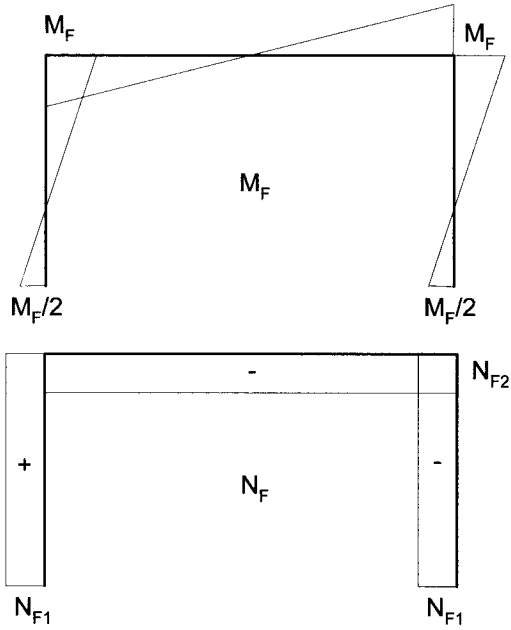

Figure 6.4 Bending moments and axial forces due to the horizontal force F

Considering also the angle difference caused by semi-rigid joints, the angle equation can be expressed as

$$\frac{FH^2}{4EI_1} - \frac{M_F H}{EI_1} = \frac{M_F L}{6EI_2} + \frac{M_F}{S_j}. \tag{6.8}$$

From Eq. (6.8) it follows that

$$M_F = \frac{FH}{4} \cdot \frac{1}{1 + \frac{LI_1}{6HI_2} + \frac{EI_1}{HS_j}}. \tag{6.9}$$

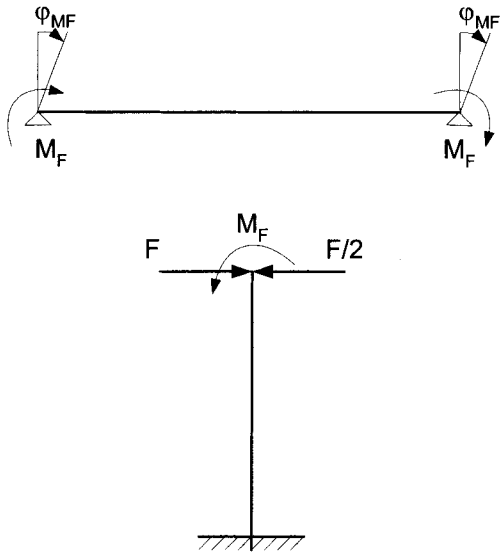

Figure 6.5 Angle deformations of the beam due to horizontal force *F*. Bending moment and horizontal forces acting on the columns in the case of the horizontal load *F*

6.2.2 Design constraints

The columns and the beam are loaded by bending and an axial force. Since rolled I-section rods are used, these should fulfil the constraints on combined bending and compression to avoid overall flexural and torsional buckling as well as lateral-torsional buckling. These stress constraints are formulated according to Eurocode 3 (2005) (EC3), Iványi (1999).

6.2.2.1 *Bending and axial compression constraint of the column CD*

The buckling constraint about the *y*-axis (Fig. 6.3) requires that:

$$\frac{N_1}{\chi_{y1} f_{y1} A_1} + k_{yy1} \frac{M_C}{\chi_{LT1} f_{y1} W_{y1}} \le 1, \tag{6.10}$$

and for buckling about *z*-axis

$$\frac{N_1}{\chi_{z1} f_{y1} A_1} \le 1, \tag{6.11}$$

where $f_{y1} = f_y / \gamma_{M1}; \gamma_{M1} = 1.1$, f_y is the yield stress, γ_{M1} is the partial safety factor.

The compression force is

$$N_1 = \frac{pL}{2} + \frac{2M_F}{L}, \tag{6.12}$$

and the bending moment is calculated as

$$M_C = M_p + M_F. \tag{6.13}$$

The overall buckling factor for the y-axis is

$$\chi_{y1} = \frac{1}{\phi_{y1} + \sqrt{\phi_{y1}^2 - \bar{\lambda}_{y1}^2}}, \tag{6.14}$$

where

$$\phi_{y1} = 0.5[1 + \alpha_{y1}(\bar{\lambda}_{y1} - 0.2) + \bar{\lambda}_{y1}^2], \tag{6.15}$$

$$\alpha_{y1} = 0.21 \quad \text{if} \quad h_1/b_1 > 1.2,$$

$$\alpha_{y1} = 0.34 \quad \text{if} \quad h_1 / b_1 \le 1.2, \tag{6.16}$$

and $$\bar{\lambda}_{y1} = \frac{K_1 H}{r_{y1}\lambda_E}; K_1 = 2; r_{y1} = \sqrt{\frac{I_{y1}}{A_1}}; \lambda_E = \pi\sqrt{\frac{E}{f_y}}. \tag{6.17}$$

According to Steenhuis et al. (1998) the joint stiffness for a bolted joint with a flush end plate and cover plate (Fig.6.6) can be approximated by the following formula

$$S_j = \frac{Ez^2 t_{fc}}{11.5}, \tag{6.18}$$

where t_{fc} is the column flange thickness and z is the arm of the bending forces in the joint, which is approximately equal to the web height, $z = h_1$.

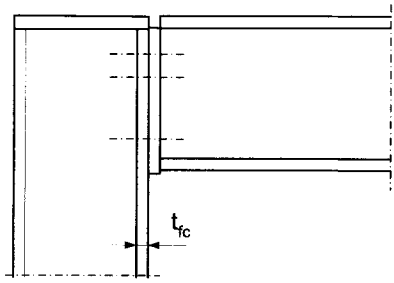

Figure 6.6 Bolted connection with flush-end plate

Furthermore

$$k_{yy1} = 0.9\left(1 + 0.6\bar{\lambda}_{y1}\frac{N_1}{\chi_{y1} f_{y1} A_1}\right). \tag{6.19}$$

The lateral-torsional buckling factor is

$$\chi_{LT1} = \frac{1}{\phi_{LT1} + \sqrt{\phi_{LT1}^2 - \overline{\lambda}_{LT1}^2}}, \tag{6.20}$$

with

$$\phi_{LT1} = 0.5[1 + \alpha_{LT1}(\overline{\lambda}_{LT1} - 0.2) + \overline{\lambda}_{LT1}^2], \tag{6.21}$$

$$\overline{\lambda}_{LT1} = \sqrt{\frac{W_{y1} f_y}{M_{cr1}}}, \tag{6.22}$$

$$M_{cr1} = 11.132\pi^2 E \frac{I_{z1}}{H} \sqrt{\frac{I_{\omega 1}}{I_{z1}} + \frac{H^2 G I_{t1}}{\pi^2 E I_{z1}}}, \tag{6.23}$$

$$\alpha_{LT1} = 0.34 \quad \text{if} \quad h_1 / b_1 \le 2,$$

and $$\alpha_{LT1} = 0.49 \quad \text{if} \quad h_1 / b_1 > 2. \tag{6.24}$$

The overall buckling factor for the z-axis is

$$\chi_{z1} = \frac{1}{\phi_{z1} + \sqrt{\phi_{z1}^2 - \overline{\lambda}_{z1}^2}}, \tag{6.25}$$

with

$$\phi_{z1} = 0.5[1 + \alpha_{z1}(\overline{\lambda}_{z1} - 0.2) + \overline{\lambda}_{z1}^2], \tag{6.26}$$

$$\overline{\lambda}_{z1} = \frac{K_1 H}{r_{z1} \lambda_E}; K_1 = 2; r_{z1} = \sqrt{\frac{I_{z1}}{A_1}}, \tag{6.27}$$

$$\alpha_{z1} = 0.34 \quad \text{if} \quad h_1 / b_1 > 1.2,$$

and $$\alpha_{z1} = 0.49 \quad \text{if} \quad h_1 / b_1 \le 1.2. \tag{6.28}$$

The calculations have shown that the torsional buckling constraint is passive.

6.2.2.2 *Bending and axial compression constraint of the beam BC*

Similar to Eqs (6.10) and (6.11) the stress constraints are as follows

$$\frac{N_2}{\chi_{y2} f_{y1} A_2} + k_{yy2} \frac{M_C}{\chi_{LT2} f_{y1} W_{y2}} \le 1, \tag{6.29}$$

and

$$\frac{N_2}{\chi_{z2} f_{y1} A_2} \le 1. \tag{6.30}$$

The other formulae are similar to those given in Section 6.2.2.1, but with subscript 2 except the following:

$$K_2 = 1.3, \tag{6.31}$$

and

$$N_2 = \frac{F}{2} + \frac{3M_p}{2H}. \tag{6.32}$$

In the above formulae the following geometric section characteristics have to be calculated:

A - cross-sectional area

I_y, I_z - moments of inertia about the y and z axis, respectively

W_y - section modulus about the y axis

r_y and r_z - radii of gyration about the y and z axis, respectively

I_t - torsional constant

I_ω - warping constant

Also the values of t_{fs} and z should be given (Eq. 6.18).

Table 6.1 Heights and cross-sectional areas of selected UB profiles according to Sales program (2007)

UB profile	h [mm]	A [mm^2]
152x89x16	152.4	2032
178x102x19	177.8	2426
203z133x25	203.2	3197
254x146x31	251.4	3968
254x146x37	256.0	4717
305x165x46.1	306.6	5875
356x171x57	358.0	7256
406x178x74	409.4	8554
457x191x74	457.0	9463
457x191x82	460.0	10450
610x229x113	607.6	14390
686x254x140	683.5	17840
838x292x194	840.7	24680

These values are given in tabulated form for available UB and UC sections of a company (Sales program 2007). To ease the calculations, approximate functions expressing the above characteristics as a function of section height h have been used.

To illustrate these approximate functions, the selected UB profiles are given in Table 6.1 with their heights and cross-sectional areas. These cross-sectional areas can be approximated by the following curve-fitting function

$$A = -489.58486 + 14.366815h + 0.01824055h^2 \quad (A \text{ in mm}^2,\ h \text{ in mm}) \qquad (6.33)$$

For instance, for UB 305x165x46.1 with h = 306.6 mm Eq.(6.33) gives A = 5629.96 mm^2 instead of the actual value of 5875 mm^2.

6.2.3 Optimization characteristics and results

The objective function to be minimized is the structural volume

$$V = 2A_1H + A_2L\,, \qquad (6.34)$$

The unknown variables are the heights of column and beam rolled I-sections h_1 and h_2.

Rosenbrock's Hillclimb algorithm has been applied to find the optimum column and beam profiles, which minimize the volume (weight) and fulfil the design constraints.

6.2.4 Cost calculation for frames with welded and bolted joints

The optimum design results in the following optimal British profiles:

Bolted version: columns UC203x203x71

beam UB356x171x51

Welded version: columns UC203x203x86

beam UB356x171x67

Costs of the frame with bolted connections:

Material cost: UB 356x171x51 20 Ł/m = 28.6 $/m, length L = 7.62 m, ... 217.9 $

UC 203x203x71 27 Ł/m = 38.6 $/m, length 2H= 7.32 m .... 282.6 $

material cost of bolts (100 bolts cost is 32.-Ł) 16 bolts 0.32x16 = 5 Ł = 7.3 $

total material cost 507.8 $

Manufacturing costs: cutting of the beam ends (main) 24 Ł = 34.3 $

Preparation (assembly) cost is calculated similarly than in the case of welded joint, with the same formula as follows

$$K_{F1} = k_F\Theta\sqrt{\kappa\rho V} = 0.6x2\sqrt{3x908.34} = 62.6\$,$$

since the total mass is 51x7.62 + 71x7.32 = 908.34 kg.

The cost of the bolted connection of medium type (endplate 25 mm thick, 200 mm wide, 410 mm deep, holing, welding to the end plate with fillet welds of leg size min 6 max 12 mm around the profile) is 81 Ł = 115.8 $

Total manufacturing costs 212.7 $

Material and manufacturing together 720.5 $

Costs of the frame with welded connections:

Material cost: UB 356x171x67 26 Ł/m = 37.2 $/m, L = 7.62 m, 283.3 $

UC 203x203x86 32 Ł/m = 45.8 $/m. 2H= 7.32 m 335.0 $

Manufacturing costs: cutting of the beam ends (main) 26 Ł = 37.2 $

welding $K_W = k_F\left(\Theta_d\sqrt{\kappa\rho V} + 1.3\sum_i \alpha_{Pi} C_{Wi} a_{Wi}^n L_{Wi}\right)$,

$$\rho V = 7.62x67.1 + 2x3.66x86.1 = 1141.6 \text{ kg/m}$$

parts of the second member:

flanges $1.3x0.5214x10^{-3}x15.7^2x2x173.2 =$ 57.9 min

web $1.3x2x0.5214x10^{-3}x9.1^2x311.6 =$ 35.0 min

flange backing $1.3x3x0.7889x10^{-3}x4^2x2x173.2 =$ 17.0 min

web backing $1.3x2x0.7889x10^{-3}x4^2x311.6 =$ 10.2 min

total 120.1 min

$$K_W = 0.6\left(2\sqrt{3x1141.6} + 120.1\right) = 142.3\$,$$

total manufacturing cost 179.5 $

Material and manufacturing together 797.8 $

The calculations show that the bolted unbraced simple planar frame is 10.7% cheaper than the welded one in the case of British cost data.

6.3 OPTIMUM SEISMIC DESIGN OF A MULTI-STOREY FRAME

An interior three storey frame structure with a column and 4 beams in each floor is investigated. The vertical and horizontal (seismic) forces, normal forces and bending moments as well as elastic interstorey drifts are calculated. Chapter 3 deals with the seismic design rules according to EC8. The welded box columns and rolled I-section beams are designed for minimum weight and cost. The beam-to-column connections are selected from a number of structural versions improved for seismic resistance. The fabrication costs are calculated in details. Design constraints relate to interstorey drifts and to stability of column parts and beams loaded by compression and bending. Calculations show that, after a connection type is selected, the fabrication cost has little effect on the optimum design, since it varies proportionally with the mass according to the present calculating method. Thus, the minimum weight design gives suitable results.

6.3.1 Problem formulation

In order to study the effect of seismic loads, a relatively simple frame is selected as shown in Figure 6.7. This is a simplified model of a central part of a three-storey building frame structure. The frame is unbraced and horizontal displacements can occur due to horizontal seismic forces. The column parts are constructed from welded square box section and the beams have a rolled universal beam (UB) profile. The frame is subject to vertical permanent and live loads as well as to horizontal seismic forces (Figures 6.7, 6.8 and 6.11). In the fishbone model the beam ends are considered to be built up for vertical loads and pinned for horizontal ones. The problem is to find suitable column and beam profiles, which fulfil the design constraints and minimize the objective function. The beams and column parts are subject to bending and compression, thus, stress constraints should be formulated for 3 beam and 3 column profiles according to Eurocode 3 (2005) (EC3). The economy of frames with semi-rigid connections was studied by Weynand et al (1998).

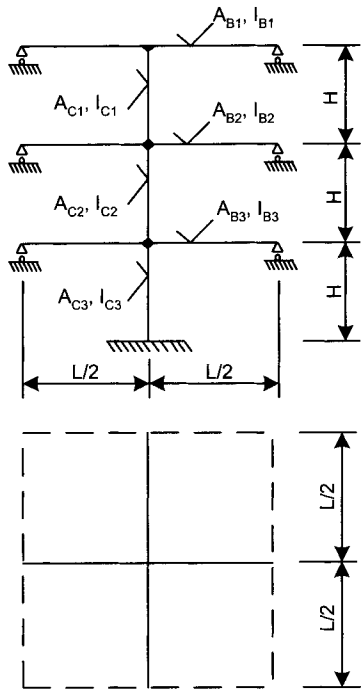

Figure 6.7 The investigated frame under horizontal loads consisting of a column and 4 beams in each storey. The frame is a central part of a building as it is seen in the top view

The seismic forces and interstorey drifts are calculated according to Eurocode 8 (1998, 2004) (EC8). Constraints on interstorey drifts are also formulated. The calculation of drifts and stability are based on the linear elastic behaviour of the structure. This is the most popular method of analysis recommended in Eurocode 8. However, the structure and the parts of it have to meet the ductility requirements inherent to the behaviour factor adopted. One of the important requirements is the

overstrength requirements for beam-to-column connections: the plastic strength of the connections should be large enough to allow formation of plastic hinges at the beam ends. The connection design was determined on the basis of the plastic analysis and experimental evidences.

6.3.2 Calculation of vertical loads

We use a slightly modified data of Design (1995) in which the seismic-resistant design of a 5-storey residential building frame is detailed.

Permanent load for roof including the structure self weight is $q_1 = 5.5$ kN/m^2.

Permanent load for floors is q_2=q_3 = 5.0 kN/m^2.

Live load for roof and floors is 2.0 kN/m^2.

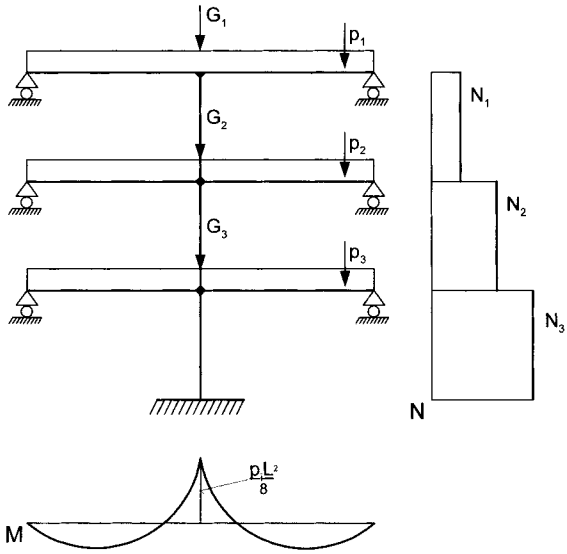

Figure 6.8 Vertical loads acting on the frame and the diagrams of bending moments (M) and axial forces (N)

According to EC8 the combination of seismic action with other actions should be performed in the following way:

$$\sum G_k + \gamma_I A_E + \sum \psi Q_k \,, \tag{6.35}$$

where G_k are the permanent actions, A_E is the earthquake action, Q_k are the variable (live) actions and $\psi = \varphi\psi_{21}$ is the combination coefficient, where for each storey

$\psi_{21} = 0.3$, for top storey (roof) $\varphi = 1$ and for other storeys $\varphi = 0.5$. For the combination of vertical and seismic load actions the EC8 rule is used, in which the importance factor for ordinary buildings not belonging to the other categories (EC8 Table 4.3) is $\gamma_I = 1$ (Class II) (see also Session 3.3.2 in this book).

Combined vertical loads for beams (we consider, that beams are in two directions)

Roof: $p_1 = (q_1 + 0.3\text{x}2.0)L/2,$ (6.36)

Other storeys $p_2 = p_3 = (q_2 + 0.15\text{x}2.0)L/2.$ (6.37)

Combined vertical loads for column parts:

Top: $G_1 = (q_1 + 0.3\text{x}2.0)\text{x}L^2.$ (6.38)

Other storeys $G_2 = G_3 = (q_2 + 0.3\text{x}2.0)\text{x}L^2.$ (6.39)

These vertical loads and the corresponding M (bending moment) and N (compression force) diagrams are given as follows:

$$N_1 = G_1,\ N_2 = G_1 + G_2, N_3 = G_1 + G_2 + G_3\,, \tag{6.40}$$

$$M_1 = p_1L^2/12, M_2 = M_3 = p_2L^2/12. \tag{6.41}$$

6.3.3 Calculation of horizontal seismic forces

According to EC8 the seismic base shear force is

$$F_b = S_d(T_1)m\lambda\,, \tag{6.42}$$

where m is the total mass of the building,

λ is the correction factor, which is equal to 0.85 since $T_1 < 2T_C$ (see below)

$$T_1 = C_tH_0^{0.75}, \tag{6.43}$$

the height of the building is $H_0 = 3H$. If H=3.6 m then H_0= 10.8 m. For moment resistant space steel frame C_t = 0.085, thus T_1 = $0.085xH_0^{0.75}$ If H_0=10.8 then T_1=0.5064 s. for this time the following formula is valid

$$S_d = \alpha S\beta_0 / q \tag{6.44}$$

For subsoil class C (Table 3.1 of EC8) (see also Table 3.1 in this book) S = 1.15, $\beta_0 = 2.5$, $T_B = 0.2$, $T_C = 0.60$, $T_D = 2.0$. For the most dangerous Japanese zones α = 0.4.

The behaviour factor q (EC8 Table 6.2, Figure 6.7) (see also Session 3.4.1 in this book) for moment resistant, unbraced multistorey buildings is q = 1.3x5 = 6.5, thus, S_d = 1.15x0.4x2.5/6.5 = 0.1769.

Horizontal shear forces for the floors are as follows $F_i = F_b \dfrac{z_im_i}{\sum_i z_im_i}$ (i = 1,2,3), since the fundamental mode shape is approximated by horizontal displacements increasing linearly along the height.

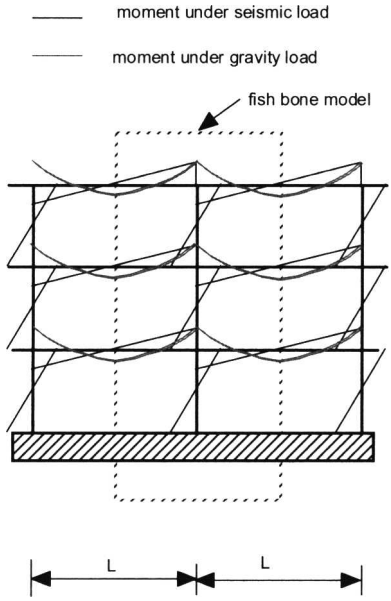

Figure 6.9 Vertical and seismic loads acting on the frame and the diagrams of bending moments

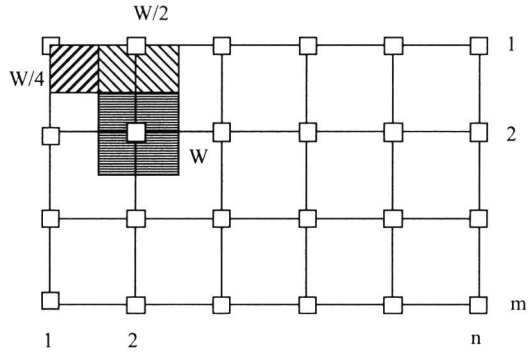

Figure 6.10 Plan view of a building with m by n columns

For the top floor it is $i = 1, z_1 = 3\text{x}3.5, m_1 = G_1$,

For the 2nd floor it is $i = 2, z_2 = 2\text{x}3.5, m_2 = G_2$,

and for first floor it is $i = 3, z_3 = 1\text{x}3.5, m_3 = G_3$.

It should be noted that the columns in a building are interior or exterior ones. A simple calculation shows how much horizontal load a column has to support. Even in a big building of m bays by n bays, each column has to support the load of about 25-100 percent of that of total column force (Figure 6.10, Table 6.2).

A plan view of a building with m by n columns. All the spans have equal length.

The number of columns:

Fully loaded columns = $(m\text{-}2)(n\text{-}2)$,

1/2 loaded columns = $2(m\text{-}2)+2(n\text{-}2)$,

1/4 loaded columns = 4.

The total weight the columns are carrying, ΣW: $\Sigma W = W(m\text{-}2)(n\text{-}2) + W(m\text{-}2) + W(n\text{-}2) + W$

The average weight, each column carrying is W (in case that interior and exterior columns have the same stiffness):

Table 6.2 Average weight each column is carrying for horizontal shear force calculation

m	n	W	m	n	W	m	n	W
2	2	0.25	3	4	0.50	4	7	0.64
2	3	0.33	3	5	0.53	5	5	0.64
2	4	0.38	3	6	0.56	5	6	0.67
2	5	0.40	3	7	0.57	5	7	0.69
2	6	0.42	4	4	0.56	6	6	0.69
2	7	0.43	4	5	0.60	6	7	0.71
3	3	0.44	4	6	0.63	7	7	0.73

$$W = \frac{mn - m - n + 1}{mn}. \tag{6.45}$$

Horizontal shear forces F_i should be multiplied by w. So $F_i = wF_i$ $(i = 1,2,3)$.
The horizontal seismic shear forces are acting on the floors as it is shown in Figure 6.10. Since the structure is statically indeterminate, in order to determine the inner forces due to these horizontal forces, an approximate method can be used. In Design (1995) the method of Ifrim (1984) is used based on the localization of inflection points (Figure 6.11). For the top floor $\alpha_1 = 0.65$, for the middle floors $\alpha_2 = 0.5$ and for bottom part of the column $\alpha_3 = 0.4$.

Using this method, the frame can be divided into 4 parts as shown in Figure 6.11. The vertical reactive forces due to the horizontal seismic forces are as follows:

$$V_1 = 0.65HF_1/L, \quad V_2 = H(0.85F_1 + 0.5F_2)/L, \tag{6.46}$$

$$V_3 = H[0.9(F_1+F_2) + 0.4F_3]/L. \tag{6.47}$$

6.3.4 Bending moments and axial forces

The bending moment and axial forces acting on beams and column parts, together with the inner forces due to vertical loads are as follows:

Beams:

$$M_{B1} = V_1L/2 + p_1L^2/12, \; M_{B2} = V_2L/2 + p_2L^2/12, \; M_{B3} = V_3L/2 + p_3L^2/12, \tag{6.48}$$

$N_{B1} = F_1, N_{B2} = F_2, N_{B3} = F_3$,

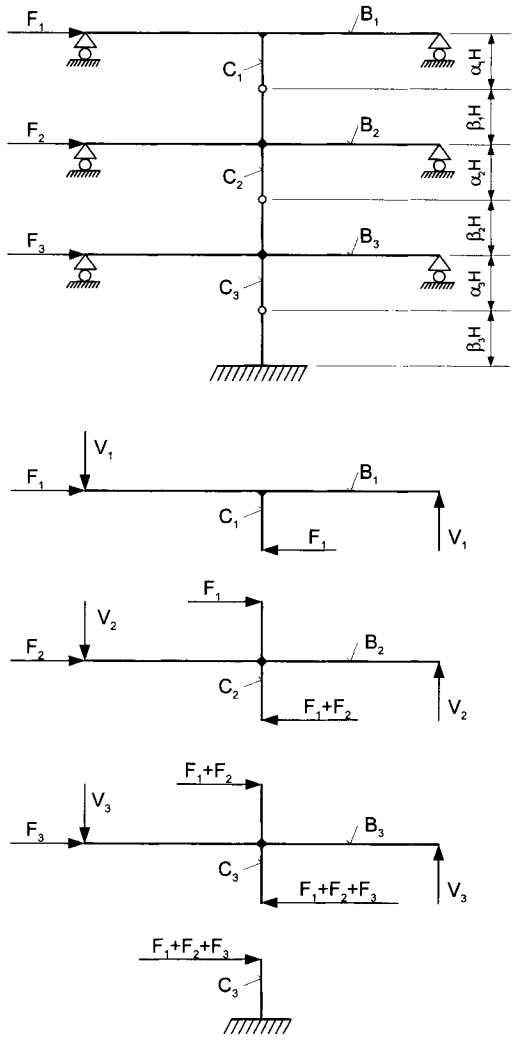

Figure 6.11 Horizontal seismic forces. The frame is divided to 4 parts by considering inflection points on the column parts

Column parts:

$$M_{C1} = 0.65HF_1,\ M_{C2} = 0.5H(F_1 + F_2),\ M_{C3} = 0.6H(F_1+F_2+F_3), \tag{6.49}$$

$$N_{C1} = N_1,\ N_{C2} = N_2,\ N_{C3} = N_3.$$

6.3.5 Calculation and constraints on interstorey drifts

Figure 6.12 shows the structural part B2. The horizontal forces acting on column parts cause a bending moment M. The angle φ due to the bending moment can be calculated using the bending moment diagram M.

$$EI_{B2}\varphi = -\frac{ML}{24} + \frac{ML}{8} = \frac{ML}{12}, \tag{6.50}$$

and the horizontal displacement from this angle is

$$d' = \beta_1 H\varphi = \beta_1 H \frac{ML}{12EI_{B2}}, \tag{6.51}$$

and from the force F_1

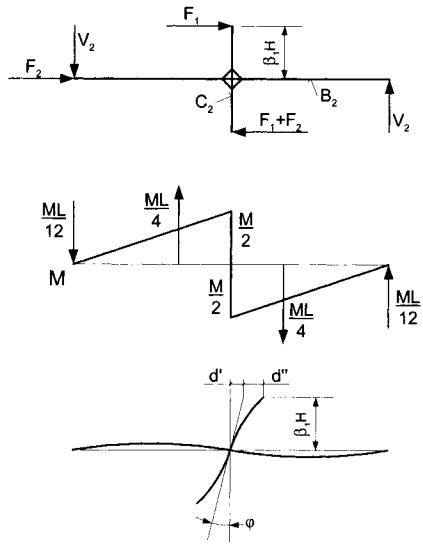

Figure 6.12 Elastic deformations of the second frame part due to bending moments. The beam deformation causes a horizontal displacement d' and the deformation of a column part causes a displacement d''

$$d'' = \frac{F_1(\beta_1 H)^3}{3EI_{C1}}. \tag{6.52}$$

Figure 6.13 illustrates the elastic deformations of the structural parts. The displacements are as follows:

$$d_1 = \frac{(F_1 + F_2 + F_3)(\beta_3 H)^3}{3EI_{C3}}, \tag{6.53}$$

$$d_2 = \frac{\alpha_3 H M_3 L}{12EI_{B3}}, \qquad M_3 = \alpha_3 H F_3 + (\alpha_3 + \beta_2) H (F_1 + F_2), \tag{6.54}$$

$$d_3 = \frac{(F_1 + F_2 + F_3)(\alpha_3 H)^3}{3EI_{C3}}, \tag{6.55}$$

$$d_4 = \frac{\beta_2 H M_3 L}{12EI_{B3}}, \tag{6.56}$$

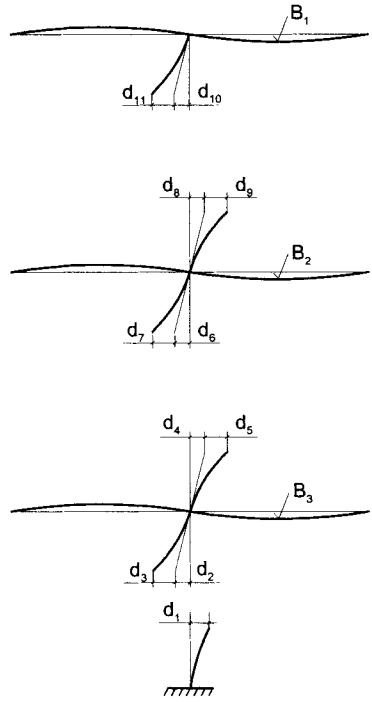

Figure 6.13 Horizontal displacements of the frame parts for the calculation of interstorey drifts

$$d_5 = \frac{(F_1 + F_2)(\beta_2 H)^3}{3EI_{C2}} = d_7, \tag{6.57}$$

$$d_6 = \frac{\alpha_2 H M_2 L}{12EI_{B2}}, \qquad M_2 = (\alpha_2 + \beta_1) H F_1 + \alpha_2 H F_2, \tag{6.58}$$

$$d_8 = \frac{\beta_1 H M_2 L}{12EI_{B2}}, \tag{6.59}$$

$$d_9 = \frac{F_1(\beta_1 H)^3}{3EI_{C1}}, \tag{6.60}$$

$$d_{10} = \frac{(\alpha_1 H)^2 F_1 L}{12EI_{B1}}, \tag{6.61}$$

$$d_{11} = \frac{F_1(\alpha_1 H)^3}{3EI_{C1}}. \tag{6.62}$$

For the interstorey drift constraint the prescription of EC8 is used. The limiting drift is given as

$$d_r \nu \le 0.01H, \tag{6.63}$$

$$d_r = q\gamma_I d_e. \tag{6.64}$$

The reduction factor for the importance category of III (EC8 2003) is $\nu = 0.4$, furthermore q = 6.5, γ_I = 1.0. The constraint on interstorey drift calculated above

$$d_{ei} \le \frac{0.01H}{q\nu} = 13.846 \text{ mm}. \tag{6.65}$$

It should be noted, that Eurocode 8 (1998) was unrealistically stringent on the storey drift limitation, Japanese rules are not so strict, but the new Final Draft of the EC 8 (2004) has similar limit to the Japanese rule.

Using the above derived displacements the interstorey drift constraints can be formulated as follows:

$$d_{e1} = (d_1 + d_2 + d_3) \le 13.846 \text{ mm}, \tag{6.66}$$

$$d_{e2} = (d_4 + d_5 + d_6 + d_7) \le 13.846 \text{ mm}, \tag{6.67}$$

$$d_{e3} = (d_8 + d_9 + d_{10} + d_{11}) \le 13.846 \text{ mm}. \tag{6.68}$$

6.3.6 Stress constraints for beams and column parts

According to EC3, for simplicity, verifications may be performed in the elastic range only. The buckling formulae use a number of factors, e.g. for the buckling length, the uniform moment factor, the critical buckling moment etc., which may vary with the stiffness conditions and moment diagrams. In the optimization fixed factors are used, which can only be approximations in general cases.

6.3.6.1 *Stress constraints for welded box column parts*

$$\frac{N_C}{\chi_{yC} A_C f_{yl}} + 2k_{yy} \frac{M_C}{W_{yC} f_{yl}} \le 1. \tag{6.69}$$

The bending moment is doubled due to the biaxial bending.

$$f_{yl} = f_y / \gamma_{M1} = f_y / 1.1,$$

$$\chi_{yC} = \frac{1}{\phi_{yC} + \sqrt{\phi_{yC}^2 - \bar{\lambda}_{yC}^2}}, \tag{6.70}$$

$$\phi_{yC} = 0.5\left[1 + \alpha_C\left(\bar{\lambda}_{yC} - 0.2\right) + \bar{\lambda}_{yC}^2\right], \tag{6.71}$$

$\alpha_C = 0.34$ for a welded box section.

$$\bar{\lambda}_{yC} = \frac{2K_{yC}H}{r_{yC}\lambda_E}; \quad \lambda_E = \pi\sqrt{\frac{E}{f_y}}; \quad r_{yC} = \sqrt{\frac{I_{yC}}{A_C}}. \tag{6.72}$$

The values of $K_{yC}H$ if H=3600 mm are 2160, 1800 and 2340 mm for bottom, middle and top column part, respectively. In Eq.(6.72) the factor 2 expresses that frame is a sway system.

For the calculation of k_{yy} the Method 2 is used:

$$k_{yy} = C_{myC}\left(1 + 0.6\bar{\lambda}_{yC}\frac{N}{\chi_{yC} A_C f_{yl}}\right) \le C_{myC}\left(1 + 0.6\frac{N}{\chi_{yC} A_C f_{yl}}\right), \tag{6.73}$$

C_{myC} =0.9.

Welded box column parts should be used. For this profile the following formulae are valid:

$$A = 4(b-t)t; I_y = I_z = \frac{2}{3}(b-t)^3 t; \tag{6.74}$$

$$r_y = r_z = \frac{b-t}{\sqrt{6}}; W_y = W_z = \frac{4}{3}(b-t)^2 t. \tag{6.75}$$

In the optimum design process the cross-sectional areas of column parts A_{ci} are selected as unknowns and the cross-sectional characteristics are expressed by A_{ci} as follows

$$I_{yCi} = \frac{A_{Ci}^2}{24\delta}; W_{yCi} = \frac{4\delta}{3}\left(\frac{A_{Ci}}{2\delta}\right)^{3/2}, \tag{6.76}$$

where δ is the limit slenderness for the flange.

Knowing A_{ci} the dimensions are the following:

$$b-t=\sqrt{\frac{A_C}{4\delta}};t=\delta(b-t)\cdot \tag{6.77}$$

6.3.6.2 *Stress constraints for beams of UB profile (I beam)*

For Universal Beam (UB) I profiles approximate formulae are determined on the basis of tabulated values of available sections (Sales program 2005). In order to

calculate with continuous values the geometric characteristics of an UB section (I_y, b_b, t_f) are approximated by curve-fitting functions as follows: h approximately equals to the first number of the profile name (Table Curve 2D 2003). The high number of decimals has been considered due to the necessary precision. During the optimization these functions are called many times and the errors can accumulate.

$$A_s = 1155.684135 + 0.034090823\ h^2, \tag{6.78}$$

$$t_f = \sqrt{33.2053380\ 8 + 0.00067012\ 88\ h^2}\ , \tag{6.79}$$

$$I_y = \exp\left(35.7363618\ 2 - \frac{156.073516\ 89}{\ln(h)}\right)10^4, \tag{6.80}$$

$$b_b = \sqrt{5851.784768098 + 0.01671843845h^2\ln(h)}\ , \tag{6.81}$$

$$t_w = \sqrt{15.62577015376 + 4.358946969\text{x}10^{-5}h^2\ln(h)}\ , \tag{6.82}$$

$$I_{zb} = exp\left(14.4133364305 - \frac{153.67541403}{\sqrt{h_b}}\right)10^4, \tag{6.83}$$

$$I_{tb} = exp\left(11.623190979 - \frac{168.5142170407}{\sqrt{h_b}}\right)10^4, \tag{6.84}$$

$$I_{\omega b} = \left(-11.8600732979 + 2.8355685391\text{x}10^{-5}h_b^2\ ln(h_b)\right)^2 10^9, \tag{6.85}$$

$$W_{yb} = exp\left(25.3497083394 - \frac{111.32333718}{ln(h_b)}\right)10^3, \tag{6.86}$$

$$W_{zb} = \left(-2.7526203118234 + h_b 0.0329915015\right)^2 10^3, \tag{6.87}$$

$$\frac{N_B}{\chi_{yB}A_B f_{yl}} + k_{yyB}\frac{M_B}{\chi_{LT}W_{yB}f_{yl}} \le 1, \tag{6.88}$$

$$\frac{N_B}{\chi_{zB} A_B f_{y1}} + k_{zy} \frac{M_B}{\chi_{LT} W_{yB} f_{y1}} \leq 1, \tag{6.89}$$

$$\chi_{yB} = \frac{1}{\phi_{yB} + \sqrt{\phi_{yB}^2 - \bar{\lambda}_{yB}^2}}, \tag{6.90}$$

$$\phi_{yB} = 0.5\left[1 + \alpha_{yB}\left(\bar{\lambda}_{yB} - 0.2\right) + \bar{\lambda}_{yB}^2\right]; \alpha_{yB} = 0.21, \tag{6.91}$$

$$\bar{\lambda}_{yB} = \frac{K_{yB} L}{r_{yB} \lambda_E}; K_{yB} = 1; r_{yB} = \sqrt{\frac{I_{yB}}{A_B}}, \tag{6.92}$$

$$k_{yyB} = C_{myB}\left(1 + 0.6\bar{\lambda}_{yB} \frac{N_B}{\chi_{yB} A_B f_{y1}}\right) \leq C_{myB}\left(1 + 0.6\frac{N_B}{\chi_{yB} A_B f_{y1}}\right), \tag{6.93}$$

$$\chi_{zB} = \frac{1}{\phi_{zB} + \sqrt{\phi_{zB}^2 - \bar{\lambda}_{zB}^2}}, \tag{6.94}$$

$$\bar{\lambda}_{zB} = \frac{K_{zB} L}{r_{zB} \lambda_E}; K_{zB} = 0.8; r_{zB} = \sqrt{\frac{I_{zB}}{A_B}}; \tag{6.95}$$

$$k_{zB} = \left(1 - \frac{0.05\bar{\lambda}_{zB}}{C_{mLT} - 0.25} \frac{N_B}{\chi_{zB} A_B f_{y1}}\right) \geq \left(1 - \frac{0.05}{C_{mLT} - 0.25} \frac{N_B}{\chi_{zB} A_B f_{y1}}\right), \tag{6.96}$$

$C_{myB} = C_{mLT} = 0.5$.

$$\chi_{LT} = \frac{1}{\phi_{LT} + \sqrt{\phi_{LT}^2 - \bar{\lambda}_{LT}^2}}, \tag{6.97}$$

$$\phi_{LT} = 0.5\left[1 + \alpha_{LT}\left(\bar{\lambda}_{LT} - 0.2\right) + \bar{\lambda}_{LT}^2\right]; \alpha_{LT} = 0.49, \tag{6.98}$$

$$\bar{\lambda}_{LT} = \sqrt{\frac{W_{yB} f_{y1}}{M_{cr}}}, \tag{6.99}$$

$$M_{cr} = C_1 \frac{\pi^2 E I_{zB}}{L^2} \sqrt{\frac{I_{\omega B}}{I_{zB}} + \frac{L^2 G I_{tB}}{\pi^2 E I_{zB}}}; C_1 = 4.0, \tag{6.100}$$

$E = 2.1x10^5; G = 0.81x10^5$ MPa.

6.3.6.3 *Shear check of cross sections at beam ends*

Additional checking for shear can be made using the following formulae according to Eurocode 3 Chapter 6.2.6.

$$\tau_{Bi} = \frac{V_i}{h_{vi} t_{vi}} \leq \frac{f_y}{\gamma_{M1}\sqrt{3}}; \qquad (i = 1,2,3), \tag{6.101}$$

where

$$V_i = V_{pi} + V_{hi}; \tag{6.102}$$

$$V_1 = \frac{p_1 L}{2} + \frac{0.65 H F_1}{L}; \tag{6.103}$$

$$V_2 = \frac{p_2 L}{2} + \frac{H(0.85F_1 + 0.5F_2)}{L}; \tag{6.104}$$

$$V_3 = \frac{p_3 L}{2} + \frac{H[0.9(F_1 + F_2) + 0.4F_3]}{L}. \tag{6.105}$$

6.3.6.4 *Local buckling constraint for welded box column profiles*

According to EC3 (2002):

$$b_i / t_i \leq 33\varepsilon; \varepsilon = \sqrt{235 / f_y}\ , \ \delta = 1/33. \tag{6.106}$$

6.3.7 Beam-to-column connections

A lot of connections have been investigated, tested and evaluated by the research team of Kurobane (Kurobane et al. 1997, Kurobane 1998, Kurobane et al. 2001, Kurobane et al. 2004, Azuma et al. 2000, Miura et al. 2002, Obukuro et al. 2002).

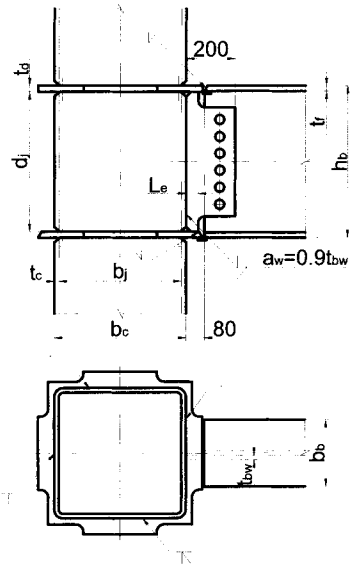

Figure 6.14 A beam-to-column connection improved for seismic resistance

From the improved connections four types have been selected and their cost has been analyzed by Shinde (2004), Shinde et al. (2003). The cheapest one is shown in Figure 6.14.

Details of the connections in Figures 6.14, 6.15 and 6.16 assume square hollow section columns. The improved field-welded connection in Figure 6.14 is constructed from two through diaphragms and a shear tab welded to the column flange by fillet welds and to the diaphragms by fillet welds of length L_e. The beam flanges are field welded to the diaphragms by butt welds with backing bars. One row of bolts connects the shear tab to the beam web.

Figures 6.14, 6.15 and 6.16 show three different connection versions each improved for seismic resistance. The versions of Figures 6.15 and 6.16 use a field-bolted beam splice and a short stub beam instead of a shear tab in the version of Figure 6.14. The version of Figure 6.15 does not use through diaphragms between the column parts but uses two internal diaphragms, so the cutting planes of a column are reduced from two to one. In this case the column widths of the two column parts had better be equal. Welding of through-diaphragms is made in shop using single-bevel PJP (partially joint penetration) welds.

It is clear without any detailed cost calculations that the version in Figure 6.14 is the cheapest. The version shown in Figure 6.15 uses many bolt holes, thus, its cost is higher because of the higher cost of drilling bolt holes. The welding costs of all the three versions are approximately the same. The version of Figure 6.16 needs the same bolt holes drilling cost as that for the version of Figure 6.15. Thus, according

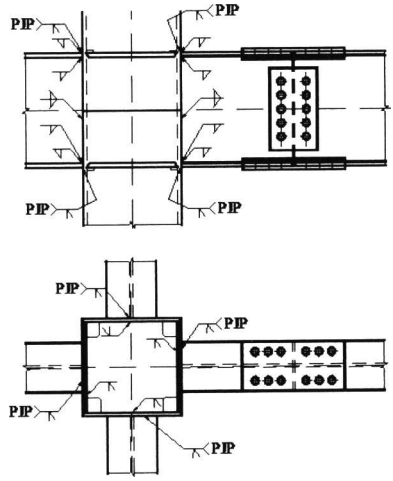

Figure 6.15 Another beam-to-column connection improved for seismic resistance

to this approximate cost comparison, the cheapest version of Figure 6.14 is selected in the present study for detailed cost calculations.

6.3.8 The connection strength

The strength of the connection is calculated by the following formulae (Kurobane et al. 2004).

The ultimate flexural strength at the column face is

$$M_f = M_{fu} + M_{wu}, \tag{6.107}$$

where M_{fu} is the ultimate moment carried by the welded joints between the beam flange and the diaphragms

$$M_{fu} = b_b t_f (h_b - t_f) f_u, \tag{6.108}$$

and M_{wu} is the ultimate moment carried by the fillet welds between the shear plate and column flange as well as the diaphragms

$$M_{wu} = m t_{bw} \frac{(h_b - 2t_f)^2}{4} f_y + L_e \frac{t_{bw}(h_b - 2t_f)}{\sqrt{3}} f_u, \tag{6.109}$$

where m is the dimensionless moment capacity of the welded web joint expressed as

$$m = 4\frac{t_c}{d_j}\sqrt{\frac{b_j f_{yc}}{t_{bw} f_{yb}}}; m \le 1.0, \tag{6.110}$$

f_{yb} and f_{yc} are the yield stresses of beam and column steel material, respectively. $f_{yb} = f_{yc} = 235$ MPa. f_u is the ultimate limit stress of the steel.

The overstrength criterion for the connection is formulated by

$$M_f \ge \alpha M_{pb}, \tag{6.111}$$

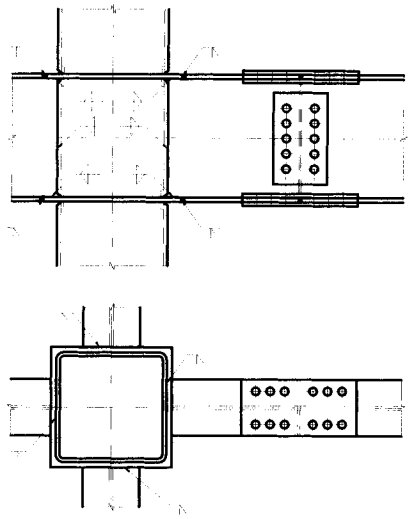

Figure 6.16 Another beam-to-column connection improved for seismic resistance

where M_{pb} is the plastic moment of the beam and the value of $\alpha \geq 1.25$ is recommended.

6.3.9 The objective function of the frame with the cost of connections

For the purpose of optimization we need the cost as a function of variables, i.e. dimensions of columns and beams (b_{ci}, t_{ci}, h_{bi}, b_{bi}, t_{fi}, i=1,2,3).

The structural volume is as follows:

$$V = H\left(A_{C1} + A_{C2} + A_{C3}\right) + 2L\left(A_{B1} + A_{B2} + A_{B3}\right). \tag{6.112}$$

The final objective function is the total cost including material and fabrication costs also for beam-to-column connections.

6.3.9.1 *Material cost*

$$K_M = K_{Mcolumn} + K_{Mbeams}, \tag{6.113}$$

$$K_{Mcolumn} = 1.05x1.08x7.85x10^{-6} H \sum_{i=1}^{3} 4t_{ci}\left(b_{ci} - t_{ci}\right), \tag{6.114}$$

$$K_{Mbeams} = 1.05x0.67x7.85x10^{-6} x2L \sum_{1}^{3} A_{bi}, \tag{6.115}$$

where the factor of 1.05 expresses the 5% material loss, the material cost factors for columns of square box section (108 ¥/kg = 1.08 $/kg) and for beams of rolled I-section (67¥/kg=0.67$/kg) are used in Japan. Material cost data were valid in 2004. These prices are floating, so they should be updated. Furthermore the steel density is 7850 kg/m^3 = 7.85x10^{-6} kg/mm^3. The material costs for plates (diaphragms and shear plates) are neglected.

6.3.9.2 *Cost of design, assembly and inspection*

According to the Japanese calculation method, the cost of design, assembly and inspection is related to the structural mass as follows:

$k_{drawing}$ = 1.55 hour/tonne, $k_{assembly}$ = 5.91 h/t, $k_{inspection}$ = 1.80 h/t, together 9.26 h/t.

The fabrication cost factor is k_F = 3125 ¥/h = 31.25 $/h.

$$K_{D,A,I} = 31.25x7.71x10^{-3}\left(\frac{K_{Mcolumn}}{1.08} + \frac{K_{Mbeams}}{0.67}\right), \tag{6.116}$$

$$K_{D,A,I} = 2.8600x10^{-5}\sum_{1}^{3} t_{ci}\left(b_{ci} - t_{ci}\right) + 4.7648x10^{-5}\sum_{1}^{3} A_{bi}. \tag{6.117}$$

6.3.9.3 *Cost of cutting*

The Japanese calculation uses times for the programming of numerical control machine. Therefore, this calculation results in very high values. Instead of these times we use times for manual cutting with acetylen gas according to speed data of ESAB (2003).

Cutting of column parts

For cutting with acetylen gas, according to ESAB (2003), quality I, for an average thickness of t_c = 25 mm, the cutting speed is 450 mm/min = 27000 mm/h. We use a beveling factor of 1.1, then the cost of cutting of column parts is

$$K_{C1} = \frac{1.1x31.25}{2.7x10^4} 16 \sum_1^3 b_{ci} = 2.0370x10^{-2} \sum_1^3 b_{ci} \cdot \tag{6.118}$$

Cutting of beams

$$K_{C2} = \frac{1.1x31.25}{2.7x10^4} 2x4 \sum_1^3 \left(2b_{bi} + h_{bi} - 2t_{fi}\right) = 1.0185x10^{-2} \sum_1^3 \left(2b_{bi} + h_{bi} - 2t_{fi}\right) \cdot \tag{6.119}$$

Cutting of diaphragms

$$K_{C3} = \frac{1.1x31.25}{2.7x10^4} 8 \sum_1^3 \left(b_{ci} + 160\right) = 1.0185x10^{-2} \sum_1^3 \left(b_{ci} + 160\right) \cdot \tag{6.120}$$

Cutting of shear plates

Cutting speed for thickness of 20 mm is 480 mm/min = 28800 mm/h.

$$K_{C4} = \frac{31.25}{2.88x10^4} 4x2 \sum_1^3 \left(h_{bi} - 2t_{fi} + 200\right) = 0.8680x10^{-2} \sum_1^3 \left(h_{bi} - 2t_{fi} + 200\right) \cdot \tag{6.121}$$

Numerically controlled drilling of bolt holes according to Japanese calculation:

Quantity: 72 holes in shear plates and 72 holes in beams

$$K_{C5} = 31.25x72\left(0.0225 + 0.038\right) = 136.1\$.$$

6.3.9.4 *Cost of welding according to the Japanese calculation*

The Japanese calculation uses welding times in function of equivalent ratios. These ratios are given in function of weld size in tabulated form. For optimization it is better to use these ratios as direct function of weld size. Using a curve fitting technique one can obtain approximate expressions of equivalent ratios for different weld types.

Welding of through-diaphragms in shop with a robot using single-bevel CJP (complete joint penetration) welds with angle of 35°, a root gap of 7 mm and backing strips. The equivalent ratio for this weld type is

$q_1 = (a_1 + b_1 t_f)^2$, $a_1 = 0.437541$, $b_1 = 0.147718$,

the required specific time is 0.0026 h/m = $2.6x10^{-6}$ h/mm,

$$K_{W1} = 31.25x2.6x10^{-6}x16\sum_{1}^{3} b_{ci}\left(a_1 + b_1 t_{fi}\right)^2 = 1.300x10^{-2}\sum_{1}^{3} b_{ci}\left(a_1 + b_1 t_{fi}\right)^2 . \quad (6.122)$$

Manual field welding of single-bevel welds with backing bars for beam flanges to diaphragms. Root gap of 7 mm and weld angle of 35° is used. The required specific time is 0.074 h/m = $7.4x10^{-5}$ h/mm, field factor is 1.5, the equivalent ratio can be approximated as

$$q_2 = \left(a_2 + b_2 t_f\right)^2 ; a_2 = 1.107405, b_2 = 0.132698 , t_f \text{ in mm.}$$

$$K_{W2} = 1.5x31.25x7.4x10^{-5}x4x2\sum_{1}^{3} b_{bi}\left(a_2 + b_2 t_{fi}\right)^2 , \quad (6.123)$$

$$K_{W2} = 0.02775\sum_{1}^{3} b_{bi}\left(a_2 + b_2 t_{fi}\right)^2 . \quad (6.124)$$

Manual shop welding of shear tabs with double fillet welds. The equivalent ratio is approximated by

$$q_3 = a_3 + b_3 s^2 ; a_3 = 0.0041975, b_3 = 0.027771 ,$$

s is the perpendicular side size of the fillet weld in mm, $s = 1.22t_{bw}$.

$$K_{W3} = 31.25x7.4x10^{-5}\sum_{1}^{3}\left(a_3 + b_3 s_i^2\right)\left[8\left(h_{bi} - 2t_{fi}\right) + 2x2x60x4x3\right], \quad (6.125)$$

$$K_{W3} = 2.312x10^{-3}\sum_{1}^{3}\left(a_3 + b_3 s_i^2\right)\left[8\left(h_{bi} - 2t_{fi}\right) + 2880\right]. \quad (6.126)$$

6.3.10 Optimization and results

Data of the calculated frame are as follows:

To show the effect of the beam length, three values of L are used: L = 4, 5, 6 m. H = 3.6 m

The interstorey drift limit is as follows (see Eq. 6.31)

$$d_{ei} \le \frac{0.01H}{qv} = \frac{0.01x3600}{6.5x2} = 13.846 \text{ mm}, \; i = 1,2,3.$$

The average weight each column is carrying, w:

$$W = \frac{mn - m - n + 1}{mn} .$$

In our example we chose m = 4 and n = 6. In this case W = 0.63 .

Table 6.3 shows the results for $H = 3.6$ m at different span length L.

6.3.11 Check the connection strength (L = 6 m)

M_{fu2} is the ultimate moment carried by the welded joints between the beam flange and the diaphragm on floor 2 according to Eq. (6.74).

The optimum sizes of the beam are as follows:

$b_{b2} = 152.9$, $t_{f2} = 13.3$, $t_{c2} = 10$ mm,

at the connection $t_{bw2} = 8.1$, $L_e = 60$ mm, $f_u = 360$ MPa.

$M_{fu2} = b_{b2}t_{f2}(h_{b2} - t_{f2})f_u = 3.2482\text{x}10^8$ Nmm.

$d_j = h_{b2} - 2t_{f2} = 430.4$

Eq. (6.75) $M_{wu2} = 4.39677\text{x}10^7 + 5.52305\text{x}10^7 = 9.91982\text{x}10^7$ Nmm

Eq.(6.76) $m_2 = 0.404$

Eq. (6.77) $\alpha M_{p2} = 3.77175\text{x}10^8$ Nmm,

$\alpha M_{p2} \le M_{fu2} + M_{wu2} = 4.24018\text{x}10^8$ OK.

We have checked the plastic hinges. In the model of EC8 (Figure 6.7) it was assumed that plastic hinges are created at the beam ends, i.e. the plastic static moment of the beams should be smaller than that of columns.

$$W_{pl.column} = 1.5b_i^2 t_i > W_{pl.y.beam} \tag{6.127}$$

Table 6.3 Optimum values of the three welded box columns and the three UB type beams

$L/2$ [mm]	b_{c1}/t_{c1} [mm]	b_{c2}/t_{c2} [mm]	b_{c3}/t_{c3} [mm]	h_{b1} [mm]	h_{b2} [mm]	h_{b3} [mm]	Cost [$]
2000	180/6	200/6.3	300/10	356	305	356	2228.1
2500	200/8	250/8	350/12	406	356	406	3256.6
3000	**250/8**	**260/10**	**350/12**	**457**	**406**	**457**	**4282.6**

On all levels Eq. (6.127) is fulfilled ($6.242\text{x}10^6 > 4.558\text{x}10^6$ mm^3), the plastic hinges were created at beam ends.

6.3.12 Conclusions

Using a relatively simple frame model it is shown how to apply the optimum design system for the case of seismic loads. The cost function to be minimized is formulated on the basis of detailed cost calculations, including the fabrication cost of beam-to-column connections. The connection type is selected from three seismic resistant types by cost comparison. For the constrained cost function minimization the Particle Swarm algorithm is used. The optimum beam and column dimensions are determined for three values of beam length.

In most cases the interstorey drift constraint is active. In some cases the stability is also active. Due to the high material cost and the cost calculation method that the design, inspection and erection costs are proportional to the weight, the mass minima do not differ from the cost minima.

Columns on the second level are a little bit larger that of the ground floor due to the interstorey drift limits. It is possible to use similar columns on the two floors, but it will increase the total cost. ArcelorMittal UB profile height is limited to 1016 mm. For larger spans other profiles are more suitable.

It is possible to use the same columns for all the floors. In this case the connection shown in Fig. 6.15 can be another economical option because the quality control of shop-welded joints is easier than field welded joints. However, this will increase the total cost according to the present cost estimation method. It is still difficult to estimate properly the cost required for the quality control. The development of a more advanced cost estimation method is a task for the future.

6.4 FIRE-RESISTANT OPTIMUM DESIGN OF A MULTI-STOREY FRAME

6.4.1 Problem formulation

In order to study the effect of fire, a relatively simple frame, which was considered at the previous example, is selected as shown in Figure 6.7. This is simplified model of a central part of a three-storey building frame structure. The frame is unbraced. The column parts are constructed from welded square box section and the beams have a rolled universal beam (UB) profile. The frame is subject to vertical permanent and live loads forces (Figures 6.7, 6.8). In the fishbone model the beam ends are considered to be built up for vertical loads and pinned for horizontal ones.

The problem is to find suitable column and beam profiles, which fulfil the design constraints, include fire safety ones and minimize the objective function. The beams and column parts are subject to bending and compression, thus, stress constraints should be formulated for 3 beam and 3 column profiles according to Eurocode 3 (2005) (EC3). One of the important requirements is the overstrength requirements for beam-to-column connections: the plastic strength of the connections should be large enough to allow formation of plastic hinges at the beam ends. The connection design was determined on the basis of the plastic analysis and experimental evidences.

Calculation of vertical loads is according to Chapter 6.3.2.

Calculation of bending moments and axial forces is according to Chapter 6.3.4 in this book.

In Chapter 4 the basic considerations of fire resistant design is shown and the way of calculation with unprotected and protected cases.

6.4.2 Stress constraints for beams and column parts

According to EC3 (2003a), for simplicity, verifications may be performed in the elastic range only.

6.4.2.1 *Stress constraints for beams of UB profile (I-beam without fire resistance)*

The equations are the same as in (6.3.6.2), but the normal forces are neglected. The beams are considered not to be restrained by the floors:

$$k_{yyB}\frac{M_{Bi}}{\chi_{LT}W_{yB}f_{y1}}\le 1\ \ (i=1,2,3), \tag{6.128}$$

$$k_{zy}\frac{M_{Bi}}{\chi_{LT}W_{yB}f_{y1}}\le 1\ \ (i=1,2,3), \tag{6.129}$$

$$\chi_{yB}=\frac{1}{\phi_{yB}+\sqrt{\phi_{yB}^2-\bar{\lambda}_{yB}^2}}, \tag{6.130}$$

$$\phi_{yB}=0.5\left[1+\alpha_{yB}\left(\bar{\lambda}_{yB}-0.2\right)+\bar{\lambda}_{yB}^2\right];\alpha_{yB}=0.21, \tag{6.131}$$

$$\bar{\lambda}_{yB}=\frac{K_{yB}L}{r_{yB}\lambda_E};K_{yB}=1;r_{yB}=\sqrt{\frac{I_{yB}}{A_B}}, \tag{6.132}$$

$$k_{yyB}=C_{myB}\left(1+0.6\bar{\lambda}_{yB}\frac{N_B}{\chi_{yB}A_Bf_{y1}}\right)\le C_{myB}\left(1+0.6\frac{N_B}{\chi_{yB}A_Bf_{y1}}\right), \tag{6.133}$$

$$\chi_{zB}=\frac{1}{\phi_{zB}+\sqrt{\phi_{zB}^2-\bar{\lambda}_{zB}^2}}, \tag{6.134}$$

$$\bar{\lambda}_{zB}=\frac{K_{zB}L}{r_{zB}\lambda_E};K_{zB}=0.8;r_{zB}=\sqrt{\frac{I_{zB}}{A_B}}; \tag{6.135}$$

$$k_{zB}=\left(1-\frac{0.05\bar{\lambda}_{zB}}{C_{mLT}-0.25}\frac{N_B}{\chi_{zB}A_Bf_{y1}}\right)\ge\left(1-\frac{0.05}{C_{mLT}-0.25}\frac{N_B}{\chi_{zB}A_Bf_{y1}}\right), \tag{6.136}$$

$C_{myB}=C_{mLT}=0.5$,

$$\chi_{LT}=\frac{1}{\phi_{LT}+\sqrt{\phi_{LT}^2-\bar{\lambda}_{LT}^2}}, \tag{6.137}$$

$$\phi_{LT}=0.5\left[1+\alpha_{LT}\left(\bar{\lambda}_{LT}-0.2\right)+\bar{\lambda}_{LT}^2\right];\alpha_{LT}=0.49\ , \tag{6.138}$$

$$\bar{\lambda}_{LT}=\sqrt{\frac{W_{yB}f_{y1}}{M_{cr}}}, \tag{6.139}$$

$$M_{cr} = C_1 \frac{\pi^2 EI_{zB}}{L^2} \sqrt{\frac{I_{\omega B}}{I_{zB}} + \frac{L^2 GI_{tB}}{\pi^2 EI_{zB}}}; C_1 = 4.0, \tag{6.140}$$

$E = 2.1x10^5; G = 0.81x10^5$ MPa.

6.4.2.2 *The stress constraint for the beam (with fire resistance) according to EC3(2003b)*

Member with Class 3 cross-sections, subject to bending:

$$\frac{k_{yyB} M_{Bi}}{W_{yB} k_{y,\theta} f_{y1}} \le 1, \qquad (i = 1,2,3). \tag{6.141}$$

The value of $\chi_{i,min\,fi}$ $(i = 1,2)$ should be taken as the lesser of the values of $\chi_{y,fi}$ and $\chi_{z,fi}$ determined according to:

$$\chi_{fi} = \frac{1}{\varphi_\theta + \sqrt{\varphi_\theta^2 - \overline{\lambda}_\theta^2}}, \tag{6.142}$$

with $\varphi_\theta = \frac{1}{2}\left(1 + \alpha\overline{\lambda}_\theta + \overline{\lambda}_\theta^{\,2}\right)$, (6.143)

and $\alpha = 0.65\sqrt{\frac{235}{f_y}}$. (6.144)

The non-dimensional slenderness for the temperature θ_a, is given by:

$$\overline{\lambda}_\theta = \overline{\lambda}\left(\frac{k_{y,\theta}}{k_{E,\theta}}\right)^{0.5}, \tag{6.145}$$

$$k_y = 1 - \frac{\mu_y N_B}{\chi_{y,fi} A k_{y,\theta} \frac{f_y}{\gamma_{M,fi}}} \le 3, \tag{6.146}$$

with $\mu_y = \left(1.2\beta_{M,y} - 3\right)\overline{\lambda}_{y,\theta} + 0.44\beta_{M,y} - 0.29 \le 0.8$, (6.147)

for beam $\beta_{M,y} = 1.4$, (6.148)

$$k_z = 1 - \frac{\mu_z N_B}{\chi_{z,fi} A k_{y,\theta} \frac{f_y}{\gamma_{M,fi}}} \le 3, \tag{6.149}$$

with $\mu_z = (1.2\beta_{M,z} - 5)\bar{\lambda}_{z,\theta} + 0.44\beta_{M,z} - 0.29 \le 0.8$, $\bar{\lambda}_{z,\Theta} \le 1.1$, (6.150)

$$\beta_{M,z} = 1.4 . \tag{6.151}$$

6.4.2.3 *Stress constraints for welded box column parts (without fire resistance)*

$$\frac{N_{Ci}}{\chi_{yC} A_C f_{y1}} + 2k_{yy} \frac{M_{Ci}}{W_{yC} f_{y1}} \le 1, \quad (i = 1,2,3). \tag{6.152}$$

The bending moment is doubled due to the biaxial bending.

$$f_{y1} = f_y / \gamma_{M1} = f_y / 1.1 ,$$

$$\chi_{yC} = \frac{1}{\phi_{yC} + \sqrt{\phi_{yC}^2 - \bar{\lambda}_{yC}^2}}, \tag{6.153}$$

$$\phi_{yC} = 0.5\left[1 + \alpha_C (\bar{\lambda}_{yC} - 0.2) + \bar{\lambda}_{yC}^2\right], \tag{6.154}$$

$\alpha_C = 0.34$ for a welded box section.

$$\bar{\lambda}_{yC} = \frac{2K_{yC}H}{r_{yC}\lambda_E}; \quad \lambda_E = \pi\sqrt{\frac{E}{f_y}}; \quad r_{yC} = \sqrt{\frac{I_{yC}}{A_C}}. \tag{6.155}$$

The values of $K_{yC}H$ if H=3600 mm are 2160, 1800 and 2340 mm for bottom, middle and top column part, respectively. In Eq.(6.155) the factor 2 expresses that frame is a sway system.

For the calculation of k_{yy} the Method 2 is used:

$$k_{yy} = C_{myC}\left(1 + 0.6\bar{\lambda}_{yC}\frac{N_C}{\chi_{yC} A_C f_{y1}}\right) \le C_{myC}\left(1 + 0.6\frac{N_C}{\chi_{yC} A_C f_{y1}}\right), \tag{6.156}$$

C_{myC} =0.9.

6.4.2.4 *Stress constraint for columns (with fire resistance) according to EC3(2003b)*

Member with Class 3 cross-sections, subject to combined bending and axial compression:

$$\frac{N_{Ci}}{\chi_{1.min.fi} A_C k_{y,\Theta} f_{y1}} + \frac{2k_{yy} M_{Ci}}{W_{yC} k_{y,\Theta} f_{y1}} \le 1 , \quad (i = 1,2,3). \tag{6.157}$$

Calculation of the parameters is according to Eqs. (6.142 - 6.151).

For column:

$$\beta_{M,\psi} = 1.8 - 0.7\psi \,, \quad \psi = -1 \,. \tag{6.158}$$

Due to the application of hollow section we need not to consider the lateral torsional buckling. Welded box column parts should be used. For this profile the following formulae are valid:

$$A = 4(b-t)t; I_y = I_z = \frac{2}{3}(b-t)^3 t; , \tag{6.159}$$

$$r_y = r_z = \frac{b-t}{\sqrt{6}}; W_y = W_z = \frac{4}{3}(b-t)^2 t \cdot \tag{6.160}$$

In the optimum design process the cross-sectional areas of column parts A_{Ci} are selected as unknowns and the cross-sectional characteristics are expressed by A_{Ci} as follows

$$I_{yCi} = \frac{A_{Ci}^2}{24\delta}; W_{yCi} = \frac{4\delta}{3}\left(\frac{A_{Ci}}{2\delta}\right)^{3/2}, \tag{6.161}$$

Knowing A_{Ci} the dimensions are the following:

$$b - t = \sqrt{\frac{A_C}{4\delta}}; t = \delta(b-t) \cdot \tag{6.162}$$

6.4.2.5 *Local buckling constraint for welded box column profiles*

According to EC3 (2003a):

$$b_i / t_i \le 33\varepsilon; \; \varepsilon = \sqrt{235 / f_y} \,. \tag{6.163}$$

where for fire resistance design:

$$\varepsilon = 0.85\sqrt{\frac{235}{f_y}} \,. \tag{6.164}$$

Approximate formulae for the UB profile are according to Chapter 6.3.6.2, Eqs. (6.78-6.87), equations are also in Appendix C.

6.4.3 The objective function

In the first design phase we use the structural volume as an objective function:

$$V = H\left(A_{C1} + A_{C2} + A_{C3}\right) + 2L\left(A_{B1} + A_{B2} + A_{B3}\right) \cdot \tag{6.165}$$

A refined objective function can be the material cost. A final objective function will be the total cost including material and fabrication costs also for beam-to-column connections.

The beam-to-column connection is calculated according to Chapter 6.3.7.

The cost function of the frame including the cost of connections is calculated according to Chapter 6.3.9.

6.4.4 Optimization and results

Dimensions of the calculated frame are as follows: the beam length L = 6 m, floor height H = 3.6 m.

Table 6.4 shows the result for the frame without fire resistance considerations. It contains unrounded (non discrete) values to be able to compare it with the results with fire resistance considerations. Discrete values are also given.

Check of the connection strength

M_{fu2} is the ultimate moment carried by the welded joints between the beam flange and the diaphragm on floor 2 according to Eq. (6.108).

The optimum sizes of the beam are as follows

b_{b2} = 142.2, t_{f2} = 11.2, t_{c2} = 10 mm, at the connection t_{bw2} = 6.8, L_e = 60 mm, f_u = 360 MPa.

$M_{fu2} = b_{b2}t_{f2}(h_{b2} - t_{f2})f_u = 2.2636\text{x}10^8$ Nmm.

$d_j = h_{b2} - 2t_{f2} = 383.6$

Eq. (6.109) $M_{wu2} = 2.8028\text{x}10^7 + 3.4378\text{x}10^7 = 6.2406\text{x}10^7$ Nmm

Eq.(6.110) $m_2 = 0.4768$

Eq. (6.111) $\alpha M_{p2} = 2.6073\text{x}10^8$ Nmm,

$\alpha M_{p2} \leq M_{fu2} + M_{wu2} = 2.8877\text{x}10^8$ is satisfied.

Table 6.4 Optimum values of the three welded box columns and the three UB type beams without fire resistance

b_{c1}/t_{c1} (mm)	b_{c2}/t_{c2} (mm)	b_{c3}/t_{c3} (mm)	h_{b1} (mm)	h_{b2} (mm)	h_{b3} (mm)	Cost ($)
241.9/7.3	266.4/8.1	378.2/11.5	419.0	393.9	418.8	**3884.3**
250/8	260/10	350/12	457	406	457	4180

Table 6.5 shows the result for the frame with fire resistance considerations. The calculation is theoretical, so we get thicker hollow sections than advisable. BS-EN 10210-2 (1997) and BS-EN 10219-2 (1997) gives the tolerances, dimensions and sectional properties for hot-finished structural hollow sections and cold formed welded structural sections. The maximum sizes for SHS are 400 mm height and 20 mm thickness for hot-finished and 16 mm thickness for cold-formed sections. If one needs a thicker section he can use welded box sections with larger thickness. In this case the cost should include the welding cost of the box section. Calculations show that the cost of the structure is proportional to the value of fire resistance time

(Figure 6.17). One hour fire resistance causes 42 % increase of cost, two hours resistance causes 79 % increase of cost.

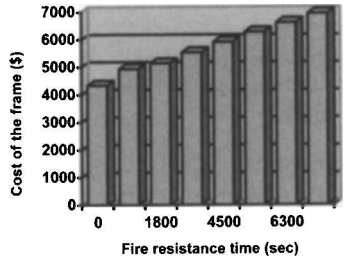

Figure 6.17. The cost of the frame in the function of the fire resistance

6.4.5 Conclusions

Optimization of steel frames for fire safety is a relatively new area. Using a rather simple frame model it is shown how to apply the optimum design system for the case of fire. The cost function to be minimized is formulated on the basis of detailed cost calculations, including the fabrication cost of beam-to-column connections. The connection type is selected from several seismic resistant types by cost comparison. A very robust optimization technique was applied, namely the modified Particle Swarm algorithm.

Table 6.5 Optimization results for the frame with fire resistance considerations

Fire resistance time (sec)	b_{c1}/t_{c1} (mm)	b_{c2}/t_{c2} (mm)	b_{c3}/t_{c3} (mm)	h_{b1} (mm)	h_{b2} (mm)	h_{b3} (mm)	Cost ($)
0	283.0/10.9	331.1/10.3	363.4/12.4	419.3	394.9	419.3	4335.3
900	240.3/16.0	334.5/10.1	371.5/11.9	425.6	403.9	420.4	4460.4
1800	237.6/16.6	209.7/31.5	317.6/16.8	436.2	394.3	422.4	4928.0
2700	279.8/15.3	281.4/17.5	304.2/20.2	466.1	411.0	428.4	5135.6
3600	193.1/31.8	258.7/23.4	258.7/30.4	443.6	416.6	425.4	**5528.6**
4500	215.8/29.9	214.5/35.7	232.4/41.6	464.1	405.9	421.9	5908.9
5400	184.4/47.5	217.8/39.2	223.6/51.3	448.1	417.1	422.9	6274.1
6300	180.2/59.6	196.1/56.7	215.7/65.5	445.6	402.9	419.7	6611.1
7200	182.8/66.3	193.8/69.9	227.2/61.7	450.3	401.0	434.9	**6940.0**

It calculated both the continuous and discrete optima. The calculation shows that optimization has a large effect. Due to the high material cost and the cost calculation method that the design, inspection and erection costs are proportional to the weight, the mass minima do not differ from the cost minima.

When we consider fire resistance, the time after which its elements still work, needs more material (steel) to be built into the structure. The present example shows, that about one hour increment in fire safety needs 42 % more cost at the structure. For a designer it is important to know the relation between mass and fire safety. Further investigation will be the application of fire resistant paintings or other materials and to optimize for the cost of the structure.

6.5 EARTHQUAKE-RESISTANT OPTIMUM DESIGN OF A TUBULAR FRAME

6.5.1 Introduction

Pressure vessels are expensive and dangerous devices, which need safe supports. Their fracture caused by earthquake can be very dangerous. Thus, the design constraints should be very strict.

A simple supporting frame consists of 4 columns and 4 beams (Fig. 6.18). The pressure vessel is fixed at the middle of the beams. The horizontal seismic load is calculated according to Eurocode 8 (2004) (see Chapter 3). Since the horizontal forces cause large bending moments in the horizontal plane and the beams should transfer at the frame corners large bending moments, their suitable profile is a welded box section or tubular hollow section. Therefore, the columns are constructed with box section as well. The welded corners are assumed to be rigid.

Eurocode 8 prescribes a strict limitation of the horizontal sway at the middle of the beams. This sway has four components as follows: the sway of the vertical frames, deformation of the beam due to bending in horizontal plane, displacement of the beam due to angular deformation of the frame corner and another displacement caused by torsion.

Optimization means a search for better solutions, which better fulfil the requirements. Requirements for a modern load-carrying structure are the safety, fitness for production and economy. In an optimum design procedure the safety and fitness for production are guaranteed by design and fabrication constraints, the economy is achieved by minimization of a cost function (Farkas & Jármai 1997, Farkas & Jármai 2003).

The fabrication (assembly and welding) cost of frame corner joints is proportional to the size of columns and beams, thus the minimum cost design is identical to the minimum mass design. Since the investigated frame is symmetric, the unknowns to be optimized are the thicknesses t_1 and t_2 for columns and beams, respectively as well as a common width $h_1 = h_2$ of the square hollow section (SHS) of the columns and beams.

The constraints relate to the sway limitation and to the stability of frame members against compression and bending according to Eurocode 3 (2005).

6.5.2 Calculation of the seismic force

According to Chapter 3

$$F_b = S_d(T_1)m\lambda\,, \tag{6.166}$$

where $S_d(T_1)$ = the ordinate of the design spectrum at period T_1, m = the pressure vessel mass, λ = correction factor. Values of the parameters describing the recommended Type 1 elastic response spectra (Table 3.1) are as follows: ground type C is selected, $S = 1.15$, $T_B = 0.20$, $T_C = 0.60$, $T_D = 2.0$.
T_1 (s) is approximated by the expression:

$$T_1 = C_1 H^{0.75}, C_1 = 0.085, H = 4, T_1 = 0.24 \text{ s}, \tag{6.167}$$

$$\text{for } T_B < T_1 < T_C, \quad S_d = \alpha S \frac{2.5}{q}. \tag{6.168}$$

We use the highest value applied for Japan $\alpha = 0.40$, the behaviour factor according to Section 3.4.1 q = 5.5. Thus S_d = 0.4x1.15x2.5/5.5 = 0.2091, required cross-section Class 1 (plastic).

For $T_1 < 2T_C$ $\lambda = 0.85$.

Thus, the pressure vessel mass m should be multiplied by 0.85x0.2091 = 0.1777. The pressure vessel mass is 300 kN, the seismic horizontal force acting on a beam is F_b = 0.1777x75 = 13.3 kN.

Load combination: $\sum G_k + \psi_E Q_k; \psi_E = \varphi \psi_{21} = 1$, *since, for storage structures,* $\varphi = \psi_{21} = 1$.

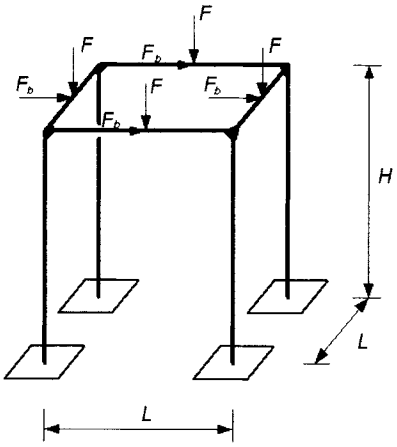

Figure 6.18 Supporting frame structure with vertical and horizontal forces

6.5.3 Normal forces and bending moments in vertical frames (Fig.6.18)

According to Glushkov et al. (1975)

$$H_A = \frac{3M_A}{H}, \tag{6.169}$$

$$M_A = \frac{M_B}{2}, \tag{6.170}$$

$$M_B = \frac{FL}{4(k+2)}, \tag{6.171}$$

$$k = \frac{I_{y2}H}{I_{y1}L}, \tag{6.172}$$

$$M_E = \frac{FL}{4} - M_B, \tag{6.173}$$

$$M_1 = \frac{3F_bHk}{2(6k+1)}, \tag{6.174}$$

$$V_{D1} = \frac{2M_1}{L}, \tag{6.175}$$

$$N_1 = F + V_{D1}, \tag{6.176}$$

$$H_{D1} = \frac{k+1}{k+2}\frac{F_b}{2}, \tag{6.177}$$

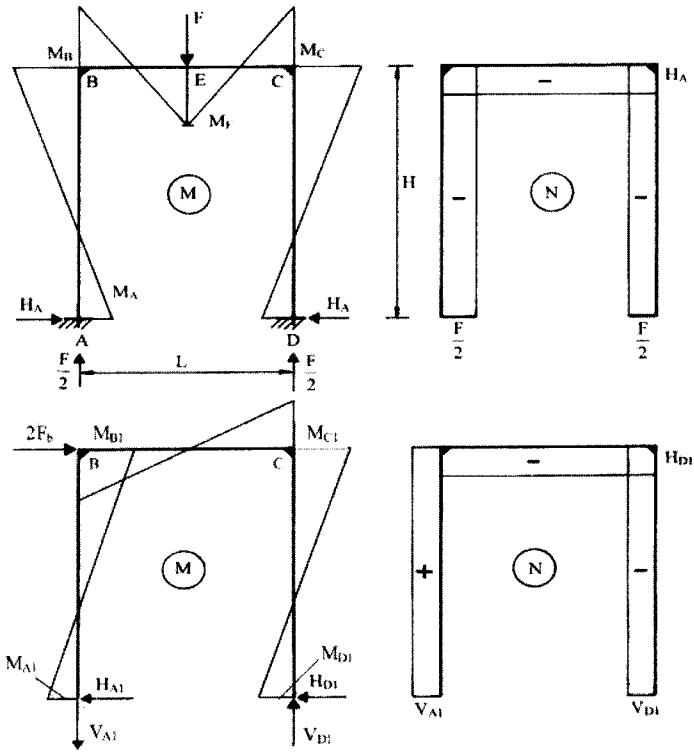

Figure 6.19 Diagrams for the bending moments and normal forces of a frame

$$M_{A1} = \frac{3k+1}{6k+1}\frac{F_b}{2}H, \tag{6.178}$$

$$M_{B1} = \frac{3k}{6k+1}\frac{F_b}{2}H, \tag{6.179}$$

$$H_2 = \frac{3k}{6k+1}H, \tag{6.180}$$

$$M_{Bt} = M_B + M_{B1}, \tag{6.181}$$

$$M_{At} = M_A + M_{A1}. \tag{6.182}$$

6.5.4 Geometric characteristics of the square hollow section (Fig.6.20)

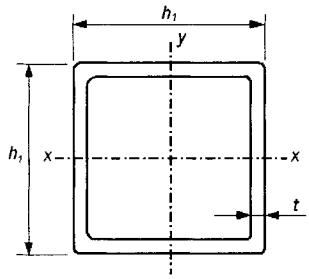

Figure 6.20 Dimensions of a square hollow section (SHS)

Areas and moments of inertia are calculated according to DASt Richtlinie 016 (1986).

Area of the cross-section for columns

$$A_1 = 4t_1(h_1 - t_1)\left(1 - 0.43\frac{2t_1}{h_1 - t_1}\right), \tag{6.183}$$

and for beams

$$A_2 = 4t_2(h_1 - t_2)\left(1 - 0.43\frac{2t_2}{h_1 - t_2}\right), \tag{6.184}$$

moment of inertia for columns

$$I_{x1} = I_{y1} = \left[\frac{2(h_1 - t_1)^3 t_1}{3}\right]\left(1 - 0.86\frac{2t_1}{h_1 - t_1}\right), \tag{6.185}$$

and for beams

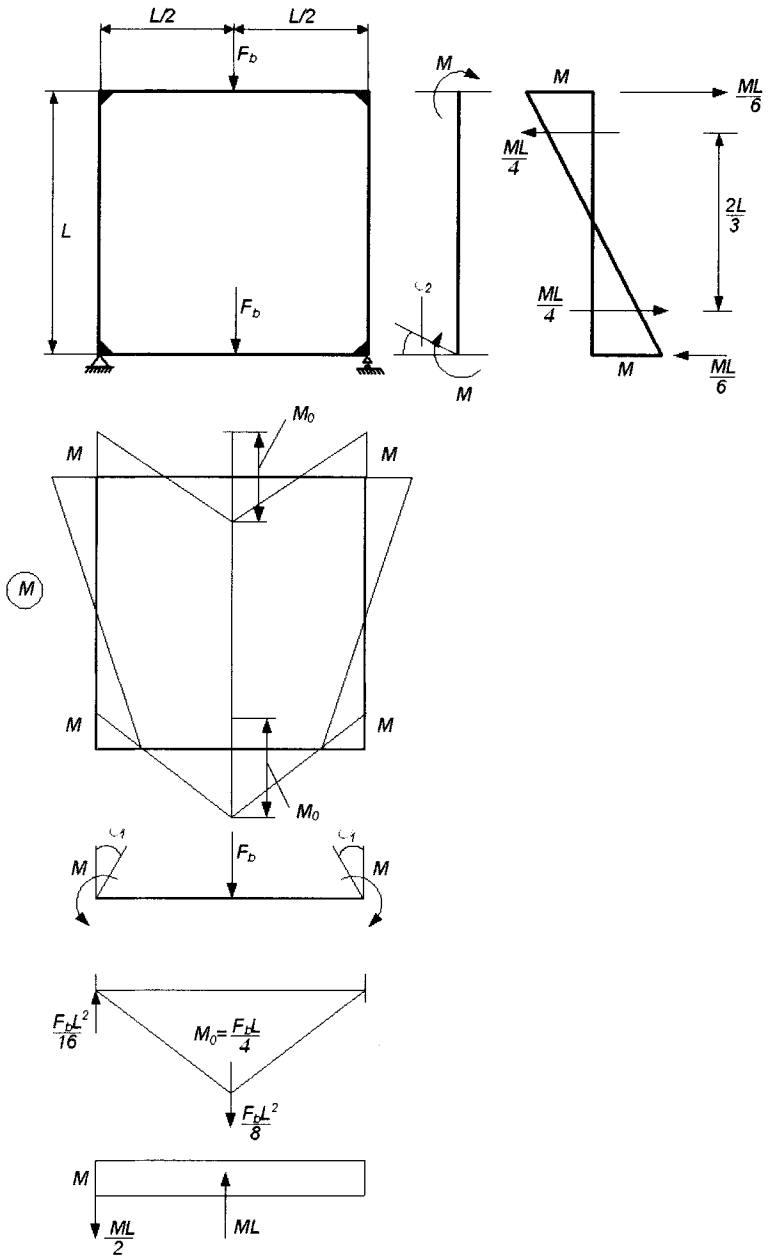

Figure 6.21 Bending moment diagram and calculation of angular deformations due to forces F_b in the horizontal plane

$$I_{x2} = I_{y2} = \left[\frac{2(h_1 - t_2)^3 t_2}{3}\right]\left(1 - 0.86\frac{2t_2}{h_1 - t_2}\right), \tag{6.186}$$

section modulus for columns

$$W_{x1} = W_{y1} = \frac{2I_{x1}}{h_1}, \tag{6.187}$$

and for beams

$$W_{x2} = W_{y2} = \frac{2I_{x2}}{h_1}, \tag{6.188}$$

6.5.5 Calculation of the elastic sway

$$u_e = u_f + u_b + u_t + u_{tl}, \tag{6.189}$$

where u_f = the sway of the frame, u_b = displacement due to bending of a beam in horizontal plane, u_t = beam displacement due to frame corner angle deformation, u_{tl} = beam displacement due to torsion.

$$u_f = \frac{2M_{A1}m_{A1}H_1}{3EI_{x1}} + \frac{2M_{B1}m_{B1}H_2}{3EI_{x1}} + \frac{M_{B1}m_{B1}L}{3EI_{x2}}, \tag{6.190}$$

where $M_{A1} = \frac{3k+1}{6k+1}F_bH; m_{A1} = \frac{3k+1}{6k+1}\frac{H}{2}; H_1 = \frac{3k+1}{6k+1}H,$ (6.191)

$$M_{B1} = \frac{3k}{6k+1}F_bH; m_{B1} = \frac{3k}{6k+1}\frac{H}{2}; H_2 = \frac{3k}{6k+1}H; k = \frac{I_{x2}H}{I_{x1}L}, \tag{6.192}$$

The displacement u_b due to two horizontal forces F_b in the horizontal plane of the frame with rigid corners is calculated as follows. The corner bending moment M can be obtained from the equation of angular deformations (Fig. 6.21)

$$\varphi_1 = \varphi_2, \tag{6.193}$$

where

$$EI_{y2}\varphi_1 = \frac{F_bL^2}{16} - \frac{ML}{2}, \tag{6.194}$$

and

$$EI_{y2}\varphi_2 = \frac{ML}{6}. \tag{6.195}$$

Considering Eqs (6.193, 6.194 and 6.195) one obtains

$$M = \frac{3F_bL}{32}, \tag{6.196}$$

and the displacement from F_b and M

$$u_b = \frac{F_b L^3}{48EI_{y2}} - \frac{ML^2}{8EI_{y2}} = \frac{7F_b L^3}{768EI_{y2}}. \tag{6.197}$$

The displacement due to angle deformation of the beam caused by the frame corner angle deformation can be obtained from

$$u_t = \frac{1}{2EI_{x1}}\left(M_{A1}H_1 - M_{B1}H_2\right)\frac{h_1}{2}. \tag{6.198}$$

Finally, the beam deformation due to torsion is

$$u_{t1} = \varphi_t \frac{h_1}{2}; \varphi_t = \frac{F_b h_1 L}{8GI_{t2}}; I_{t2} = h_1^3 t_2; u_{t1} = \frac{F_b L}{16Gh_1 t_2}. \tag{6.199}$$

6.5.6 Constraint on sway limitation

The allowable sway according to Chapter 3 is calculated as follows. The elastic displacement for ductile non-structural elements should fulfil the following limitation

$$u_e \le \frac{0.0075H}{\gamma_1 q \nu} = \frac{0.0075x4000}{1.4x5.5x0.4} = 9.74 \text{ mm}. \tag{6.200}$$

Importance class for power plants is IV (Chapter 3). Structural height $H = 4000$ mm. The recommended safety factor for importance class IV (Section 3.3.2) is $\gamma_1 = 1.4$. The reduction factor $\nu = 0.4$. Behaviour factor $q = 5.5$.

6.5.7 Local buckling constraints

For SHS columns and beams of section class 1 (plastic) the constraint is given by:

$$\frac{h_1 - 3t_i}{t_i} = \frac{h_1}{t_i} - 3 \le 33\varepsilon, \varepsilon = \sqrt{\frac{235}{f_y}}, i = 1,2. \tag{6.201}$$

6.5.8 Stress constraint for the columns

According to Eurocode 3 (2005) the SHS section is not susceptible to torsional deformations, thus $\chi_{LT} = 1$, $k_{yx} = 0$ and the second constraint in EC3 should not be considered.

$$\frac{N_1}{\chi_{1.min} A_1 f_{y1}} + \frac{k_{yy1}(M_C + M_{B1})}{W_{y1} f_{y1}} + \frac{k_{zz1}(M_C)}{W_{z1} f_{y1}} \le 1, \tag{6.202}$$

$$k_{yy1} = min\left(C_{my1}\left(1+\frac{0.6\lambda_{y1}(H_A+H_{D1})}{\chi_{y1}A_1 f_{y1}} \right), C_{my1}\left(1+\frac{0.6(H_A+H_{D1})}{\chi_{y1}A_1 f_{y1}} \right) \right), \quad (6.203)$$

$C_{my1} = 0.4$,

$$k_{xy1} = min\left(C_{my1}\left(1+\frac{0.6\lambda_{y1}(H_A+H_{D1})}{\chi_{y1}A_1 f_{y1}} \right), C_{my1}\left(1+\frac{0.6(H_A+H_{D1})}{\chi_{y1}A_1 f_{y1}} \right) \right), \quad (6.204)$$

$C_{mz1} = 0.4$,

$$r_{y1} = \left(\frac{I_{y1}}{A_1} \right)^{0.5}; r_{z1} = \left(\frac{I_{z1}}{A_1} \right)^{0.5}; \bar{\lambda}_{y1} = \frac{K_{y1}H}{r_{y1}\lambda_E}; \quad (6.205)$$

The value of K_{y1} and K_{z1} are taken according to EC3 (2005)

$$K_{y1} = 2.19; \bar{\lambda}_{z1} = \frac{K_{z1}H}{r_{z1}\lambda_E}; K_{z1} = 0.5, \quad (6.206)$$

$$\bar{\lambda}_{1.\max} = \max(\bar{\lambda}_{y1}, \bar{\lambda}_{z1}), \quad (6.207)$$

$$\chi_{i.min} = \frac{1}{\phi_i + \left(\phi_i^2 - \bar{\lambda}_{i.max}^2 \right)^{0.5}}; \quad (6.208)$$

$$\phi_i = 0.5\left[1+0.34\left(\bar{\lambda}_{i.max} - 0.2 \right) + \bar{\lambda}_{i.max}^2 \right]. \quad (6.209)$$

6.5.9 Stress constraint for the beams

$$\frac{H_A + H_{D1}}{\chi_{2.min}A_2 f_{y1}} + \frac{k_{yy2}M_E}{W_{y2}f_{y1}} + \frac{k_{yz2}M}{W_{z2}f_{y1}} \le 1, \; f_{y1} = \frac{f_y}{\gamma_{M1}}. \quad (6.210)$$

The flexural buckling factor is

$$\chi_i = \frac{1}{\phi_i + \left(\phi_i^2 - \bar{\lambda}_i^2 \right)^{0.5}}; \quad (6.211)$$

$$\phi_i = 0.5\left[1+0.34\left(\bar{\lambda}_i - 0.2 \right) + \bar{\lambda}_i^2 \right], \quad (6.212)$$

$$\bar{\lambda}_{y2} = \frac{K_{y2}L}{r_{y2}\lambda_E}; \text{ the effective length factor is } K_{y2} = 0.5, \quad (6.213)$$

$$r_{y2}=\left(\frac{I_{y2}}{A_2}\right)^{0.5};\lambda_E=\pi\left(\frac{E}{f_y}\right)^{0.5}. \tag{6.214}$$

E is the elastic modulus.

$$\bar{\lambda}_{z2}=\frac{K_{z2}L}{r_{z2}\lambda_E};\text{ the effective length factor is} \tag{6.215}$$

$$K_{z2}=0.5, \tag{6.216}$$

$$r_{z2}=\left(\frac{I_{z2}}{A_2}\right)^{0.5}, \tag{6.217}$$

$\chi_{2.min}$ is calculated from $\bar{\lambda}_{2.max}=max\left(\bar{\lambda}_{y2},\bar{\lambda}_{z2}\right)$.

$$k_{yy2}=min\left(C_{my2}\left(1+\frac{0.6\lambda_{y2}\left(H_A+H_{D1}\right)}{\chi_{y2}A_2f_{y1}}\right),C_{my2}\left(1+\frac{0.6\left(H_A+H_{D1}\right)}{\chi_{y2}A_2f_{y1}}\right)\right), \tag{6.218}$$

$$C_{my2}=0.9,$$

$$k_{zz2}=min\left(C_{mz2}\left(1+\frac{0.6\lambda_{z2}\left(H_A+H_{D1}\right)}{\chi_{z2}A_2f_{y1}}\right),C_{mz2}\left(1+\frac{0.6\left(H_A+H_{D1}\right)}{\chi_{z2}A_2f_{y1}}\right)\right), \tag{6.219}$$

$$C_{mz2}=0.4,$$

$$k_{yz2}=0.8k_{yy2}. \tag{6.220}$$

6.5.10 Optimization and results

Numerical data

$E=2.1\text{x}10^5$ MPa, $G=0.8\text{x}10^5$ MPa, $H=4000$, $L=4000$ mm, $F=75$ kN, $F_b=13.3$ kN.

The objective function *is the structural volume*

$$V=4A_1H+4A_2L. \tag{6.221}$$

or the structural mass

$$m=\rho V,\rho=7.85x10^{-6}\text{ kg/mm}^3.$$

The suitable SHS for columns and beams are selected using a cold-formed SHS catalogue BS EN 10219 (1997). Since the minimum thickness is limited by the local

buckling constraint (Eq.28), only that thicknesses can be used, which are larger than this limit, e.g. for $h_1 = 220$ $t = 6.3$, for $h_1 = 250$ $t = 8$, for $h_1 = 260$ $t = 8$ and for $h_1 = 300$ $t = 10$ mm. Therefore, the number of SHS to be investigated is limited.

Table 6.6 shows the results of the calculations to find the optimum SHS sizes. The governing constraint is that on sway limitation (Eq.6.200), the stress constraints are always fulfilled. The common width is h_1 and the thicknesses are t_1 for columns and t_2 for beams.

Table 6.6 Results of the systematic search to find the optimum SHS sizes (in mm)

h_1	t_1	t_2	sway constraint	m (kg)
220	6.3	6.3	13.6>9.74	
220	8	8	11.1>9.74	
220	10	8	9.9>9.74	
220	8	10	10.6>9.74	
220	10	10	9.3<9.74	2024
250	8	8	7.434<9.74	1890
260	8	8	6.6<9.74	1970
300	10	10	3.5<9.74	2828

It can be seen that the optimum sizes are as follows: $h_1 = 250$, $t = t_1 = t_2 = 8$ mm, the minimum mass is $m = 1890$ kg.

In the case of the optimum solution, the stress constraints are fulfilled as follows: Eq.(6.202): 0353<1 and Eq.(6.210): 0.601<1.

The components of the sway are the following: Eq.(6.190) $u_f = 6.769$, Eq.(6.197) $u_b = 0.518$, Eq.(6.198): $u_t = 0.127$ and Eq.(6.199): $u_{t1} = 0.021$ mm, thus, u_t and u_{t1} can be neglected.

Figure 6.22 shows the welded frame corner.

6.5.11 Cost calculation

The cost function includes the material and fabrication costs as follows:

$$K = K_M + K_F, \quad K_M = k_M \rho V_1, \rho = 7.85x10^{-6}\,\text{kg/mm}^3, \tag{6.222}$$

$V_1 = V + V_h$, volume of head plates $V_h = 4x3.5h_1^2 t_h, t_h = 8$ mm,

$$K_F = k_F\left(\Theta\sqrt{\kappa\rho V_1} + 1.3\sum_i C_i a_{wi}^n L_{wi}\right). \tag{6.223}$$

Number of assembled elements $\kappa = 12$, difficulty factor for a spatial structure $\Theta = 3$, welding time for the connection of a SHS beam to a SHS column with 2 vertical, one overhead and one downhand single bevel (1/2V) butt weld of size t_2 and length h_1

$$0.9518x10^{-3}x3t_2^2h_1 + 0.5214x10^{-3}t_2^2h_1, \tag{6.224}$$

welding time for the connection of a head plate to the frame corner with overhead fillet welds of size 5 mm and length $6h_1$ and with downhand fillet welds of length $2h_1$

$$1.667x10^{-3}x5^2x6h_1 + 0.7889x10^{-3}x5^2x2h_1. \tag{6.225}$$

For the optimum values of $h_1 = 250$, $t_2 = 8$ mm and for cost factors of $k_M = 1$ \$/kg and $k_F = 1$ \$/min

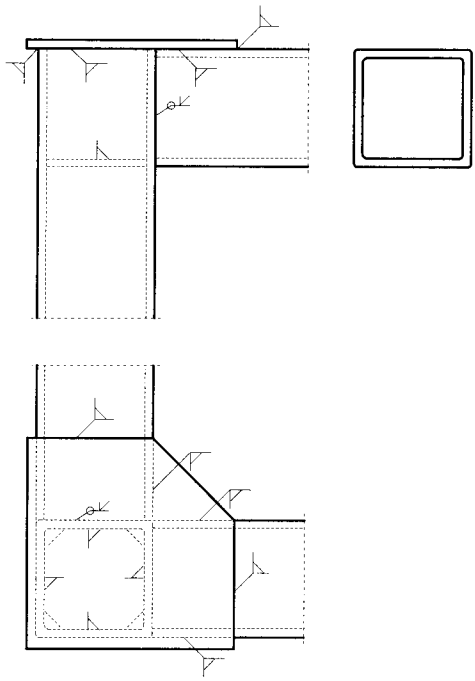

Figure 6.22 The welded frame corner.

$K_M = 1944$ \$ and $K_F = 1395$ \$.

It can be seen that the fabrication cost gives a significant part of the total cost.

6.5.12 Conclusions

The horizontal seismic forces and the allowable horizontal sway of a simple frame is calculated according to the Eurocode 8 (2004) (Chapter 3). The frame with rigid joints supports a pressure vessel, the failure of which caused by earthquake can be dangerous. The stress constraints for columns and beams are formulated according to Eurocode 3 (2005). The frame is welded from SHS profiles.

For fabrication reasons, the section width of columns and beams should be equal. Thus, the unknowns are the common width and the different two thicknesses. The

minimum thicknesses are limited by the local buckling constraint for section of class 1 (plastic).

The detailed calculation of sway due to bending deformations of the frame in vertical and horizontal plane and due to the torsion of the beams is presented. The objective function is the structural volume or mass, since the minimum cost design coincides with minimum mass design.

The optimum cross-sections are selected from a discrete series for SHS using a systematic search. The sway limitation is the governing constraint. Calculating the sway components, it is found that the deformation due to torsion of beams and the sway from the angular deformation of frame corners can be neglected.

6.6 FIRE-RESISTANT OPTIMUM DESIGN OF A TUBULAR FRAME

6.6.1 Introduction

Steel structures have been used in industrial and residential buildings, because they offer a wide range of advantages. However, these structures, when unprotected, behave poorly in fire situation. The high thermal conductivity of steel, together with the deterioration of its mechanical properties as a function of temperature, can lead to large deformations of structural elements and the premature failure of the buildings. The calculation of these steel frames can be according to Eurocode 1 (2002) and Eurocode 3 (2005).

The steel can be protected by materials such as mineral fibres, gypsum boards, concrete, intumescent paints and water-filled structures. In this study the optimal fire design of a steel frame structure is investigated. Using a relatively simple frame model it is shown how to apply the optimum design system for the case of fire resistance of a welded steel structure. Hollow sectional columns and beams are designed for minimum volume and weight. Overall and local buckling constraints are considered.

In this part we continue the calculation of the steel frame described in Chapter 6.5, but this case we concentrate not the earthquake behaviour, but the fire resistance (Fig. 6.18). In the first design phase the structural mass is used as an objective function. A refined objective function can be the material cost.

6.6.2 Calculation of the frame members

Beams are made of RHS or SHS, unknowns are h_2, b_2, t_{f2}, columns are made of SHS, unknowns are h_1, t_{f1}.

The cross-section area of a RHS beam profile with a height h, width b and thickness t, considering rounded corners of corner radius of $R = 2t$ and supposing that $b_2 = h_2/2$, using the formulae given by Eurocode 3 Part 1.3 (2005), can be calculated as

$$A_2 = 2t_2\left(1.5h_2 - 2t_2\right)\left(1 - 0.43\frac{4t_2}{1.5h_2 - 2t_2}\right), \tag{6.226}$$

For SHS column it is

$$A_1 = 4t_1(h_1 - t_1)\left(1 - 0.43\frac{2t_1}{h_1 - t_1}\right), \tag{6.227}$$

For RHS beams the second moments of area are as follows (Figure 6.23).

$$I_{x2} = \left[\frac{(h_2 - t_2)^3 t_2}{6} + \frac{t_2}{2}\left(\frac{h_2}{2} - t_2\right)(h_2 - t_2)^2\right]\left(1 - 0.86\frac{4t_2}{1.5h_2 - 2t_2}\right), \tag{6.228}$$

$$I_{y2} = \left[\frac{(0.5h_2 - t_2)^3 t_2}{6} + \frac{t_2}{2}\left(\frac{h_2}{2} - t_2\right)^2(h_2 - t_2)\right]\left(1 - 0.86\frac{4t_2}{1.5h_2 - 2t_2}\right). \tag{6.229}$$

For SHS columns

$$I_{x1} = I_{y1} = \left[\frac{2(b_1 - t_1)^3 t_1}{3}\right]\left(1 - 0.86\frac{2t_1}{b_1 - t_1}\right). \tag{6.230}$$

6.6.2.1 *Bending moments and forces from the vertical loads*

Bending moments and forces from the vertical loads F can be seen on Figure 6.19 and their calculations according to Glushkov et al. (1975) are as follows (Farkas & Jármai (1997, 2003) Eqs. (169-181).

6.6.2.2 *Bending moment in the horizontal frame due to horizontal force F_b*

The horizontal force is the tenth of the vertical one.

$$F_b = 0.1F, \tag{6.231}$$

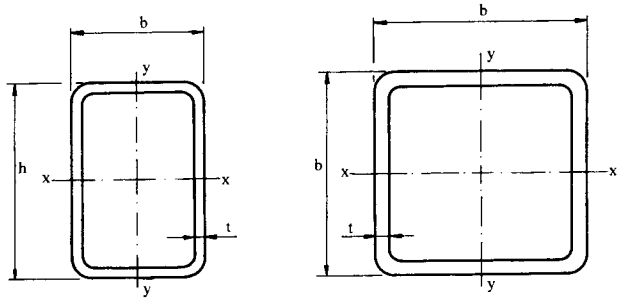

Figure 6.23. Dimensions of RHS and SHS profiles

$$M_{Bz1} = \frac{F_b L}{4}, \tag{6.232}$$

$$M_{Bz2} = \frac{5F_b L}{64}, \tag{6.233}$$

$$M_{Bz3} = \frac{F_b L}{64}, \tag{6.234}$$

$$M_{Bz} = M_{Bz1} - \left(M_{Bz2} + M_{Bz3}\right). \tag{6.235}$$

6.6.2.3 *The stress constraint for the beam (point E, no fire resistance) according to* Eurocode 3 (2005)

$$\frac{H_A + H_{D1}}{\chi_{2.min} A_2 f_{y1}} + \frac{k_{yy2} M_E}{W_{y2} f_{y1}} + \frac{k_{yz2} M_{Bz}}{W_{z2} f_{y1}} \le 1, \quad f_{y1} = \frac{f_y}{\gamma_{M1}}. \tag{6.236}$$

The parameters are according to Eqs. (6.211-6.220).

6.6.2.4 *The stress constraint for the beam (point E, with fire resistance) according to* Eurocode 1 (2002)

Member with Class 3 cross-sections, subject to combined bending and axial compression

$$\frac{H_A + H_{D1}}{\chi_{2.min} k_{y,\theta} A_2 f_{y1}} + \frac{k_{yy2} M_E}{W_{y2} k_{y,\theta} f_{y1}} + \frac{k_{yz2} M_{Bz}}{W_{z2} k_{y,\theta} f_{y1}} \le 1, \tag{6.237}$$

The value of $\chi_{i,min\,fi}$ (i = 1,2) should be taken as the lesser of the values of $\chi_{y,fi}$ and $\chi_{z,fi}$ determined according to Eqs. (6.237, 6.144). $k_{y,\theta}$ is reduction factor according to Chapter 4, Eq. (4.1).

The non-dimensional slenderness for the temperature θ_a, is given by Eq. (6.145).
Due to the application of hollow section we need not consider the lateral torsional buckling according to Eqs. (6.146-6.151).

6.6.2.5 *Stress constraint for columns (point C, with fire resistance) according to* Eurocode 1 (2002)

Member with Class 3 cross-sections, subject to combined bending and axial compression

$$\frac{N_1}{\chi_{1.min.fi} A_1 k_{y,\theta} f_{y1}} + \frac{k_y (M_C + M_{B1})}{W_{y1} k_{y,\theta} f_{y1}} + \frac{k_z M_C}{W_{z1} k_{y,\theta} f_{y1}} \le 1. \tag{6.238}$$

Calculation of the parameters is according to Eqs. (6.142-6.151).

For column

$$\beta_{M,\psi} = 1.8 - 0.7\psi\,, \quad \psi = -1, \tag{6.239}$$

Due to the application of hollow section we need not to consider the lateral torsional buckling.

6.6.3 Local buckling of plates

For the local buckling calculation we use limit slendernesses, given by Eurocode 3 (2005).

For the beam flange

$$\frac{b_2}{t_{f2}} - 3 \le 42\varepsilon\,. \tag{6.240}$$

For the beam web

$$\frac{h_2}{t_{w2}} - 3 \le 69\varepsilon\,. \tag{6.241}$$

For the column flange

$$\frac{b_1}{t_{f1}} \le 42\varepsilon\,. \tag{6.242}$$

For the column web

$$\frac{h_1}{t_{w1}} - 3 \le 42\varepsilon\,. \tag{6.243}$$

where for fire resistance design

$$\varepsilon = 0.85\sqrt{\frac{235}{f_y}}\,. \tag{6.244}$$

Calculation of loading is according to Chapter 6.5.3.

6.6.4 Numerical data

The sizes of the frame are $H = 4000$, $L = 4000$ mm. The vertical and horizontal loads are $F = 75$ kN, $F_b = 0.1F$ for the normal design and $F = 0.74$x75 kN, $F_b = 0.1F$ for the fire resistant design. The Young modulus and the shear modulus and the yield stress $E = 2.1\text{x}10^5$ MPa, $G = 0.8\text{x}10^5$ MPa, $f_y = 355$ MPa respectively. The frame is a sway one with class 3 section.

The objective function is the structural mass M according to Eq. (6.221). The unknowns are the dimensions of SHS columns (b_1, t_1) and those of RHS beams (h_2, t_2). If SHS beams are taken into account, the formulae for SHS columns should be used with subscript 2 and their unknowns are b_2 and t_2.

Fabrication limitation

$$b_2 = \frac{h_2}{2} \leq b_1 \ . \tag{6.245}$$

To ease the fabrication, the solution of $b_2 = b_1$ is recommended. In this case the number of unknowns is 3.

6.6.5 Optimization results

Table 6.7 shows the optimum sizes of the frame, when we consider the same SHS section for the column and beam members, means 3 variables (SHS 3v), or different SHS sections for columns and beams, with 4 variables (SHS 4v), or different SHS and RHS sections for columns and beams, with 4 variables, assuming that the width of RHS section is the half of its height. We have used the tables of Dutta (1999) to get the available SHS and RHS sections. Both continuous (unrounded) and discrete optima have been calculated. The two different SHS sections version gives the best solution.

For the frame with the same SHS section at columns and beams we have calculated the optima considering fire resistance. The fire resistance time vary from 225 sec up to 4500 sec. At each timestep we calculate the temperature of the steel with an inner iteration and we can calculate the correction factors for yield stress and Young modulus. The optimization algorithm checks the constraints at each outer iterations.

Table 6.7 Optimization results for the frame (no fire resistance has been taken into account)

Section		h_1 (mm)	t_1 (mm)	h_2 (mm)	t_2 (mm)	K (kg)
SHS 3v	continuous	187.78	4.17	-	4.17	754.87
SHS 3v	discrete	180	5	-	4	775.57
SHS 4v	continuous	195.37	4.34	154.70	3,44	664.69
SHS 4v	**discrete**	**200**	**5**	**150**	**4**	**765.53**
SHS-RHS 4v	continuous	193.35	4.29	187.84	4.17	679.30
SHS-RHS 4v	discrete	180	5	200	5	782.24

Both continuous and discrete optima have been calculated. Optima show that increasing the time of fire resistance, considerable increment of mass can be detected (Table 6.8). If increase the time from 450 sec to 4500 sec (10 times more) we get an increment of mass from 1561 up to 4703 kg (3 times more). One more hour safety means three times more steel in the structure (Figure 5.24).

Table 6.8 Optimization results for the frame (with fire resistance considerations)

Fire resistance time [sec]		h_1 [mm]	t_1 [mm]	t_2 [mm]	K [kg]
225	continuous	256.34	6.33	6.33	1557.57
225	discrete	250	8	6.3	1699.19
450	continuous	256.63	6.34	6.34	1561.07
450	discrete	250	8	6.3	1699.19
900	continuous	257.31	6.36	6.36	1569.39
900	discrete	250	8	6.3	1699.19
1800	continuous	226.47	12.18	7.60	2058.94
1800	discrete	250	12	8	2317.63
2700	continuous	209.16	20.22	12.46	2907.60
2700	discrete	220	20	12	3028.55
3600	continuous	207.12	28.44	17.46	3736.45
3600	discrete	220	25	18	3865.90
4500	continuous	214.83	35.15	22.21	4575.00
4500	discrete	220	35	22	4703.10

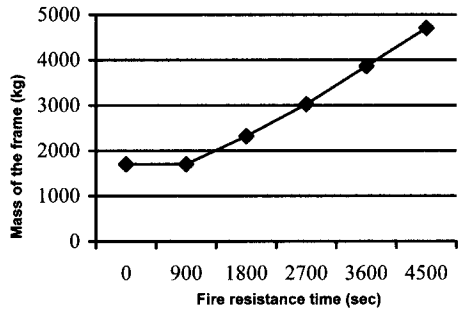

Figure 6.24 Mass of the frame in the function of fire resistance time

6.6.6 Conclusion

Optimization of steel frames for fire safety is a relatively new area. We have calculated the members of a high pressure vessel supporting frame without fire resistance. Using different cross sections (SHS, RHS) the mass of the frame is also different. The best solution occurred, when both columns and beams were made of SHS sections, with four variable sizes. When we consider fire resistance, the time after which its elements still work, needs more material (steel) to be built into the structure. The present example shows, that about 1 hour increment in fire safety needs 3 time more material in the structure. For a designer it is important to know the relation between mass and fire safety. The applied optimization technique was very robust, the modified particle swarm optimization. It calculated both the continuous and discrete optima. The calculation shows that optimization has a large effect. Further investigation will be the application of fire resistant paintings or other materials and to optimize for the cost of the structure.

7

Stiffened Plates

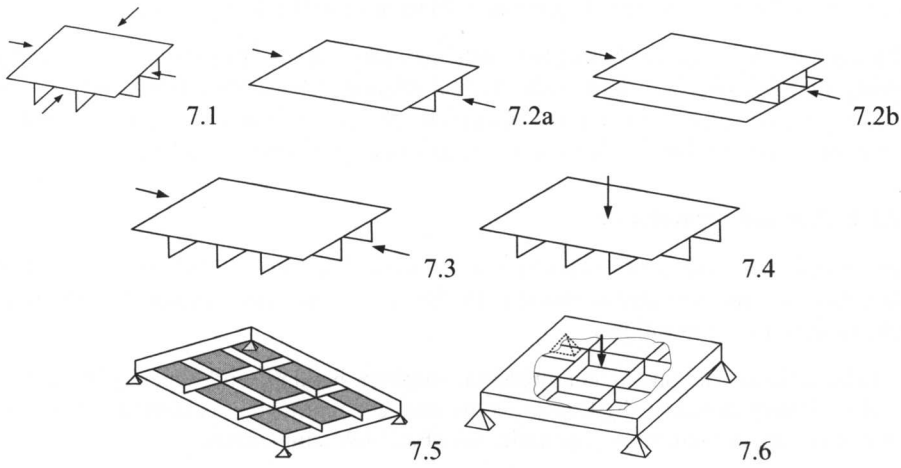

Overview of the sections in Chapter 7

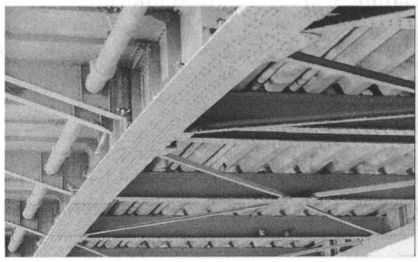

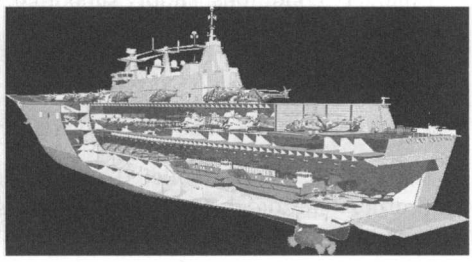

7.1 MINIMUM COST DESIGN OF A WELDED STIFFENED SQUARE PLATE LOADED BY BIAXIAL COMPRESSION

7.1.1 Introduction

Our aim is to show the application of efficient mathematical methods to an important optimization problem. Stiffened plates are used as load-carrying elements of ships, bridges, offshore platforms, roofs, etc. In stability problems of welded structures the effect of initial imperfections and residual welding stresses should be taken into account.

Based on their own experimental results Mikami and Niwa (1996-97) have proposed formulae for the calculation of ultimate buckling strength of orthogonally stiffened plates loaded by uniaxial compression considering the above mentioned effects. Their method is used in an article of Farkas and Jármai (2000) and extended here for plates compressed biaxially.

For the objective function an advanced cost function is used including material, welding and painting costs. Fabrication cost plays an important role in the whole cost and the comparison of the minimum costs of different structural versions enables designers to achieve significant cost savings in the design stage.

To illustrate the effectiveness of the mathematical methods, the problem is solved by using the Rosenbrock's Hillclimb method (Farkas and Jármai 1997), and by an entropy-based unconstrained minimization for the optimization of continuous design variables associated with a branch and bound strategy (Simões and Negrão 1999).

7.1.2 Problem formulation

In an effective structural optimization the variables are selected on the basis of analysis of structural characteristics. In the case of stiffened plates the structural characteristics are as follows:

Loads: uniaxial or biaxial compression, in-plane bending and shear (plate girder webs), lateral pressure, hydrostatic pressure, concentrated, distributed on a line, uniformly distributed, static, dynamic, variable, high temperature.

Material: normal or high-strength steels, aluminium-alloys.

Plate geometry: square, rectangular, triangular, trapezoidal, circular.

Boundary conditions: simply supported, clamped, free, elastic support.

Stiffening geometry: edge-parallel, diagonal-parallel, unidirectional, orthogonal, tridirectional, circular.

Topology: number of stiffeners (variable).

Stiffener shape: flat, rolled T- and L-profile, welded T-profile, cold-formed L-profile, trapezoidal, rectangular hollow section. Possible variables: dimensions of stiffeners.

Connections of stiffeners to base plate: welded, riveted, bolted or bonded.

Fabrication of nodes: welded, riveted, bolted or bonded with L-elements.

From these characteristics we have selected for this study the following:
The investigated plate structure (Figure 7.1) consists of a simply supported square base plate stiffened with an orthogonal grid of flat stiffeners welded to the base plate by fillet welds. It is assumed that the stiffeners in one direction are continuous and in the other direction they are intermittent. The connections of stiffeners are welded by transverse fillet welds.

The uniformly distributed compressive load is acting biaxially in the plane determined by the gravity centers of T-sections, which consist of a part of the base plate and of a stiffener.
The unknown variables are as follows. $\varphi = b/a; t_F; h_S; t_S$. b is the whole side length of the base plate, t_F is the thickness of the base plate, h_S and t_S are the height and the thickness of a flat stiffener. Thus, the number of stiffeners in one direction is $\varphi - 1$. The optima of the variables are sought, which minimize the cost function and fulfil the design constraints.

Numerical data: $b = 8$ m; $N = 9800$ kN; the yield stress is $f_y = 235$ MPa.

7.1.3 Cost function

According to Farkas and Jármai (1997, 2000) the cost function includes material, fabrication (welding) and painting costs

$$K = k_M \rho_0 V + k_F \left[\Theta(\kappa \rho_0 V)^{1/2} + 1.3\left(T_2' + T_2'' + T_2'''\right)\right] + k_P S\,, \tag{7.1}$$

The cost factors are as follows:

Material cost factor is $k_M = 0.5 - 1.0$ \$/kg, fabrication cost factor is $k_F = 12 - 48$ \$/h $= 0.2 - 0.8$ \$/min, painting cost factor is $k_P = 15$ \$/m^2 . We calculate with $k_M = 0.5$ \$/kg and $k_F = 0.6$ \$/min.

The density of the steel is $\rho_0 = 7.85x10^{-6}$ kg/mm^3

The volume of the structure is

$$V = b^2 t_F + 2b(\varphi - 1)h_S t_S\,, \tag{7.2}$$

the difficulty factor expressing the complexity of the structure is $\Theta = 3$
the number of structural parts to be assembled is

$$\kappa = 16 + \varphi - 1 + \varphi(\varphi - 1) = 17 + \varphi^2\,. \tag{7.3}$$

Welding times are as follows:

(a) butt welds of the base plate, in the numerical example the base plate side length is b=8 m, and it is assumed that this base plate is welded from plate elements of dimensions 6mx1.5 m, so the weld length is $L_W = 8b = 64$ m, weld size is t_F , welding technology is GMAW-M (Gas metal arc welding with mixed gas)

for $t_F \leq 15$ mm $\quad T_2' = 0.1861 t_F^2 x64$, (7.4)

for $t_F > 15$ mm $\quad T_2' = 0.1433 t_F^{1.9035} x64$, (7.5)

(b) longitudinal fillet welds connecting the flat stiffeners to the base plate, welding technology is GMAW-M,

$$T_2'' = 0.3258x10^{-3} a_W^2 x4b(\varphi - 1) \tag{7.6}$$

$a_W = 0.4t_S$, but $a_{W.min} = 4$ mm

(c) transversal fillet welds connecting the intermittent flat stiffeners to the continuous ones.

Number of nodes is $(\varphi - 1)^2$, welding technology is SMAW (Shielded metal arc welding)

$$T_2''' = 0.7889x10^{-3} a_W^2 x4h_S(\varphi - 1)^2 \tag{7.7}$$

The superficies to be painted is

$$S = 2b^2 + 4b(\varphi - 1)h_S \tag{7.8}$$

7.1.4 Design constraints

7.1.4.1 *Constraint on global buckling*

$$\frac{N}{A} \leq \sigma_U^* = \sigma_U \frac{\rho_P + \delta_S}{1 + \delta_S}, \tag{7.9}$$

where N is the compression force,

$$A = bt_F + (\varphi - 1)A_S, \tag{7.10}$$

$b = \varphi a$ is the side length of the whole plate, a is the distance between stiffeners, t_F is the thickness of the base plate,

$$\delta_S = \frac{A_S}{at_F}, \tag{7.11}$$

σ_U is the ultimate global buckling strength of the whole, simply supported plate. It is calculated on the basis of the classic formula (American Petroleum Institute 1987)

$$\sigma_{cr} = \frac{\pi^2 D_1}{hb^2}, \tag{7.12}$$

$$h = t_F + A_S/a, \tag{7.13}$$

$$D_1 = D + EI_X/a, \tag{7.14}$$

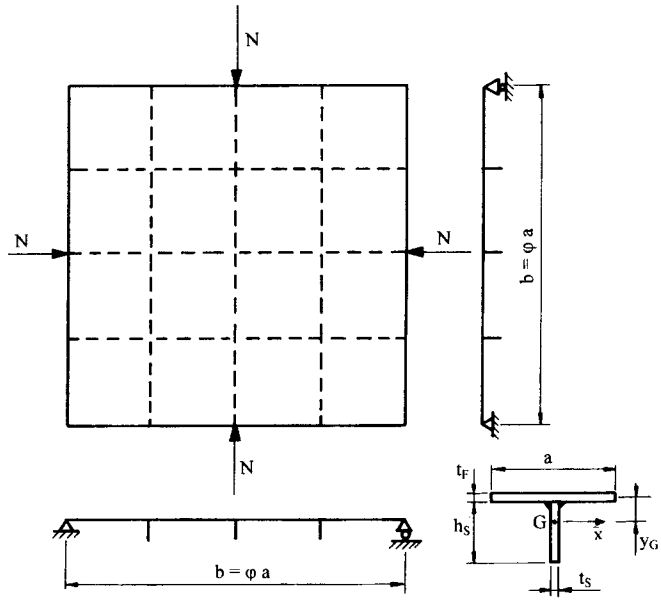

Figure 7.1 Welded square plate with flat stiffeners

$$D = \frac{Et_F^3}{12(1-\nu^2)} = \frac{Et_F^3}{10.92}\ , \tag{7.15}$$

I_X is the moment of inertia of a cross-section containing the flat stiffener and a strip of the base plate of the width of a. The distance of the gravity center of this T-section is

$$y_G = \frac{h_S + t_F}{2}\frac{\delta_S}{1+\delta_S}\ , \tag{7.16}$$

$$I_X = \frac{h_S^3 t_S}{12}\frac{4+\delta_S}{1+\delta_S}, \tag{7.17}$$

$A_S = h_S t_S$ is the cross-sectional area of a flat stiffener, h_S is the height and t_S is the thickness of a flat stiffener.

Since the classic buckling strength formula does not take into account the effect of the initial imperfection and residual welding stresses, we use a reduced buckling strength according to Mikami and Niwa method based on a reduced slenderness

$$\lambda_R = \left(f_y / \sigma_{cr}\right)^{1/2}, \tag{7.18}$$

where f_y is the yield stress. Note that the method of this reduced slenderness is used also in Eurocode 3 (2005)

$$\sigma_U / f_y = 1, \qquad \text{for} \quad \lambda_R \le 0.3, \tag{7.19}$$

$$\sigma_U / f_y = 1 - 0.63(\lambda_R - 0.3), \qquad \text{for} \quad 0.3 < \lambda_R \le 1, \tag{7.20}$$

$$\sigma_U / f_y = 1/(0.8 + \lambda_R^2), \qquad \text{for} \quad \lambda_R > 1, \tag{7.21}$$

The factor of ρ_P is introduced in order to take into consideration the local buckling of the base plate

$$\rho_P = 1 \qquad \text{if} \quad \sigma_{UP} \ge \sigma_U, \tag{7.22}$$

$$\rho_P = \sigma_{UP} / f_y \quad \text{if} \quad \sigma_{UP} < \sigma_U, \tag{7.23}$$

σ_{UP} is the ultimate local buckling strength of a base plate square field, which is assumed to be simply supported and loaded by biaxial compression. The ultimate strength is calculated also by using a reduced slenderness derived from the classic buckling strength

$$\frac{\sigma_{Pcr}}{f_y} = \frac{2\pi^2 E}{10.92 f_y}\left(\frac{t_F}{a}\right)^2, \tag{7.24}$$

$$\lambda_P = \left(\frac{f_y}{\sigma_{Pcr}}\right)^{1/2} = \frac{a/t_F}{40.19\varepsilon}, \qquad \varepsilon = (235/f_y)^{1/2}, \tag{7.25}$$

f_y is the actual yield stress in MPa.

$$\frac{\sigma_{UP}}{f_y} = 1 \qquad \text{for} \quad \lambda_P \le 0.526, \tag{7.26}$$

$$\frac{\sigma_{UP}}{f_y} = \left(\frac{0.526}{\lambda_P}\right)^{0.7} \qquad \text{for} \quad \lambda_P \ge 0.526. \tag{7.27}$$

7.1.4.2 *Constraint on local buckling of flat stiffeners*
According to Eurocode 3 (2005)

$$h_S / t_S \le 14\varepsilon. \tag{7.28}$$

7.1.4.3 *Distortion constraint*

In order to assure the quality of this type of welded structures large deflections due to weld shrinkage should be avoided. It has been shown that the curvature of a beam like structure due to shrinkage of longitudinal and transverse welds can be calculated by relatively simple formulae (Farkas and Jármai 1997). The allowable maximal

residual deformation f_0 is prescribed by design rules. For compression Eurocode 3 (1992) prescribes $f_0 = b/1000$, thus the distortion constraint is defined as

$$f_{max} = 1.5\, C\, b^2/8 \leq f_0 = b/1000. \tag{7.29}$$

Considering fillet welds in two directions we multiply with 1.5 instead of 2, since the interruption of ribs and the residual plastic zones decrease the deflection.
The curvature for steel is

$$C = 0.844\text{x}10^{-3}\, Q_T\, y_T/I_x, \tag{7.30}$$

Q_T is the heat input for double fillet weld

$$Q_T = 1.3\text{x}59.5a_W^2\,. \tag{7.31}$$

In the case of a double fillet weld, we multiply with 1.3 instead of 2, assuming that the second weld is performed after cooling of the first one and its plastic zone overlaps the first one. y_T is the weld eccentricity

$$y_T = y_G - t_F/2\,, \tag{7.32}$$

y_G and I_x are given by Eqs (7.16) and (7.17).

7.1.4.4 *Limitation of the number of spacings between the stiffeners*

Since the classic overall buckling strength is calculated on the basis of the theory of orthotropic plates, a limitation of the number of spacings

$$\varphi \geq 3 \tag{7.33}$$

should be introduced.

7.1.5 Results and conclusions

The results are given in Tables 7.1-7.2. Minimum material cost and minimum total cost results for continuous design variables can be found in Table 7.1 Optimum discrete design variables are given in Table 7.2. The optima are marked by bold letters.

Table 7.1 Minimum material and total cost for continuous variables

φ	t_f	t_s	K_M[\$]	K [\$]
3	18.7	19.8	5362	11603
4	16.1	18.7	5000	**11423**
5	14.5	18.0	**4774**	12714
6	14.6	17.1	4951	13847
7	15.5	16.4	5310	13695

It can be seen that the optimum number of spacings for minimum material cost differs from that for minimum whole cost. The optimal number of spacings

(stiffeners) is smaller for minimum whole cost. This decrease is caused by high fabrication costs. The cost differences between the best and worst structural solutions indicated in tables are 18-22%, thus, it is worth using the optimization procedure. Both mathematical optimization methods have been efficient for this problem.

Table 7.2 Minimum material and total cost for discrete variables

φ	t_f	t_s	K_M[$]	K [$]
3	19	20	5476	**11787**
4	17	19	5222	11905
5	15	18	**4907**	12349
6	16	17	5289	13087
7	17	17	5795	14779

When φ is increases t_S becomes smaller to reduce distortion. t_f is reduced with φ, but for larger φ it must compensate the diminishing t_S.

7.2 OPTIMUM DESIGN AND COST COMPARISON OF A WELDED PLATE STIFFENED ON ONE SIDE AND A CELLULAR PLATE BOTH LOADED BY UNIAXIAL COMPRESSION

7.2.1 Introduction

Stiffened plate is one of the most frequently used structural component in welded structures. Two types of stiffened plates can be constructed: plate stiffened on one side (in the following briefly *stiffened plate*) and cellular plate (Figs 1 and 2). Cellular plates have some advantages over stiffened ones as follows. (a) their torsional stiffness contributes to the overall buckling strength significantly, therefore, their dimensions (height and thickness) can be smaller, (b) their symmetry eliminates the large residual welding distortions, which can occur in stiffened plates due to shrinkage of eccentric welds.

In the present study it is shown that the cellular plates can be cheaper than the stiffened ones. This economy is caused by the advantage mentioned above in (a).
The stiffened and cellular plates have the following structural characteristics:

--loads: uniaxial and biaxial compression, lateral loads, hydrostatic load, static and dynamic (variable) forces;

--material: normal or high-strength steel, aluminium alloys, fiber-reinforced plastics (FRP);

--stiffening topology: stiffening on one, two or more directions;

--stiffener type: flat plate, halved rolled I-section, cold-formed L-shape, trapezoidal;

--fabrication technology: welding, bolting, riveting, bonding (FRP).

In the present study the load is uniaxial compression, the stiffening is constructed with longitudinal halved rolled I-section stiffeners, the material is a higher-strength

steel with yield stress of 355 MPa, the fabrication technology is welding (continuous longitudinal fillet submerged arc – SAW- welds).

We have developed a cost calculation method mainly for welded structures (Farkas & Jármai 1997, Jármai & Farkas 1999, Farkas & Jármai 2003), by which it is possible to give a realistic cost comparison of optimized structural versions. The cost function includes the costs of material, assembly, welding, post-welding works and painting.

The analysis and optimization of cellular plates have been first treated in the doctoral dissertation of Farkas (1984, 1977). The large torsional stiffness of cellular plates is demonstrated by deflection measurements in a welded steel cellular plate model and in a glued plexiglas model. A detailed literature survey is worked out for cellular plates in the book (Farkas & Jármai 1997). The book (Farkas & Jármai 2003) contains studies on stiffened and cellular plates relating to hydrostatic loads, ship deck panels, different kinds of stiffeners, combination of axial compression and lateral load.

This study is a part of our systematic research on economy of welded structures. The economy of some structural types is demonstrated by the comparison of minimum costs of different structural versions. Such a comparison has been performed for various kinds of stiffened cylindrical shells as well (see Chapter 8).

7.2.2 Overall buckling strength of orthogonally stiffened uniaxially compressed plates

The Huber's differential equation of uniaxially compressed orthotropic plates is given by

$$B_x w'''' + 2Hw'''' + B_y w'''' + N_x w'' = 0, \tag{7.34}$$

where the prime (') and dot (˙) superscripts denote partial derivatives with respect to x and y respectively. The corresponding bending and torsional stiffnesses are defined as

$$B_x = \frac{E_1 I_y}{a_y}; B_y = \frac{E_1 I_x}{a_x}; E_1 = \frac{E}{1-\nu^2}, \tag{7.35}$$

for cellular plates in the calculation of B_{xy} and B_{yx} the moments of inertia I_y and I_x can be used, since the shear stresses act similarly than the normal stresses due to bending as it is shown in Figure 7.2.

$$B_{xy} = \frac{GI_y}{a_y}; B_{yx} = \frac{GI_x}{a_x}; G = \frac{E}{2(1+\nu)}, \tag{7.36}$$

$$H = B_{xy} + B_{yx} + \frac{\nu}{2}\left(B_x + B_y\right) = \frac{E_1}{2}\left(\frac{I_y}{a_y} + \frac{I_x}{a_x}\right), \tag{7.37}$$

for plates of quadratic symmetry $H = B_x = B_y$, (7.37a)

i.e. this calculation of the torsional stiffness shows that it equals to the mean value of bending stiffnesses. This fact is verified by a torsional test of a welded steel cellular plate.

For stiffened plates with open-section stiffeners $B_{xy} = B_{yx} = H \approx 0$.

The solution of Eq (7.34) yields the classic buckling formula for critical force of a simply supported rectangular plate

$$N_E = \frac{\pi^2}{b_0^2}\left(B_x \frac{b_0^2}{a_0^2} + 2H + B_y \frac{a_0^2}{b_0^2}\right) \tag{7.38}$$

For a cellular plate with longitudinal stiffeners only

$$B_y = E_1 \frac{t(h+2t)^2}{8}, B_{yx} \approx 0,$$
$$B_{xy} = \frac{Gt(h+2t)^2}{8}, H = B_{xy} + \frac{\nu}{2}B_y + \frac{\nu}{2}B_x. \tag{7.39}$$

For stiffened plates with longitudinal ribs only

$$B_y = 0; N_E = \frac{\pi^2 B_x}{a_0^2}. \tag{7.40}$$

7.2.3 Verification of the torsional stiffness of cellular plates

7.2.3.1 *Derivation of the fundamental differential equation of an orthotropic plate in the case of a uniform transverse load*

On the basis of the theory of plates (Timoshenko 1959), the relationships between the in-plane strains and the derivatives of the transverse deflection w are as follows:

$$\varepsilon_x = -zw'', \varepsilon_y = -zw'', \gamma_{xy} = -2zw''. \tag{7.41}$$

The formulae for stress components are

$$\sigma_x = E_1(\varepsilon_x + \nu\varepsilon_y) = -E_1 z(w'' + \nu w''), \tag{7.42}$$

$$\sigma_y = -E_1 z(w'' + \nu w''), \tau_{xy} = -2Gw''. \tag{7.43}$$

The formulae for the bending and twisting moments per unit length are as follows:

$$m_x = \int \sigma_x z dA = -B_x(w'' + \nu w''), \tag{7.44}$$

$$m_y = -B_y(w'' + \nu w''), \tag{7.45}$$

$$m_{xy} = \int \tau_{xy} z dA = 2B_{xy} w'', m_{yx} = -2B_{yx} w'' . \tag{7.46}$$

From the equilibrium equations of a plate element (Fig.A1) one obtains

$$q_x = m_x' + m_{xy}' = -\left[B_x w''' + \left(2B_{yx} + \nu B_x\right) w'''\right], \tag{7.47}$$

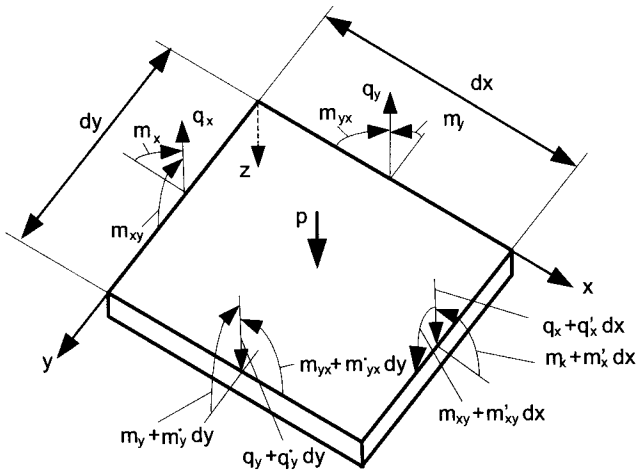

Figure 7.2 Equilibrium of an orthotropic plate element

$$q_y = m_y' - m_{xy}' = -\left[B_y w''' + \left(2B_{xy} + \nu B_y\right) w'''\right], \tag{7.48}$$

and $$q_x' + q_y' + p = 0 . \tag{7.49}$$

Inserting Eq.(7.47) and Eq.(7.48) into Eq.(7.49) yields the Huber's equation for orthotropic plates in the case of a uniform transverse load

$$B_x w'''' + 2Hw'''' + B_y w'''' = p , \tag{7.50}$$

where $$H = B_{xy} + B_{yx} + \frac{\nu}{2}\left(B_x + B_y\right), \tag{7.51}$$

is the torsional stiffness of an orthotropic plate (Farkas 1976).

7.2.3.2 *Verification of the torsional stiffness by a torsional test on a welded steel cellular plate model*

The torsional stiffness of an anisotropic plate can be experimentally determined by measuring the deflection of the free corner of a quadratic plate supported at four corners (Fig. 7.3). For this purpose a welded steel cellular plate model has been used (Fig. 7.4) (Farkas 1974).

The corner deflection can be derived as follows. Using a force F acting on the free corner, the specific torsional moment in one direction is $m_{xy} = -F/2$. In the case of quadratic symmetry the torsional stiffness Eq. (7.50) is

$$H = 2B_{xy} + \nu B_x , \tag{7.51}$$

and from Eq. (7.51) one obtains

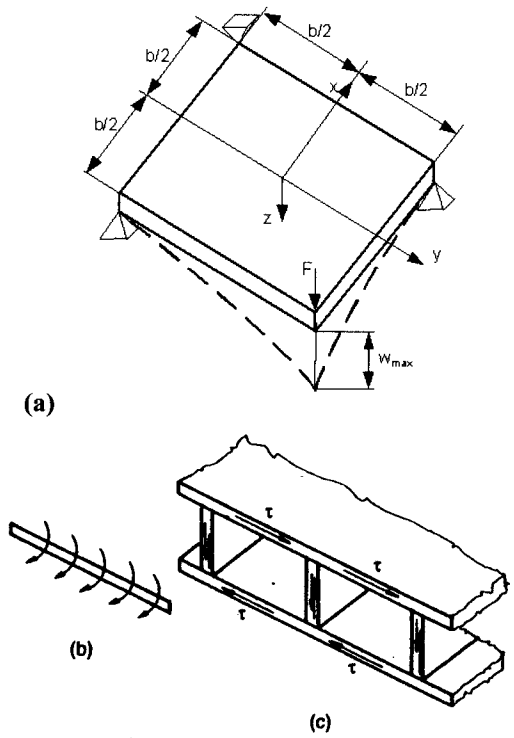

Figure 7.3. (a) A quadratic plate supported at four corners, (b) torsional moments acting on a side, (c) shear stresses in a cellular plate due to torsion

$$2B_{xy} = H - \nu B_x . \tag{7.52}$$

Our aim is to verify that the torsional stiffness of a cellular plate equals to its bending stiffness i.e. $H = B_x$ as it is calculated using formulae of Eq.(7.37) and (7.37a). In this case Eq. (7.46) can be written as

$$m_{xy} = H(1-\nu)w'' = -F/2 , \tag{7.53}$$

or $$w'' = \frac{F}{2H(1-\nu)} . \tag{7.54}$$

Integrating Eq. (7.54) two times and using the boundary conditions

$$w(x=y=b/2)=0, w(x=y=-b/2)=0, w(x=-y=b/2)=0, \tag{7.55}$$

one obtains

$$w=-\frac{F}{2H(1-\nu)}\left(xy+\frac{b}{2}x-\frac{b}{2}y-\frac{b^2}{4}\right), \tag{7.56}$$

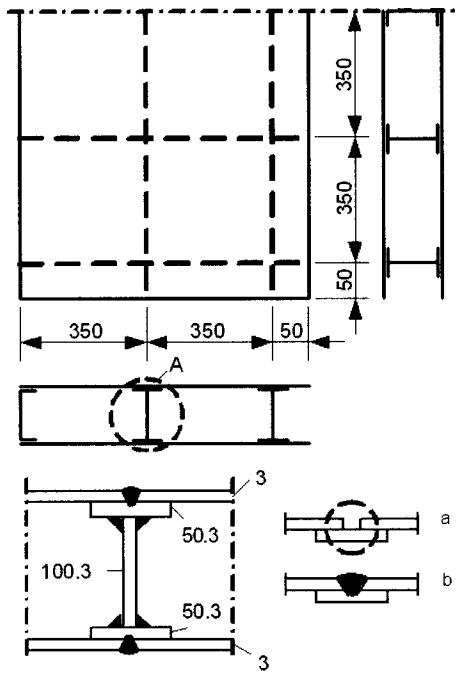

Figure 7.4 Dimensions of the welded steel cellular plate model

The deflection due to bending of the point $x = y = -b/2$ is

$$w_{b.\max}=\frac{Fb^2}{2H(1-\nu)}, \tag{7.57}$$

and the whole deflection considering also the shear deflection is

$$w_{\max}=\frac{Fb^2}{2H(1-\nu)}+\frac{Fb}{2A_wG}=w_{b.\max}+w_q, \tag{7.58}$$

where A_w is the cross-sectional area of a stiffener web. If w_{max} is measured, the torsional stiffness can be calculated from Eq. (7.58) as

$$H=\frac{Fb^2}{2(w_{\max}-w_q)(1-\nu)}, \tag{7.59}$$

The deflection due to a force $F = 40$ kN was $w_{max} = 12.94$ mm, $b = 1400$ mm, $w_q = 1.17$ mm, from Eq. (7.59) one obtains $H = 4.76\text{x}10^9$ Nmm. Since the stresses in the plate due to $F = 40$ kN are small, it is not necessary to consider an effective plate width for the deck plates.

The moment of inertia of a stiffener is

$$I_{xs} = \frac{3x100^3}{12} + 2x150x51.5^2 = 1.0457x10^6 \text{ mm}^4.$$

The value of H obtained from measurement can be compared to the following bending stiffness

$$B_x = E\left(\frac{I_{xs}}{a} + \frac{t_f h_1^2}{2(1-\nu^2)}\right) = 2.1x10^5\left(\frac{1.0457x10^6}{350} + \frac{3x109^2}{0.91x2}\right) = 4.74x10^9 \text{ Nmm}.$$

It can be seen that the measured torsional stiffness equals to the calculated bending stiffness, thus, it is verified that the torsional stiffness of a cellular plate equals to its bending stiffness. Therefore, a cellular plate can be calculated as an isotropic one.

7.2.4 The plate stiffened on one side by longitudinal stiffeners (Fig.7.5)

Overall buckling constraint according to DNV (1995)

Effective cross-sectional area

$$A_e = \frac{h_1 t_w}{2} + b\, t_f + s_e t, s = \frac{b_0}{n}. \tag{7.60}$$

Effective plate width for global plate buckling according to DNV (1995)

$$s_e = \left(\frac{1.8}{\beta} - \frac{0.8}{\beta^2}\right)s \ , \tag{7.61}$$

$$\beta = \frac{s}{t}\sqrt{\frac{f_y}{E}} \quad \text{if} \quad \beta \geq 1 \ , \tag{7.62}$$

$$\beta = 1 \qquad \text{if} \quad \beta < 1 ,$$

$$\sigma = \frac{N}{n\, A_e} \leq \sigma_{cr} = \frac{f_{y1}}{\sqrt{1+\lambda^4}}, f_{y1} = \frac{f_y}{1.1} , \tag{7.63}$$

$$\lambda = \sqrt{\frac{f_{y1}}{\sigma_E}}, \sigma_E = \frac{N_E s}{A_e}, N_E = \frac{\pi^2 B_x}{a_0^2} , \tag{7.64}$$

$$B_x = \frac{EI_y}{s} .$$

The distance of the gravity centre G

$$z_G = \frac{1}{A_e}\left[\frac{h_1 t_w}{2}\left(\frac{h_1}{4}+\frac{t}{2}\right)+ b\ t_f\left(\frac{h_i + t - t_f}{2}\right)\right], \tag{7.65}$$

The moment of inertia

$$I_y = s_e t z_G^2 + \frac{h_1^3 t_w}{96} + \frac{h_1 t_w}{2}\left(\frac{h_1}{4}+\frac{t}{2}-z_G\right)^2 + b\ t_f\left(\frac{h\ + t - t_f}{2} - z_G\right)^2. \tag{7.66}$$

Constraint on stiffener induced failure according to DNV (1995)

$$s_{e1} = \left(1.1 - 0.1\beta\ \right)s_y\ , \tag{7.67}$$

but $s_{e1.\max} = 1$

$$A_{e1} = \frac{h_1 t_w}{2} + b t_f + s_{e1} t, \tag{7.68}$$

$$z_{G1} = \frac{h_1 t_w}{2A_{e1}}\left(\frac{h_1}{4}+\frac{t}{2}\right)+ \frac{b t_f}{2A_{e1}}\left(h_1 + t - t_f\right), \tag{7.69}$$

$$I_{y1} = s_{e1} t z_{G1}^2 + \frac{h_1^3 t_w}{96} + \frac{h_1 t_w}{2}\left(\frac{h_1}{4}+\frac{t}{2}-z_{G1}\right)^2 + I_{y11}, \tag{7.70}$$

$$I_{y11} = b t_f\left(\frac{h + t - t_f}{2} - z_{G1}\right)^2,$$

$$\sigma_{Ex} = \frac{\pi^2 E I_{y1}}{A_{e1} a_0^2}, \tag{7.71}$$

$$\sigma_{ET} = \frac{A_w + A_f\left(\dfrac{t_f}{t_w}\right)^2}{A_{wf}} G\left(\frac{2t_w}{h_1}\right)^2 + \frac{3x2.6\pi^2 E I_z}{A_{wf} a_0^2}, \tag{7.72}$$

where

$$A_w = \frac{h_1 t_w}{2}, A_f = b t_f, A_{wf} = A_w + 3A_f, I_z = \frac{b^3 t_f}{12}, \tag{7.73}$$

$$\lambda_T = \sqrt{\frac{f_y}{\sigma_{ET}}}\ , \tag{7.74}$$

$$\sigma_T = \frac{f_{y1}}{\phi_T + \sqrt{\phi_T^2 - \lambda_T^2}}, \phi_T = 0.5\left(1 + \mu_T + \lambda_T^2\right), \tag{7.75}$$

$$\mu_T = 0.007\left(\lambda_T - 0.6\right), \tag{7.76}$$

$$\lambda_S = \sqrt{\frac{\sigma_k}{\sigma_{Ex}}}, \tag{7.77}$$

where

$$\sigma_k = f_y \quad \text{if} \quad \lambda_T < 0.6, \tag{7.78}$$

$$\sigma_k = \sigma_T \quad \text{if} \quad \lambda_T \geq 0.6.$$

The constraint is formulated as

$$\sigma_1 = \frac{N}{n\ A_{e1}} \leq \sigma_{acr} = \frac{\sigma_k}{\phi + \sqrt{\phi^2 - \lambda_S^2}}, \tag{7.79}$$

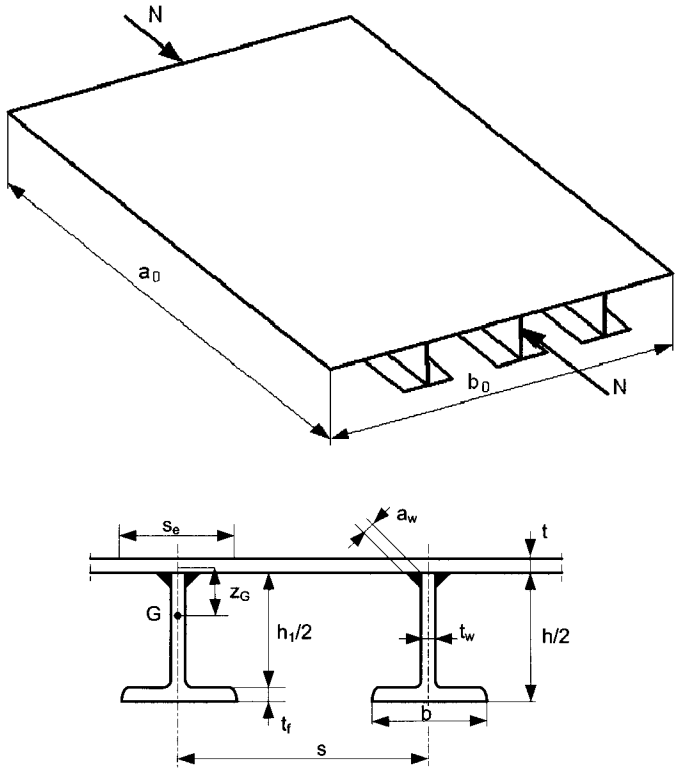

Figure 7.5 A plate longitudinally stiffened on one side

where

$$\phi = 0.5\left(1+\mu+\lambda_S^2\right), \tag{7.80}$$

$$\mu = \frac{\delta z_t A_{el}}{I_{yl}} \quad \text{if} \quad \lambda_T < 0.6, \tag{7.81}$$

$$\mu = \frac{2.3\delta z_t A_{el}}{I_{yl}} \quad \text{if} \quad \lambda_T \geq 0.6,$$

$$\delta = 0.0015 s_x, \tag{7.82}$$

$$z_t = z_{Gyl} + \frac{t_f}{2}. \tag{7.83}$$

The fabrication constraint is expressed as

$$s - b \geq 300\,\text{mm}. \tag{7.84}$$

The cost function includes the cost of material and welding

$$K = K_M + K_W, \tag{7.85}$$

$$K_M = k_M \rho V, k_M = 1\$/kg, \rho = 7.85x10^{-6} kg/mm^3, \tag{7.86}$$

$$V = a_0 b_0 t + (n-1)a_0\left(\frac{h_1 t_w}{2} + b t_f\right), \tag{7.87}$$

$$K_W = k_W\left[\Theta\sqrt{n\rho V} + 1.3Ca_w^2(n-1)2a_0\right], \tag{7.88}$$

where

$$\Theta = 2, k_W = 1.0\$/min, a_w = 0.4t_w, C = 0.3394x10^{-3}\ min/mm^3.$$

The unknowns are as follows: h, n and t.

The other dimensions of a halved rolled I-section are expressed by the main height h according to (Table Curve 2003) (see Appendix C, Eqs C1-C3).

The discrete values of h are according to (Profil Arbed 2001) as follows: 152.4, 177.8, 203.2, 257.2, 308.7, 353.4, 403.2, 454.6, 533.1, 607.6, 683.5, 762.2, 840.7, 910.4 mm.

7.2.5 The longitudinally stiffened cellular plate (Fig.7.6)

The buckling constraint is given by

$$\frac{N}{n_c A_{ec}} \leq \sigma_{crc} = \frac{f_{yl}}{\sqrt{1+\lambda_c^4}}, \tag{7.89}$$

where

$$A_{ec} = \frac{h_{1c} t_{wc}}{2} + b_c t_{fc} + 2 s_{ec} t_c, \tag{7.90}$$

$$s_c = \frac{b_0}{n_c}, \tag{7.91}$$

$$\lambda_c = \sqrt{\frac{f_{y1}}{\sigma_{Ec}}}, \sigma_{Ec} = \frac{N_{Ec} s}{A_{ec}}, \tag{7.92}$$

$$N_{Ec} = \frac{\pi^2}{b_0^2}\left[B_{xc}\left(\frac{b_0}{a_0}\right)^2 + 2H_c + B_{yc}\left(\frac{a_0}{b_0}\right)^2 \right], \tag{7.93}$$

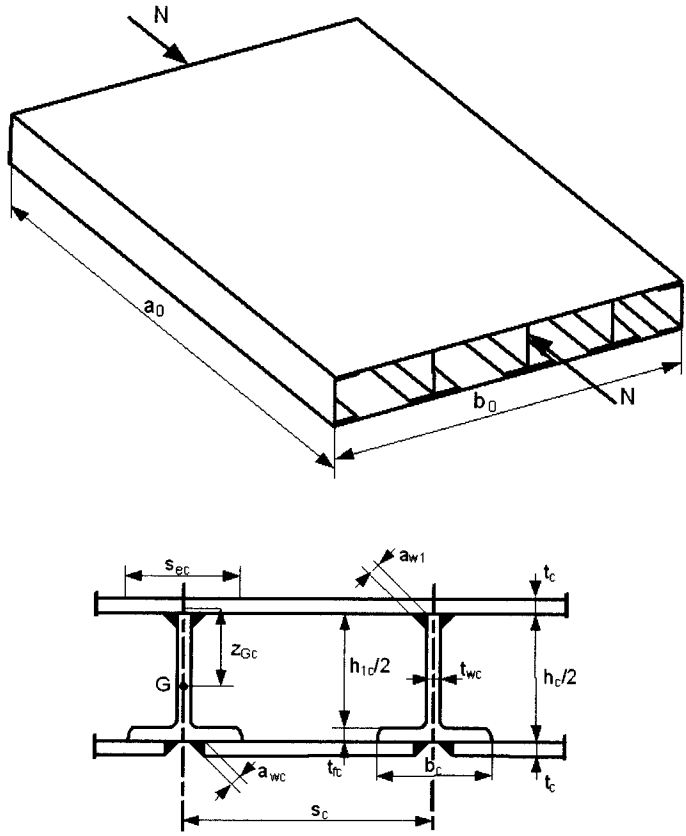

Figure 7.6 A cellular plate with longitudinal stiffeners

where

$$B_{xc} = \frac{E_1 I_{yc}}{s_{1c}}, E_1 = \frac{E}{1-\nu^2}, \tag{7.94}$$

using Eqs (7.35) and (7.39)

$$B_{yc} = \frac{E_1 t_c (h_c + 2t_c)^2}{8}, H_c = \frac{B_{yc}}{2} + \frac{\nu B_{xc}}{2}, \tag{7.95}$$

The distance of the gravity centre is

$$z_{Gc} = \frac{1}{A_{ec}}\left[s_{ec} t_c \left(\frac{h_c}{2} + t_c \right) + \frac{h_{1c} t_{wc}}{2} \left(\frac{h_{1c}}{4} + \frac{t_c}{2} \right) + b_c t_{fc} \left(\frac{h_c + t_c - t_{fc}}{2} \right) \right], \tag{7.96}$$

and the moment of inertia is expressed as

$$I_{yc} = s_{ec} t_c z_{Gc}^2 + s_{ec} t_c \left(\frac{h_c}{2} + t_c - z_{Gc} \right)^2 + \frac{h_{1c}^3 t_{wc}}{96} +$$

$$+ \frac{h_{1c} t_{wc}}{2} \left(\frac{h_{1c}}{4} + \frac{t_c}{2} - z_{Gc} \right)^2 + b_c t_{fc} \left(\frac{h_c + t_c - t_{fc}}{2} - z_{Gc} \right)^2. \tag{7.97}$$

The fabrication constraint is given by

$$s_c - b_c \geq 300 \text{ mm}. \tag{7.98}$$

The cost function includes the material and fabrication costs as follows:

$$K_c = K_{Mc} + K_{Wc}, \tag{7.99}$$

where

$$K_{Mc} = k_M \rho V_c, V_c = 2a_0 b_0 t_c + a_0 (n_c - 1)\left(\frac{h_{1c} t_{wc}}{2} + b_c t_{fc} \right), \tag{7.100}$$

$$K_{Wc} = k_W \left[\Theta \sqrt{n_c \rho V} + 1.3 C a_{w1}^2 2(n_c - 1) a_0 \right] + k_W \left[\Theta \sqrt{n_c \rho V_c} + 1.3 C a_{wc}^2 2 n_c a_0 \right], \tag{7.101}$$

$$a_{w1} = 0.4 t_{wc}, a_{wc} = 0.5 t_c, a_{w1\,min} = 3 \text{ mm}.$$

The unknowns are as follows: n_c, h_c, t_c.

7.2.6 Numerical data

b_0 = 8000, a_0 = 24000 mm, N = 3x10^7 [N], f_y = 355 MPa, E = 2.1x10^5 MPa. Ranges of variables are as follows: t = 4 – 40 mm, h = 152.4 – 910.4 mm, the maximum value of n is given by the fabrication constraint (Eq.7.84 or 7.98)

$$n_{\max} = \frac{b_0}{b + 300} \tag{7.102}$$

The n_{max} values are given in the Table 7.3.

Table 7.3 n_{max}- values for rolled I-sections – dimensions in mm

h	353.4	403.2	454.6	533.1	607.6	683.5	762.2	840.7	910.4	1008.1
b	126.0	142.2	152.9	209.3	228.2	253.7	266.7	292.4	304.1	302.1
n	18	18	17	15	15	14	14	13	13	13

7.2.7 Minimum cost design of the stiffened plate

The optimal values of unknowns are sought, which minimize the cost K and fulfil the design and fabrication constraints. In the ranges defined above it is easy to find these values by a systematic search. The following tables show the details of this search.

Table 7.4 Cost for h = 1008.1, constraint on stiffener failure

n	t mm	constraint MPa	K $
13	9	87.4<87.8	82930
12	10	91<92	78700
11	11	96<96.6	70470
10	12	100.6<100.8	70230
9	14	103<106	67530
8	15	109<110	63300
7	17	113<113.9	60580
6	20	114<116	59390
5	**23**	**115.8<115.9**	**58190**
4	29	108.3<108.8	61540
3	43	84.1<84.6	77000

Table 7.5 Cost K for h = 910.4 mm

n	t [mm]	constraint [MPa]	K [$]
13	26	76<78	83330
12	27	78<79	81220
11	29	77<78	80650
10	**31**	**77<78**	**80070**
9	34	76<77	81000
8	37	73.9<74.1	81930

Table 7.6 Cost K for h = 840.7 mm

n	t [mm]	constraint [MPa]	K [$]
13	34	69<70	89650
12	**36**	**69.0<69.4**	**89560**
11	39	67.2<67.9	90990
10	42	65.5<65.7	92420

From these Tables it is clear that the optimum is h = 1008.1 mm, n = 5 and K = 58190 $.

7.2.8 Minimum cost design of the cellular plate

Similar systematic search can be performed for the cellular plate. The results are summarized in Table 7.7. It should be mentioned that, for $h \leq$ 403.2 mm the fabrication constraint of $a_{wl} \geq 3mm$ is governing instead of $a_{wl} = 0.4t_{wC}$.

Table 7.7 Optimum values of n_C and t_C (mm) as well as the minimum cost for different values of h_C (mm). The optimum is marked by bold letters

h_C	n_C	t_C	constraint [MPa]	K_C [$]
152.4	19	7	286<292	32360
177.8	18	7	291<304	32580
203.2	16	7	307<312	32740
257.2	16	7	307<318	32750
308.7	19	6	310<319	31460
353.4	17	6	305<320	32400
403.2	**18**	**5**	**320.6<321.2**	**31040**
454.6	16	5	308<321	32470
533.1	13	4	317<321	32140
607.6	11	4	317<322	32320
683.5	10	4	291<322	34340

7.2.9 Comparison of the stiffened and the cellular plate

It can be seen from Tables 7.4, 7.5, 7.6 and 7.7 that the minimum cost for the stiffened plate is K_{min} = 58190 $ and for the cellular plate is K_{Cmin} = 31040 $, i.e. the cellular version is 46% cheaper than the stiffened one. This great difference is caused by the different torsional stiffnesses of the two structural types, which allows for the cellular plate to use much more smaller plate thickness and smaller stiffeners than for the plate stiffened on one side.

7.3 ECONOMIC ORTHOGONALLY WELDED STIFFENING OF A UNIAXIALLY COMPRESSED STEEL PLATE

7.3.1 Introduction

The main requirements of a modern engineering structure are the safety, fitness for production and economy. In the optimum design process the safety and producibility are fulfilled by design and fabrication constraints as well as the economy is achieved by the minimization of a cost function.

We have developed a cost calculation method mainly for welded structures, thus, we are able to determine the economy of a structural version and to compare the costs of these versions to each other (Farkas & Jármai 2003). Welded stiffened plates are applied in many steel structures. Our aim is to determine the most economic stiffening of a uniaxially compressed plate. Our structural model is a rectangular

steel plate with simply supported edges, stiffened orthogonally by halved rolled I-section stiffeners welded to the base plate by double fillet welds.

In our other study we have compared the costs of a plate stiffened on one side and a cellular plate both stiffened longitudinally and loaded by uniaxial compression (Farkas & Jármai 2006). Economic stiffening has been determined for an orthogonally stiffened plate loaded by bending (Jármai et al. 2006).
In the optimization process the base plate thickness, as well as the number and height of stiffeners in both directions are sought, which fulfil the buckling constraints and minimize the cost function.

The applied mathematical method is the particle swarm algorithm. The classic buckling stress is derived from the Huber's differential equation (Timoshenko & Gere 1961). This stress is modified taking into account the effect of residual welding stresses and initial imperfections.

The cost function includes the material and fabrication (welding and painting) costs and is formulated according to the fabrication sequence. A series of rolled I-section stiffeners is selected according to the ARCELOR catalogue (Sales Program 2007). The flange width and thickness, as well as the web thickness are expressed by the section height using approximate formulae (see Appendix), thus, in the optimization only five unknowns should be determined.

7.3.2 Problem formulation

Determine the economic orthogonal stiffening of a rectangular plate with given main dimensions a_0 and b_0, subject to a uniformly distributed uniaxial compression of intensity N_x (Figure 7.7), which fulfils the design and fabrication constraints and minimizes the cost function. Halved rolled I-section stiffeners are welded to the base plate by double fillet welds.

Numerical data (Figure 7.7): $a_0 = 24000$, $b_0 = 8000$ mm, $N_x = 3\text{x}10^7$ [N], steel yield stress $f_y = 355$ MPa, elastic modulus $E = 2.1\text{x}10^5$ MPa, shear modulus $G = 0.8\text{x}10^5$, density $\rho = 7.85\text{x}10^{-6}$ kg/mm^3, selected rolled I-sections UB profiles.

Unknowns to be optimized: base plate thickness t, sizes and number of stiffeners in both directions: h_y, h_x, n_y, n_x. Ranges of unknowns: $4 < t < 20$ mm, $152 < h < 1016$ mm, $4<n<n_{max}$, n_{max} are determined by the following fabrication constraints:

$$\frac{b_0}{n_y} - b_y \geq 300\,\text{mm}, \quad \frac{a_0}{n_x} - b_x \geq 300\,\text{mm}. \tag{7.103}$$

The other dimensions of a halved rolled I-section are given by approximate functions of h in Appendix C, Eqs C1-C3.

$$h_1 = h - 2t_f\,.$$

The discrete values of h are as follows: 152.4, 177.8, 203.2, 257.2, 308.7, 353.4, 403.2, 454.6, 533.1, 607.6, 683.5, 762.2, 840.7, 910.4, 1016 mm.

The maximum values of n_i is given by the fabrication constraints Eq. (7.103). The n_{max} values are given in the Table 7.3.

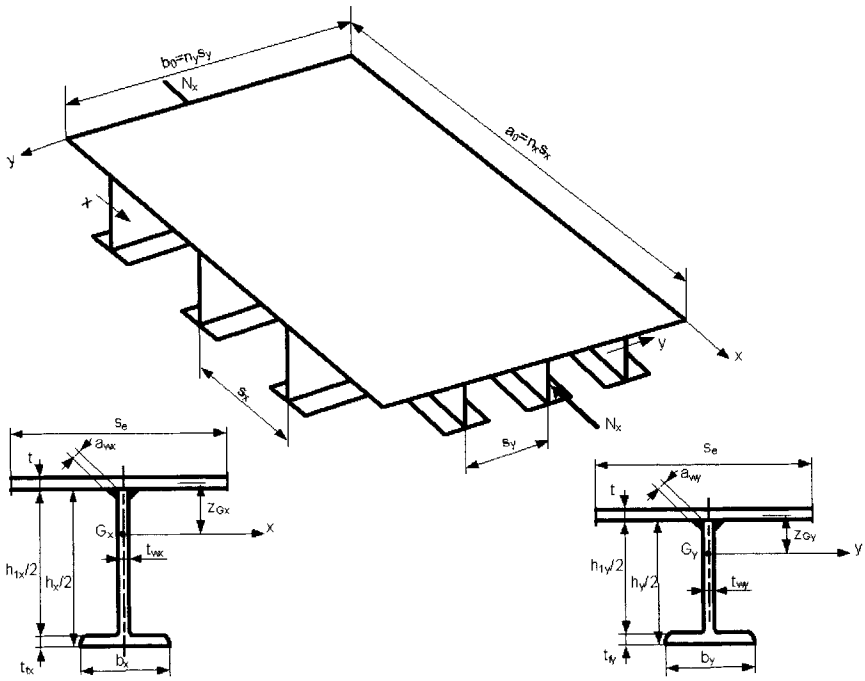

Figure 7.7 Orthogonally stiffened plate loaded by uniaxial compression

7.3.3 Geometric characteristics of stiffeners

Effective cross-sectional areas ($i = x,y$)

$$A_{ei} = \frac{h_{1i}t_{wi}}{2} + b_i t_{fi} + s_{ei}t, s_y = \frac{b_0}{n_y}, s_x = \frac{a_0}{n_x}. \tag{7.104}$$

Effective plate widths in two directions for global plate buckling according to DNV (Det Norske Veritas 1995)

$$s_{ey} = \left(\frac{1.8}{\beta_y} - \frac{0.8}{\beta_y^2}\right)s_y, \quad s_{ex} = \left(\frac{1.8}{\beta_x} - \frac{0.8}{\beta_x^2}\right)s_x, \tag{7.105}$$

$$\beta_y = \frac{s_y}{t}\sqrt{\frac{f_y}{E}} \quad \text{if} \quad \beta_y \geq 1, \tag{7.106a}$$

$$\beta_y = 1 \qquad \text{if} \quad \beta_y < 1,$$

$$\beta_x = \frac{s_x}{t}\sqrt{\frac{f_y}{E}} \quad \text{if} \quad \beta_x \geq 1, \tag{7.106b}$$

$$\beta_x = 1 \qquad \text{if} \quad \beta_x < 1.$$

The distances of the gravity centres G_i

$$z_{Gi} = \frac{1}{A_{ei}}\left[\frac{h_{1i}t_{wi}}{2}\left(\frac{h_{1i}}{4}+\frac{t}{2}\right)+b_i t_{fi}\left(\frac{h_i+t-t_{fi}}{2}\right)\right], \tag{7.107}$$

The moments of inertia

$$I_i = s_{ei}tz_{Gi}^2 + \frac{h_{1i}^3 t_{wi}}{96} + \frac{h_{1i}t_{wi}}{2}\left(\frac{h_{1i}}{4}+\frac{t}{2}-z_{Gi}\right)^2 + b_i t_{fi}\left(\frac{h_i+t-t_{fi}}{2}-z_{Gi}\right)^2. \tag{7.108}$$

The bending stiffnesses

$$B_x = \frac{EI_y}{s_y}; B_y = \frac{EI_x}{s_x}. \tag{7.109}$$

7.3.4 Design constraints

Overall buckling constraint according to DNV (Det Norske Veritas 1995)

$$\sigma = \frac{N_x}{n_y A_{ey}} \leq \sigma_{cr} = \frac{f_{y1}}{\sqrt{1+\lambda^4}}, f_{y1} = \frac{f_y}{1.1}, \tag{7.110}$$

$$\lambda = \sqrt{\frac{f_{y1}}{\sigma_E}}, \sigma_E = \frac{N_E s_y}{A_{ey}}, N_E = \frac{\pi^2}{b_0^2}\left(B_x\frac{b_0^2}{a_0^2}+B_y\frac{a_0^2}{b_0^2}\right). \tag{7.111}$$

It can be seen from the load-carrying capacity formula N_E that, when $a_0 > b_0$, to have a larger N_E, B_x (h_x) should be larger than B_y (h_y).

Constraint on stiffener induced failure according to DNV (1995)

$$s_{ey1} = (1.1 - 0.1\beta_y)s_y, \tag{7.112}$$

but $s_{ey1.\max} = 1$

$$A_{ey1} = \frac{h_1 t_w}{2} + bt_f + s_{ey1}t, \tag{7.113}$$

$$z_{Gy1} = \frac{h_1 t_w}{2A_{ey1}}\left(\frac{h_1}{4}+\frac{t}{2}\right)+\frac{bt_f}{2A_{ey1}}\left(h_1+t-t_f\right), \tag{7.114}$$

$$I_{y1} = s_{ey1} t z_{Gy1}^2 + \frac{h_1^3 t_w}{96} + \frac{h_1 t_w}{2}\left(\frac{h_1}{4} + \frac{t}{2} - z_{Gy1}\right)^2 + I_{y11}, \tag{7.115}$$

$$I_{y11} = b t_f \left(\frac{h + t - t_f}{2} - z_{Gy1}\right)^2,$$

$$\sigma_{Ex} = \frac{\pi^2 E I_{y1}}{A_{ey1} s_x^2}, \tag{7.116}$$

$$\sigma_{ET} = \frac{A_w + A_f\left(\frac{t_f}{t_w}\right)^2}{A_{wf}} G\left(\frac{2t_w}{h_1}\right)^2 + \frac{3x2.6\pi^2 E I_z}{A_{wf} s_x^2}, \tag{7.117}$$

where

$$A_w = \frac{h_1 t_w}{2}, A_f = b t_f, A_{wf} = A_w + 3A_f, I_z = \frac{b^3 t_f}{12}, \tag{7.118}$$

$$\lambda_T = \sqrt{\frac{f_y}{\sigma_{ET}}}, \tag{7.119}$$

$$\sigma_T = \frac{f_{y1}}{\phi_T + \sqrt{\phi_T^2 - \lambda_T^2}}, \phi_T = 0.5\left(1 + \mu_T + \lambda_T^2\right), \tag{7.120}$$

$$\mu_T = 0.007\left(\lambda_T - 0.6\right), \tag{7.121}$$

$$\lambda_S = \sqrt{\frac{\sigma_k}{\sigma_{Ex}}}, \tag{7.122}$$

where

$$\sigma_k = f_y \quad \text{if} \quad \lambda_T < 0.6, \tag{7.123}$$

$$\sigma_k = \sigma_T \quad \text{if} \quad \lambda_T \geq 0.6.$$

The constraint is formulated as

$$\sigma_1 = \frac{N_x}{n_y A_{ey1}} \leq \sigma_{acr} = \frac{\sigma_k}{\phi + \sqrt{\phi^2 - \lambda_S^2}}, \tag{7.124}$$

where

$$\phi = 0.5\left(1 + \mu + \lambda_S^2\right), \tag{7.125}$$

$$\mu = \frac{\delta z_t A_{ey1}}{I_{y1}} \quad \text{if} \quad \lambda_T < 0.6\,, \tag{7.126}$$

$$\mu = \frac{2.3\delta z_t A_{ey1}}{I_{y1}} \quad \text{if} \quad \lambda_T \geq 0.6\,,$$

$$\delta = 0.0015 s_x\,, \tag{7.127}$$

$$z_t = z_{Gy1} + \frac{t_f}{2}\,. \tag{7.128}$$

7.3.5 Cost function

The cost function includes the cost of material, assembly, welding as well as painting and is formulated according to the fabrication sequence.
The cost of material

$$K_M = k_M \rho V_2; k_M = 1.0 \text{ \$/kg.} \tag{7.129}$$

Welding of the base plate from butt welds (3 in direction of a_0 and 3 in direction of b_0) (SAW - submerged arc welding) (Farkas & Jármai 2003)

The fabrication cost factor is taken as k_F = 1.0 \$/min, the factor of complexity of the assembly $\Theta_W = 2$:

$$K_0 = k_F\left[\Theta_W \sqrt{16\rho V_0} + 1.3 C_W t^n (3a_0 + 3b_0)\right], \tag{7.130}$$

$$V_0 = a_0 b_0 t, \tag{7.131}$$

$$\text{for } t < 11 \qquad C_W = 0.1346 x 10^{-3}; n = 2\,, \tag{7.132a}$$

$$\text{for } t \geq 11 \qquad C_W = 0.1033 x 10^{-3}; n = 1.904\,. \tag{7.132b}$$

Welding (n_x-1) stiffeners to the base plate in y direction with double fillet welds (GMAW-C - gas metal arc welding with CO_2):

$$K_{W1} = k_F\left[\Theta_W \sqrt{n_x \rho V_1} + 1.3 x 0.3394 x 10^{-3} a_{wx}^2 2 b_0 (n_x - 1)\right], \tag{7.133}$$

$$a_{Wx} = 0.4\, t_{wx} \text{ but } a_{wx.min} = 3 \text{ mm},$$

$$V_1 = a_0 b_0 t + \left(\frac{h_{1x} t_{wx}}{2} + b_x t_{fx}\right) b_0 (n_x - 1) \tag{7.134}$$

Welding of (n_y – 1) stiffeners to the base plate in x direction with double fillet welds. These stiffeners should be interrupted and welded with fillet welds to the stiffeners in the y direction.

$$K_{W2} = k_F\left[\Theta_W\sqrt{(n_y n_x - n_x + 1)\rho V_2} + 1.3x0.3394x10^{-3} a_{wy}^2 2a_0(n_y - 1) + T_1\right], \qquad (7.135)$$

$$T_1 = 1.3x0.3394x10^{-3} a_{wy}^2 4(n_y - 1)(n_x - 1)\left(\frac{h_{1y}}{2} + b_y\right), \qquad (7.136)$$

$a_{Wy} = 0.4\, t_{wy}$ but $a_{Wy.min} = 3$ mm,

$$V_2 = V_1 + \left(\frac{h_{1y} t_{wy}}{2} + b_y t_{fy}\right) a_0(n_y - 1). \qquad (7.137)$$

Painting

$$K_P = k_P \Theta_P S_P, \qquad k_P = 14.4x10^{-6}\ \$/\text{mm}^2,\ \Theta_P = 2. \qquad (7.138)$$

Surface to be painted

$$S_P = 2a_0 b_0 + a_0 (n_y - 1)(h_{1y} + 2b_y) + b_0 (n_x - 1)(h_{1x} + 2b_x). \qquad (7.139)$$

The total cost

$$K = K_M + K_0 + K_{W1} + K_{W2} + K_P. \qquad (7.140)$$

7.3.6 Optimization and results

The optimization is performed by using the Particle Swarm Optimization algorithm (Kennedy & Eberhardt 1995, Jármai 2005).

The optima of unknowns are as follows.

$h_y = 353.4$, $h_x = 533.1$, $t = 12$ mm, $n_y = 14$, $n_x = 5$. The constraints are fulfilled, since $\sigma = 292 < \sigma_{cr} = 299$ MPa and $\sigma_S = 230 < \sigma_{acr} = 243$ MPa. The minimum cost is $K = 51087$ \$.

It should be mentioned that the calculation of the critical buckling stress (Eqs 7.110, 7.111) according to DNV (1995) takes into account the effect of residual welding stresses and distortions. The considered measure of welding distortion is about $L/1000$ where L is the span length. This distortion can be approximately calculated using our formulae published earlier (Farkas & Jármai 1998).

For the optimum solution with fillet weld size $a_w = 4$ mm, for double fillet welds taking a factor of 1.5: $Q_T = 1.5x59.5a_w^2 = 1428$ J/mm, $z_{Gx}' = 100.36 - 6 = 94.36$ mm,

$$I_x = 1.658x10^8\ \text{mm}^4,\ b_0 = 8000\ \text{mm},$$

$$C = \frac{0.844x10^{-3} Q_T z_G'}{I_x} = 0.6859x10^{-6}\ 1/\text{mm},\ f = \frac{Cb_0^2}{8} = 5.5 < 8 = \frac{b_0}{1000}.$$

Thus, the calculation of the critical buckling stress gives safe values.

7.3.7 Conclusions

Orthogonally stiffened plates are important elements of welded structures, thus their minimum cost design influences the economy of these structures significantly. The basic formula for overall buckling strength shows that the transverse stiffening increases the plate strength in a greater measure.

In the optimization process the height and number of halved rolled I-section stiffeners as well as the base plate thickness is sought, which fulfil the design constraints and minimize the cost function. Both the global buckling and the stiffener induced failure constraints are active.

The particle swarm algorithm has been proved to be efficient in finding the optima.

An approximate calculation shows that the deflections caused by the shrinkage of longitudinal welds are smaller than the deflection taking into account as initial imperfections in the buckling strength formulae.

7.4 ECONOMIC WELDED STIFFENING OF A STEEL PLATE LOADED BY BENDING

7.4.1 Introduction

In the present study a simply supported rectangular plate is chosen with orthogonal stiffening, subject to a uniformly distributed normal load, stiffeners of halves rolled I-section are welded to the base plate on one side with double fillet welds.

The main point of a structural optimization procedure is the selection of variables from the structural characteristics, with the change of which the most suitable structural version can be found. Design constraints relate to the maximum deflection and stresses in the base plate as well as in stiffeners. Fabrication constraints express the need for the free space between stiffener flanges to guarantee suitable place for welding of stiffeners to the base plate.

From the large amount of publications relating to the strength and design of stiffened plates we mention only the following: Mikami and Niwa (1996-1997) have given a design method for orthogonally stiffened uniaxially compressed plates considering the effect of residual welding stresses and initial imperfections. Stability problems have been investigated by Grondin (1999) and Fujikubo (1999). Design of ship panels has been dealt with by Paik (2001, 2003). Some optimum design problems are worked out by authors in the book (Farkas & Jármai 2003).

Our specialty is the use of a cost function, for which the realistic data are collected from literature and industry. Our book (Farkas & Jármai 2003) contains problems of finding economic structural versions by minimization of a cost function. The cost function contains the cost of material, assembly, welding and painting. Since the functions are highly nonlinear, special effective mathematical methods should be used to perform the constrained function minimization. Because of the complexity of problems only numerical treatments is possible to work out. Therefore, the conclusions cannot be general. In spite of this the conclusions can help designers to find suitable structural versions.

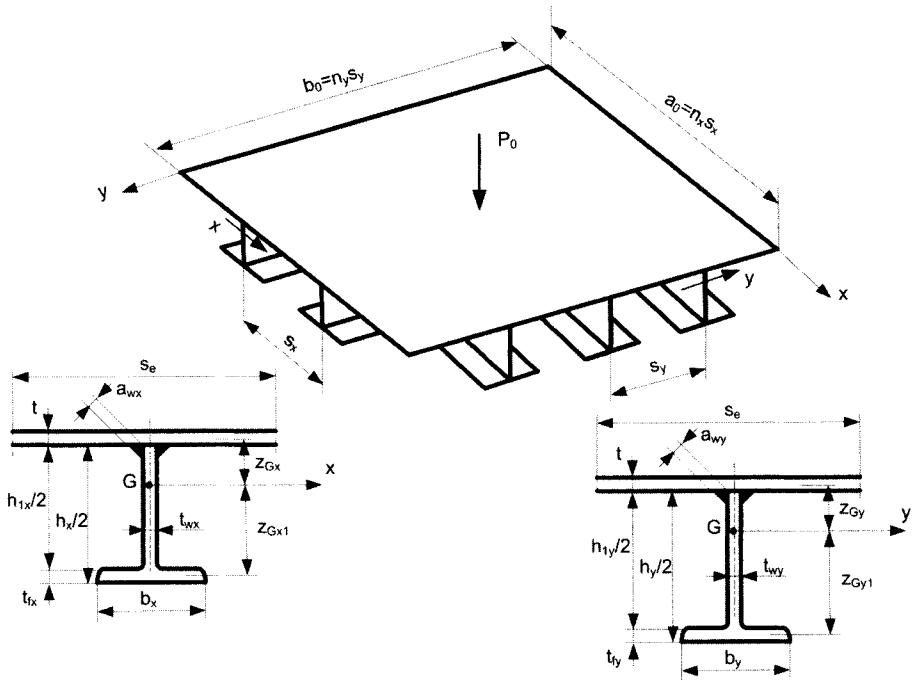

Figure 7.8 Orthogonally stiffened plate subject to a uniformly distributed normal load. Halved rolled I-section stiffeners are used in both directions

7.4.2 Problem formulation

Determine the economic orthogonal stiffening of a rectangular plate with given main dimensions a_0 and b_0, subject to a uniformly distributed normal load of intensity p_0 (Figure 7.8), which fulfils the design and fabrication constraints and minimizes the cost function. Halved rolled I-section stiffeners are welded to the base plate by double fillet welds.

Numerical data (Figure 1): a_0 = 9000, b_0 = 9000 - 18000 mm, p_0 = 0.01 MPa, steel yield stress f_y = 355 MPa, elastic modulus $E = 2.1\text{x}10^5$ MPa, density $\rho = 7.85\text{x}10^{-6}$ kg/mm^3, selected rolled I-sections UB profiles (see Appendix).

Unknowns to be optimized: base plate thickness t, sizes and number of stiffeners in both directions: h_y, h_x, n_y, n_x. Ranges of unknowns: $4 < t < 20$ mm, $152 < h < 1016$ mm, $4<n<n_{max}$, n_{max} are determined by the following fabrication constraints:

$$\frac{b_0}{n_y} - b_y \geq 300 \text{ mm}, \quad \frac{a_0}{n_x} - b_x \geq 300 \text{ mm}. \tag{7.141}$$

7.4.3 Geometric characteristics of stiffeners

The sizes of the halved rolled I-sections UB profiles are calculated according to the size of h in Appendix C, Eqs C1-C3.

Effective cross-sectional areas ($i = x, y$)

$$A_{ei} = \frac{h_{1i}t_{wi}}{2} + b_i t_{fi} + s_{ei}t, s_y = \frac{b_0}{n_y}, s_x = \frac{a_0}{n_x}; s_E = 1.9t\sqrt{\frac{E}{f_y}}. \tag{7.142}$$

when $s_E < s_i$ $\quad s_{ei} = s_E$,
when $s_E > s_i$ $\quad s_{ei} = s_i$.

Note that the formula of s_E is given by ECCS rules (1988)

The distances of the gravity centre G

$$z_{Gi} = \frac{1}{A_{ei}}\left[\frac{h_{1i}t_{wi}}{2}\left(\frac{h_{1i}}{4} + \frac{t}{2}\right) + b_i t_{fi}\left(\frac{h_i + t - t_{fi}}{2}\right)\right], \tag{7.143}$$

$$z_{Gi1} = \frac{h_{1i} + t + t_{fi}}{2} - z_{Gi}. \tag{7.144}$$

The moments of inertia

$$I_i = s_{ei}tz_{Gi}^2 + \frac{h_{1i}^3 t_{wi}}{96} + \frac{h_{1i}t_{wi}}{2}\left(\frac{h_{1i}}{4} + \frac{t}{2} - z_{Gi}\right)^2 + b_i t_{fi}\left(\frac{h_i + t - t_{fi}}{2} - z_{Gi}\right)^2. \tag{7.145}$$

The bending stiffnesses

$$B_x = \frac{EI_y}{s_y}; B_y = \frac{EI_x}{s_x}. \tag{7.146}$$

It should be noted that the torsional stiffnesses for open section ribs are very small and can be neglected when the orthotropic plate theory is used.

7.4.4 Design constraints

7.4.4.1 *Limitation of stresses in the base plate*

stresses from the bending of the whole stiffened plate

$$\sigma_{x\max} = c_x p a_0^2 z_{Gy}\sqrt{\frac{E}{B_x}}, \tag{7.147}$$

$$\sigma_{y\max} = c_y p a_0^2 z_{Gx}\sqrt{\frac{E}{B_x B_y}}, \tag{7.148}$$

stresses from the local bending of a base plate field with clamped edges

$$\sigma_{fx} = 6c_{fx}p_0 s_{\min}^2 / t^2, \tag{7.149}$$

$$\sigma_{fy} = 6c_{fy}p_0 s_{\min}^2 / t^2, \tag{7.150}$$

$$s_{\min} = \min(s_x, s_y). \tag{7.151}$$

The factors of c_{fx} and c_{fy} are given in function of s_{max}/s_{min} in the Appendix B

where

$$s_{\max} = \max(s_x, s_y). \tag{7.152}$$

The stress constraint is defined by

$$\sigma_r = \sqrt{\sigma_1^2 + \sigma_2^2 - \sigma_1\sigma_2} \le f_{y1}; f_{y1} = f_y / 1.1, \tag{7.153}$$

where

$$\sigma_1 = \sigma_{x\,max} + \sigma_{fx}, \tag{7.154}$$

$$\sigma_2 = \sigma_{y\,max} + \sigma_{fy}. \tag{7.155}$$

7.4.4.2 *Limitation of stress in stiffeners*

$$\sigma_{xs\max} = c_{xs} p a_0^2 z_{Gy1} \frac{E}{B_x} \le f_{y1}, \tag{7.156}$$

$$\sigma_{ys\max} = c_{ys} p a_0^2 z_{Gx1} \frac{E}{B_x B_y} \le f_{y1}. \tag{7.157}$$

Note that the local buckling of base plate fields is limited by consideration of the effective width s_E.

7.4.4.3 *Limitation of maximum deflection*

$$w_{x\max} = c_w \frac{p_0 a_0^4}{B_x} \le w_0, \tag{7.158}$$

In the intensity of load the effect of self mass is considered:

$$p = p_0 + \frac{\rho_0 V_2}{a_0 b_0}; \rho_0 = 7.85x10^{-5} \text{ N/mm}^3, \tag{7.159}$$

$$V_1 = a_0 b_0 t + a_0 (n_y - 1)\left(\frac{h_{1y} t_{wy}}{2} + b_y t_{fy}\right), \tag{7.160}$$

$$V_2 = V_1 + b_0 (n_x - 1)\left(\frac{h_{1x} t_{wx}}{2} + b_x t_{fx}\right). \tag{7.161}$$

The factors of c_x, c_y, c_{xs}, c_{ys} and c_w can be calculated in function of

$$\Theta_B = \frac{b_0}{a_0}\sqrt[4]{\frac{B_x}{B_y}}, \tag{7.162}$$

according to Schade (1941) who has given diagrams as a result of the solution of the differential equation for orthotropic plates (Farkas 1983). These diagrams can be approximated by formulae given in Appendix A.

7.4.5 Cost function

The cost function includes the cost of material, assembly, welding and painting and is formulated according to the fabrication sequence.

The cost of material

$$K_M = k_M \rho V_2; k_M = 1.0 \text{ \$/kg.} \tag{7.163}$$

Welding of the base plate from butt welds (one in direction of a_0 and 5 in direction of b_0) (SAW - submerged arc welding) (Farkas & Jármai 2003):

The fabrication cost factor is taken as $k_F = 1.0$ \$/min, the factor of complexity of the assembly $\Theta_W = 2$:

$$K_0 = k_F\left[\Theta_W\sqrt{12\rho V_0} + 1.3C_W t^n(a_0 + 5b_0)\right], \tag{7.164}$$

$$V_0 = a_0 b_0 t, \tag{7.165}$$

for $t < 11 \qquad C_W = 0.1346x10^{-3}; n = 2,$ (7.166a)

for $\qquad C_W = 0.1033x10^{-3}; n = 1.904.$ (7.166b)

Welding (n_y-1) stiffeners to the base plate in x direction with double fillet welds (GMAW-C - gas metal arc welding with CO_2):

$$K_{W1} = k_F\left[\Theta_W\sqrt{n_y \rho V_1} + 1.3x0.3394x10^{-3} a_{wy}^2 2a_0(n_y - 1)\right], \tag{7.167}$$

$a_{Wy} = 0.4\, t_{wy}$ but $a_{wy.min} = 3$ mm.

Welding of $(n_x - 1)$ stiffeners to the base plate in y direction with double fillet welds. These stiffeners should be interrupted and welded with fillet welds to the stiffeners in the x direction.

$$K_{W2} = k_F\left[\Theta_W\sqrt{(n_y n_x - n_y + 1)\rho V_2} + 1.3x0.3394x10^{-3} a_{wx}^2 2b_0(n_x - 1) + T_1\right], \tag{7.168}$$

$$T_1 = 1.3x0.3394x10^{-3} a_{wx}^2 4(n_y - 1)(n_x - 1)\left(\frac{h_{1x}}{2} + b_x\right), \tag{7.169}$$

$a_{Wx} = 0.4\, t_{wx}$ but $a_{wx.min} = 3$ mm.

Painting

$$K_P = k_P \Theta_P S_P, \tag{7.170}$$

$k_P = 14.4\text{x}10^{-6}$ \$/mm^2, $\Theta_P = 2$.

Surface to be painted

$$S_P = 2a_0b_0 + a_0\,(n_y - 1)(h_{1y} + 2b_y) + b_0\,(n_x - 1)(h_{1x} + 2b_x). \tag{7.171}$$

The total cost

$$K = K_M + K_0 + K_{W1} + K_{W2} + K_P. \tag{7.172}$$

7.4.6 Optimization and results

In the numerical example we have kept a_0 constant and change the value of b_0 to determine the optimum sizes and number stiffeners for the stiffened plate.

$b_0 = 9000 - 18000$ mm, $a_0 = 9000$ mm, $p_0 = 0.01$ N/mm^2, yield stress $f_y = 355$ MPa, Young modulus $E = 210000$ MPa.

Size limitations

$$152 \le x_1 \le 1016 \text{ mm},$$

$$152 \le x_2 \le 1016 \text{ mm},$$

$$4 \le x_3 = t \le 20 \text{ mm},$$

$$4 \le x_4 = n_y \le \text{see Eq.(7.141)},$$

$$4 \le x_5 = n_x \le \text{see Eq.(7.141)}.$$

Results are shown in Table 7.8.

Table 7.8 The optimum sizes in mm of the stiffened plate in the function of the length of the plate b_0

b_0	a_0	h_y	h_x	t	n_y	n_x	K [\$]
9000	9000	610	610	10	4	4	18037.5
12000	9000	914	152	7	4	8	21529.4
15000	9000	914	152	8	4	7	25969.3
18000	9000	914	152	9	4	7	31217.3

7.4.7 Conclusions

The analysis and optimization of an orthogonally stiffened plate is shown subject to uniformly distributed normal load. The stiffeners are halved rolled I-sections in both directions. The design constraints relate to the limitation of deflection and stresses in the base plate and in the stiffeners. Fabrication constraints express the limitation of numbers of stiffeners to make it possible to weld the stiffeners to the base plate by double fillet welds. For the calculation of stresses the Schade diagrams are used based on the orthotropic plate theory.

The cost function includes the material, assembly, welding and painting costs. In the structural optimization process the variables are the base plate thickness, the numbers and dimensions of stiffeners in both directions. The optimum design was made using an evolutionary technique, the particle swarm optimization, which is very robust finding the global optima.

Results show that the deflection constraint is active while the other stress and fabrication constraints are passive. In a rectangular plate the stiffeners in the direction of the longer plate side should be smaller. When b_0 approaches to infinite, the stiffeners in x-direction are only working without any stiffeners in y-direction.

7.5 MINIMUM COST DESIGN OF A WELDED SQUARE STIFFENED PLATE SUPPORTED AT FOUR CORNERS

7.5.1 Introduction

A square plate is investigated subject to uniformly distributed normal static load, supported at four corners, stiffened by a square symmetrical orthogonal grid of ribs. Halved rolled I-section stiffeners are used welded to the base plate by double fillet welds (Fig.7.9).

The bending moments are calculated using the force method for torsionless gridworks with different numbers of stiffeners. Constraints on stress in the base plate and in stiffeners as well as on deflection of edge beams and of internal stiffeners are formulated. The cost function includes material, welding as well as painting costs and is formulated according to the fabrication sequence.

The unknowns are the base plate thickness, the dimensions of edge and internal stiffeners and the number of internal stiffeners.
Fig.7.9 shows a schematic drawing of a square stiffened plate supported at four corners.

7.5.2 Geometric characteristics of stiffeners

Edge stiffeners (Fig.7.9)

Effective cross-sectional area

$$A_e = \frac{h_{1e}t_{we}}{2} + b_e t_{fe} + s_E t; s_E = 1.9t\sqrt{\frac{E}{f_y}}. \tag{7.173}$$

The effective plate width s_E is calculated according to design rules of ECCS (1988).

$$h_{1e} = h_e - 2t_{fe}. \tag{7.174}$$

The distances of the gravity centre G_e

$$z_{Ge} = \frac{1}{A_e}\left[\frac{h_{1e}t_e}{2}\left(\frac{h_{1e}}{4} + \frac{t}{2}\right) + b_e t_{fe}\left(\frac{h_e + t - t_{fe}}{2}\right)\right], \tag{7.175}$$

$$z_{Ge1} = \frac{h_{1e} + t + t_{fe}}{2} - z_{Ge}\,. \tag{7.176}$$

The moment of inertia

$$I_{ye} = s_E t z_{Ge}^2 + \frac{h_{1e}^3 t_{we}}{96} + \frac{h_{1e} t_{we}}{2}\left(\frac{h_{1e}}{4} + \frac{t}{2} - z_{Ge}\right)^2 + b_e t_{fe}\left(\frac{h_e + t - t_{fe}}{2} - z_{Ge}\right)^2. \tag{7.177}$$

For internal stiffeners the same formulae hold but without index e (Fig. 7.9).

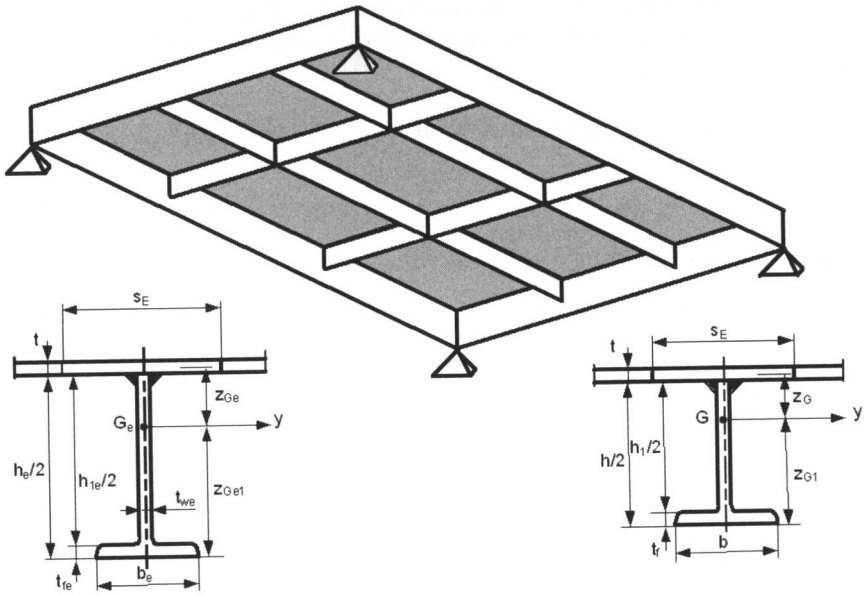

Figure 7.9 A schematic illustration of a stiffened square plate supported at four corners as well as the cross-sections of the edge and the internal stiffeners

7.5.3 Costs as a function of number of internal stiffeners in one direction (*n*)

The corresponding structural volumes are as follows.

$$V_0 = L^2 t;\;\; V_1 = V_0 + 4A_{eS}L;\;\; V_2 = V_1 + nLA_S; \tag{7.178}$$

$$V_3 = V_2 + nLA_S;\;\; A_{eS} = b_e t_{fe} + h_{1e} t_{we}/2\,; \tag{7.179}$$

$$A_S = bt_f + h_1 t_w/2. \tag{7.180}$$

Welding of the base plate with 36 plate parts of dimension 6x1.5 m using GMAW-C single-bevel welds with complete joint penetration

$$K_{F1} = k_F\left(\Theta\sqrt{36\rho V_0} + 1.3C_W x10^{-3} t^{n1} 13L\right). \tag{7.181}$$

Welding of four edge beams to the base plate by double fillet welds using GMAW-C

$$K_{F2} = k_F\left(\Theta\sqrt{5\rho V_1} + 1.3x0.3394x10^{-3}a_{we}^2 8L\right), \tag{7.182}$$

$$a_{we} = 0.4t_{we}, \text{ but } a_{we.min} = 3 \text{ mm}. \tag{7.183}$$

Welding of n continuous internal stiffeners to the base plate and to the edge beams by double fillet welds using GMAW-C

$$K_{F3} = k_F\left[\Theta\sqrt{(n+1)\rho V_2} + 1.3x0.3394x10^{-3}a_w^2 2n(L + h_1 + 2b)\right], \tag{7.184}$$

$$a_w = 0.4t_w, \text{ but } a_{w.min} = 3 \text{ mm}. \tag{7.185}$$

Welding of n intermittent internal stiffeners to the base plate, to the edge beams and to the continuous internal stiffeners (at the internal nodes butt welds are used for connection of bottom flanges)

$$K_{F4} = k_F\left(\Theta\sqrt{[(n+1)n+1]\rho V_3} + 1.3x0.3394x10^{-3}a_w^2\{2nL + 2(n+1)nh_1 + 2n(n+4)b\} + T_1\right)$$

$$T_1 = 1.3C_w t_f^{n1} 2n^2 b\,. \tag{7.186}$$

for butt welds using GMAW-C

for t_f<15 mm C_w =0.1939x10^{-3}, $n_1 = 2$, (7.187a)

for t_f>15 mm $C_w = 0.1496x10^{-3}$, $n_1 = 1.9029$. (7.187b)

Cost of material

$$K_M = k_M \rho V_3\,. \tag{7.188}$$

Cost of painting

$$K_P = \Theta_P k_P S_P\,, \tag{7.189}$$

$$S_P = 2L^2 + 4L(h_{1e} + 2b_e) + 2nL(h_1 + 2b). \tag{7.190}$$

Total cost

$$K = K_M + K_{f1} + K_{f2} + K_{f3} + K_{f4} + K_P. \tag{7.191}$$

7.5.4 Constraints

Stresses in edge beams from bending moment M_e in the top fiber and from local bending of the base plate

$$\sigma_e = \frac{M_e}{I_{ye}} z_{Ge} + cp_0 \frac{a^2}{t^2} \le f_{y1}\,, \tag{7.192}$$

$c = 0.3078$,

the distance between the internal stiffeners $a = \dfrac{L}{n+1}$.

Stress in edge beam bottom fiber from the bending moment

$$\sigma_{e1} = \frac{M_e}{I_{ye}} z_{Ge1} \leq f_{y1} \ . \tag{7.193}$$

Stresses in the internal stiffeners from bending moment M in the top fiber and from local bending of the base plate

$$\sigma = \frac{M}{I_y} z_G + cp_0 \frac{a^2}{t^2} \leq f_{y1} . \tag{7.194}$$

Stress in the internal stiffener bottom fiber from bending moment

$$\sigma_1 = \frac{M}{I_y} z_{G1} \leq f_{y1} . \tag{7.195}$$

Deflection of the edge beams

$$w_e \leq w_{adm} . \tag{7.196}$$

Deflection of the internal stiffener

$$w \leq w_{adm} . \tag{7.197}$$

Bending moments and deflections should be derived for each number of internal stiffeners n.

7.5.5 Numerical data

Yield stress of steel f_y = 355 MPa, $f_{y1} = f_y/1.1$, elastic modulus $E = 2.1\text{x}10^5$ MPa, edge length of the base plate L = 18.0 m, factored load intensity p_0 = 0.0015 N/mm^2, load intensity considering the self mass

$$p = p_0 + \rho_0 \frac{V_3}{L^2}, \tag{7.198}$$

density of steel $\rho = 7.85x10^{-6}$ kg/mm^3, $\rho_0 = 7.85x10^{-5}$ N/mm^3,
admissible deflection $w_{adm} = L/300$, factor for the complexity of assembly $\Theta = 3$, factor for the complexity of painting $\Theta_P = 3$, cost factors: k_M = 1.0 \$/kg, k_F = 1.0 \$/min, $k_P = 14.4\text{x}10^{-6}$ \$/mm^2.

The ranges of unknowns: t = 4 – 40 mm, h and h_e = 152 – 1008.1 mm.
The discrete values of h and the nominal size of I-beam (UB)(in the parenthesis) are as follows according to ARCELOR catalogue

Approximate expressions for other dimensions of rolled I-profiles as a function of h or h_e according to the ARCELOR catalogue are detailed in Appendix C, Eqs C10-C12.

7.5.6 Special case of three internal stiffeners ($n = 3$) (Fig.7.10)

The internal forces in the nodes of the gridwork are F_1, F_2 and F_3 (Fig.7.10), since in the nodes locating in the diagonals internal forces do not occur because of square symmetry. The unknown forces can be determined solving two equilibrium and one deflection equation.

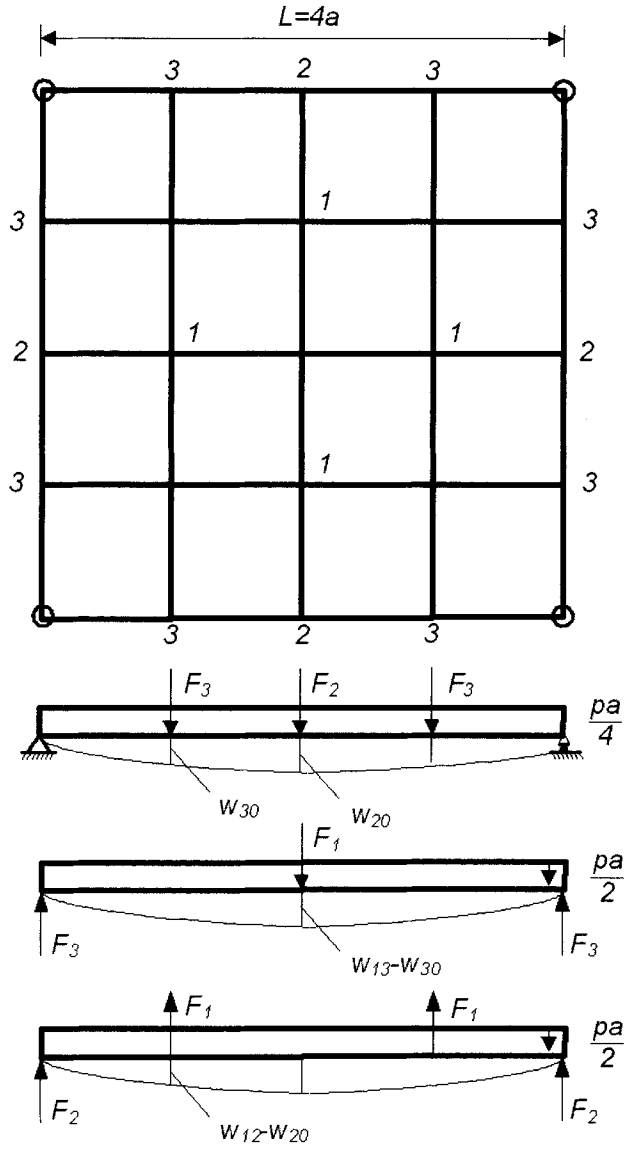

Figure 7.10 A square plate with three internal stiffeners in one direction. Internal forces and deflections

The equilibrium equations are as follows (Fig.7.10):

$$2pa^2 + F_1 = 2F_3, \tag{7.199}$$

$$2pa^2 - 2F_1 = 2F_2. \tag{7.200}$$

The deflection equation expresses the fact that the two internal stiffeners in the nodes No.1 have the same deflection

$$w_{13} - w_{30} = w_{12} - w_{20}, \tag{7.201}$$

where w_{30} and w_{20} are the deflections of the edge beams.

$$EI_{ye} w_{20} = \frac{5pL^5}{48x8x16} + \frac{F_2 L^3}{48} + \frac{11F_3 L^3}{6x64}, \tag{7.202}$$

$$EI_{ye} w_{30} = \frac{57pL^5}{48x32x64} + \frac{11F_2 L^3}{12x64} + \frac{F_3 L^3}{48}, \tag{7.203}$$

$$EI_y w_{13} = \frac{5pL^5}{48x64} + \frac{F_1 L^3}{48}, \tag{7.204}$$

$$EI_y w_{12} = \frac{57pL^5}{48x64x16} - \frac{F_1 L^3}{48}. \tag{7.205}$$

Introducing the notation $\eta = I_{ye} / I_y$ one obtains the equation

$$\frac{11pL^2}{64} + \frac{51.5pL^2\eta}{64} + 32F_1\eta + 5F_2 + 6F_3 = 0. \tag{7.206}$$

Together with the equilibrium equations the solution of the three equations is

$$F_1 = -\frac{pL^2}{256(16\eta - 1)}(103\eta + 111), \tag{7.207}$$

$$F_2 = \frac{pL^2}{16} - F_1, \tag{7.208}$$

$$F_3 = \frac{pL^2}{16} + \frac{F_1}{2}. \tag{7.209}$$

The maximum bending moment in the edge beams

$$M_e = \frac{pL^3}{16x8} + \frac{F_A L}{2} - \frac{F_3 L}{4}, F_A = \frac{pL^2}{16} + \frac{F_2}{2} + F_3, \tag{7.210}$$

and in the internal stiffener

$$M = \frac{pL^3}{16x4} + \frac{F_1 L}{4}, \tag{7.211}$$

The constraint on maximum deflection for an edge beam is expressed as

$$w_{20.0} \le L/300\,, \tag{7.212}$$

and for an internal stiffener

$$w_{13.0} \le L/300\,, \tag{7.213}$$

$w_{20.0}$ and $w_{13.0}$ should be calculated with p_0 instead of p:

$$EI_{ye}w_{20} = \frac{5pL^5}{48x8x16} + \frac{F_2L^3}{48} + \frac{11F_3L^3}{6x64}\,, \tag{7.202}$$

$$F_{10} = -\frac{p_0L^2}{256(16\eta - 1)}(103\eta + 111)\,, \tag{7.214}$$

$$F_{20} = \frac{p_0L^2}{16} - F_{10}\,, \tag{7.215}$$

$$F_{30} = \frac{p_0L^2}{16} + \frac{F_{10}}{2}\,, \tag{7.216}$$

$$w_{20.0} = \frac{5p_0L^5}{48x8x16EI_{ye}} + \frac{F_{20}L^3}{48EI_{ye}} + \frac{11F_{30}L^3}{6x64EI_{ye}}\,, \tag{7.217}$$

$$w_{13.0} = \frac{5p_0L^5}{48x64EI_y} + \frac{F_{10}L^3}{48EI_y}\,. \tag{7.218}$$

7.5.7 Special case of four internal stiffeners (n = 4) (Fig.7.11)

Similar than in the case of n = 3, there are also three unknown forces F_2, F_3 and F_5, since in the nodes No.1 and No.4 internal forces do not occur because of symmetry. The two equilibrium equations are as follows:

$$\frac{5}{2}pa^2 + 2F_2 = 2F_5\,, \tag{7.219}$$

$$\frac{5}{2}pa^2 - 2F_2 = 2F_3\,. \tag{7.220}$$

The deflection equation is expressed as

$$w_{23} - w_{30} = w_{25} - w_{50}\,, \tag{7.221}$$

where

$$EI_y w_{23} = \frac{29pa^5}{12} - \frac{11F_2a^3}{6}\,, \tag{7.222}$$

$$EI_y w_{25} = \frac{31pa^5}{8} + \frac{14F_2a^3}{3}, \tag{7.223}$$

$$EI_{ye} w_{30} = \frac{31pa^5}{16} + \frac{14F_3a^3}{3} + \frac{17F_5a^3}{6}, \tag{7.224}$$

$$EI_{ye} w_{50} = \frac{29pa^5}{24} + \frac{17F_3a^3}{6} + \frac{11F_5a^3}{6}. \tag{7.225}$$

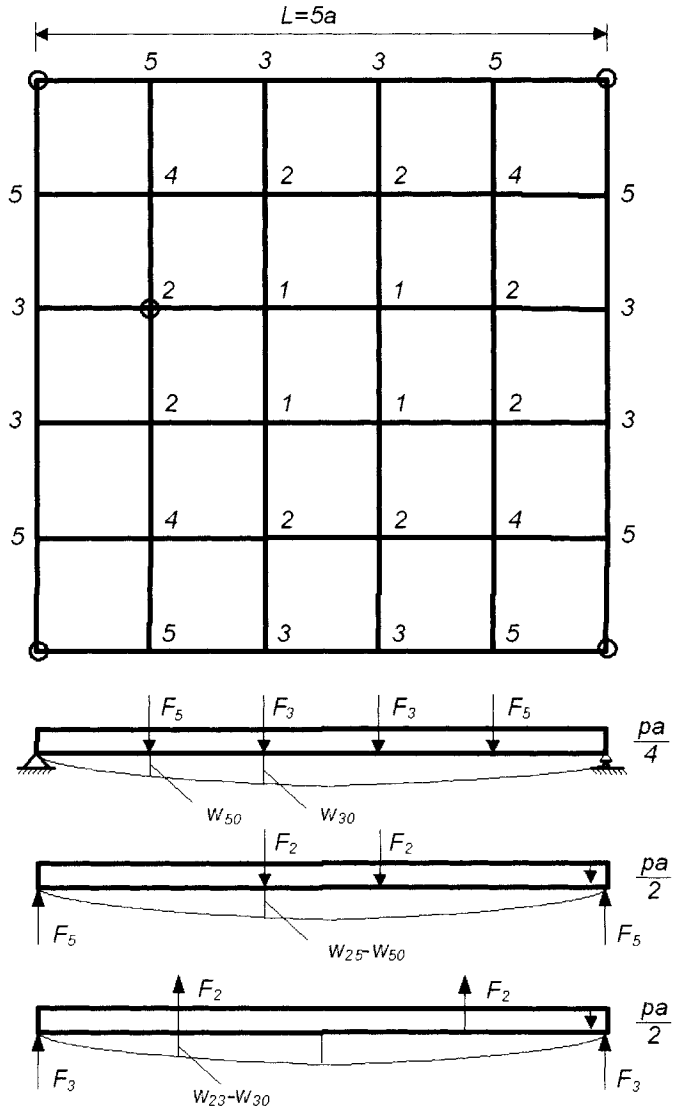

Figure 7.11 A square plate with four internal stiffeners in one direction. Internal forces and deflections

Solving the two equilibrium and one deflection equation one obtains

$$F_3 = \frac{460\eta + 155}{312\eta - 40} pa^2, \tag{7.226}$$

$$F_2 = \frac{F_5}{2} - \frac{F_3}{2}, \tag{7.227}$$

$$F_5 = \frac{5pa^2}{2} - F_3, \tag{7.228}$$

The maximum bending moment in the edge beam is given by

$$M_e = \frac{pL^3}{160} + \frac{2F_3L}{5} + \frac{F_5L}{5}. \tag{7.229}$$

The maximum bending moment in the internal stiffeners is the larger of the following two values

$$M_3 = \frac{pL^3}{80} - \frac{F_2L}{5}, \tag{7.230}$$

$$M_5 = \frac{pL^3}{80} + \frac{2F_2L}{5}, \tag{7.231}$$

$$M = \max(M_3, M_5). \tag{7.232}$$

Deflection constraints should be calculated with forces using p_0 instead of p:

$$F_{30} = \frac{460\eta + 155}{312\eta - 40} p_0a^2, F_{50} = \frac{5p_0a^2}{2} - F_{30}. \tag{7.233}$$

Deflection constraint for edge beams

$$w_e = \frac{1}{EI_{ye}}\left(\frac{3125p_0a^5}{384x4} + \frac{59F_{30}a^3}{12} + \frac{71F_{50}a^3}{24}\right) \le \frac{L}{300}, \tag{7.234}$$

and for internal stiffener

$$w = \frac{1}{EI_y}\left(\frac{3125p_0a^5}{384x2} + \frac{59F_2a^3}{12}\right) \le \frac{L}{300}. \tag{7.235}$$

7.5.8 Special case of five internal stiffeners (n = 5) (Fig.7.12)

Unknowns: $F_2, F_4, F_5, F_6, F_8, F_9$
Equilibrium equations:

$$3pa^2 + 2F_5 + F_4 = 2F_9, \tag{7.236}$$

$$3pa^2 - 2F_5 + F_2 = 2F_8, \tag{7.237}$$

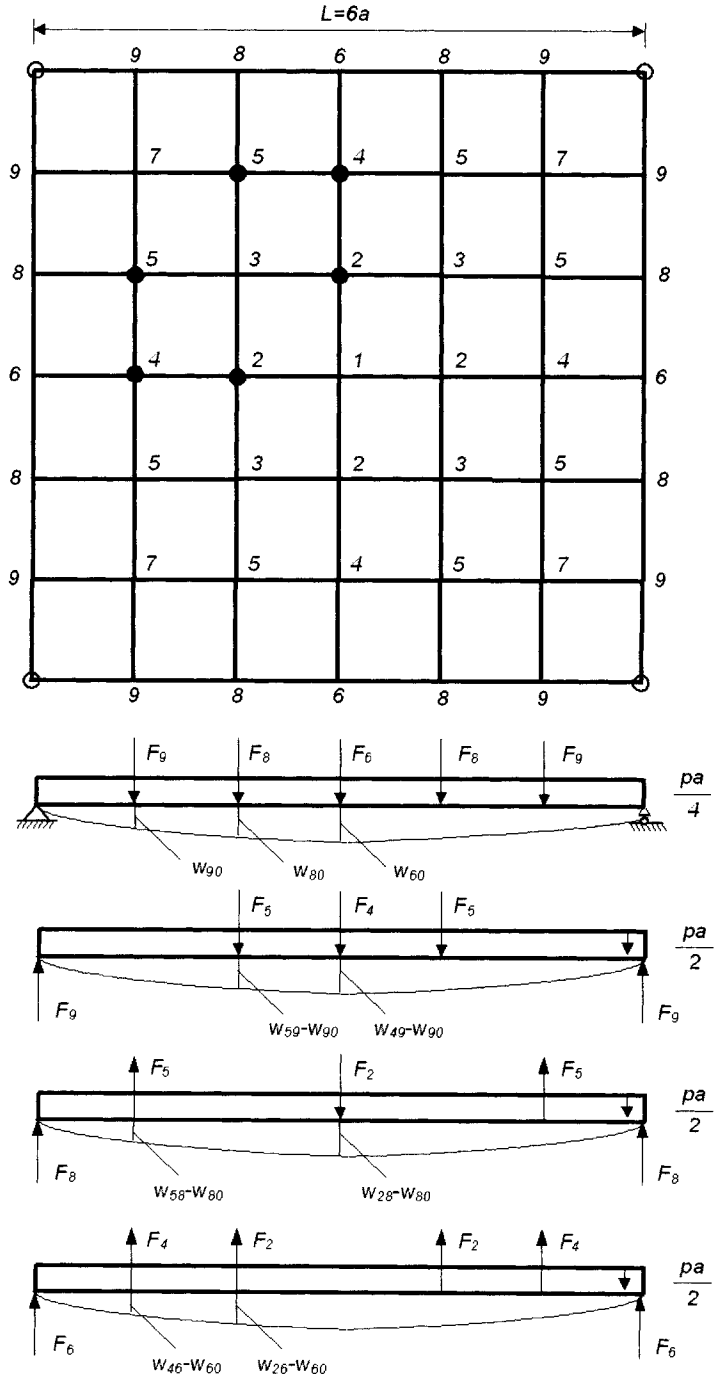

Figure 7.12 A square plate with five internal stiffeners in one direction. Internal forces and deflections

$$3pa^2 - 2F_4 - 2F_2 = 2F_6 . \tag{7.238}$$

Deflection equations:

For the node 5

$$w_{59} - w_{90} = w_{58} - w_{80} . \tag{7.239}$$

For the node 4

$$w_{49} - w_{90} = w_{46} - w_{60} . \tag{7.240}$$

For the node 2

$$w_{28} - w_{80} = w_{26} - w_{60} . \tag{7.241}$$

The deflections are as follows
for edge beam

$$EI_{ye} w_{60} = \frac{135pa^5}{32} + \frac{9F_6 a^3}{2} + \frac{23F_8 a^3}{3} + \frac{13F_9 a^3}{3} , \tag{7.242}$$

$$EI_{ye} w_{80} = \frac{11pa^5}{3} + \frac{23F_6 a^3}{6} + \frac{20F_8 a^3}{3} + \frac{23F_9 a^3}{6} , \tag{7.243}$$

$$EI_{ye} w_{90} = \frac{205pa^5}{96} + \frac{13F_6 a^3}{6} + \frac{23F_8 a^3}{6} + \frac{7F_9 a^3}{3} , \tag{7.244}$$

for the stiffener 9-9

$$EI_y w_{59} = \frac{22pa^5}{3} + \frac{23F_4 a^3}{6} + \frac{20F_5 a^3}{3} , \tag{7.245}$$

$$EI_y w_{49} = \frac{135pa^5}{16} + \frac{9F_4 a^3}{2} + \frac{23F_5 a^3}{3} , \tag{7.246}$$

for the stiffener 8-8

$$EI_y w_{58} = \frac{205pa^5}{48} + \frac{13F_2 a^3}{6} - \frac{7F_5 a^3}{3} , \tag{7.247}$$

$$EI_y w_{28} = \frac{135pa^5}{16} + \frac{9F_2 a^3}{2} - \frac{13F_5 a^3}{3} , \tag{7.248}$$

for the stiffener 6-6

$$EI_y w_{46} = \frac{205pa^5}{48} - \frac{23F_2 a^3}{6} - \frac{7F_4 a^3}{3} , \tag{7.249}$$

$$EI_y w_{26} = \frac{22pa^5}{3} - \frac{20F_2 a^3}{3} - \frac{23F_4 a^3}{6} , \tag{7.250}$$

After the substitution of Eqs (7.242-7.250) into Eqs (7.239, 7.240 and 7.241) one obtains

$$-208F_2\eta + 368F_4\eta + 864F_5\eta + 160F_6 + 272F_8 + 144F_9 = -147pa^2(1+2\eta) \quad (7.251)$$

$$368F_2\eta + 656F_4\eta + 736F_5\eta + 224F_6 + 368F_8 + 192F_9 = -200pa^2(1+2\eta) \quad (7.252)$$

$$1072F_2\eta + 368F_4\eta - 416F_5\eta + 64F_6 + 96F_8 + 48F_9 = -53pa^2(1+2\eta) \quad (7.253)$$

After the solution of six equations (7.236, 7.237, 7.238, 7.251, 7.252, 7.253) we calculate the bending moments and deflections to check the constraints. The maximum bending moment in the edge beam can be expressed as

$$M_e = \frac{9pa^3}{8} + 3F_A a - 2F_9 a - F_8 a\,. \quad (7.254)$$

The governing bending moment in the internal stiffeners M is the maximum from the following three bending moments

$$M_1 = \frac{9pa^3}{4} + 3F_9 a - F_5 a\,, \quad (7.255)$$

$$M_2 = \frac{9pa^3}{4} + 3F_8 a + 2F_5 a\,, \quad (7.256)$$

$$M_3 = \frac{9pa^3}{4} + 3F_6 a + 2F_4 a + F_2 a\,, \quad (7.257)$$

$$M = \max(M_1, M_2, M_3)\,. \quad (7.258)$$

Deflection constraints should be calculated with forces using p_0 instead of p (F_{20},F_{40},F_{50},F_{60},F_{80},F_{90}):

$$w_e = w_{60} = \frac{1}{EI_{ye}}\left(\frac{135p_0a^5}{32} + \frac{9F_{60}a^3}{2} + \frac{23F_{80}a^3}{3} + \frac{13F_{90}a^3}{3}\right) \le \frac{L}{300}\,, \quad (7.259)$$

$$w_1 = \frac{1}{EI_y}\left(\frac{135p_0a^5}{16} - \frac{23F_{20}a^3}{3} - \frac{13F_{40}a^3}{3}\right) \le \frac{L}{300}\,. \quad (7.260)$$

7.5.9 Optimization results

Results obtained for continuous variables by the Snyman-Fatti global minimization algorithm are summarized in Table 7.9.

Table 7.9 Results obtained by the global minimization algorithm. Dimensions and deflections in mm, stresses in MPa, costs in $

n	h_e	h	t	σ_{e1}	σ_e	σ_1	σ	w_e	w	K
3	941.40	557.27	14.50	224	316	110	104	38	47	108423
4	1005.13	590.02	8.34	87	190	272	150	58.7	50.9	98253
5	961.47	778.45	11.98	148	243	259	314	50.8	42.7	122502

Results obtained for continuous and discrete variables by PSO are summarized in Table 7.10.

Table 7.10 Results obtained by PSO for continuous (cont) and discrete (disc) variables. Dimensions and deflections in mm, stresses in MPa, costs in $

N	h_e	h	t	σ_{e1}	σ_e	σ_1	σ	w_e	w	K
3 cont	945.14	560.44	14.08							112025
3 disc	1016	607.6	14	208	310	112	106	36.1	47.6	118500
4 cont	1004.38	589.97	8.35							97993
4 disc	1016	607.6	9	109	286	205	285	51.6	51.7	106800
5 cont	953.43	818.95	12.78							127210
5 disc	1008.1	762.2	12	142	233	301	299	45.9	42.7	134200

It can be seen that $n_{opt} = 4$. The stress constraints are active for $n = 3$ and $n = 5$, the deflection constraint is active for $n = 4$.

7.5.10 Conclusions

A plate supported at four corners and stiffened by open section ribs can be calculated as a torsionless gridwork. In the case of square symmetry the equations of the force method can be significantly simplified. Halved rolled I-section stiffeners can be used with different dimensions for edge and internal ribs.

The uniformly distributed normal load causes also local bending stresses in the base plate fields. Design constraints relate to the stresses in the base plate and in stiffeners as well as to deflections of stiffeners. Fabrications constraints guarantee the suitable welding technology.

The cost function includes the material, welding and painting costs and is formulated in function of the number of stiffeners in one direction (n). The costs are analyzed considering the fabrication sequence.

Since the formulae of constraints are different for different number of stiffeners, the optimization should be carried out separately for each stiffener number. In our numerical problem the optimization is performed for $n = 3$, 4 and 5 and it is found that the minimum cost design can be realized taking $n = 4$.

The used two different mathematical function minimization methods, namely the Snyman-Fatti global optimization algorithm and the particle swarm optimization (PSO) have proved to be suitable for such optimization problems and have given nearly the same results.

7.6 MINIMUM COST DESIGN OF A WELDED STEEL SQUARE CELLULAR PLATE SUPPORTED AT FOUR CORNERS

7.6.1 Introduction

Cellular plates can be applied in various structures e.g. in floors and roofs of buildings, in bridges, ships, machine structures etc. Cellular plates have the following advantages over the plates stiffened on one side: (a) because of their large torsional stiffness the plate thickness can be decreased, which results in decrease of welding cost, (b) their planar surface is more suitable to corrosion protection, (c) their symmetric welds do not cause residual distortion.

In previous studies (Farkas 1985, Farkas & Jármai 2006) it has been shown that cellular plates can be calculated as isotropic ones, bending moments and deflections can be determined by using classic results of isotropic plates for various load and support types.

A large research project was performed by Williams (1969) who used a welded cellular plate model for double bottom of ships. Pettersen (1979) has worked out a detailed analysis of double-bottom plates of ships. Evans and Shanmugam (1984), Shanmugam and Evans (1984) and Shanmugam and Balendra (1986) have treated the analytical problems of cellular plates relating to the ship construction.

A base plate for transportation of heavy structures may be built by using an orthogonal grid welded from rolled I-beams. The lower face plate has been joined to the grid by plug welds (Sahmel 1978). In the revolving frame of surface mining equipment (dragline) a platform for boom, cab, power unit and other structural parts forms an all-welded multi-cell structure (Birchfield 1981). Laser welding technology has been used for welding of "Norsial" metallic sandwich plates and a corrugated sheet sandwiched between them (Haroutel 1982).

In the book (Farkas & Jármai 1997) some problems can be found about cellular plates. Welded cellular plates for ships investigated in (Jármai et al. 1999, Farkas & Jármai 2003) consist of two face sheets and some longitudinal ribs of square hollow section welded between them using arc-spot welding technology.

In the present chapter a cellular plate is designed, which is supported at four corners and subject to a uniformly distributed normal load.

In order to guarantee a suitable fabrication procedure halved rolled I-section stiffeners are used, their web is welded to the upper base plate by double fillet welds and the bottom base plate parts are welded to the stiffener flanges also by fillet welds (Fig. 7.13).

7.6.2 Derivation of the fundamental differential equation of an orthotropic plate in the case of a uniform transverse load

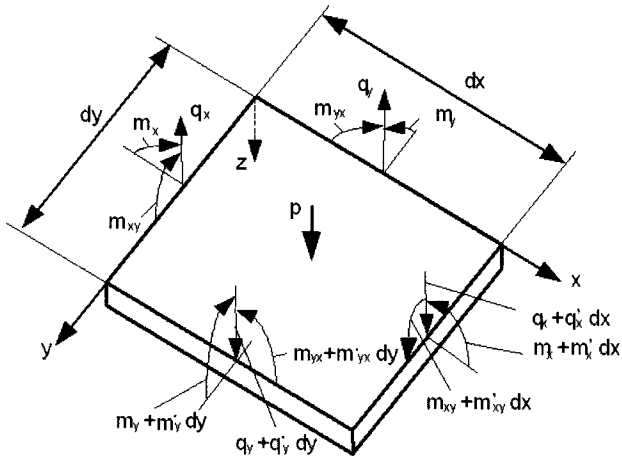

Fig. 7.13 Equilibrium of an orthotropic plate element

On the basis of the theory of plates the relationships between the in-plane strains and the derivatives of the transverse deflection w are as follows:

$$\varepsilon_x = -zw'', \varepsilon_y = -zw'', \gamma_{xy} = -2zw'. \tag{7.261}$$

The prime (') and dot (˙) superscripts denote partial derivatives with respect to x and y respectively.

The formulae for stress components are

$$\sigma_x = E_1\left(\varepsilon_x + \nu\varepsilon_y\right) = -E_1 z\left(w'' + \nu w''\right), \tag{7.262}$$

$$\sigma_y = -E_1 z\left(w'' + \nu w''\right), \tau_{xy} = -2Gw'. \tag{7.263}$$

The formulae for the bending and twisting moments per unit length are as follows:

$$m_x = \int \sigma_x z dA = -B_x\left(w'' + \nu w''\right), \tag{7.264}$$

$$m_y = -B_y\left(w'' + \nu w''\right), \tag{7.265}$$

$$m_{xy} = \int \tau_{xy} z dA = 2B_{xy} w', m_{yx} = -2B_{yx} w'. \tag{7.266}$$

From the equilibrium equations of a plate element (Fig.7.13) one obtains

$$q_x = m_x' + m_{xy}' = -\left[B_x w''' + \left(2B_{yx} + \nu B_x\right)w'''\right], \tag{7.267}$$

$$q_y = m_y' - m_{xy}' = -\left[B_y w''' + \left(2B_{xy} + \nu B_y\right)w'''\right], \tag{7.268}$$

and $q_x' + q_y' + p = 0$. (7.269)

Inserting Eq.(7.267) and Eq.(7.268) into Eq.(7.269) yields the Huber's equation for orthotropic plates in the case of a uniform transverse load

$$B_x w'''' + 2Hw'''' + B_y w'''' = p, \tag{7.270}$$

where

$$H = B_{xy} + B_{yx} + \frac{\nu}{2}\left(B_x + B_y\right), \tag{7.271}$$

is the torsional stiffness of an orthotropic plate.

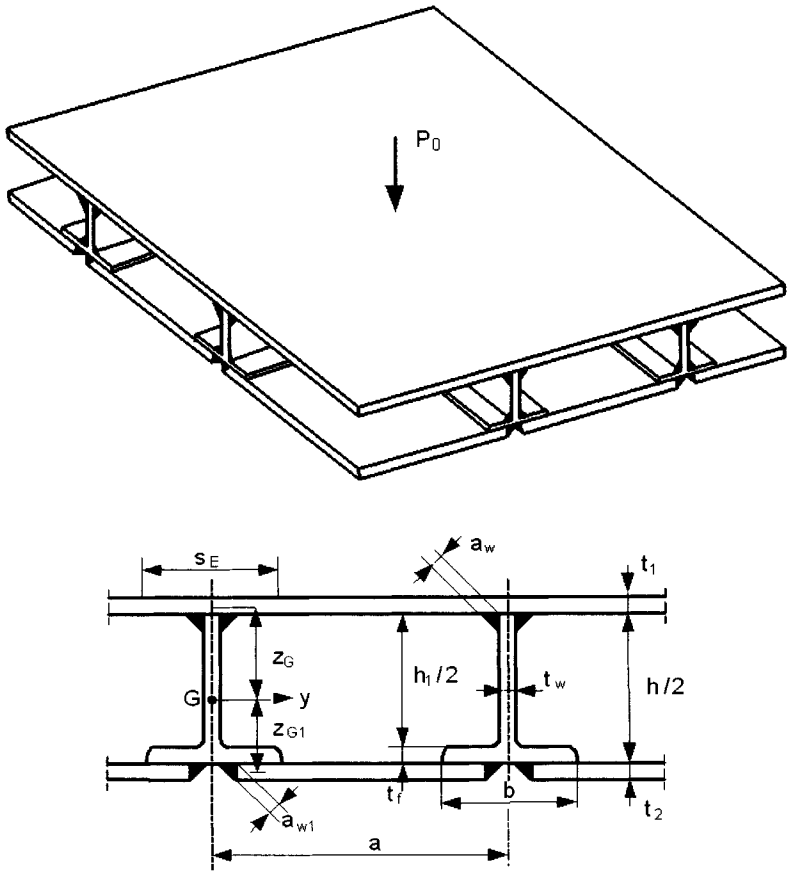

Fig. 7.14 Cellular plate and dimensions of halved rolled I-section stiffeners

The corresponding bending and torsional stiffnesses are defined as

$$B_x = \frac{E_1 I_y}{a_y}; B_y = \frac{E_1 I_x}{a_x}; E_1 = \frac{E}{1-\nu^2}, \tag{7.272}$$

for cellular plates

$$B_{xy} = \frac{GI_y}{a_y}; B_{yx} = \frac{GI_x}{a_x}; G = \frac{E}{2(1+\nu)}, \tag{7.273}$$

$$H = B_{xy} + B_{yx} + \frac{\nu}{2}(B_x + B_y) = \frac{E_1}{2}\left(\frac{I_y}{a_y} + \frac{I_x}{a_x}\right), \tag{7.274}$$

for plates of quadratic symmetry

$$H = B_x = B_y \,. \tag{7.275}$$

Thus, the torsional stiffness of a cellular plate of quadratic symmetry equals to its bending stiffness.

7.6.3 Bending moments and deflections

Lee et al. (1971) have solved the differential equation for rectangular orthotropic plates (Eq.7.270) supported at four corners by using a polynomial function.

Formulae have given for bending moments and deflections as a function of bending and torsional stiffnesses. In the case of a square cellular plate the bending stiffnesses are equal to the torsional stiffness ($B_x = B_y = H$) and the maximum bending moment is

$$M_{max} = 0.15pL^2, \tag{7.276}$$

and the maximum deflection is expressed by

$$w_{max} = 0.025p_0L^4/B_x, \tag{7.277}$$

where L is the plate edge length, p_0 is the factored intensity of the uniformly distributed normal load and p is the load intensity including the self mass of the plate.

Results for square isotropic plates according to Timoshenko & Woinowsky-Krieger (1959)

for $\nu = 0.3$,

$$M_{max} = 0.1404pL^2, \tag{7.278}$$

and

$$w_{max} = 0.0249p_0L^4/B_x \,. \tag{7.279}$$

It can be seen that the constants are nearly the same.

7.6.4 Geometric characteristics (Fig. 7.14)

Effective width of the compressed upper base plate according to ECCS (1988)

$$s_E = 1.9t\sqrt{\frac{E}{f_y}}. \tag{7.280}$$

Cross-sectional area of a halved rolled I-section stiffener

$$A_S = \frac{h_1 t_w}{2} + bt_f, \quad h_1 = h - 2t_f. \tag{7.281}$$

Cross-sectional area of a stiffener with upper and bottom base plate parts

$$A = s_E t_1 + at_2 + A_S, \quad a = \frac{L}{n+1}. \tag{7.282}$$

Distances of the gravity center

$$z_G = \frac{1}{A}\left[at_2\left(\frac{h}{2} + \frac{t_1}{2} + \frac{t_2}{2}\right) + bt_f\left(\frac{h_1 + t_1 + t_f}{2}\right) + \frac{h_1 t_w}{2}\left(\frac{h_1}{4} + \frac{t_1}{2}\right)\right], \tag{7.283}$$

$$z_{G1} = \frac{h + t_1 + t_2}{2} - z_G. \tag{7.284}$$

Moment of inertia

$$I_y = s_E t_1 z_G^2 + at_2 z_{G1}^2 + bt_f\left(\frac{h_1 + t_1 + t_f}{2} - z_G\right)^2 + I_{y1}, \tag{7.285}$$

$$I_{y1} = \frac{h_1^3 t_w}{96} + \frac{h_1 t_w}{2}\left(\frac{h_1}{4} + \frac{t_1}{2} - z_G\right)^2, \tag{7.286}$$

Bending stiffness

$$B_x = \frac{E_1 I_y}{a}, E_1 = \frac{E}{1-\nu^2}. \tag{7.287}$$

Structural volumes corresponding to each fabrication phase are as follows:

$$V_1 = L^2 t_1, V_2 = V_2 + (n+2)A_S, V_3 = V_2 + (n+2)A_S, \tag{7.288}$$

$$V_4 = V_3 + L^2 t_2. \tag{7.289}$$

Load intensity including the self mass

$$p = p_0 + \frac{\rho_0 V_4}{L^2}. \tag{7.290}$$

7.6.5 Design constraints

Stress constraint including normal stress due to local bending of an upper base plate part with built-in edges according to Timoshenko & Woinowsky-Krieger (1959)

$$\sigma_P = 0.0513\frac{p_0 a^2}{t_1^2/6} = 0.3078\frac{p_0 a^2}{t_1^2}, \tag{7.291}$$

$$\sigma_2 = \frac{0.15pL^2 z_G}{I_y} + \sigma_P \le \frac{f_y}{1.1}, \tag{7.292}$$

$$\sigma_1 = \frac{0.15pL^2 z_{G1}}{I_y} \le \frac{f_y}{1.1}. \tag{7.293}$$

Deflection constraint

$$w_{\max} \le w_{allow} = \frac{L}{300}. \tag{7.294}$$

Shear stress constraint at the corners

$$\tau = \frac{pL^2}{4h_1 t_w} \le \frac{f_y}{1.1\sqrt{3}}. \tag{7.295}$$

7.6.6 Fabrication constraints

Thickness limitation: $t_{min} = 4$ mm.

Limitation of the distance between stiffener flanges to allow the welding of the stiffener web to the upper base plate:

$$a - b \ge 300 \text{ mm}. \tag{7.296}$$

7.6.7 Structural characteristics to be changed (variables)

Number of stiffeners in one direction (square symmetry) n,

--thicknesses of the upper and bottom base plates t_1 and t_2,

--height of the rolled I-section stiffener h.

Another dimensions of UB profiles are given in Table 7.11. Note that for these dimensions approximate formulae can be applied as well.

Available series of rolled I-sections: UB profiles selected according to the ARCELOR catalogue (Sales Program 2007) (necessary for the optimization)

Table 7.11 Selected UB profiles according to the ARCELOR catalogue

UB profile	h	B	t_w	t_f
610x229x113	607.6	228.2	11.1	17.3
686x254x140	683.5	253.7	12.4	19.0
762x267x173	762.2	266.7	14.3	21.6
838x292x194	840.7	292.4	14.7	21.7
914x305x224	910.4	304.1	15.9	23.9
1016x305x349	1008.1	302.0	21.1	40.0

7.6.8 Numerical data

Plate edge length: L = 18 m, factored load intensity p_0 = 150 kg/m^2 = 0.0015 N/mm^2, yield stress of steel f_y = 355 MPa, elastic modulus E = 2.1x10^5 MPa, Poisson ratio v = 0.3, steel density ρ = 7.85x10^{-6} kg/mm^3, ρ_0 = 7.85x10^{-5} N/mm^3.

7.6.9 Cost function

The cost function is formulated according to the fabrication sequence.
Welding of the upper base plate (18x18 m) from 36 pieces of size 6 m x 1.5 m using single or double bevel welds with complete joint penetration (GMAW-C gas metal arc welding with CO_2):

$$K_{w1} = k_w\left[\Theta\sqrt{36\rho V_1} + 1.3C_1 t_1^{n1} 13L\right], \tag{7.297}$$

welding cost factor k_w = 1 \$/kg, factor for the complexity of assembly Θ = 3,

$$\text{for } t_1 < 15 \text{ mm } C_1 = 0.1939 \text{ and } n1 = 2, \tag{7.298a}$$

$$\text{for } t_1 > 15 \text{ mm } C_1 = 0.1496 \text{ and } n1 = 1.9029. \tag{7.298b}$$

Welding of n+2 continuous stiffeners to the upper base plate by double fillet welds (GMAW-C)

$$K_{w2} = k_w\left[\Theta\sqrt{(n+3)\rho V_2} + 1.3x0.3394x10^{-3} a_w^2 2(n+2)L\right], \tag{7.299}$$

$a_w = 0.4t_w$, but $a_{wmin} = 4$ mm.

Welding of n+2 intermittent stiffeners to the upper base plate and to the continuous stiffeners (webs with fillet welds, flanges with butt welds GMAW-C)

$$K_{w3} = k_w\left[\Theta\sqrt{(n^2+3n+3)\rho V_3} + T_1 + T_2\right], \tag{7.300}$$

$$T_1 = 1.3x0.3394x10^{-3} a_w^2 (h_1 + b)2(n+1)(n+2), \tag{7.301}$$

$$T_2 = 1.3C_1 t_f^{n1} 2b(n+1)(n+2). \tag{7.302}$$

Welding of the bottom plate parts to the flanges of stiffeners by fillet welds (GMAW-C)

$$K_{w4} = k_w\left[\Theta\sqrt{(n^2+2n+2)\rho V_4} + 1.3x0.3394x10^{-3}a_{w1}^2 4L(n+1)\right], \qquad (7.303)$$

$a_{w1} = 0.4t_2$, but $a_{w1min} = 3$ mm.

Cost of material

$$K_M = k_M \rho V_4, \quad k_M = 1 \text{ \$/kg}, \qquad (7.304)$$

Cost of painting

$$K_P = k_P \Theta_P S_P, \Theta_P = 3, \quad k_P = 14.4x10^{-6} \text{ \$/mm}^2, \qquad (7.305)$$

surface to be painted

$$S_P = 3L^2 + 2L(h_1 + b)(n+2). \qquad (7.306)$$

Total cost

$$K = K_M + K_{w1} + K_{w2} + K_{w3} + K_{w4} + K_P. \qquad (7.307)$$

7.6.10 Optimization and results

In the optimization process the optimum values of variables are sought, which fulfil the design and fabrication constraints and minimize the cost function. Calculation shows that the deflection constraint is always active, and the minimum cost corresponds to the minimum value of plate thickness t_2 = 4 mm. The results are summarized in Table 7.12.

It can be seen that the cost increases when h decreases, thus it is not necessary to continue with the search. The optimum is marked by bolt letters. Each result given in Table 7.12 satisfies all the constraints.

Table 7.12 Optimization results. Allowable deflection is 60 mm. Dimensions and deflections in mm, stresses in MPa

h	n	t_1	t_2	σ_2	w_{max}	$10^{-5} K$ [\$]
1008.1	3	8	7	191	57.2	1.125
	4	7	4	122	57.2	1.071
	5	**5**	**4**	**166**	**59.6**	**1.061**
	6	4	4	191	56.8	1.094
910.4	3	12	4	65	57.6	1.158
	4	10	4	60	59.1	1.121
	5	9	4	51	56.9	1.129
840.7	3	14	4	47	57.7	1.232
	4	12	4	41	58.4	1.188
	5	11	4	34	56.0	1.191
	6	10	4	30	55.0	1.195
	7	9	4	29	55.2	1.200

7.6.11 Conclusions

It has been shown in previous studies that, in the case of square symmetry, the torsional stiffness of cellular plates equals to their bending stiffness. Thus, they can be calculated as isotropic ones and the bending moments and deflection for a square plate supported at four corners can be obtained by using the formulae for isotropic plates.

In the optimization process the four variables are as follows: height and number of halved rolled I-section stiffeners as well as the thicknesses of upper and bottom face plates. A systematic search considers the constraints on stresses and deflection as well as the cost function to be minimized. It is found that the deflection constraint and the limitation of the bottom face plate thickness are always active.

8

Welded Stiffened Cylindrical and Conical Shells

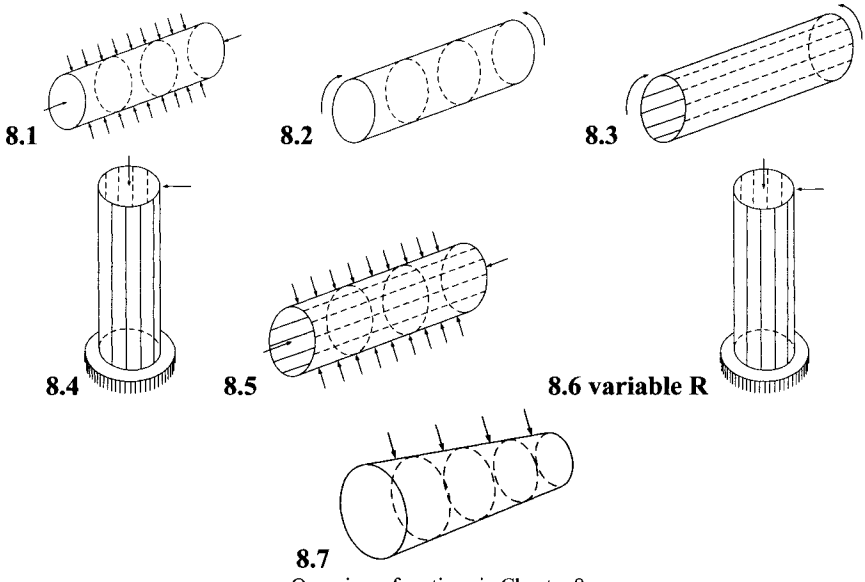

Overview of sections in Chapter 8

The economy of some structural types is demonstrated by the comparison of minimum costs of different structural versions. Such a comparison has been performed for various kinds of stiffened cylindrical shells as follows: ring stiffeners, external pressure (Farkas et al. 2002), ring stiffeners, bending (Farkas et al. 2004), stringer stiffeners, axial compression and bending (Farkas & Jármai 2005a), stringer stiffeners, bending (Farkas & Jármai 2005b), ring and stringer stiffeners, axial compression and external pressure (Jármai et al. 2006). Finite element calculations of circular and conical shells are treated by Ross (1984).

8.1 RING-STIFFENED CYLINDRICAL SHELLS SUBJECT TO AXIAL COMPRESSION AND EXTERNAL PRESSURE

8.1.1 Introduction

The buckling strength for both load cases is calculated according to the American Petroleum Institute design rules (API 1987) Since the API interaction curves are too complicated, i.e. need an iteration process, we use here the simpler linear interaction relation according to ECCS Recommendations (ECCS 1988).

The design constraints relate to the general and local shell buckling as well as to the limitation of imperfections. Ring stiffeners of welded box section are used to avoid tilting of flat stiffeners. The effect of imperfections caused by shrinkage of circumferential welds is considered by an imperfection factor proposed by Farkas (2002).

The cost function includes the material and fabrication costs. For the calculation of welding costs we use our recently developed formulae (Jármai & Farkas 1999). For the constrained function minimization two effective optimization methods are used: the mathematical programming Hillclimb and the evolutionary Particle Swarm Optimization (PSO) techniques. The PSO algorithm was modified to find discrete optima. Recently, we have worked out the case of external pressure (Farkas et al. 2002).

In an illustrative numerical problem the total shell length and the shell radius is given, the unknowns are the shell thickness, the dimensions and number of ring stiffeners. The cost comparison shows that, using the optimum number of stiffeners significant cost savings can be achieved in the design stage by optimization.

8.1.2 Design constraints

8.1.2.1 *Axial compression* (dimensions according to Fig. 8.1)

$$\sigma_D = \frac{F}{2\pi Rt} \le \eta\sigma_U \,, \tag{8.1}$$

8.1.2.2 *External pressure and interaction*

$$p_D = \gamma_b p \frac{R}{t} \le p_U \quad \text{if} \qquad \sigma_D \le \frac{Rp_U}{2t} \,, \tag{8.2}$$

$$\frac{p_D}{p_U}+\frac{\sigma_D-\dfrac{Rp_U}{2t}}{\eta\sigma_U-\dfrac{Rp_U}{2t}}\le 1 \quad \text{if} \quad \sigma_D>\frac{Rp_U}{2t}, \tag{8.3}$$

$$p_U=\min\left(\eta_L\sigma_{UL},\eta_G\sigma_{UG}\right), \tag{8.4}$$

$$\eta\sigma_U=\eta\alpha_{xg}(1.5-50\beta)0.605\frac{Et}{R}\sqrt{\bar{A}_r+1}, \quad \bar{A}_r=\frac{A_r}{L_r t}, \tag{8.5}$$

where A_r is the cross-sectional area of a ring-stiffener, L_r is the distance between ring-stiffeners, $\gamma_b=1.5$ is the safety factor and the plasticity reduction factor.

For $\bar{A}_r\ge 0.2$, $\alpha_{xg}=0.72$. (8.6)

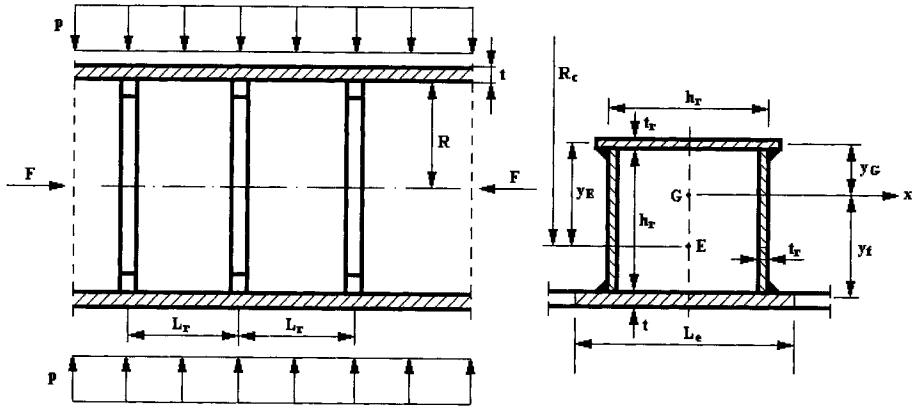

Figure 8.1 The ring-stiffened shell and the cross-section of a ring-stiffener.

The reduction factors are as follows:

η is the plastic reduction factor, β is the imperfection factor.

For $\Delta=\dfrac{\sigma_U}{f_y}\le 0.55$, $\eta=1$, (8.7a)

for $0.55<\Delta<1.6$, $\eta=\dfrac{0.45}{\Delta}+0.18$, (8.7b)

for $1.6<\Delta\le 6.25$, $\eta=\dfrac{1.31}{1+1.15\Delta}$, (8.7c)

for $\Delta>6.25$, $\eta=\dfrac{1}{\Delta}$. (8.7d)

$$0.01 \le \beta = \frac{u_{max}}{4\sqrt{Rt}} \le 0.02 \qquad \text{when} \quad \beta \le 0.01, \quad \beta = 0.01, \tag{8.8}$$

$$u_{\max} = 0.64\text{x}0.844\text{x}10^{-3} \frac{Q_T}{t}\sqrt{\frac{R}{t}}. \tag{8.9}$$

For butt welds $Q_T = 60.7 A_W$ (A_W in mm^2), (8.10)

when $t \le 10$ mm, $A_W = 10t$,

when $t > 10$ mm, $A_W \cong 3.05t^{1.45}$

The cross-sectional area of a stiffener is $A_r = 3h_r t_r = 3\delta_r h_r^2$ (8.11)

The ultimate local and global buckling strengths are

$$\sigma_{UL} = \alpha_L p_{eL} \frac{R}{t} K_L, \qquad \alpha_L = 0.8, \tag{8.12}$$

is the imperfection factor, and for our numerical example $K_L = 1$,

$$\sigma_{UG} = \frac{\alpha_G}{1.2} p_{eG} \frac{R}{t} K_G, \tag{8.13}$$

$\alpha_G = 0.8$ is the imperfection factor, the factor of 1.2 is recommended to avoid the mode interaction (coupled instability).

The distances of centroid G are as follows (Fig. 8.1)

$$y_G = \frac{h_r}{3}; y_r = \frac{2h_r}{3} + \frac{t}{2}, \tag{8.14}$$

$$y_E = \frac{L_e t\left(h_r + \frac{t}{2}\right) + \delta_r h_r^3}{3\delta_r h_r^2 + L_e t}, \tag{8.15}$$

$$L_e = 1.1\sqrt{2Rt} \quad \text{if} \quad M_x = \frac{L_r}{\sqrt{Rt}} > 1.56, \tag{8.16}$$

$$L_e = L_r \qquad \text{if} \qquad M_x \le 1.56. \tag{8.17}$$

The distance of the centroid E of the cross-section consisting of the stiffener and the effective part of shell is characterized by

$$R_C = R - \left(h_r - y_E + t/2\right). \tag{8.18}$$

The moment of inertia of the stiffener and the effective part of shell is

$$I_{er} = \frac{\delta_r h_r^4}{6} + A_r y_r^2 K_G + \frac{L_e t^2}{12}; K_G = \frac{L_e t}{A_r + L_e t}, \tag{8.19}$$

η_L is calculated in function of $\delta_L = \sigma_{UL} / f_y$ as follows

$$\eta_L = 1 \quad \text{if} \quad \delta_L \le 0.55, \tag{8.20}$$

$$\eta_L = \frac{0.45}{\delta_L} + 0.18 \quad \text{if} \quad 0.55 < \delta_L \le 1.6, \tag{8.21}$$

$$\eta_L = \frac{1.31}{1 + 1.15\delta_L} \quad \text{if} \quad 1.6 < \delta_L < 6.25, \tag{8.22}$$

$$\eta_L = \frac{1}{\delta_L} \quad \text{if} \quad \delta_L \ge 6.25, \tag{8.23}$$

$$p_{eL} = \frac{1.27E}{A^{1.18} + 0.5}\left(\frac{t}{R}\right)^2 \quad \text{if } M_x > 1.5 \text{ and } A = M_x - 1.17 < 2.5, \tag{8.24}$$

$$p_{eL} = \frac{0.92E}{A}\left(\frac{t}{R}\right)^2 \quad \text{if} \quad 2.5 < A < 0.208R/t, \tag{8.25}$$

$$p_{eL} = 0.836C_P^{-1.061}E\left(\frac{t}{R}\right)^3 \text{ if } 0.208 < C_P = \frac{A}{R/t} < 2.85, \tag{8.26}$$

$$p_{eL} = 0.275E\left(\frac{t}{R}\right)^3 \quad \text{if} \quad C_P > 2.85, \tag{8.27}$$

and E is the elastic modulus of steel.

The plasticity reduction factor η_G is calculated in function of $\delta_G = \sigma_{UG} / f_y$ with the same formulae as in the case of η_L.

$$p_{eG} = \frac{E\frac{t}{R}\lambda_G^4}{\left(n^2 - 1\right)\left(n^2 + \lambda_G^2\right)^2} + \frac{EI_{er}\left(n^2 - 1\right)}{L_r R_C^2 R}, \tag{8.28}$$

where

$$\lambda_G = \frac{\pi R}{L_b} = \frac{1850\pi}{15000} = 0.3875, \tag{8.29}$$

n is that value, which gives the minimum value of p_{eG}, $n_{min} = 2$, $n_{max} = 10$. For our case $n = 2$ is used.

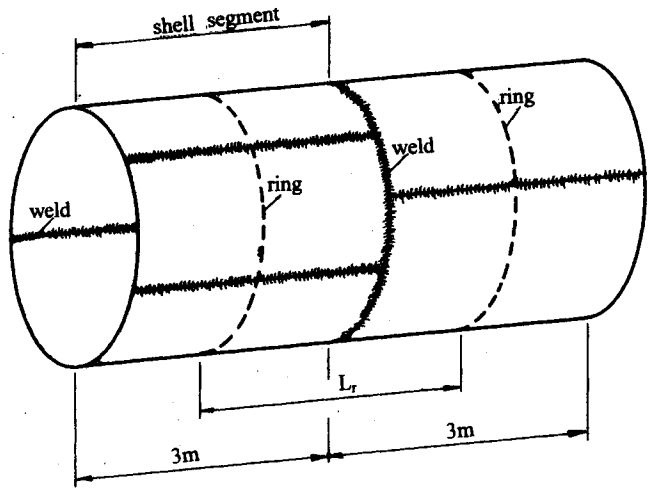

Figure 8.2. Shell segments of the cylindrical shell.

8.1.2.3 *Local buckling constraint*

$$t_r \geq \delta_r h_r ; \delta_r = 1/42\varepsilon ; \varepsilon = \sqrt{235/f_y} ; \delta_r = 1/34 . \tag{8.30}$$

Considering the local buckling constraint of the stiffener flange as active, we use the following correlation between the height and thickness $t_r = \delta_r h_r$.

Data: length of shell L_b = 15 m, welded from 5 m long segments, radius of shell R = 1850 mm, intensity of the external pressure p = 0.5 MPa, the compression force is varied up to $F = 10^8$ N, yield stress of steel f_y = 355 MPa. To avoid tilting of ring-stiffeners, welded square box section is used, which is characterized by the height h_r and thickness t_r.

8.1.3 The cost function

The cost function includes the material, fabrication and painting costs:

$$K = K_M + K_F + K_P . \tag{8.31}$$

The material cost is

$$K_M = k_M \rho V , \tag{8.32}$$

k_M [$/kg] is the material cost factor, the volume of the structure is

$$V = 2\pi RtL_b + n_r\left[4\pi\delta_r h_r^2\left(R - \frac{h_r}{2}\right) + 2\pi\delta_r h_r^2(R - h_r)\right], \tag{8.33}$$

where n_r is the number of ring-stiffeners.

The fabrication cost function is formulated according to the fabrication sequence. For a fabrication phase it is

$$K_F = k_F\left(\Theta_{dW}\sqrt{\kappa\rho V} + 1.3C_W a_W^n L_W\right), \tag{8.34}$$

where k_F (\$/min) is the fabrication cost factor, Θ_{dW}=3 is the difficulty factor expressing the complexity of a structure regarding the assembly, the first member calculates the time for assembly and tacking, κ is the number of structural parts to be assembled, the second member calculates the time of welding and additional works (changing the electrode, deslagging, chipping). The additional works are considered by the factor of 1.3. L_W is the weld length, a_W is the weld size, C_W and n are given for different welding technologies and weld type (butt or fillet).

The fabrication cost function is formulated according to the fabrication sequence as follows.

(1) *Welding of a shell segment from 3 parts without stiffeners* with GMAW-C (Gas Meta Arc Welding with CO_2) butt welds, number of structural parts to be assembled is 3

$$K_{W1} = 3\sqrt{3\rho V_S} + 1.3x0.2245x10^{-3}t^2x3L_S, \tag{8.35}$$

where $L_S = 3000$ mm, $V_S = 2R\pi tL_S$.

(2) *Welding of a ring-stiffener from 3 plate parts* with 2 fillet welds of GMAW-C, weld size $a_W = 0.7t_r$

$$K_{F2} = 3\sqrt{3\rho V_r} + 1.3x0.3394x10^{-3}a_W^2x4\pi(R - h_r), \tag{8.36}$$

where $V_r = 4\pi\delta_r h_r^2\left(R - \frac{h_r}{2}\right) + 2\pi\delta_r h_r^2(R - h_r)$.

(3) *Welding of n_r/5 stiffeners to a shell segment* with 2 fillet welds of size a_W = $0.7t_r$,, GMAW-C

$$K_{F3} = 3\sqrt{\left(\frac{n_r}{5} + 1\right)\rho V_3} + 1.3x0.3394x10^{-3}a_w^2x4\pi Rn_r/5, \tag{8.37}$$

where $V_3 = V_S + V_r n_r/5$.

(4) *Welding of 5 stiffened shell segments together* with butt welds GMAW-C

$$K_{F4} = 3\sqrt{5\rho 5V_3} + 1.3x0.2245x10^{-3}t^2x8R\pi\,. \tag{8.38}$$

Total material cost is

$$K_M = k_M \rho 5V_3\,. \tag{8.39}$$

Total fabrication cost is

$$K_F = k_F\left(5K_{F1} + n_r K_{F2} + 5K_{F3} + K_{F4}\right). \tag{8.40}$$

The painting cost is

$$K_P = k_P\left[2R\pi L_b + 2R\pi\left(L_b - n_r h_r\right) + 2\pi\left(R - h_r\right)h_r + 4\pi\left(R - \frac{h_r}{2}\right)\right]. \tag{8.41}$$

In the numerical example the following cost factors are used: $k_M = 1.0$ \$/kg, $k_F = 1.0$ \$/min and $k_P = 28.8\text{x}10^{-6}$ \$/mm^2.

8.1.4 Optimization techniques and results

The optimization problem can be defined as follows:

Minimize the objective function $f(x_i) \rightarrow$ min.

Design constraints are: explicit $x_i^L \le x_i \le x_i^U$ $(i = 1,2,...,N)$,

implicit $g_j(x_i) \ge 0$ $(j = 1;2,..,M)$. (8.42)

Table 8.1 Discrete optima in the function of the compression force

F [10^{7}N]	t [mm]	t_r [mm]	n_r	K [\$]
0	9	5	19	38857
1	9	5	19	38857
2	9	5	19	38857
3	10	5	16	39242
4	13	5	8	40867
5	16	5	5	45157
6	18	5	5	50259
7	21	4	5	54255
8	23	4	5	58252
9	25	4	5	62559
10	27	4	5	66277

We have used two conceptually different optimization techniques. One of them is the Rosenbrock's Hillclimb technique (Rosenbrock 1960, Farkas & Jármai 1997), which is very quick, but reliable results need more starting points. The other one is

an evolutionary technique, the Particle Swarm Optimization (PSO) (Kennedy 1977, Wilke et al. 2003), which uses the swarm intelligence.

Changing the compression force the number of stiffeners and the objective function are also changing. Low number of stiffeners is ineffective for buckling, high shell thickness is needed for the stress constraint, high number of stiffeners increases the objective function. The two optimization techniques gave nearly the same solutions.

Higher compression forces increase the shell thickness and decrease the number of stiffeners. If $F< 3x10^7$ then the buckling constraint is active, if $F> 3x10^7$ the stress constraint is more important.

8.2 A RING-STIFFENED SHELL SUBJECT TO BENDING

8.2.1 Introduction

Design rules for the shell buckling strength have been worked out by ECCS (1988), API (2000) and DNV (1995). The optimum design of stiffened shells has been treated in some of our articles (Farkas et al. 2002, Farkas 2002a, Jármai et al. 2003). The optimum design of a stiffened shell belt-conveyor bridge has been treated in (Liszkai & Farkas 1989). The buckling behaviour of stiffened cylindrical shells has been investigated by several authors, e.g. Harding (1981), Dowling & Harding (1982), Ellinas et al. (1984), Frieze et al. (1984), Shen et al (1993), Tian et al. (1999).

In the calculation of shell buckling strength the initial imperfections should be taken into account. These imperfections are caused by fabrication and by shrinkage of circumferential welds. A calculation method for the effect of welding has been worked out by the first author (Farkas 2002b) and it is used in the calculation of the local shell buckling strength.

In this study the design rules of Det Norske Veritas (DNV) are used for ring-stiffened cylindrical shells. The shape of rings is a simple flat plate, which is welded to the shell by double fillet welds. In the calculation of the fabrication cost the cost of forming the shell elements into the cylindrical shape and the cutting of the flat ring-stiffeners is also taken into account.

The shell is a supporting bridge for a belt-conveyor, simply supported with a given span length of L = 60 m and radius of R = 1800 mm (Figures 1,2). The intensity of the factored uniformly distributed vertical load is p = 16.5 N/mm + self mass. Factored live load is 12 N/mm, dead load (belts, rollers, service-walkway) is 4.5 N/mm. For self mass a safety factor of 1.35 is used, which is prescribed by Eurocode 3 (note that ECCS gives 1.3). The safety factor for variable load is 1.5.

The flat plate rings are uniformly distributed along the shell. Note that the belt-conveyor supports are independent of the ring stiffeners, they can be realized by using local plate elements.

The unknown variables are as follows: shell thickness t, stiffener thickness t_r and number of stiffeners n.

We do not consider the case of an unstiffened shell, since to assure a stable cylindrical shape, a certain number of ring-stiffeners should be used. In the present study we consider a range of ring numbers $n = 6 - 30$. The range of thicknesses t and t_r is taken as 4 – 20 mm, rounded to 1 mm.

8.2.2 The design constraints

8.2.2.1 *Local buckling of the flat ring-stiffeners* (Fig. 8.3)
According to DNV

$$\frac{h_r}{t_r} \le 0.4\sqrt{\frac{E}{f_y}}\,. \tag{8.43}$$

Considering this constraint as active one, for $E = 2.1\text{x}10^5$ MPa and yield stress $f_y =$ 355 MPa one obtains

$$h_r = 9t_r\,. \tag{8.44}$$

8.2.2.2 *Constraint on local shell buckling (as unstiffened)* (Fig. 8.5)

$$p = 16.5 + 1.35\rho(2R\pi t + nA_r)\,;$$

$$\rho = 7.85x10^{-6}\ \text{kg/mm}^3\,; \quad A_r = h_r t_r\,, \tag{8.45}$$

$$M_{\max} = \frac{pL^2}{8}\,; \tag{8.46}$$

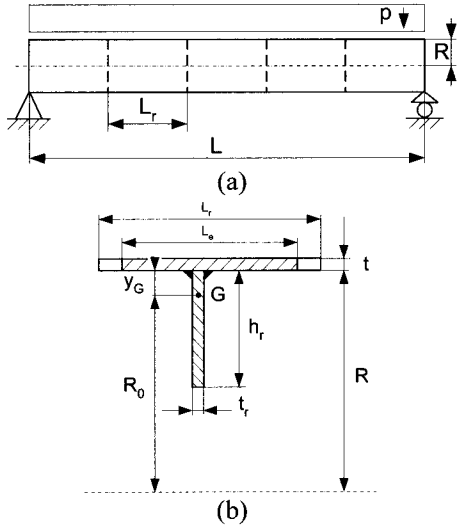

Figure 8.3 (a) A simply supported belt conveyor bridge constructed as a ring stiffened cylindrical shell, (b) the cross-section of a ring stiffener including the effective width of the shell

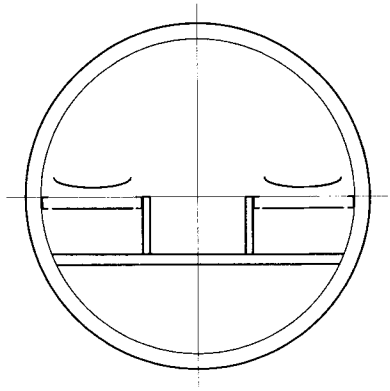

Figure 8.4 Cross-section of a belt conveyor bridge with two belt conveyors and a service walkway in the middle

$$\sigma_{\max} = \frac{M_{\max}}{\pi R^2 t} \le \sigma_{cr} = \frac{f_y}{\sqrt{1+\lambda^4}}, \tag{8.47}$$

$$\lambda^2 = \frac{f_y}{\sigma_E}, \sigma_E = (1.5 - 50\beta) C \frac{\pi^2 E}{10.92} \left(\frac{t}{L_r} \right)^2, \tag{8.48}$$

$$L_r = \frac{L}{n+1}. \tag{8.49}$$

The factor of $(1.5\text{-}50\beta)$ in Eq. (8.48) expresses the effect of initial radial shell deformation caused by the shrinkage of circumferential welds and can be calculated as follows (Farkas 2002b).

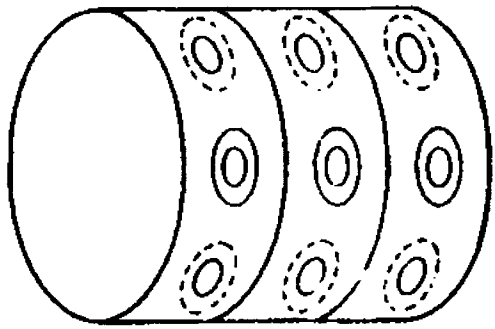

Figure 8.5. Top-view of the shell with local buckling

The maximum radial deformation of the shell caused by the shrinkage of a circumferential weld is

$$u_{\max} = 0.64 A_T \sqrt{R/t}\,, \tag{8.50}$$

where $A_T t$ is the area of specific strains near the weld. According to our results (Farkas & Jármai 1998)

$$A_T t = \frac{0.3355 Q_T \alpha_0}{c_0 \rho}. \tag{8.51}$$

For steels it is

$$A_T t = 0.844 x 10^{-3} Q_T \quad (A_T t \text{ in mm}^2,\ Q_T \text{ in J/mm}), \tag{8.52}$$

$$Q_T = \eta_0 \frac{UI}{v_W} = C_A A_W \cdot \tag{8.53}$$

For manually arc welded butt welds it is

$$Q_T = 60.7 A_W \quad (A_W \text{ in mm}^2) \tag{8.54}$$

When $t \le 10$ mm, $A_W = 10t$, (8.55)

When $t > 10$ mm, $A_W \cong 3.05 t^{1.45}$, (8.56)

Introducing a reduction factor of β for which

$$0.01 \le \beta = \frac{u_{\max}}{4\sqrt{Rt}} \le 0.02\,, \tag{8.57}$$

and the imperfection factor for shell buckling strength should be multiplied by $(1.5 - 50\beta)$.

For $\beta \le 0.01$ $\beta = 0.01$, for $\beta \ge 0.02$ $\beta = 0.02$. (8.58)

Furthermore

$$C = \psi \sqrt{1 + \left(\frac{\rho_0 \xi}{\psi}\right)^2}, Z = 0.9539 \frac{L_r^2}{Rt}, \tag{8.59}$$

$$\psi = 1, \xi = 0.702 Z, \rho_0 = 0.5 \left(1 + \frac{R}{300t}\right)^{-0.5} \cdot \tag{8.60}$$

It can be seen that σ_E does not depend on L_r, since in Eq. (8.48) L_r^2 is in nominator and in C (Eq.8.59) it is in denominator. The fact that the buckling strength does not depend on the shell length is first derived by Timoshenko & Gere (1961).

Note that API design rules (2000) give another formulae. On the contrary, in the case of external pressure the distance between ring-stiffeners plays an important role (Farkas et al. 2002, Jármai et al. 2003).

8.2.2.3 *Constraint on panel ring buckling* (Fig. 8.6)

Requirements for a ring stiffener are as follows:

$$A_r = h_r t_r \geq \left(\frac{2}{Z^2} + 0.06 \right) L_r t \ , \tag{8.61}$$

$$I_r = \frac{h_r^3 t_r}{12} \cdot \frac{1+4\omega}{1+\omega} \geq \frac{\sigma_{\max} t R_0^4}{500 E L_r} \ , \tag{8.62}$$

$$R_0 = R - y_G ; y_G = \frac{h_r}{2(1+\omega)} ; \omega = \frac{L_e t}{h_r t_r} \ , \tag{8.63}$$

$$L_e = \min\left(L_r, L_{e0} = 1.5\sqrt{Rt} \right) . \tag{8.64}$$

8.2.2.4 *Deflection constraint*

$$w_{\max} = \frac{5 p_0 L^4}{384 E I_x} \leq \frac{L}{500} \ , \tag{8.65}$$

$$I_x = \pi R^3 t \ . \tag{8.66}$$

The unfactored load is

$$p_0 = 12/1.5 + 4.5/1.35 + \rho(2R\pi t + nA_r) = 11.33 + \rho(2R\pi t + nA_r) . \tag{8.67}$$

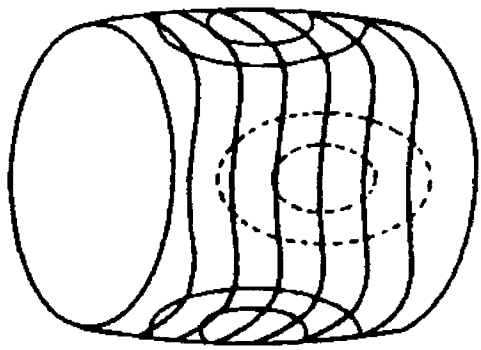

Figure 8.6 Top-view of panel ring buckling

8.2.3 The cost function

The cost function is formulated according to the fabrication sequence. A possible fabrication sequence is as follows:

(1) Fabricate 20 shell elements of length 3 [m] without rings (using 2 end ring stiffeners to assure the cylindrical shape). For one shell element 2 axial butt welds are needed (GMAW-C). The welding of end ring stiffeners is not calculated, since it does not influence the variables. The cost of the forming of the shell element to a cylindrical shape is also included (K_{F0}). According to the time data obtained from a Hungarian production company (Jászberényi Aprítógépgyár, Crushing Machine Factory, Jászberény) for plate elements of 3 m width (Table 8.2), the times ($T_a + T_b$) can be approximated by the following function of the plate thickness (Eq. 8.68).

Table 8.2 Time for forming the shell elements of 3m width into circular shape (T_a),as well as for reducing the initial imperfections due to forming (T_b)

t [mm]	T_a [min]	T_b [min]	$T_a + T_b$ [min]
6	270	184	454
8	336	204	540
10	395	228	623
15	495	304	799
20	588	374	962
25	680	442	1122
30	744	538	1282
40	834	692	1526

$$K_{F0} = k_F \Theta (212.18 + 42.824t - 0.2483t^2). \tag{8.68}$$

The cost of welding of a shell element is

$$K_{F1} = k_F \left[\Theta \sqrt{\kappa \rho V_1} + 1.3x0.2245x10^{-3} t^2 (2x3000) \right], \tag{8.69}$$

where Θ is a difficulty factor expressing the complexity of the assembly and κ is the number of elements to be assembled

$$\kappa = 2; V_1 = 2R\pi tx3000; \Theta = 2. \tag{8.70}$$

The first term of Equation (8.69) expresses the time of assembly and the second calculates the time of welding and additional works (Farkas & Jármai 1997).

(2) Welding the whole unstiffened shell from 20 elements with 19 circumferential butt welds

$$K_{F2} = k_F \left(\Theta \sqrt{20 \rho V_1} + 1.3x0.2245x10^{-3} t^2 x19x2R\pi \right), \tag{8.71}$$

(3) Cutting of n flat plate rings with acetylene gas (Farkas & Jármai 2003)

$$K_{F3} = k_F \Theta_c C_c t_r^{0.25} L_c \tag{8.72}$$

where Θ_c, C_c and L_c are the difficulty factor for cutting, cutting parameter and length respectively, Θ_c =3, C_c= 1.1388, $L_c \approx 2R\pi n + 2(R - h_r)\pi n$.

(4) Welding n rings into the shell with double-sided GMAW-C fillet welds. Number of fillet welds is $2n$

$$K_{F4} = k_F \left(\Theta \sqrt{(n+1)\rho V_2} + 1.3x0.3394x10^{-3} a_W^2 x4R\pi n \right), \tag{8.73}$$

$a_W = 0.5t_r$, but a_{Wmin} = 3 mm,

$$V_2 = 20V_1 + 2\left(R - \frac{h_r}{2} \right) \pi h_r t_r n, \tag{8.74}$$

a_W is taken so that the double fillet weld joint be equivalent to the stiffener thickness.

The total material cost is

$$K_M = k_M \rho V_2 , \tag{8.75}$$

The total cost is

$$K = K_M + 20(K_{F0} + K_{F1}) + K_{F2} + K_{F3} + K_{F4} . \tag{8.76}$$

k_M = 1 \$/kg; k_F = 1 \$/min.

8.2.4 Results of the optimum design

Table 8.3 Computational results: the number of stiffeners, thickness of the stiffeners, material and total costs in the case of optimum shell thickness t = 7 mm. The optimum solution is marked by bold letters

n	t_r	K_M	K
6	21	39291	76041
7	**19**	**39211**	**75870**
8	18	39266	76296
9	17	39278	76531
10	16	39252	76595
11	16	39448	77640
12	15	39365	77446
13	15	39538	78384
14	14	39404	77965
15	14	39555	78803
16	13	39379	78191
17	13	39509	78935
18	13	39640	79679
19	12	39409	78819

The optimization has been worked out using the Hillclimb technique (Farkas & Jármai 1997). Results can be found in Table 8.3. Those results for which the place of stiffeners coincides with the circumferential welds of the shell segments are not applicable for fabrication reasons ($n = 3, 4, 9, 19$).

Table 8.4 Cost distribution for the optimum solution

n	t_r	$20\,K_{F0}$	$20\,K_{F1}$	K_{F2}	K_{F3}	K_{F4}	K_M	K
7	19	19991	4707	3459	1076	7425	39211	75870
		26%	6%	5%	2%	10%	51%	100%

Table 8.4 shows the value of the different cost elements.

8.2.5 Conclusions

The shell thickness is determined by the constraints on local shell buckling as well as on deflection. Since the number of ring-stiffeners does not influence these constraints, in order to assure a stable circular shell shape, a certain number of rings should be used.

Since the design rules do not give any prescriptions for the minimum number of ring-stiffeners, for the investigated case we have selected a ring number domain of $n = 6 - 30$ and have performed the optimization in this domain.

The Det Norske Veritas design rules give suitable formulae for the design of rings, the dimensions of which decrease with the increase of the number of rings.

The initial radial deformation of the shell caused by the shrinkage of circumferential welds affects the local shell buckling strength significantly. Cost calculation methods are proposed for the forming of shell elements into circular shape and for the cutting of flat plate ring-stiffeners. The cost function is formulated according to the fabrication sequence.

The optimization results (Table 2) show that, due to the cutting and welding costs of stiffeners, the smaller number of stiffeners is more economic. The optimum ring number is 7, which minimizes the total mass (material cost) and the total cost.

Material cost is about half of the total one and is insensitive to the variation of ring numbers. The forming cost of the shell elements (K_{F0}) is significant. The difference between the best and worst optima indicated in Table 2 is 7 %, thus it is worth using an optimization process in the design stage.

8.3 A STRINGER-STIFFENED SHELL SUBJECT TO BENDING

8.3.1 Introduction

An interesting problem relating to the economy of structures is how to achieve cost savings by using thinner stiffened plates or shells instead of thick unstiffened ones. The stiffened structure is economic, if the thicknesses can be decreased in such a manner that the cost savings caused by this decreasing is higher than the additional cost of stiffening material and welding. The cost of forming the plate elements into

cylindrical shapes and that of welding can significantly be decreased by the reduction of plate thickness.

Our previous studies relating to the economy of stiffened shells have shown that the cost effectiveness of stiffening depends on the load (axial compression, bending or external pressure), stiffening geometry (ring-, stringer-stiffeners or both) and the cross-sectional shape of stiffeners (flat, rolled I, welded box, cold-formed L, trapezoidal etc.). We have found that the ring-stiffening is economic for external pressure (Farkas et al. 2004), but it is uneconomic for axial compression or bending, since the shell thickness cannot be decreased by rings with realistic distances between them (Farkas et al. 2004).

Our another result is that the stringer-stiffening can be economic for bending in the case when an allowable lateral displacement (e.g. horizontal displacement of a column top) is prescribed (Farkas & Jármai 2005). In this case it is advantageous to use stringers of halved rolled I-section welded outside to the shell.

Circular cylindrical shells are often used for belt-conveyor bridges, since the closed shape is advantageous for such purposes (Fig.8.7). We have worked out the minimum cost design of a belt-conveyor bridge using ring-stiffened shell (Farkas & Jármai 2004). In the present study it is shown that the stringer-stiffened shell with stiffeners of halved rolled I-section welded outside of the shell (Fig.8.8) can be economic, when the deflection constraint is active.

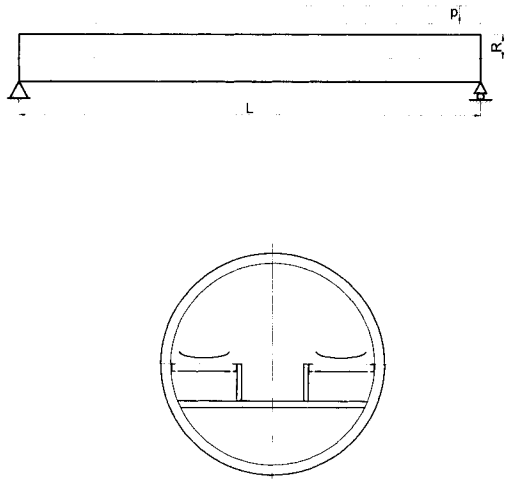

Figure 8.7 A simply supported belt-conveyor bridge with two belts, side view and cross-section

In order to show the economy of stringer-stiffening, a stiffened and an unstiffened version is optimized for minimum cost and their costs are compared to each other.

Design constraints are formulated according to the rules of Det Norske Veritas (1995). The cost function is formulated according to the fabrication sequence. In the case of the stiffened version, the unknowns are the shell thickness as well as the dimension and number of stiffeners. The constraints relate to the shell buckling, panel stiffener buckling and fabrication limitations.

8.3.2 Problem formulation

Structural optimization procedures have to be carried out for a stringer-stiffened and an unstiffened circular cylindrical shell and the cost effectiveness of stiffening should be evaluated by a comparison of their minimal cost.

For both versions the given data are as follows: L = 60 m span length of the simply supported bridge, R = 1850 mm shell radius, ϕ - allowable deflection factor, f_y = 355 MPa yield stress of steel, $E = 2.1\text{x}10^5$ MPa elastic modulus, ν = 0.3 Poisson ratio, k_M, k_F, k_P -cost factors for material, fabrication and painting.

The intensity of the factored uniformly distributed vertical load is p = 26 N/mm + self mass. Factored live load is 20 N/mm, dead load (belts, rollers, service-walkway) is 6 N/mm. For self mass a safety factor of 1.35 is used. The safety factor for variable load is 1.5.

The unknowns are as follows: the shell thickness (t), the dimension (h_S) and number of stringers (n_S). The dimensions of a halved rolled I-section (Universal Beam – UB according to ARBED 2001) can be determined by their height h_S, since we use approximate expressions for another dimensions and geometric characteristics (h_I, t_w, b, t_f, A, I_y) (Fig. 8.8) using a special software (Table Curve 2003) (Appendix C, Eqs C4-C9).

Note that the use of halved rolled I-section stringers is advantageous because of their large moment of inertia and small web thickness, which enables the use of small fillet welds to connect the stringers to the shell.

In the optimum design, the optimum values of unknowns are sought, which minimize the cost function and fulfil the design constraints. We use for constrained function minimization an effective mathematical method.

8.3.3 The stringer-stiffened shell

8.3.3.1 *Design constraints*

Shell (curved panel) buckling

$$\sigma_a = \frac{M}{R^2\pi t_e} \le \sigma_{cr} = \frac{f_y}{\sqrt{1+\lambda^4}};\ \lambda^2 = \frac{f_y}{\sigma_E};\ t_e = t + \frac{A_s}{2s};\ s = \frac{2R\pi}{n_s}, \tag{8.77}$$

$$M = \frac{pL^2}{8};\ p = 26.0 + 1.35\rho\left(2R\pi t_e\right),\ \rho = 9.81x7.85x10^{-6}, \tag{8.78}$$

$$\sigma_E = C(1.5-50\beta)\frac{\pi^2 E}{12(1-\nu^2)}\left(\frac{t}{s}\right)^2, \tag{8.79}$$

$$C = 4\sqrt{1+\left(\frac{\rho_e \xi}{4}\right)^2}; Z = \frac{s^2}{Rt}\sqrt{1-\nu^2}\ ;\ \rho_e = 0.5\left(1+\frac{R}{150t}\right)^{-0.5}; \xi = 0.702Z, \tag{8.80}$$

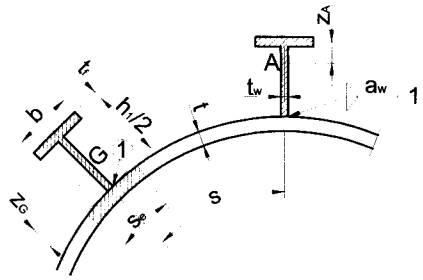

Figure 8.8 Halved rolled I-section stringers welded outside to the shell

The calculation of the factor $1.5-50\beta$ is detailed in Sec. 8.2.2.2 (Eqs 8.50 – 8.57). Note that the residual welding distortion factor $1.5-50\beta = 1$ when t>9 mm.

Stringer panel buckling

$$\sigma_a = \frac{M}{R^2\pi t_e} \le \sigma_{crp} = \frac{f_y}{\sqrt{1+\lambda_p^4}};\ \lambda_p^2 = \frac{f_y}{\sigma_{Ep}}; \sigma_{Ep} = C_p \frac{\pi^2 E}{10.92}\left(\frac{t}{L}\right)^2, \tag{8.81}$$

$$C_p = \psi_p\sqrt{1+\left(\frac{0.5\xi_p}{\psi_p}\right)^2}; Z_p = 0.9539\frac{L^2}{Rt};\ \xi_p = 0.702Z_p; \gamma_s = 10.92\frac{I_{sef}}{st^3};$$

$$\psi_p = \frac{1+\gamma_s}{1+\frac{A_s}{s_e t}}; \tag{8.82}$$

according to ECCS (1988)

$$s_E = 1.9t\sqrt{\frac{E}{f_y}}\ ;\ \text{if } s_E < s \quad s_e = s_E\ ;\ \text{if } s_E > s \quad s_e = s, \tag{8.83}$$

I_{sef} is the moment of inertia of a cross section containing the stiffener and a shell part of width s_e.

$$I_{sef} = s_e t z_G^2 + \frac{t_w}{12}\left(\frac{h_1}{2}\right)^3 + \frac{h_1 t_w}{2}\left(\frac{h_1}{4}-z_G\right)^2 + bt_f\left(\frac{h_1}{2}-z_G\right)^2;$$

$$z_G = \frac{h_1^2 t_w / 8 + h_1 b t_f / 2}{h_1 t_w / 2 + b t_f + s_e t}. \tag{8.84}$$

Deflection limitation

$$w_{\max} = \frac{5 p_0 L^4}{384 E I_{y0}} \le \frac{L}{\phi}. \tag{8.85}$$

p_0 is the load intensity without safety factors:

$$p_0 = 20/1.5 + 6.0/1.35 + \rho 2R\pi t_e = 17.78 + \rho 2R\pi t_e, \tag{8.86}$$

the deflection limitation factor ϕ is varied between 400 – 1000.
The moment of inertia of the stiffened shell is

$$I_{y0} = \pi R^3 t + \left[I_y + \left(\frac{h_1}{2} t_w + b t_f \right) \left(R + \frac{h_1 + t_f}{2} - z_A \right)^2 \right] \sum_{i=1}^{n_S} \sin^2 \left(\frac{2\pi i}{n_S} \right), \tag{8.87}$$

$$z_A = \frac{h_1 t_w / 2 \left(h_1 / 4 + t_f / 2 \right)}{h_1 t_w / 2 + b t_f}. \tag{8.88}$$

The characteristic data of the UB rolled I-sections are expressed by the main parameter of the section height h_S (see Appendix C, Eqs C4-C9).

8.3.3.2 *The cost function*

The fabrication sequence can be as follows:

(1) Fabrication of 20 shell elements of length 3 m without stiffeners. For one shell element 2 axial butt welds are needed (GMAW-C – Gas Metal Arc Welding with CO_2) (K_{F1}) (Farkas & Jármai 2003). The cost of forming a shell element into the cylindrical shape is also included (K_{F0}).

(2) Welding of an unstiffened shell unit from 4 shell segments of 3m length with 3 butt welds with 4 circumferential butt welds (K_{F2}).

(3) Welding the n_s stiffeners into the unit with $2n_s$ fillet welds of size a_w and length 12 m (K_{F3}), $a_w = 0.3t_w$, $a_{wmin} = 3$ mm..

(4) Welding the 5 units together with 4 butt welds and butt welds connecting the halved UB stiffeners.

The material cost is

$$K_M = k_{M1} 5 \rho_1 V_2, \tag{8.89}$$

$$V_2 = 4V_1 + n_S \frac{A_s L}{2x5}; V_1 = 3000x2R\pi t, \tag{8.90}$$

$$K_{F0} = k_F \Theta e^{\mu}; \mu = 6.8582513 - 4.527217t^{-0.5} + 0.009541996(2R)^{0.5}, \quad (8.91)$$

$$K_{F1} = k_F \left(\Theta \sqrt{\kappa \rho_1 V_1} + 1.3x0.152x10^{-3} t^{1.9358} x6000 \right), \quad (8.92)$$

$$\Theta = 2; \kappa = 2; \rho_1 = 7.85x10^{-6} \text{ kg/mm}^3, \quad (8.93)$$

$$K_{F2} = k_F \left(\Theta \sqrt{4x4\rho_1 V_1} + 1.3x0.152x10^{-3} t^{1.9358} 6R\pi \right), \quad (8.94)$$

k_F = 1.0 \$/min, k_{MI} = 1.0 \$/kg.

where Θ is a difficulty factor expressing the complexity of the assembly and κ is the number of elements to be assembled. Furthermore

$$K_{F3} = k_F \left(\Theta \sqrt{(n_s + 1)\rho_1 V_2} + 1.3x0.3394x10^{-3} a_W^2 2Ln_s / 5 \right), \quad (8.95)$$

$$K_{F4} = k_F \left(\Theta \sqrt{5x5\rho_1 V_2} \right) +$$

$$+ k_F 1.3x0.152x10^{-3} \left(8R\pi t^{1.9358} + n_S \frac{h_1}{2} t_w^{1.9358} + n_S b t_f^{1.9358} \right). \quad (8.96)$$

The cost of painting is

$$K_P = k_P \left(4R\pi L + n_S \frac{A_L L}{2} \right); k_P = 14.4x10^{-6} \text{ \$/mm}^2. \quad (8.97)$$

The total cost is

$$K = K_M + 20K_{F1} + 20K_{F0} + 5K_{F2} + 5K_{F3} + K_{F4} + K_P. \quad (8.98)$$

8.3.4 The unstiffened shell

8.3.4.1 *Design constraints*

Shell buckling

$$\sigma_a = \frac{M}{R^2 \pi t} \le \sigma_{cr} = \frac{f_y}{\sqrt{1 + \lambda^4}}; \quad \lambda^2 = \frac{f_y}{\sigma_E}; t_e = t, A_S = 0, \quad (8.99)$$

$$M = \frac{pL^2}{8}; p = 20 + 6 + 1.35\rho(2R\pi t), \quad \rho = 9.81x7.85x10^{-6} \text{ N/mm}^3, \quad (8.100)$$

$$\sigma_E = C \frac{\pi^2 E}{12(1 - \nu^2)} \left(\frac{t}{L} \right)^2. \quad (8.101)$$

Note that the residual welding distortion factor $1.5 - 50\beta = 1$ when t>9 mm.

$$C=\sqrt{1+\left(\rho_e\xi\right)^2};Z=\frac{L^2}{Rt}\sqrt{1-\nu^2};\ \rho_e=0.5\left(1+\frac{R}{300t}\right)^{-0.5};\xi=0.702Z\cdot \tag{8.102}$$

Deflection limitation

$$w_{\max}=\frac{5p_0L^4}{384E\pi R^3t}\le\frac{L}{\phi};\ p_0=20/1.5+6.0/1.35+\rho 2R\pi t=17.78+\rho 2R\pi t\cdot \tag{8.103}$$

8.3.4.2 *The cost function*

Fabrication sequence:

(1) Fabrication of 20 shell elements of length 3 m without stiffeners. For one shell element 2 axial butt welds are needed (GMAW-C) (K_{FI}). The cost of forming of a shell element into the cylindrical shape is also included (K_{F0}).

(2) Welding the 20 units together with 19 butt welds (K_{F2}).

The material cost is

$$K_M=k_{M1}20\rho_1V_1;\ V_1=3000x2R\pi t, \tag{8.104}$$

$$K_{F0}=k_F\Theta e^{\mu};\mu=6.8582513-4.527217t^{-0.5}+0.009541996\left(2R\right)^{0.5}, \tag{8.105}$$

$$K_{F1}=k_F\left(\Theta\sqrt{\kappa\rho_1V_1}+1.3x0.152x10^{-3}t^{1.9358}x6000\right), \tag{8.106}$$

$$K_{F2}=k_F\left(\Theta\sqrt{20x20\rho_1V_1}+1.3x0.152x10^{-3}t^{1.9358}38R\pi\right);$$

$$k_F=1.0\ \$/\text{min},\ k_{MI}=1.0\ \$/\text{kg}. \tag{8.107}$$

The cost of painting is

$$K_P=k_P\left(4R\pi L\right);k_P=14.4x10^{-6}\ \$/\text{mm}^2. \tag{8.108}$$

The total cost is

$$K=K_M+20K_{F1}+20K_{F0}+K_{F2}+K_P\cdot \tag{8.109}$$

8.3.5 Optimization and comparison of results

The optimization is performed by using the Particle Swarm algorithm, which is an effective mathematical method (Farkas & Jármai 2003). The optimization results are summarized in Table 1. It can be seen that significant cost savings can be achieved by stringer stiffening when the deflection constraint is active. In our case the cost difference is 11-34% when the deflection factor is 700-1000. For the factor of 400-500 the stiffening is uneconomic, since the cost of the unstiffened version is 9% smaller than that of the stiffened one.

Table 8.5 Results of the optimization. Negative cost difference means savings by stiffening

	Stiffened shell					Unstiffened shell			
ϕ	t mm	h_S mm	n_S	$w_{max} \le L/\phi$ mm	K$	t mm	$w_{max} \le L/\phi$ mm	K$	Cost difference
400	9	152	5	95.7<150	102030	9	116<150	93930	+9
500	9	152	5	95.7<120	102030	9	116<120	93930	+9
600	8	533	6	78.5<100	112433	12	96<100	118000	-5
700	8	762	5	73.6<85.7	126398	15	84<85.7	142300	-11
800	8	914	5	68.3<75	137336	19	74<75	175300	-22
900	7	838	9	58.4<66.6	158800	24	66<66.6	217900	-27
1000	7	838	12	52.5<60	185086	31	59<60	280800	-34

8.3.6 Conclusions

Economy of stiffened steel shells is investigated in the case of a welded stringer-stiffened cylindrical shell constructed for a belt-conveyor bridge. Both the stiffened and unstiffened structural version is optimized for minimum cost.

Halved rolled I-section stringers are welded outside the shell. In this case the stiffened shell has much larger moment of inertia (stiffness against deflection) than that of stringers welded inside the shell. In the case of halved I-section their web can be welded to the shell by small fillet welds. It is advantageous, since the welding cost is proportional to the square of weld size.

The shell thickness plays an important role in decreasing the structural cost. It can be seen that, in the case of an active deflection constraint the thickness of the unstiffened shell can be decreased by stiffening in such a measure that the stiffening can significantly be economic.

In our numerical model the deflection limitation is active for $w_{max} < L/700$, thus, for these cases significant cost savings can be achieved by stringer-stiffeners.

8.4 A STRINGER-STIFFENED SHELL SUBJECT TO AXIAL COMPRESSION AND BENDING

8.4.1 Introduction

An important requirement from modern welded structures is the economy, since the cost of welding is high. Therefore, the basis of comparison of different structural versions is the cost. Since only the optimum versions can be realistically compared to each other, the minimum cost design should be performed for each structural version.

The economy of stiffened cylindrical shells depends on several parameters as follows: load (axial compression, bending, external pressure or combined load), type of stiffening (ring-, stringer-stiffeners or orthogonal stiffening), stiffener profile (flat, rolled I, halved rolled I, L-, hollow section or trapezoidal).

It has been shown that ring-stiffening is economic in the case of external pressure (Farkas & Jármai 2003, Farkas et al. 2002). In the case of bending the ring-stiffening should be used to assure the sufficient cylindrical shape. In this case the cost of stiffened shell is higher than that of unstiffened one, since the shell thickness cannot be decreased by ring-stiffeners (Farkas et al. 2004).

Stiffening is economic only in those cases, when the thickness can be decreased in such a measure that the cost savings caused by this decreasing is higher that the additional cost of stiffening material and welding.

As a part of our systematic research relating to stiffened cylindrical shells, in the present study a column is investigated subject to an axial compression and a horizontal force acting on the top of the column (Fig. 8.9).

The column is fixed at the bottom and free on the top. It is shown that a shell stiffened outside with stringers can be economic, when a constraint on horizontal displacement of the column top is active.

In order to decrease the welding cost of stiffeners, their cross-sectional area is increased, i.e. halved rolled I-section (UB) stiffeners are used instead of flat ones. The halved I-sections are advantageous, since the web can be easier welded to the shell than the flange.

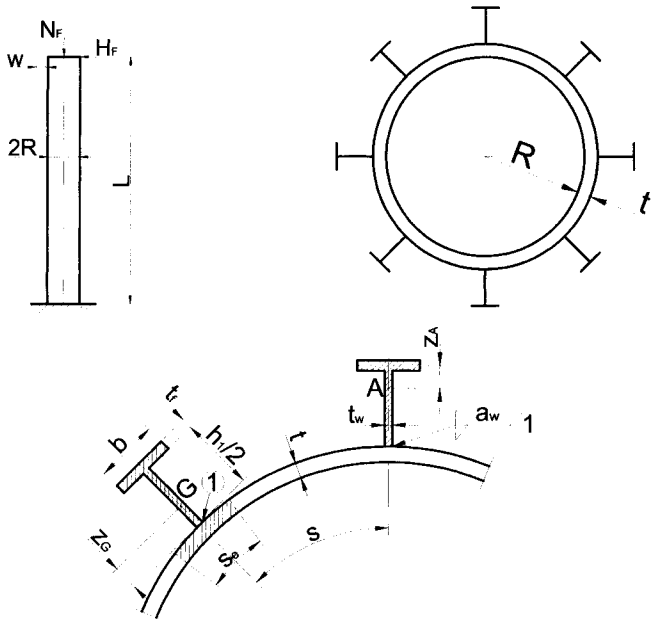

Figure 8.9 A column constructed as a stiffened cylindrical shell loaded by a compression force N_F and a horizontal force H_F. Cross-section and a detail of the cross-section with outside stiffeners of halved rolled I-section. The horizontal displacement of the top (w) is limited

It should be mentioned that stringer-stiffening can also be economic in those cases, when the corresponding unstiffened version needs a very thick shell (more than 40 mm).

The cross-section of the stiffened shell is constant along the whole height. Constraints on local shell buckling, on stringer panel buckling and on horizontal displacement are taken into account.

The buckling constraints are formulated according to the DNV design rules (1995). The cost function to be minimized includes the cost of material, forming of shell elements into cylindrical shape, assembly, welding and painting.

In order to demonstrate the economy of the stiffened shell, the unstiffened version is also optimized. The results show that the cost savings depends on the active displacement constraint.

8.4.2 Problem formulation

The investigated structure is a supporting column loaded by an axial and horizontal force (Fig. 8.9). The horizontal displacement of the top is limited by the reasons of serviceability of the supported structure. Both the stiffened and unstiffened shell version is optimized and their cost is compared to each other. In the stiffened shell outside longitudinal stiffeners of halved rolled I-section (UB) are used. The cost function is formulated according the fabrication sequence.

Given data are as follows: column height L, shell radius R, factored axial compression force N_F, factored horizontal force H_F, yield stress of steel f_y, cost factors for material, fabrication and painting k_m, k_f, k_p. The unknowns are the shell thickness t as well as the height h and number n_s of halved rolled I-section stiffeners. The characteristics of the selected UB profiles are given in Appendix C.

In order to calculate with continuous values the geometric characteristics of an UB section (I_y, b, t_f) are approximated by curve-fitting functions (see Appendix C, Eqs C1-C3, Table Curve 2D 2003).

8.4.3 The stiffened shell

8.4.3.1 *Constraints*

Shell buckling (unstiffened curved panel buckling)

The sum of the axial and bending stresses should be smaller than the critical buckling stress

$$\sigma_a + \sigma_b = \frac{N_F}{2R\pi t_e} + \frac{H_F L}{R^2 \pi t_e} \le \sigma_{cr} = \frac{f_y}{\sqrt{1+\lambda^4}}, \tag{8.110}$$

where the reduced slenderness

$$\lambda^2 = \frac{f_y}{\sigma_a + \sigma_b}\left(\frac{\sigma_a}{\sigma_{Ea}} + \frac{\sigma_b}{\sigma_{Eb}}\right); t_e = t + \frac{A_s}{2s}; s = \frac{2R\pi}{n_s}, \tag{8.111}$$

t_e is the equivalent thickness. The elastic buckling stress for the axial compression is

$$\sigma_{Ea} = C_a(1.5 - 50\beta)\frac{\pi^2 E}{10.92}\left(\frac{t}{s}\right)^2, \tag{8.112}$$

$$C_a = 4\sqrt{1 + \left(\frac{\rho_a \xi}{4}\right)^2}; Z = \frac{s^2}{Rt}0.9539, \tag{8.113}$$

$$\rho_a = 0.5\left(1 + \frac{R}{150t}\right)^{-0.5}; \xi = 0.702Z \cdot \tag{8.114}$$

The elastic buckling stress for bending is

$$\sigma_{Eb} = C_b(1.5 - 50\beta)\frac{\pi^2 E}{10.92}\left(\frac{t}{s}\right)^2, \tag{8.115}$$

$$C_b = 4\sqrt{1 + \left(\frac{\rho_b \xi}{4}\right)^2}, \tag{8.116}$$

$$\rho_b = 0.5\left(1 + \frac{R}{300t}\right)^{-0.5} \cdot \tag{8.117}$$

Note that the residual welding distortion factor $1.5 - 50\beta = 1$ when t>9 mm. The detailed derivation of it is treated in Sec.8.2.2.2 (Eqs 8.50 – 8.57).

Stringer panel buckling

$$\sigma_a + \sigma_b \le \sigma_{crp} = \frac{f_y}{\sqrt{1 + \lambda_p^4}}, \tag{8.118}$$

$$\lambda_p^2 = \frac{f_y}{\sigma_{Ep}}; \sigma_{Ep} = C_p \frac{\pi^2 E}{10.92}\left(\frac{t}{L}\right)^2, \tag{8.119}$$

$$C_p = \psi_p \sqrt{1 + \left(\frac{0.5\xi_p}{\psi_p}\right)^2}; Z_p = 0.9539\frac{L^2}{Rt}, \tag{8.120}$$

$$\xi_p = 0.702Z_p; \gamma_s = 10.92\frac{I_{sef}}{st^3}, \tag{8.121}$$

$$\psi_p = \frac{1+\gamma_s}{1+\dfrac{A_s}{2s_e t}}; \tag{8.122}$$

Since the effective shell part s_e (Fig.8.9) is given by DNV with a complicate iteration procedure, we use here the simpler method of ECCS (1988)

$$s_E = 1.9t\sqrt{\frac{E}{f_y}}, \tag{8.123}$$

if $s_E < s$ $\quad s_e = s_E$,

if $s_E > s$ $\quad s_e = s$.

I_{sef} is the moment of inertia of a cross section containing the stiffener and a shell part of width s_e (Fig. 8.9). For a stiffener of halved rolled I-section it is

$$I_{sef} = s_e t z_G^2 + \frac{t_w}{12}\left(\frac{h_1}{2}\right)^3 + \frac{h_1 t_w}{2}\left(\frac{h_1}{4} - z_G\right)^2 + bt_f\left(\frac{h_1}{2} - z_G\right)^2, \tag{8.124}$$

$$z_G = \frac{h_1^2 t_w/8 + h_1 b t_f/2}{h_1 t_w/2 + bt_f + s_e t}. \tag{8.125}$$

Horizontal displacement

$$w_h = \frac{ML^2}{3EI_{x0}} \le w_{allow} = \frac{L}{\phi}, \tag{8.126}$$

ϕ is the varied between 400 and 1000 (Table 8.6).
The exact calculation of the moment of inertia for the horizontal displacement uses the following formulae (Fig.8.9):
The distance of the center of gravity for the halved UB section is

$$z_A = \frac{h_1 t_w/2\left(h_1/4 + t_f/2\right)}{h_1 t_w/2 + bt_f}. \tag{8.127}$$

The moment of inertia of the halved UB section is expressed by

$$I_x = bt_f z_A^2 + \frac{t_w}{12}\left(\frac{h_1}{2}\right)^3 + \frac{h_1 t_w}{2}\left(\frac{h_1}{4} - z_A\right)^2. \tag{8.128}$$

The moment of inertia of the whole stiffened shell cross-section is

$$I_{x0} = \pi R^3 t + I_x \sum_{i=1}^{n_s} \sin^2\left(\frac{2\pi i}{n_s}\right) +$$

$$+\left(\frac{h_1 t_w}{2}+bt_f\right)\left(R+\frac{h_1+t_f}{2}-z_A\right)^2\sum_{i=1}^{n_s}\sin^2\left(\frac{2\pi i}{n_s}\right), \tag{8.129}$$

$$M=H_F L/\gamma_M;\gamma_M=1.5;H_F=0.1N_F. \tag{8.130}$$

Numerical data: N_F = 34000 kN, f_y = 355 MPa, R = 1850 mm, L = 15 m.

8.4.3.2 *The cost function*

Fabrication sequence:

(1) Fabrication of 5 shell elements of length 3 m without stiffeners. For one shell element 2 axial butt welds are needed (GMAW-C) (K_{F1}). The cost of forming of a shell element into the cylindrical shape is also included (K_{F0}).

(2) Welding of the whole unstiffened shell from 5 elements with 4 circumferential butt welds (K_{F2}).

(3) Welding of n_s stiffeners to the shell with double-sided GMAW-C fillet welds. Number of fillet welds is $2n_s$. (K_{F3}).

The material cost is

$$K_M=k_{M1}5\rho V_1+k_{M2}\rho n_s A_s L/2, \tag{8.131}$$

$$V_1=3000x2R\pi t;\rho=7.85x10^{-6}\ \text{kgmm}^{-3}.\ k_F=1.0\ \$/\text{min},\ k_{Ml}=1.0\ \$/\text{kg}. \tag{8.132}$$

The cost of forming of a shell element into the cylindrical shape according to (Farkas et al. 2004) is

$$K_{F0}=k_F\Theta e^{\mu};\mu=6.8582513-4.527217t^{-0.5}+0.009541996(2R)^{0.5}, \tag{8.133}$$

$$K_{F1}=k_F\left[\Theta\sqrt{\kappa\rho V_1}+1.3x0.1520x10^{-3}t^{1.9358}(2x3000)\right], \tag{8.134}$$

where Θ is a difficulty factor expressing the complexity of the assembly and κ is the number of elements to be assembled

$$\kappa=2;V_1=2R\pi tx3000;\Theta=2, \tag{8.135}$$

$$K_{F2}=k_F\left(\Theta\sqrt{25\rho V_1}+1.3x0.1520x10^{-3}t^{1.9358}x4x2R\pi\right), \tag{8.136}$$

$$K_{F3}=k_F\left(\Theta\sqrt{(n_s+1)\rho V_2}+1.3x0.3394x10^{-3}a_W^2 2Ln_s\right). \tag{8.137}$$

The fillet weld size $a_w=0.3t_w$, a_{wmin} = 3 mm.

$$V_2=5V_1+n_s A_s L/2 \tag{8.138}$$

The cost of painting is

$$K_P = k_P\left(4R\pi L + n_S A_L L/2\right); k_P = 14.4x10^{-6}\,\$/\text{mm}^2. \tag{8.139}$$

The total cost is

$$K = K_M + 5K_{F1} + 5K_{F0} + K_{F2} + K_{F3} + K_P. \tag{8.140}$$

8.4.4 The unstiffened shell

8.4.4.1 *Constraints*

Shell buckling

$$\sigma_a + \sigma_b = \frac{N_F}{2R\pi t} + \frac{H_F L}{R^2\pi t} \le \sigma_{cr} = \frac{f_y}{\sqrt{1+\lambda^4}}, \tag{8.141}$$

$$\lambda^2 = \frac{f_y}{\sigma_a + \sigma_b}\left(\frac{\sigma_a}{\sigma_{Ea}} + \frac{\sigma_b}{\sigma_{Eb}}\right), \tag{8.142}$$

$$\sigma_{Ea} = C_a\left(1.5 - 50\beta\right)\frac{\pi^2 E}{10.92}\left(\frac{t}{L}\right)^2 \tag{8.143}$$

$$C_a = \sqrt{1+\left(\rho_a\xi\right)^2}; Z = \frac{L^2}{Rt}0.9539, \tag{8.144}$$

$$\rho_a = 0.5\left(1+\frac{R}{150t}\right)^{-0.5}; \xi = 0.702Z, \tag{8.145}$$

$$\sigma_{Eb} = C_b\left(1.5 - 50\beta\right)\frac{\pi^2 E}{10.92}\left(\frac{t}{L}\right)^2, \tag{8.146}$$

$$C_b = \sqrt{1+\left(\rho_b\xi\right)^2}, \tag{8.147}$$

$$\rho_b = 0.5\left(1+\frac{R}{300t}\right)^{-0.5}. \tag{8.148}$$

Horizontal displacement

$$w_h = \frac{ML^2}{3E\pi R^3 t} \le w_{allow} = \frac{L}{\phi}, \tag{8.149}$$

$$M = H_F L/\gamma_M; \gamma_M = 1.5; H_F = 0.1N_F. \tag{8.150}$$

8.4.4.2 *The cost function*

Fabrication sequence:

(1) Fabrication of 5 shell elements of length 3 m without stiffeners. For one shell element 2 axial butt welds are needed (GMAW-C) (K_{F1}). The cost of forming of a shell element into the cylindrical shape is also included (K_{F0}).

(2) Welding the 5 units together with 4 circumferential butt welds (K_{F2}).

The material cost is

$$K_M = k_{M1} 5 \rho_1 V_1, \tag{8.151}$$

$$V_1 = 3000 x 2R\pi t, \tag{8.152}$$

$$K_{F0} = k_F \Theta e^{\mu}; \mu = 6.8582513 - 4.527217 t^{-0.5} + 0.009541996 (2R)^{0.5}, \tag{8.153}$$

$$K_{F1} = k_F \left(\Theta \sqrt{\kappa \rho_1 V_1} + 1.3 x 0.152 x 10^{-3} t^{1.9358} x 6000 \right), \tag{8.154}$$

$$\Theta = 2; \kappa = 2; \rho_1 = 7.85 x 10^{-6} \text{ kg/mm}^3,$$

$$K_{F2} = k_F \left(\Theta \sqrt{5 x 5 \rho_1 V_1} + 1.3 x 0.152 x 10^{-3} t^{1.9358} 8R\pi \right), \tag{8.155}$$

k_F = 1.0 \$/min, k_{Ml} = 1.0 \$/kg.

The cost of painting is

$$K_P = k_P (4R\pi L); k_P = 14.4 x 10^{-6} \text{ \$/mm}^2. \tag{8.156}$$

The total cost is

$$K = K_M + 5K_{F1} + 5K_{F0} + K_{F2} + K_P. \tag{8.157}$$

8.4.5 Optimization and results

The optimization is performed using the Particle Swarm mathematical algorithm (Farkas & Jármai 2003). The results are summarized in Table 8.6.

Table 8.6 Results of the optimization for stiffened and unstiffened shell. The positive cost difference means savings due to stiffening

	Stiffened						Unstiffened				cost difference
ϕ	h mm	n_S	t	$w_h<w_{allow}$ mm	$\sigma < \sigma_{cr}$ MPa	K \$	t	$w_h<w_{allow}$ mm	$\sigma < \sigma_{cr}$ MPa	K \$	%
400	203	5	24	25<37.5	314<317	56310	22	27.7<37.5	349<351	49480	-14
500	610	5	22	24<30	307<311	56082	22	27.7<30	349<351	49480	-13
600	406	5	23	24.8<25	313<314	55760	25	24.4<25	307<352	55800	0
700	686	14	16	21<21.4	293<294	57751	29	21<21.4	264<353	64440	12
800	914	10	16	18.2<18.7	268<282	62294	33	18.5<18.7	232<354	73370	18
900	914	15	12	16<16.7	248<254	66545	37	16.5<16.7	207<354	82580	24
100	914	18	11	14.4<15	227<253	70571	41	14.9<15	187<354	92100	30

It can be seen that the buckling (stress) constraint is active when the allowable horizontal displacement is $L/400 - L/500$ and for these cases the unstiffened shell is cheaper than the stiffened one.
On the other hand, for $L/700$-$L/1000$ the displacement constraint is active and the stringer-stiffened shell is cheaper than the unstiffened one. The cost savings achieved by stiffening is 12-30%.

Comparison of the costs for unstiffened and stiffened shells

This comparison is shown in Table 8.7.

Table 8.7 Summary of costs (positive difference means cost savings) (Costs in $)

Cost	Unstiffened shell	Stiffened shell	Difference %
Material K_M	56117	45321	24
Forming $5K_{F0}$	8385	4342	93
Welding $5K_{F1}+K_{F2}$	22577		
Welding $5K_{F1}+K_{F2}+K_{F3}$		10169	122
Painting K_P	5021	10739	-114
Total	92100	70571	30

It can be seen that the cost savings caused by stringer stiffening are significant in forming and welding costs, but the painting for unstiffened shell is 114% cheaper than that for stiffened one.

It can be concluded that the cost factors of fabrication and painting play an important role in the achievable cost savings.

8.4.6 Multiobjective optimization

The Particle Swarm Optimizer has been built into this interactive decision support program system (Jármai 1989a) as it was written in Chapter 1, which contains the following single objective optimization methods

Complex method of Box (1965)

Flexible Tolerance (*FT*) method of Himmelblau (1971),

Direct Random Search (*DRS*) method (Siddal 1982),

Hillclimb method (*HILL*) of Rosenbrock (1960),

Davidon-Flecher-Powell (*DFP*) method of Rao (1984),

Particle Swarm Optimization (*PSO*), (Jármai 2005).

The efficiencies of these methods are different. All of them use the same objective, constraints subroutines. For a problem like this, which is highly non-linear, several local minima exist. They find different ones. The advantage of Particle swarm optimization is that it can find optimum for a nonconvex problem. It has found the minimum cost structure. Table 8.8 shows the single objective optima.

The interactive decision support program system contains several multiobjective optimization methods. They are the following:

Min-max method,

Global criterion method: type - I,

Global criterion method: type - II,

Weighted min-max method,

Weighted global criterion method,

Pure weighting method,

Normalized weighting method.

Weighting coefficients are similar to all four objectives 0.25 each.

Table 8.8 Different optima for the total cost, using different single objective optimization techniques

Method	h_s (mm)	n_s	t (mm)	Total cost ($)	2nd Material cost	3rd Fabrication cost	4th Painting cost
Flexible tolerance	257.2	25	21	79081.4	46463.6	22912.1	9705.6
Hillclimb	257.2	15	24	82361.4	49678.7	24632.6	8050.1
Davidon Fletcher Powell	257.2	17	23	81593.5	49014.2	23634.2	8945.0
Particle swarm optimization	257.2	24	21	78639.7	46283.1	22746.1	9610.6

The objective functions are as follows:

Total cost of the structure in $, K (1st),

Material cost of the structure in $, K_M (2nd),

Fabrication cost of the structure in $, $K_F = 5K_{F1}+5K_{F0}+K_{F2}$ (3rd),

Painting cost in $, K_P (4th).

Table 8.9 shows the different multiobjective optima. The material cost is dominating, 55-65 % of the total cost. The other two objectives are around 35-45 %. The height of stiffener is nearly the same at all optima; the number of stiffeners and the shell thickness is changing on an opposite way due to the necessary stiffness. The greatest conflict is between the total and the painting costs. The painting cost minimum gives the greatest shell thickness t.

The optimization is performed using the Particle Swarm mathematical algorithm. The results are summarized in Table 8.9.

Table 8.9 Multiobjective optima for the stringer stiffened shell

Method	h_s (mm)	n_s	t (mm)	1st Total cost ($)	2nd Material cost ($)	3rd Fabrication cost ($)	4th Painting cost ($)
1st objective	257.2	24	21	**78639.7**	46283.1	22746.1	9610.6
2nd objective	257.2	24	21	78639.7	**46283.1**	22746.1	9610.6
3rd objective	683.5	25	15	87516.6	56295.1	**17691.4**	13530.0
4th objective	257.2	5	26	85276.8	52840.0	24632.6	**7804.1**
Min-max	257.2	24	21	78629.7	46283.1	22746.1	9610.6
Weighted min-max	257.2	24	21	78629.7	46283.1	22746.1	9610.6
Global criterion 1 exp. 3	308.7	23	21	79432.3	46994.2	22599.6	9838.6
Global criterion 2 exp. 2	257.2	21	22	80336.5	47738.9	23272.2	9325.4
Weighted global	257.2	21	22	80336.5	47738.9	23272.2	9325.4
Pure weighting	257.2	25	21	79081.4	46463.6	22912.1	9705.7
Normalized weighting	257.2	24	21	78629.7	46283.1	22746.1	9610.6

8.4.7 Conclusions

Cylindrical shells stiffened outside by stringers are economic for axial compression and bending with an active deflection constraint, but without a deflection constraint they are uneconomic.

In order to decrease the welding cost, the stiffeners should have cross-sectional area as large as possible and should welded to shell with welds as small as possible, thus the outside halved rolled I-section stringers are advantageous for this purpose.

In the investigated numerical problem 12-30 % cost savings can be achieved using this stiffening in the case of displacement limit of $L/700$-$L/1000$. It should be noted that cost savings cannot be achieved by stringers welded inside of the shell.

The decision support system, which contains several single and multiobjective optimization techniques, is an efficient tool for structural optimization. Using the same constraints, the optimizers can find the optima. If these optima are similar, or close to each other, the designer can be sure, that he has found, or close to the global optimum. Discrete solutions are useful for the application of the results. The robustness of PSO is visible, when the problem is non-convex. In this case the material cost is dominant; the optima for the total and for the material cost minimum are identical. Using different multiobjective optimization techniques, different weighting coefficients, we can get a great number of optima to get more information about the behaviour of the structure.

The PSO technique was found to be a robust method for multiobjective optimization as well. Some of the objectives are in conflict. The material cost represents more than 60 % of the total cost. Optimization for the cost of forming the shell elements into the cylindrical shape, assembly and welding means a smaller shell thickness and more and larger stiffeners. Optimization for the painting cost means a thicker shell with fewer and smaller stiffeners.

8.5 A WELDED ORTHOGONALLY STIFFENED CYLINDRICAL SHELL SUBJECT TO AXIAL COMPRESSION AND EXTERNAL PRESSURE

8.5.1 Introduction

In the present study the combined load of axial compression and external pressure is considered, as it acts on parts of the columns of a truss tower of a fixed offshore platform (see Figures 8.10 and 8.11). The cylindrical-shell member that is orthogonally stiffened by using ring stiffeners of box cross-section and stringers of halved rolled I-section (see Figures 8.12 and 8.13), is to be optimized with respect to a cost function, which includes material, manufacturing and painting costs.

In order to demonstrate the economy of the stiffening, both stiffened and un-stiffened assemblies are optimized and their costs are compared to each other . The design rules used here are formulated according to the design rules of Det Norske Veritas (1995). The cost function is formulated in correspondence to the manufacturing sequence. The specified constraints relate to shell buckling, panel stringer and panel ring buckling, as well as to manufacturing limitations.

In the case of the orthogonally stiffened assemblies, the particular design variable to be considered are the shell thickness (t), the number of longitudinal stiffeners (stringers) (n_s), the number of ring-stiffeners (n_r), the box height (h_r) and the stringer stiffener height ($h=h_1+2t_f$), (see Figures 8.12 and 8.13).

8.5.2 Constraints for the orthogonally stiffened cylindrical shell

Some of the quantities that appear in the definitions of the constraints are given below, are also indicated in Figure 8.12.

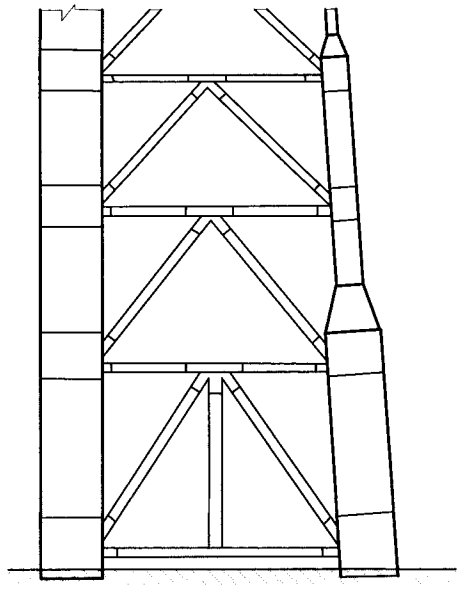

Figure 8.10 A part of a fixed offshore structure, the main columns are stiffened cylindrical shells

8.5.2.1 *Shell (curved panel) buckling*

The equivalent stress σ_e must satisfy the constraint:

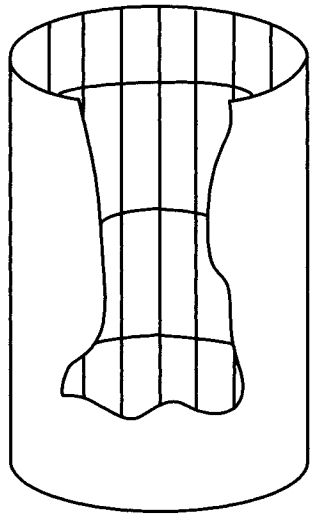

Figure 8.11 An illustrative sketch of a part of an orthogonally stiffened cylindrical shell

$$\sigma_e = \sqrt{\sigma_a^2 - \sigma_a \sigma_p + \sigma_p^2} \le \frac{f_{y1}}{\sqrt{1+\lambda_s^4}}, \tag{8.158}$$

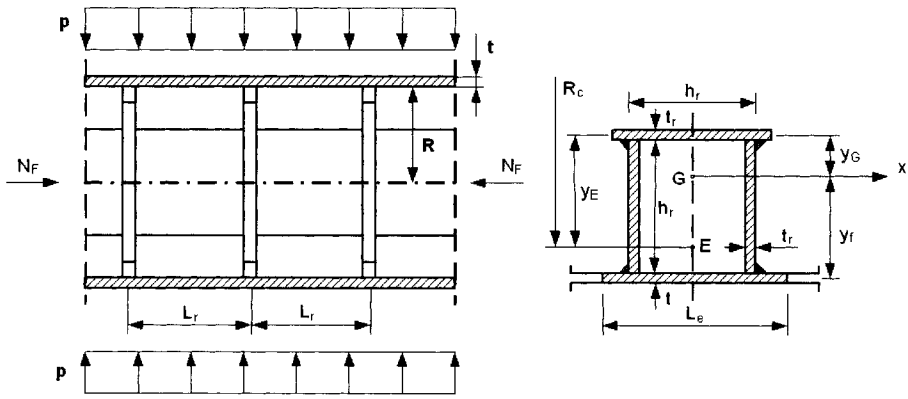

Figure 8.12 Stringer and ring stiffened cylindrical shell with compression and external pressure

where $f_{y1} = \dfrac{f_y}{1.1}$, and the stress due to axial compression is given by

$$\sigma_a = \frac{N_F}{2R\pi t_e}, \text{ where } t_e = t + \frac{A_S}{s} \text{ and } s = \frac{2R\pi}{n_s}, \tag{8.159}$$

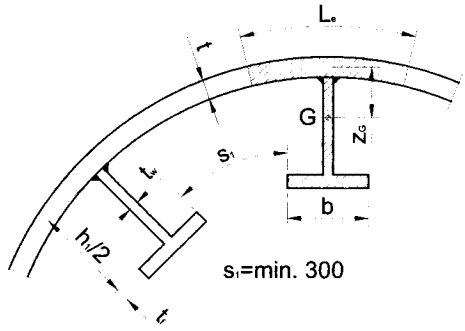

Figure 8.13 Cross-section of the stiffened shell

Here f_y is the yield stress, N_F is the factored compression force, R is the shell radius, t is the shell thickness, A_s is the cross-sectional area of a stringer, n_s is the number of longitudinal stiffeners (stringers). Also appearing in the above constraint definition is the stress due to external pressure

$$\sigma_p = \frac{p_F R}{t(1+\alpha)}, \ \alpha = \frac{A_R}{L_{e0}t}, \ L_{e0} = \min(L_r, L_{er} = 1.56\sqrt{Rt}) \text{ and } L_r = \frac{L}{n_r - 1}. \tag{8.160}$$

Here p_F is the factored external pressure intensity, A_r is the cross-sectional area of a ring-stiffener, L is the shell length, n_r is the number of ring-stiffeners, L_r is the distance between rings. Also used in the definition above is λ_s^2 defined by

$$\lambda_s^2 = \frac{f_{y1}}{\sigma_e}\left(\frac{\sigma_a}{\sigma_{Eas}} + \frac{\sigma_p}{\sigma_{Eps}}\right), \text{ where } \sigma_{Eas} = C_{as}\frac{\pi^2 E}{12(1-\nu^2)}\left(\frac{t}{s}\right)^2, \tag{8.161}$$

E and ν are the Young modulus and the Poisson ratio, respectively

$$C_{as} = \psi_{as}\sqrt{1+\left(\frac{\rho_{as}\xi_{as}}{\psi_{as}}\right)^2}, \ \psi_{as} = 4, \ Z_{as} = \frac{s^2}{Rt}\sqrt{1-\nu^2}, \xi_{as} = 0702Z_{as}, \tag{8.162}$$

$$\rho_{as} = 0.5\left(1+\frac{R}{150t}\right)^{-05}, \ \sigma_{Eps} = C_{ps}\frac{\pi^2 E}{10.92}\left(\frac{t}{s}\right)^2, \tag{8.163}$$

$$C_{ps} = \psi_{ps}\sqrt{1+\left(\frac{\rho_{ps}\xi_{ps}}{\psi_{ps}}\right)^2}, \ \rho_{ps} = 0.6, \tag{8.164}$$

and

$$\xi_{ps} = 1.04\frac{s}{L_r}\sqrt{Z_{ps}},\ Z_{ps} = Z_{as},\ \text{and}\ \psi_{ps} = \left[1+\left(\frac{s}{L_r}\right)^2\right]^2. \tag{8.165}$$

8.5.2.2 *Panel stiffener (stringer) buckling*

In this case the equivalent stress σ_e must satisfy the constraint:

$$\sigma_e \le \frac{f_{y1}}{\sqrt{1+\lambda_P^4}}, \tag{8.166}$$

where

$$\lambda_P^2 = \frac{f_{y1}}{\sigma_e}\left(\frac{\sigma_a}{\sigma_{Eap}}+\frac{\sigma_p}{\sigma_{Epp}}\right),\ \sigma_{Eap} = C_{ap}\frac{\pi^2 E}{10.92}\left(\frac{t}{L_r}\right)^2,\ C_{ap} = \psi_{ap}\sqrt{1+\left(\frac{\rho_{ap}\xi_{ap}}{\psi_{ap}}\right)^2}, \tag{8.167}$$

$$\rho_{ap} = 0.5,\ \xi_{ap} = 0.702Z_{ap},\ Z_{ap} = \frac{L_r^2}{Rt}0.9539, \tag{8.168}$$

$$\psi_{ap} = \frac{1+\gamma_s}{1+\dfrac{A_S}{s_e t}},\ \gamma_s = 10.92\frac{I_{Sef}}{st^3},\ \text{and}\ s_E = 1.9t\sqrt{\frac{E}{f_y}}. \tag{8.169}$$

With respect to further quantities to be computed below, the following rule is applied:

$$\text{if}\ \ s_E \le s,\ s_e = s_E\ ,\ \text{and if}\ \ s_E \ge s,\ s_e = s\,. \tag{8.170}$$

I_{Sef} is the moment of inertia of a stiffener including effective shell plating s_e. In the case of a stiffener of halved UB section (flange width b, flange thickness t_f, web height $h_1/2$, and web thickness t_w as shown in Figure 8.13), the distance of the centre of gravity is

$$z_G = \frac{\dfrac{h_1}{2}t_w\left(\dfrac{h_1}{4}+\dfrac{t}{2}\right)+bt_f\left(\dfrac{h_1+t+t_f}{2}\right)}{s_e t+bt_f+h_1 t_w/2}, \tag{8.171}$$

and I_{sef} is given by

$$I_{Sef} = s_e t z_G^2+\left(\frac{h_1}{2}\right)^3\frac{t_w}{12}+\frac{h_1 t_w}{2}\left(\frac{h_1}{4}+\frac{t}{2}-z_G\right)^2+bt_f\left(\frac{h_1+t+t_f}{2}-z_G\right)^2, \tag{8.172}$$

and

$$A_s = bt_f+h_1 t_w/2\,. \tag{8.173}$$

Furthermore

$$\sigma_{Epp} = C_{pp}\frac{\pi^2 E}{10.92}\left(\frac{t}{L_r}\right)^2,\quad C_{pp} = \psi_{pp}\sqrt{1+\left(\frac{\rho_{pp}\xi_{pp}}{\psi_{pp}}\right)^2}, \tag{8.174}$$

$$\xi_{pp} = 1.04\sqrt{Z_{pp}},\ Z_{pp} = Z_{ap},\ \rho_{pp} = 0.6,\ \text{and}\ \psi_{pp} = 2\left(1+\sqrt{1+\gamma_s}\right). \tag{8.175}$$

8.5.2.3 *Panel ring buckling*

The ring-stiffeners are welded square box sections, (see Figure 8.12), constructed from three plate elements of width b_r and thickness t_r. The relationship that must be satisfied between the width and thickness, is prescribed by the Eurocode 3 (2002) rule for compression plates against buckling, and is given by

$$t_r \geq \delta_r h_r,\ 1/\delta_r = 42\varepsilon,\ \varepsilon = \sqrt{235/f_y},\ f_y = 355,\ \delta_r = 1/34. \tag{8.176}$$

Assuming the buckling constraint, given by (Eq. 8.176), to be active, then the cross-sectional area of a ring-stiffener is

$$A_R = 3h_r t_r = 3\delta_r h_r^2. \tag{8.177}$$

The required cross-sectional area of ring-stiffener, excluding the effective shell width, is

$$A_{Rreq} = \left(\frac{2}{Z^2} + 0.06\right)L_r t,\ \text{where}\ Z = \frac{L_r^2}{Rt}0.9539. \tag{8.178}$$

Thus the constraint is:

$$A_{Rreq} \leq A_R. \tag{8.179}$$

The effective flange width is given by

$$L_e = \min\left(L_r, 2\times 1.56\sqrt{Rt}\right).$$

The distance of the centroid of ring (point E in Figure 8.12), including the effective shell flange width is given by

$$y_E = \frac{L_e t(h_r + t/2) + \delta_r h_r^3}{3\delta_r h_r^2 + L_e t}. \tag{8.180}$$

The moment of inertia of the ring about x-axis is

$$I_R = \frac{\delta_r h_r^4}{6} + 2\delta_r h_r^2\left(\frac{h_r}{2} - y_E\right)^2 + \delta_r h_r^2 y_E^2 + L_e t\left(h_r + \frac{t}{2} - y_E\right)^2. \tag{8.181}$$

The required moment of inertia of a ring is given by

$$I_{Rreq} = I_a + I_p, \tag{8.182}$$

where I_a is the required moment of inertia for axial compression, and I_p that for external pressure, respectively given by

$$I_a = \frac{\sigma_a t\left(1+\frac{A_S}{st}\right)R_0^4}{500EL_R}, \quad R_0 = R-\left(h_r - y_E\right), \tag{8.183}$$

and

$$I_p = \frac{p_F R R_0^2 L_r}{3E}\left[2+\frac{3Ey_E\delta_0}{R_0^2\left(\frac{f_y}{2}-\sigma_p\right)}\right] \text{ with } \delta_0 = 0.005R. \tag{8.184}$$

The constraint is:

$$I_{Rreq} \le I_R. \tag{8.185}$$

8.5.2.4 *Manufacturing limitations*

In order to ensure that the welding of the webs of the halved rolled I-section stringers into the shell is possible, the minimum distance between the stringer flanges should satisfy the following condition:

$$\frac{2\left(R-h_r/2\right)\pi}{n_s} - b \ge 300 \text{ mm}. \tag{8.186}$$

or:

$$n_s \le \frac{2\left(R-h_r/2\right)\pi}{b+300}. \tag{8.187}$$

Another limitation is related to the minimum value of fillet welds connecting the stringer webs to the shell, and that for connecting the plate elements of ring-stiffeners. They are respectively given by $a_{ws} = 0.4t_w$, $a_{ws.min} = 3$ mm, and $a_{wr} = 0.4t_r$, $a_{wr.min} = 3$ mm.

8.5.3 Cost function for the orthogonally stiffened cylindrical shell

The cost function (K) includes material (K_M) and manufacturing costs (K_{Fi}), as well as the cost of painting (K_P) the final assembly, i.e. the total cost is given by

$$K = K_M + \sum_i K_{Fi} + K_P. \tag{8.188}$$

The manufacturing sequence, determining the associated total manufacturing cost, is as follows:

(1) Form plate elements of L_s = 3 m length, into cylindrical shapes, (K_{F0}).

(2) Weld shell segments of L_s = 3 m length, from 2 curved plate elements, with 2 butt welds using GMAW-C (Gas Metal Arc Welding with CO_2), (K_{F1}).

(3) Weld whole un-stiffened shell of L = 15 m length, from 5 shell segments with 4 circumferential butt welds, using GMAW-C, (K_{F2}).

(4) Weld n_r ring-stiffeners from 3 plate elements with 2 fillet welds, each using SMAW (Shielded Metal Arc Welding), (K_{F3}).

(5) Weld n_r ring-stiffeners into the whole shell with 2 n_r circumferential fillet welds, using SMAW, (K_{F4}).

(6) Weld n_s stringers into the shell with 2 n_s fillet welds, using SMAW, (K_{F5}).

The volume of a shell segment is

$$V_1 = 2R\pi tL_s, \tag{8.189}$$

and the volume of a ring-stiffener is given by

$$V_R = 2\pi\delta_r h_r^2(R - h_r) + 4\pi\delta_r h_r^2(R - h_r/2). \tag{8.190}$$

The material cost is expressed as

$$K_M = k_{M1}5\rho V_1 + k_{M1}\rho n_r V_R + k_{M2}\rho n_s A_s L, \tag{8.191}$$

where k_{M1} and k_{M2} are the respective cost factors for plates and rolled I-sections.

The manufacturing cost components are as follows:

$$K_{F0} = 5k_F\Theta e^{\mu}, \mu = 6.8582513 - 4.527217t^{-0.5} + 0.009541996(2R)^{0.5}, \tag{8.192}$$

$$K_{F1} = 5k_F\left(\Theta\sqrt{\kappa\rho V_1} + 1.3\times 0.1520\times 10^{-3}t^{1.9358}\times 2L_s\right),\ \Theta = 2,\ \kappa = 2, \tag{8.193}$$

$$K_{F2} = k_F\left(\Theta\sqrt{25\rho V_1} + 1.3\times 0.1520\times 10^{-3}t^{1.9358}\times 4\times 2R\pi\right), \tag{8.194}$$

$$K_{F3} = n_r k_F\left[3\sqrt{3\rho V_R} + 1.3\times 0.3394\times 10^{-3}a_{wr}^2 4\pi(R - h_r)\right], \tag{8.195}$$

$$K_{F4} = k_F\left[3\sqrt{(n_r+1)\rho(5V_1 + n_r V_R)} + 1.3\times 0.3394\times 10^{-3}a_{wr}^2 n_r 4R\pi\right], \tag{8.196}$$

and

$$K_{F5} = k_F\left[3\sqrt{(n_r + n_s + 1)\rho(5V_1 + n_r V_R + n_s A_s L)} + 1.3\times 0.3394\times 10^{-3}a_{ws}^2 n_s 2L\right]. \tag{8.197}$$

Finally, the cost of painting is given by

$$K_P = k_P\left[2R\pi L + 2R\pi(L - n_r h_r) + 2n_r\pi h_r(R - h_r) + 4\pi n_r h_r\left(R - \frac{h_r}{2}\right) + n_s L(h_1 + 2b)\right]. \tag{8.198}$$

8.5.4 Constraint and cost function for the unstiffened shell

8.5.4.1 *Constraint on shell buckling*

The equivalent stress σ_e must satisfy the constraint:

$$\sigma_e = \sqrt{\sigma_{aa}^2 - \sigma_a\sigma_p + \sigma_p^2} \le \frac{f_{y1}}{\sqrt{1+\lambda^4}}, \tag{8.199}$$

where $f_{y1} = \dfrac{f_y}{1.1}$,

$$\lambda_S^2 = \frac{f_{y1}}{\sigma_e}\left(\frac{\sigma_a}{\sigma_{Ea}} + \frac{\sigma_p}{\sigma_{Ep}}\right),\ \sigma_a = \frac{N_F}{2R\pi t},\quad \sigma_p = \frac{p_F R}{t}, \tag{8.200}$$

$$\sigma_{Ea} = C_a\frac{\pi^2 E}{12(1-\nu^2)}\left(\frac{t}{L}\right)^2,\ C_a = \psi_a\sqrt{1+\left(\frac{\rho_a\xi_a}{\psi_a}\right)^2},\ \psi_a = 1, \tag{8.201}$$

$$Z_a = \frac{L^2}{Rt}\sqrt{1-\nu^2},\ \xi_a = 0702Z_a,\ \rho_a = 0.5\left(1+\frac{R}{150t}\right)^{-0.5}, \tag{8.202}$$

$$\sigma_{Ep} = C_p\frac{\pi^2 E}{10.92}\left(\frac{t}{L}\right)^2,\ C_p = \psi_p\sqrt{1+\left(\frac{\rho_p\xi_p}{\psi_p}\right)^2},\ \rho_p = 0.6, \tag{8.203}$$

and $\xi_p = 1.04Z_p,\quad Z_p = Z_a,\ \psi_p = 4.$ (8.204)

8.5.4.2 *Cost function for the unstiffened shell*

The cost function includes cost of material, manufacturing and painting:

$$K = K_M + \sum_i K_{Fi} + K_P. \tag{8.205}$$

The manufacturing sequence in this case is as follows:

(1) Form plate elements of L_s = 3 m length, into cylindrical shapes, (K_{F0}).

(2) Weld shell segments of L_s = 3 m length from 2 curved plate elements, with 2 butt welds, using GMAW-C (Gas Metal Arc Welding with CO_2), (K_{F1}).

(3) Weld whole un-stiffened shell of L = 15 m length, from 5 shell segments with 4 circumferential butt welds, using GMAW-C (K_{F2}).

The volume of a shell segment is

$$V_1 = 2R\pi tL_s . \tag{8.206}$$

The material cost is expressed as

$$K_M = k_{M1} 5\rho V_1 . \tag{8.207}$$

where k_{Ml} is the cost factor for plates.
The manufacturing cost components are as follows:

$$K_{F0} = 5k_F \Theta e^{\mu}, \mu = 6.8582513 - 4.527217t^{-0.5} + 0.009541996(2R)^{0.5}, \tag{8.208}$$

$$K_{F1} = 5k_F\left(\Theta\sqrt{\kappa\rho V_1} + 1.3\times 0.1520\times 10^{-3} t^{1.9358} \times 2L_S\right),\ \Theta = 2, \kappa = 2, \tag{8.209}$$

$$K_{F2} = k_F\left(\Theta\sqrt{25\rho V_1} + 1.3\times 0.1520\times 10^{-3} t^{1.9358} \times 4\times 2R\pi\right), \tag{8.210}$$

k_F = 1.0 \$/min, k_{Ml} = 1.0 \$/kg.

The cost of painting is given by $K_P = 4R\pi Lk_P, k_P = 14.4\times 10^{-6}\ \$/\text{mm}^2$.

8.5.5 Numerical optimization results

8.5.5.1 *Numerical data*

The loading is specified by N_F = 5.4x10^7 N and p_F = 1.5 MPa. The values of the remaining data used are: L = 15 m, R = 1850 mm, f_y = 355 MPa, E = 2.1x10^5 MPa, $\nu = 0.3$. The cost factor values are k_{Ml} =k_{M2} = 1.0 \$/kg, k_F = 1.0 \$/min and k_P = 14.4x10^{-6} \$/mm^2.

The geometric characteristics of an UB section, namely (t_w, b, t_f, h) are approximated by curve-fitting functions (Table Curve 2D 2003)(see in Appendix C, Eqs C1-C3).

Practical considerations restrict the final values of the design variables. The thicknesses t may assume any integer mm value. The height of the ring stiffeners h_r is restricted to steps of 10 mm. For the UB sections, according to the ARBED catalogue, the only acceptable values for h are 152, 203, 254, 305, 356, 406, 457, 533, 610, 686, 762, 838, 914 mm (Profil Arbed 2001).

For the optimization the leap-frog, the dynamic-Q and the particle swarm algorithms are used. These methods are described in Chapter 1.

8.5.5.2 *Results for the orthogonally stiffened cylindrical shell*

The best continuous solution obtained, together with the discrete solution are listed in Table 8.10.

Table 8.10 Results for the 5 variables: continuous and discrete solutions (M=500).

t [mm]	n_s	n_r	h_r [mm]	h [mm]	K [$]
13.82	26.85	8.31	260.96	225.79	54444.62 (cont.)
14	**27**	**9**	**270**	**203**	**55342.9** (disc.)

8.5.5.3 *Results for the unstiffened shell*

The shell buckling constraint is satisfied if the shell thickness is t = 50 mm. In this case the objective function is K = 112131.3 $. Thus, a cost saving of 51 % can be achieved by the orthogonal stiffening of the shell member.

8.5.6 Conclusions

The results show that if the member is stiffened, a cost saving of more than 50 percent, compared to that of the unstiffened shell, may be obtained. This is due to the fact that stiffening allows the thickness of the shell to be reduced to 14 mm, which represents a significant material saving, compared to the unstiffened shell that requires a minimum thickness of 50 mm. This material saving overshadows the increase in labour and welding costs associated with the stiffening.

8.6 A STRINGER-STIFFENED STEEL CYLINDRICAL SHELL OF VARIABLE DIAMETER SUBJECT TO AXIAL COMPRESSION AND BENDING

8.6.1 Introduction

A column is investigated subject to an axial compression and a horizontal force acting on the top of the column (Fig.8.14). The column is fixed at the bottom and free on the top. It is shown that a shell stiffened outside with stringers can be economic, when a constraint on horizontal displacement of the column top is active. In order to decrease the welding cost of stiffeners, their cross-sectional area is increased, i.e. halved rolled I-section (UB) stiffeners are used instead of flat ones.

The halved I-sections are advantageous, since the web can be easier welded to the shell than the flange. It should be mentioned that stringer-stiffening can also be economic in those cases, when the corresponding unstiffened version needs a very thick shell (more than 40 mm).

The cross-section of the stiffened shell is constant along the whole height. Constraints on local shell buckling, on stringer panel buckling and on horizontal displacement are taken into account. The buckling constraints are formulated according to the DNV design rules (1995). The cost function to be minimized includes the cost of material, forming of shell elements into cylindrical shape, assembly, welding and painting.

In order to demonstrate the economy of the stiffened shell, the unstiffened version is also optimized. The results show that the cost savings depends on the active displacement constraint.

8.6.2 Problem formulation

The investigated structure is a supporting column loaded by an axial and horizontal force (Fig.8.14). The horizontal displacement of the top is limited by the reasons of serviceability of the supported structure. Both the stiffened and unstiffened shell version is optimized and their cost is compared to each other. In the stiffened shell outside longitudinal stiffeners of halved rolled I-section (UB) are used. The cost function is formulated according the fabrication sequence.

Given data are as follows: column height L, factored axial compression force N_F, factored horizontal force H_F, yield stress of steel f_y, cost factors for material, fabrication and painting k_m, k_f, k_p. The unknowns are the shell thickness t and radius R as well as the height h and number n_s of halved rolled I-section stiffeners.
The characteristics of the selected UB profiles are given in Appendix C.

In order to calculate with continuous values the geometric characteristics of an UB section (I_y, b, t_f) are approximated by curve-fitting functions as follows: h approximately equals to the first number of the profile name (Table Curve 2D, 2003) (Appendix C, Eqs C11-C13).

8.6.3 The stiffened shell

8.6.3.1 *Constraints*

Shell buckling (unstiffened curved panel buckling)

The sum of the axial and bending stresses should be smaller than the critical buckling stress

$$\sigma_a + \sigma_b = \frac{N_F}{2R\pi t_e} + \frac{H_F L}{R^2 \pi t_e} \le \sigma_{cr} = \frac{f_y}{\sqrt{1+\lambda^4}}, \tag{8.211}$$

where the reduced slenderness

$$\lambda^2 = \frac{f_y}{\sigma_a + \sigma_b}\left(\frac{\sigma_a}{\sigma_{Ea}} + \frac{\sigma_b}{\sigma_{Eb}}\right); t_e = t + \frac{A_s}{2s}; s = \frac{2R\pi}{n_s}, \tag{8.212}$$

t_e is the equivalent thickness. The elastic buckling stress for the axial compression is

$$\sigma_{Ea} = C_a(1.5 - 50\beta)\frac{\pi^2 E}{10.92}\left(\frac{t}{s}\right)^2, \tag{8.213}$$

$$C_a = 4\sqrt{1+\left(\frac{\rho_a \xi}{4}\right)^2}; Z = \frac{s^2}{Rt}0.9539, \tag{8.214}$$

$$\rho_a = 0.5\left(1+\frac{R}{150t}\right)^{-0.5}; \xi = 0.702Z. \tag{8.215}$$

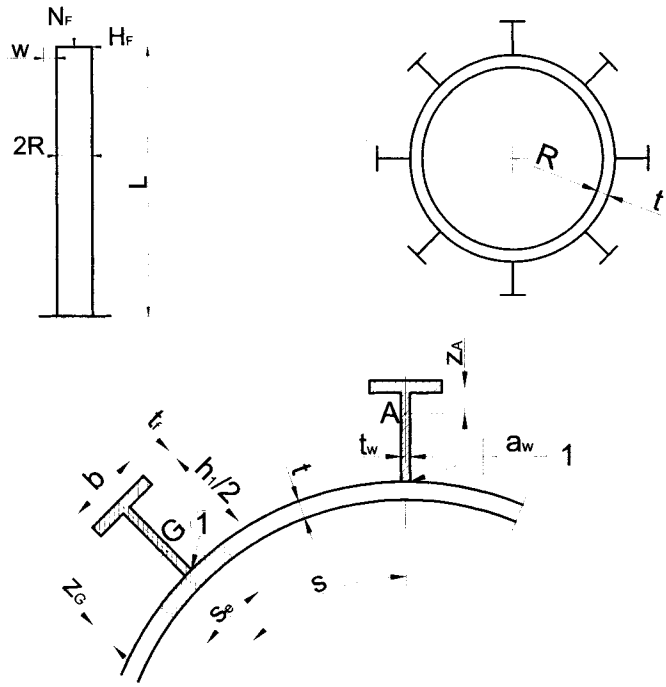

Figure 8.14 A column constructed as a stiffened cylindrical shell loaded by a compression force N_F and a horizontal force H_F. Cross-section and a detail of the cross-section with outside stiffeners of halved rolled I-section. The horizontal displacement of the top (w) is limited

The elastic buckling stress for bending is

$$\sigma_{Eb} = C_b\left(1.5-50\beta\right)\frac{\pi^2 E}{10.92}\left(\frac{t}{s}\right)^2, \tag{8.216}$$

$$C_b = 4\sqrt{1+\left(\frac{\rho_b \xi}{4}\right)^2}, \tag{8.217}$$

$$\rho_b = 0.5\left(1+\frac{R}{300t}\right)^{-0.5}. \tag{8.218}$$

Note that the residual welding distortion factor $1.5-50\beta = 1$ when t>9 mm. The detailed derivation of it is treated in (Farkas 2002).

Stringer panel buckling

$$\sigma_a + \sigma_b \le \sigma_{crp} = \frac{f_y}{\sqrt{1+\lambda_p^4}}, \tag{8.219}$$

$$\lambda_p^2 = \frac{f_y}{\sigma_{Ep}}; \sigma_{Ep} = C_p \frac{\pi^2 E}{10.92}\left(\frac{t}{L}\right)^2, \tag{8.220}$$

$$C_p = \psi_p \sqrt{1+\left(\frac{0.5\xi_p}{\psi_p}\right)^2}; Z_p = 0.9539\frac{L^2}{Rt}, \tag{8.221}$$

$$\xi_p = 0.702 Z_p; \gamma_s = 10.92\frac{I_{sef}}{st^3}, \tag{8.222}$$

$$\psi_p = \frac{1+\gamma_s}{1+\frac{A_s}{2s_e t}}; \tag{8.223}$$

Since the effective shell part s_e (Fig.8.14) is given by DNV with a complicated iteration procedure, we use here the simpler method of ECCS (1988).

$$s_E = 1.9t\sqrt{\frac{E}{f_y}}, \tag{8.224}$$

if $s_E < s$ $\quad s_e = s_E$,

if $s_E > s$ $\quad s_e = s$.

I_{sef} is the moment of inertia of a cross section containing the stiffener and a shell part of width s_e (Fig. 8.14). For a stiffener of halved rolled I-section it is

$$I_{sef} = s_e t z_G^2 + \frac{t_w}{12}\left(\frac{h_1}{2}\right)^3 + \frac{h_1 t_w}{2}\left(\frac{h_1}{4} - z_G\right)^2 + bt_f\left(\frac{h_1}{2} - z_G\right)^2, \tag{8.225}$$

$$z_G = \frac{h_1^2 t_w/8 + h_1 b t_f/2}{h_1 t_w/2 + bt_f + s_e t}. \tag{8.226}$$

Horizontal displacement

$$w_h = \frac{ML^2}{3EI_{x0}} \le w_{allow} = \frac{L}{\phi}. \tag{8.227}$$

The exact calculation of the moment of inertia for the horizontal displacement uses the following formulae (Fig.8.14):
The distance of the centre of gravity for the halved UB section is

$$z_A = \frac{h_1 t_w/2\left(h_1/4 + t_f/2\right)}{h_1 t_w/2 + bt_f}. \tag{8.228}$$

The moment of inertia of the halved UB section is expressed by

$$I_x = bt_f z_A^2 + \frac{t_w}{12}\left(\frac{h_1}{2}\right)^3 + \frac{h_1 t_w}{2}\left(\frac{h_1}{4} - z_A\right)^2. \tag{8.229}$$

The moment of inertia of the whole stiffened shell cross-section is

$$I_{x0} = \pi R^3 t + I_x \sum_{i=1}^{n_s} \sin^2\left(\frac{2\pi i}{n_s}\right) + \\ + \left(\frac{h_1 t_w}{2} + bt_f\right)\left(R + \frac{h_1 + t_f}{2} - z_A\right)^2 \sum_{i=1}^{n_s} \sin^2\left(\frac{2\pi i}{n_s}\right), \tag{8.230}$$

$$M = H_F L / \gamma_M; \gamma_M = 1.5; H_F = 0.1 N_F. \tag{8.231}$$

Numerical data: N_F = 6x10^7 kN, f_y = 355 MPa, L = 15 m, the radius is varied between R = 1900-3500 mm.

8.6.3.2 *The cost function*

Fabrication sequence:

(1) Fabrication of 5 shell elements of length 3 m without stiffeners. For one shell element 2 axial butt welds are needed (GMAW-C) (K_{F1}). The cost of forming of a shell element into the cylindrical shape is also included (K_{F0}).

(2) Welding of the whole unstiffened shell from 5 elements with 4 circumferential butt welds (K_{F2}).

(3) Welding of n_s stiffeners to the shell with double-sided GMAW-C fillet welds. Number of fillet welds is $2n_s$. (K_{F3}).

The material cost is

$$K_M = k_{M1} 5\rho V_1 + k_{M2} \rho n_s A_s L / 2, \tag{8.232}$$

$$V_1 = 3000x2R\pi t; \rho = 7.85x10^{-6}\ \text{kgmm}^{-3}.$$

$$k_F = 1.0\ \$/\text{min}, k_{MI} = 1.0\ \$/\text{kg}. \tag{8.233}$$

The cost of forming of a shell element into the cylindrical shape according to (Farkas et al. 2004) is

$$K_{F0} = k_F \Theta e^{\mu}; \mu = 6.8582513 - 4.527217 t^{-0.5} + 0.009541996(2R)^{0.5}, \tag{8.234}$$

$$K_{F1} = k_F \left[\Theta\sqrt{\kappa\rho V_1} + 1.3x0.1520x10^{-3} t^{1.9358}(2x3000)\right], \tag{8.235}$$

where Θ is a difficulty factor expressing the complexity of the assembly and κ is the number of elements to be assembled

$$\kappa = 2; V_1 = 2R\pi t x 3000; \Theta = 2, \tag{8.236}$$

$$K_{F2} = k_F\left(\Theta\sqrt{25\rho V_1} + 1.3x0.1520x10^{-3}t^{1.9358}x4x2R\pi\right), \tag{8.237}$$

$$K_{F3} = k_F\left(\Theta\sqrt{(n_s+1)\rho V_2} + 1.3x0.3394x10^{-3}a_W^2 2Ln_s\right). \tag{8.238}$$

The fillet weld size $a_w = 0.3t_w$, $a_{wmin} = 3$ mm.

$$V_2 = 5V_1 + n_s A_s L/2. \tag{8.239}$$

The cost of painting is

$$K_P = k_P\left(4R\pi L + n_S A_L L/2\right); k_P = 14.4x10^{-6}\ \$/\text{mm}^2. \tag{8.240}$$

The total cost is

$$K = K_M + 5K_{F1} + 5K_{F0} + K_{F2} + K_{F3} + K_P. \tag{8.241}$$

8.6.4 The unstiffened shell

8.6.4.1 *Constraints*

Shell buckling

$$\sigma_a + \sigma_b = \frac{N_F}{2R\pi t} + \frac{H_F L}{R^2\pi t} \le \sigma_{cr} = \frac{f_y}{\sqrt{1+\lambda^4}}, \tag{8.242}$$

$$\lambda^2 = \frac{f_y}{\sigma_a + \sigma_b}\left(\frac{\sigma_a}{\sigma_{Ea}} + \frac{\sigma_b}{\sigma_{Eb}}\right), \tag{8.243}$$

$$\sigma_{Ea} = C_a(1.5 - 50\beta)\frac{\pi^2 E}{10.92}\left(\frac{t}{L}\right)^2, \tag{8.244}$$

$$C_a = \sqrt{1+(\rho_a\xi)^2}; Z = \frac{L^2}{Rt}0.9539, \tag{8.245}$$

$$\rho_a = 0.5\left(1+\frac{R}{150t}\right)^{-0.5}; \xi = 0.702Z, \tag{8.246}$$

$$\sigma_{Eb} = C_b(1.5 - 50\beta)\frac{\pi^2 E}{10.92}\left(\frac{t}{L}\right)^2, \tag{8.247}$$

$$C_b = \sqrt{1+(\rho_b\xi)^2}, \tag{8.248}$$

$$\rho_b = 0.5\left(1+\frac{R}{300t}\right)^{-0.5}. \tag{8.249}$$

Horizontal displacement

$$w_h = \frac{ML^2}{3E\pi R^3 t} \le w_{allow} = \frac{L}{\phi}, \tag{8.250}$$

$$M = H_F L/\gamma_M; \gamma_M = 1.5; H_F = 0.1N_F. \tag{8.251}$$

8.6.4.2 *The cost function*

Fabrication sequence:

(1) Fabrication of five shell elements of length 3 m without stiffeners. For one shell element two axial butt welds are needed (GMAW-C) (K_{F1}). The cost of forming of a shell element into the cylindrical shape is also included (K_{F0}).

(2) Welding the five units together with 4 circumferential butt welds (K_{F2}).

The material cost is

$$K_M = k_{M1} 5\rho_1 V_1, \tag{8.252}$$

$$V_1 = 3000x2R\pi t, \tag{8.253}$$

$$K_{F0} = k_F \Theta e^{\mu}; \mu = 6.8582513 - 4.527217t^{-0.5} + 0.009541996(2R)^{0.5}, \tag{8.254}$$

$$K_{F1} = k_F\left(\Theta\sqrt{\kappa\rho_1 V_1} + 1.3x0.152x10^{-3}t^{1.9358}x6000\right), \tag{8.255}$$

$$\Theta = 2; \kappa = 2; \rho_1 = 7.85x10^{-6}\ \text{kg/mm}^3,$$

$$K_{F2} = k_F\left(\Theta\sqrt{5x5\rho_1 V_1} + 1.3x0.152x10^{-3}t^{1.9358}8R\pi\right), \tag{8.256}$$

k_F = 1.0 \$/min, k_{Ml} = 1.0 \$/kg.

The cost of painting is

$$K_P = k_P(4R\pi L); k_P = 14.4x10^{-6}\ \$/\text{mm}^2. \tag{8.257}$$

The total cost is

$$K = K_M + 5K_{F1} + 5K_{F0} + K_{F2} + K_P. \tag{8.258}$$

8.6.5 Optimization and results

The optimization is performed using the Particle Swarm mathematical algorithm (Farkas & Jármai 2003). The results are summarized in Table 8.11 for deflection limit factor of ϕ = 1000 only.

Table 8.11 Results of the optimization for stiffened and unstiffened shell. The positive cost difference means savings due to stiffening. Dimensions in mm

	Stiffened				Unstiffened				
R	h	n_S	t	K \$	t	$\sigma<\sigma_{cr}$ MPa	w mm	K \$	cost diff.%
1900	1016	24	9	124600	67	193<350	14.80	165162	24
2100					50	220<343	14.73	133675	
2300	910.4	18	17	94560	38	251<331	14.75	105959	29
2500	607.6	16	21	84980	30	280<311	14.55	88744	4
2700	257.2	14	24	83309	26	287<289	13.33	82177	-1
2900	203.2	17	22	84650	25	268<275	11.19	85924	1
3100	257.2	18	21	86110	24	252<260	9.54	87413	1
3300	257.2	14	20	87240	23	240<245	8.25	88546	1
3500	203.2	21	19	88510	23	220<235	6.92	93206	5

Comparison of the costs for unstiffened and stiffened shells

This comparison is shown in Table 8.12.

Table 8.12 Summary of costs (positive difference means cost savings)

Cost [\$]	Unstiffened shell	Stiffened shell	Difference %
Material K_M	56117	45321	24
Forming $5K_{F0}$	8385	4342	93
Welding $5K_{F1}+K_{F2}$	22577		
Welding $5K_{F1}+K_{F2}+K_{F3}$		10169	122
Painting K_P	5021	10739	-114
Total	92100	70571	30

It can be seen that the cost savings caused by stringer stiffening are significant in forming and welding costs, but the painting for unstiffened shell is 114% cheaper than that, for stiffened one. It can be concluded that the cost factors of fabrication and painting play an important role in the achievable cost savings.

8.6.6 Conclusions

Table 8.12 shows that both stiffened and unstiffened versions have an optimum radius, in our numerical problem $R_{opt} = 2700$ mm.

It can be seen that, for smaller radii (R<2100 mm) the required thickness is unrealistically large (t>50 mm), thus, stiffening is needed to decrease this thickness and the thickness reduction by stiffening results in considerable cost savings.

Cost difference is considerable only for radii smaller than the optimum, thus, the stiffening is economic only for these radii. For radii larger than the optimum, the difference between the thicknesses and between the costs is small, since the unstiffened shell can be realized with larger radius and not too large thickness.

It can also be seen that, for both structural versions the stress constraint is active for radii smaller than R_{opt} and the deflection constraint governs for radii larger than R_{opt}.

8.7 A RING-STIFFENED CONICAL SHELL LOADED BY EXTERNAL PRESSURE

8.7.1 Introduction

Conical shells are applied in numerous structures e.g. in submarine and offshore structures, aircraft, tubular structures, towers, tanks, etc. Their structural characteristics are as follows.

- Material: steels, Al-alloys, fibre-reinforced plastics,
- Geometry: slightly conical (transition parts between two circular shells), strongly conical (storage tank roofs), truncated,
- Stiffening: ring-stiffeners, stringers, combined, equidistant, non-equidistant,
- Stiffener profile: flat, box, T-, L-, Z-shape,
- Loads: external pressure, axial compression, torsion, combined,
- Fabrication technology: welding, riveting, bolting, gluing.

Klöppel and Motzel (1976) have carried out buckling experiments with truncated unstiffened and ring-stiffened steel conical shell specimens and proposed simple formulae for critical buckling stress.

Rao and Reddy (1981) have worked out an optimization procedure for minimum weight of truncated conical shells. Rectangular ring-stiffeners and stringers are used and constraints on shell buckling as well as on natural frequency are considered. In the book, written by Ellinas et al. (1984), experimental results and design of stiffened conical shells are treated.

Spagnoli has written a PhD thesis on buckling behaviour and design of stiffened conical shells under axial compression (Spagnoli 1997). Rectangular stringers are considered. Later Spagnoli also with co-authors (Spagnoli & Chryssanthopoulos 1999a, 1999b, Spagnoli 2001) has published other articles in this field.

Chryssanthopoulos et al. (1998) have used finite element method for buckling analysis of stringer-stiffened conical shells in compression.

Singer et al. (2002) have given a detailed description of experiments carried out with stiffened conical shell models.

Minimum cost design has been worked out for ring-stiffened circular cylindrical shell in our study Farkas et al. 2002, Farkas & Jármai 2003).

In the present study we select the following structural characteristics: steel, slightly conical shell, ring-stiffeners of welded square box section to avoid tripping, equidistant stiffening, external pressure, welding. Design rules of Det Norske Veritas (1995, 2002) are applied for shell and stiffener buckling constraints.

The variables to be optimized are as follows: number of shell segments (n) (Fig. 8.15), shell thicknesses (t_i), dimensions of ring-stiffeners (h_i, t_{ri}). The number of

stiffeners is n+1, since stiffeners should be used at the ends of the shell, thus, two stiffeners are used in the first shell segment.

The ring stiffeners are placed in a small distance from the circumferential welds connecting two segments to allow the inspection of welds, this is marked in Figure 8.15 by dotted lines. The cost function includes the cost of material, assembly, welding and painting and is formulated according to the fabrication sequence.
The optimization process has the following parts:

(a) design of thicknesses for each shell segment given by two radii (R_i and R_{i+1}) using the shell buckling constraint,

(b) design of ring-stiffeners for each shell segment using the stiffener buckling constraint,

(c) cost calculation for each shell segment and for the whole shell structure.

These design steps should be carried out for a series of segment-numbers. On the basis of calculated costs the optimum solution corresponding to the minimum cost can be determined.

8.7.2 Design of shell thicknesses

According to DNV rules (2002), for shell segments between two ring-stiffeners of radii R_i and R_{i+1} the buckling constraint valid for circular cylindrical shells with equivalent radius

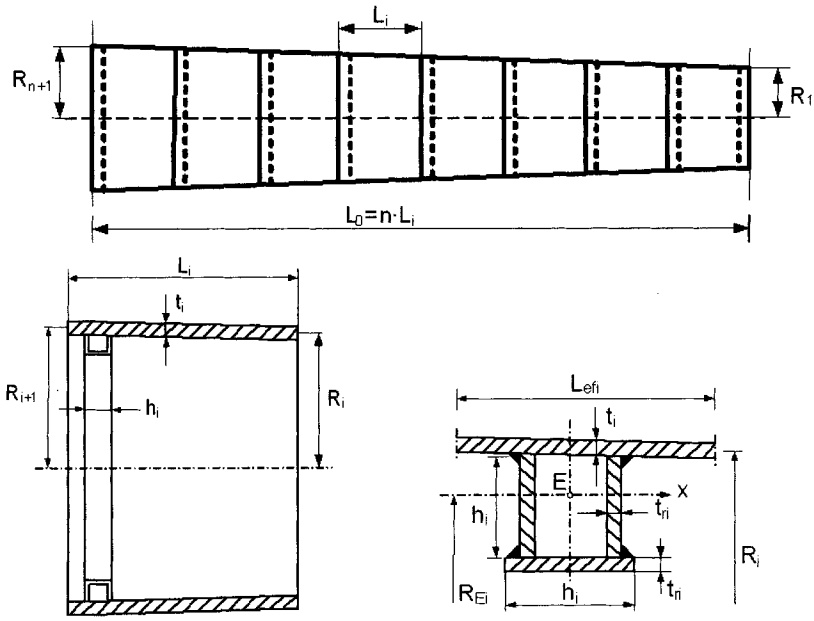

Figure 8.15. The main dimensions of the conical shell – a shell segment with the ring-stiffener of welded square box section

$$R_{ei} = \frac{R_{i+1} + R_i}{2\cos\alpha}, \cos\alpha = \frac{1}{\sqrt{\tan^2\alpha + 1}}, \tag{8.259}$$

$$\tan\alpha = \frac{R_{n+1} - R_1}{L_0}, R_{i+1} = L_i \tan\alpha + R_i, L_i = \frac{L_0}{n}, \tag{8.260}$$

and equivalent thickness

$$t_{ei} = t_i \cos\alpha . \tag{8.261}$$

The normal stress due to external pressure in a shell segment should be smaller than the critical buckling stress

$$\sigma_i = \frac{\gamma_b p R_i}{t_{ei}} \le \sigma_{cri} = \frac{f_{y1}}{\sqrt{1+\lambda_i^4}}, \qquad \lambda_i = \sqrt{\frac{f_{y1}}{\sigma_{Ei}}}, \tag{8.262}$$

$$\sigma_{Ei} = \frac{C_i \pi^2 E}{12(1-\nu^2)}\left(\frac{t_{ei}}{L_{ei}}\right)^2, L_{ei} = \frac{L_i}{\cos\alpha}, \tag{8.263}$$

where

$$C_i = 4\sqrt{1+\left(\frac{0.6\xi_i}{4}\right)^2}, \xi_i = 1.04\sqrt{Z_i}, \; Z_i = \frac{L_{ei}^2}{R_{ei}t_{ei}}\sqrt{1-\nu^2} . \tag{8.264}$$

Using Eqs (8.263), Eq (8.264) can be written in the form of

$$C_i = 4\sqrt{1+0.023214\frac{L_{ei}^2}{R_{ei}t_{ei}}} . \tag{8.265}$$

From the shell buckling constraint Eq (8.262) the unknown t_i can be calculated using a Mathcad algorithm.

8.7.3 Design of a ring-stiffener for each shell segment

For ring-stiffeners a square box section welded from 3 parts is selected to avoid tripping, which is dangerous failure mode for open-section stiffeners (Fig.8.15). The constraint on local buckling of the compressed stiffener flange according to Eurocode 3 (2002) is expressed by

$$t_{ri} \ge \delta h_i, 1/\delta = 42\varepsilon, \varepsilon = \sqrt{235/f_y} \tag{8.266}$$

for $f_y = 355$ MPa $1/\delta = 34$.

Calculating with Eq (8.266) as equality, the only unknown for a square ring-stiffener is the height h_i. This dimension can be determined from the stiffener buckling constraint relating to the required moment of inertia of a stiffener section about the

axis x of the point E, which is the gravity center of the cross-section including the 3 stiffener parts and the effective part of the shell (Fig.8.15)

$$I_{xi} \geq I_{reqi} = \frac{\gamma_b p R_i R_{Ei}^2 L_{efi}}{3E}\left[2+\frac{3Ey_{ei}0.005R_i}{R_{Ei}^2\left(f_{y1}/2-\sigma_i\right)}\right], \tag{8.267}$$

where

$$I_{xi} = \frac{\delta h_i^4}{6} + 2\delta h_i^2\left(\frac{h_i}{2}-y_{Ei}\right)^2 + \delta h_i^2\left(h_i-y_{Ei}\right)^2 + \frac{L_{efi}t_i^3}{12} + L_{efi}t_i y_{Ei}^2 \tag{8.268}$$

$$y_{Ei} = \frac{2\delta h_i^3}{3\delta h_i^2 + L_{efi}t_i} \tag{8.269}$$

$$L_{efi} = \min\left(L_i, L_{ef0i}\right), L_{ef0i} = 1.56\sqrt{R_i t_i}\,, \tag{8.270}$$

$$R_{Ei} = R_i - \left(h_i + \frac{t_i}{2} + \frac{\delta h_i}{2} - y_{Ei}\right). \tag{8.271}$$

The required h_i can be calculated from Eq (8.267).

8.7.4 The cost function

The cost function is formulated according to the fabrication sequence as follows (Farkas & Jármai 2003).

(1) Forming of 3 plate elements for shell segments into slightly conical shape (K_{F0}).

(2) Welding 3 curved shell elements into a shell segment with GMAW-C (gas metal arc welding with CO_2) butt welds (K_{F1}).

(3) Welding of n+1 ring-stiffeners each from 3 elements with 2 GMAW-C fillet welds (K_{F2}).

(4) Welding of a ring-stiffener into each shell segment with 2 GMAW-C fillet welds (K_{F3}).

(5) Assembly of the whole stiffened shell structure from n shell segments (K_{F4A}).

(6) Welding of n shell segments to form the whole shell structure with n-1 circumferential GMAW-C butt welds (K_{F4W}).

(7) Painting of the whole shell structure from inside and outside (K_P).

The total cost includes the cost of material, assembly, welding and painting

$$K = K_M + K_{F0} + K_{F1} + K_{F2} + K_{F3} + K_{F4} + K_P\,, \tag{8.272}$$

$$K_M = k_M \rho V, k_M = 1.0\,\$/\text{kg} \tag{8.273}$$

The volume of the whole structure includes the volume of shell segments (V_{1i}) and ring-stiffeners (V_{ri})

$$V = \sum_{i=1}^{n} V_{1i} + \sum_{i=1}^{n+1} V_{ri} \,, \tag{8.274}$$

$$K_{F0i} = k_F \Theta e^{\mu}, \mu = 6.8582513 - 4.527217 t_i^{-0.5} + 0.009541996 (2R_{ei})^{0.5} \,,$$

$$K_{F0} = \sum_{i=1}^{n} K_{F0i} \,, \tag{8.275}$$

where the factor of fabrication difficulty is taken as $\Theta = 3$ and the steel density is $\rho = 7.85 \text{x} 10^{-6}$ kg/mm^3.

$$K_{F1i} = k_F \left[\Theta \sqrt{3 \rho V_{1i}} + 1.3 x 0.152 x 10^{-3} t_i^{1.9358} x 3 L_{ei} \right], \quad K_{F1} = \sum_{i=1}^{n} K_{F1i} \,, \tag{8.276}$$

$$V_{1i} = 2\pi R_{ei} L_{ei} t_i \,, \tag{8.277}$$

$$K_{F2i} = k_F \left[\Theta \sqrt{3 \rho V_{ri}} + 1.3 x 0.3394 x 10^{-3} a_{wi}^2 x 4\pi (R_i - h_i) \right], \tag{8.278}$$

where

$$V_{ri} = 4\pi t_{ri} h_i (R_i - h_i / 2) + 2\pi t_{ri} h_i (R_i - h_i),$$

and the fillet weld size $a_{wi} = 0.7 \delta h_i$.

$$K_{F3i} = k_F \left[\Theta \sqrt{2 \rho V_{3i}} + 1.3 x 0.3394 x 10^{-3} a_{wi}^2 x 4\pi R_i \right], \qquad V_{3i} = V_{1i} + V_{ri} \,, \tag{8.279}$$

$$K_{F4} = K_{F4A} + K_{F4W}, K_{F4A} = k_F \Theta \sqrt{n \rho V} \,, \; K_{F4W} = \sum_{i=2}^{n} K_{F4Wi} \,, \tag{8.280}$$

$$K_{F4Wi} = 1.3 k_F x 0.152 x 10^{-3} t_i^{1.9358} x 2\pi R_i \,, \tag{8.281}$$

$$K_P = K_{P1} + \sum_{i=1}^{n+1} K_{Pi}, K_{P1} = k_P 4\pi \frac{R_{\max} + R_1}{2} L_0 \,, \tag{8.282}$$

$$K_{Pi} = k_P 4\pi h_i (R_i - h_i / 2), \tag{8.283}$$

$k_P = 2 \text{x} 14.4 \text{x} 10^{-6}$ \$/mm^2.

8.7.5 Numerical data (Figure 8.15)

Total shell length L = 15000, side radii $R_{min} = R_1 = 1850$ and $R_{max} = R_{n+1} = 2850$ mm, yield stress of steel f_y = 355 MPa, with a safety factor for yield stress $f_{y1} = f_y / 1.1$, external pressure intensity p = 0.5 MPa, safety factor for loading γ_b = 1.5, Poisson ratio $\nu = 0.3$, elastic modulus $E = 2.1 \text{x} 10^5$ MPa.

8.7.6 Results of the optimization

The detailed calculations are carried out for numbers of shell segments n = 3-15. The corresponding material and total costs are summarized in Table 8.11.

Table 8.11 The material and total costs in $ for investigated numbers of shell segments. The optima are marked by bold letters

N	3	4	5	6	8	10	12	15
K_M	48540	43540	40350	36830	33390	31390	**29840**	31192
K	85390	82360	81430	**79210**	80260	82120	84811	95818

It can be seen that the optimum number of shell segments for material cost is n_{Mopt} = 12 and for total cost n_{opt} = 6. This difference is caused by the fact that the fabrication (assembly, welding and painting) cost represents a large amount of total cost. The cost data show that, in the fabrication cost a significant part have the forming of plate elements into shell shape, welding and painting.

Table 8.12 Main dimensions (in mm) of the optimum shell structure (n = 6)

i	R_i	t_i	h_i	t_{ri}
1	1850	18	121	4
2	2017	19	132	4
3	2184	20	143	5
4	2351	20	156	5
5	2518	21	155	5
6	2685	22	153	5
7	2852	23	152	6

In order to characterize the dimensions of the optimum structure, the main data are given in Table 8.12.

The fabrication and painting cost components for the optimum structure are given in Table 8.13.

Table 8.13 Fabrication and painting cost components in $ for the optimum structure of n = 6

K_{F0}	K_{F1}	K_{F2}	K_{F3}	K_{F4A}	K_{F4W}	K_{P1}	ΣK_{Pi}
1	5330	1329	3202	1410	5681	12760	689

8.7.7 Conclusions

The optimum design problem is solved for a slightly conical shell loaded in external pressure with equidistant ring-stiffeners of a welded square box section. The optimum number of shell segments is found, which minimizes the cost function and fulfils the design constraints.

The thickness of each shell segment is calculated from the shell buckling constraint. This constraint is similar to that for circular cylindrical shells, but an equivalent thickness and segment length is used according to the DNV design rules (2002).

The dimensions of ring-stiffeners for each shell segment are determined on the basis of the ring buckling constraint. This constraint is expressed by the required moment of inertia of the ring-stiffener cross-section.

The cost function includes the cost of material, forming of plate elements into shell shape, assembly, welding and painting. The fabrication cost function is formulated according to the fabrication sequence. The forming, welding and painting costs play an important role in the total cost.

The cost difference between the maximum and minimum cost in the investigated range of shell segment number (n = 3 – 15) is (95818-79210)/95818x100 = 17%, thus, a significant cost savings can be achieved by optimization.

The ring-stiffening is very effective, since the unstiffened shell needs a thickness of 42 mm, which is unrealistic for fabrication.

9

Tubular Structures

9.1 COST COMPARISON OF A RING-STIFFENED SHELL AND A TUBULAR TRUSS STRUCTURE FOR A WIND TURBINE TOWER

9.1.1 Introduction

Steel towers for wind turbines can be constructed in various structural versions. Ring-stiffened cylindrical shells or tubular trusses are usually applied. Since the main requirements of engineering structures are the safety, fitness for production and economy, an important problem for designers is the cost comparison of these structural versions.

A cost calculation method has been developed and applied for various welded structures (Farkas and Jármai 2003, Jármai and Farkas 1999). The cost function includes the cost of material, cutting and grinding of tubular member ends, assembly and welding. This cost function has been applied in various problems of minimum

cost design, e.g. for a triangular truss (Farkas 2001), for a ring-stiffened cylindrical shell loaded by external pressure (Farkas and Jármai 2002). Some other problems of economic design are treated in the book of Farkas and Jármai 2003).

This cost calculation method is applied now to two structural versions of a wind turbine tower. The tower is 45 m high, loaded on the top by a factored vertical force of 950 kN (self weight of the nacelle), a bending moment of 997 kNm and a horizontal force of 282 kN from the turbine operation. The tower width is limited to 2.5 m due to the rotating turbine blades of length 27 m.

Both the shell and the truss structure are constructed from 3 parts each of 15 length with stepwise increasing widths. The shell parts are designed against shell buckling and panel ring buckling according to the design rules of the Det Norske Veritas (1995). The number of flat ring-stiffeners is determined by the designer to avoid larger ovalization of the cylindrical shell. The 3 shell parts are joined by bolted connections.

Wind turbines are used worldwide with various capacities and tower height. In the book (Spera 1994) a detailed description is given of various wind turbine towers. Koumousis and Dimou (1995) have treated the minimum volume design of a cylindrical shell tower with varying diameter and thickness considering stress and displacement constraints. Horváth and Tóth (2001) have investigated the most suitable shape of a cylindrical shell tower with variable diameter regarding the natural frequency using the finite element method.

Bazeos et al. (2002) have studied the stability and seismic behaviour of a 38 m high shell tower structure for a 450 kW wind turbine with cylindrical and conical parts of varying diameters and thicknesses. Lavassas et al. (2003) have investigated for gravity, seismic and wind loadings a 1 MW capacity and 44 m high tower of tubular shape with variable diameter and thickness using two different finite element models.

9.1.2 Ring-stiffened shell structure

For the cost minimization, the procedure already developed by Farkas et al. (2004) to optimize the design of a ring-stiffened cylindrical shell loaded in bending, is used. Design constraints on shell buckling and on local buckling of flat ring-stiffeners are formulated according to DNV (1995) and API (2000) design rules. The wind load acting on the shell tower is calculated according to Eurocode 1 Part 2-4 (EC1) (1999). The wind force and bending moment acting on the top of the 45 m high tower for a 1 MW wind turbine in Greece, is given by Lavassas et al. (2003). The load due to the self-weight of the nacelle is furthermore considered.

To avoid shell ovalization, a minimum number of 5 and a maximum number of 15 stiffeners is prescribed. In the shell buckling constraint, an imperfection factor as proposed by Farkas (2002), is used which expresses the effect of radial shell deformation due to shrinkage of circumferential welds.
Figure 9.1 shows the diameters, loads, bending moment diagram and the optimum shell thicknesses.

For the three shell segments, the wind loads are as follows: $p_{w1} = 6.334$, $p_{w2} = 6.883$ and $p_{w3} = 6.864$ kN/m. $F_{w1} = 95.01$, $F_{w2} = 103.25$, $F_{w3} = 102.95$ kN.

The factored bending moments due to wind load F_w, are given in Figure 9.1 (c), with $M_{w0} = 997$ kNm, the safety factor being 1.5. The factored load $F_{w0} = 282$ kN and nacelle (rotor) selfweight $G_w = 950$ kN.

9.1.2.1 *Design constraints*

Local buckling of the flat ring-stiffeners

The limitation on the height to thickness ratio of a flat ring-stiffener is (API 2000)

$$\frac{h_r}{t_r} \le 0.375\sqrt{\frac{E}{f_y}}, \tag{9.1}$$

where t_r is the ring stiffener thickness to be determined. Using the upper limit to obtain a larger moment of inertia, one obtains

$$h_r = 9t_r, \tag{9.2}$$

for $E = 2.1\text{x}10^5$ MPa and yield stress $f_y = 355$ MPa.

Constraint on local shell buckling (unstiffened)

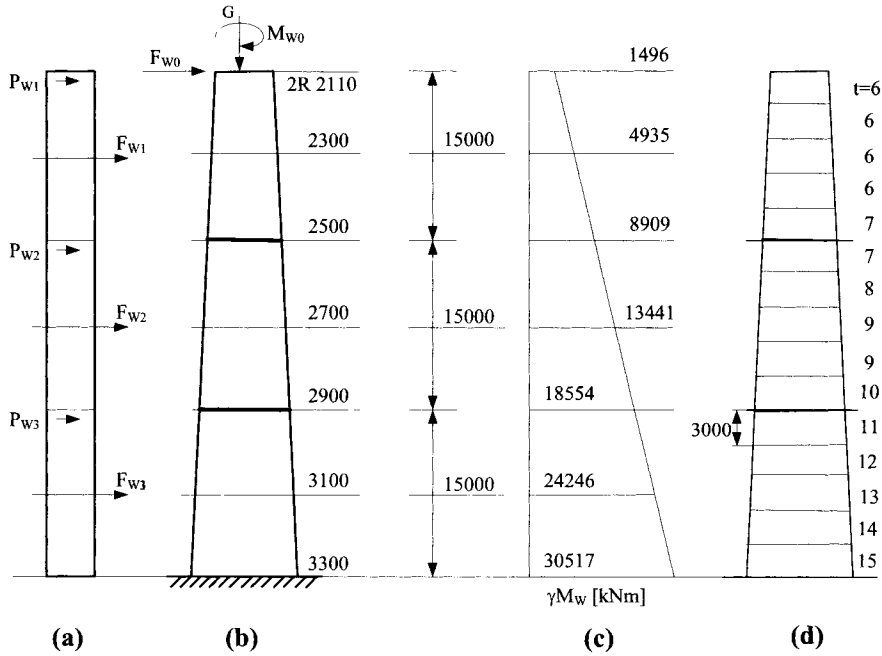

Figure 9.1 Loads, bending moments and optimal shell thicknesses in three tower parts of length 15 m

According to Det Norske Veritas (1995), for the length of one shell part L = 15 m, the number of ring stiffeners in one shell part n, R the radius and t the thickness of the shell, M pertaining to the moment on the shell part (see Figure 9.1(b)) :

The sum of the axial and bending stresses should be smaller than the critical buckling stress

$$\sigma_a + \sigma_b = \frac{G_w}{2R\pi t} + \frac{M}{\pi R^2 t} \le \sigma_{cr} = \frac{f_y}{\sqrt{1+\lambda^4}} \quad , \tag{9.3}$$

where

$$\lambda^2 = \frac{f_y}{\sigma_a + \sigma_b}\left(\frac{\sigma_a}{\sigma_{Ea}} + \frac{\sigma_b}{\sigma_{Eb}}\right) \tag{9.4}$$

$$\sigma_{Ea} = (1.5 - 50\beta)C_a \frac{\pi^2 E}{12(1-\nu^2)}\left(\frac{t}{L_r}\right)^2 \tag{9.5}$$

$$\sigma_{Eb} = (1.5 - 50\beta)C_b \frac{\pi^2 E}{12(1-\nu^2)}\left(\frac{t}{L_r}\right)^2 \tag{9.6}$$

$$C_a = \sqrt{1+(\rho_a \xi)^2} \tag{9.7}$$

$$C_b = \sqrt{1+(\rho_b \xi)^2} \tag{9.8}$$

$$\rho_a = 0.5\left(1 + \frac{R}{150t}\right)^{-0.5} \tag{9.9}$$

$$\rho_b = 0.5\left(1 + \frac{R}{300t}\right)^{-0.5} \tag{9.10}$$

$$\xi = 0.702Z, Z = \frac{L_r^2}{Rt}\sqrt{1-\nu^2} \tag{9.11}$$

and $$L_r = \frac{L}{n+1} \ . \tag{9.12}$$

The factor of (1.5-50 β) in Eqs (9.5,9.6) expresses the effect of initial radial shell deformation caused by the shrinkage of circumferential welds (Farkas 2002). For the detailed calculation see Eqs (8.50-8.58).

Furthermore

$$Z = 0.9539\frac{L_r^{\,2}}{Rt},\ \xi = 0.702Z\,, \tag{9.13}$$

From Eq (9.5) it can be deduced that σ_E does not depend on L_r, since L_r^2 is in the denominator and from (Eq 9.7), C has L_r^2 in the numerator. The fact that the buckling strength does not depend on the shell length, was first derived by Timoshenko & Gere (1961). Note that this dependence of σ_E on L_r is very small according to the API design rules (2000). It has, however, been determined that in the case of external pressure, the distance between ring-stiffeners does play an important role (Farkas et al. 2002, Farkas and Jármai 2003).

Constraint on panel ring buckling

Requirements for a ring stiffener are as follows (DNV1995):

$$A_r = h_r t_r \geq \left(\frac{2}{Z^2} + 0.06\right) L_r t \tag{9.14}$$

$$I_r = \frac{h_r^3 t_r}{12}\cdot\frac{1+4\omega}{1+\omega} \geq \frac{\sigma_{\max} t R_0^4}{500 E L_r} \tag{9.15}$$

$$R_0 = R - y_G\,, \qquad y_G = \frac{h_r}{2(1+\omega)}\,, \tag{9.16}$$

$$\omega = \frac{L_e t}{h_r t_r} \tag{9.17}$$

and $$L_e = \min\left(L_r, L_{e0} = 1.5\sqrt{Rt}\right). \tag{9.18}$$

9.1.2.2 *Cost function*

A possible manufacturing sequence is as follows:

(1) Manufacture five shell elements with a length of 3 m without rings. Two axial butt welds (GMAW-C) are needed for every shell element. The cost to form a shell element into a slightly conical, near cylindrical shape, is included in the factor K_{F0} described below. From data obtained from the Hungarian production company Jászberényi Aprítógépgyár, Crushing Machine Factory, Jászberény, the time T for bending a plate element of 3m width can be approximated by the following function:

$$\ln T = 6.85825 - 4.5272 t^{-0.5} + 0.0095419 D^{0.5}\,. \tag{9.19}$$

(4 mm < t < 40mm and 1750 mm < D < 3500 mm). In this equation, which also includes the time to form the plate and reduce the initial imperfections due to forming, t is the plate thickness and D is the diameter. The cost for shell formation is thus given by

$$K_{F0} = k_F \Theta_F T \tag{9.20}$$

where $\Theta_F = 3$ is the difficulty factor indicative of the complexity of fabrication and k_F is the specific manufacturing cost per unit time.
The welding cost of a shell element is (Farkas and Jármai 2003)

$$K_{F1} = k_F\left(\Theta_W \sqrt{\kappa \rho V_1}\right) + k_F[1.3\text{x}0.224\text{x}10^{-3} t^2(2\text{x}3000)], \tag{9.21}$$

where Θ_W is a difficulty factor expressing the complexity of the assembly and κ is the number of elements to be assembled. For the elements of radius R and density ρ to be welded

$\kappa = 2$, $V_1 = 2R\pi t$ x 3000 and $\Theta_W = 2$, where V_1 is the volume of an element.

(2) Weld a complete unstiffened shell part, combining the five elements by using four circumferential butt welds. This implies welding costs of

$$K_{F2} = k_F\left(\Theta_W \sqrt{5x5\rho V_1} + 1.3x0.2245x10^{-3} t^2 x4x2R\pi\right) \tag{9.22}$$

for a shell part.

(3) Cut n flat plate rings using acetylene gas. The cutting cost amounts to

$$K_{F3} = k_F \Theta_c C_c t_r^{\,0.25} L_c\,, \tag{9.23}$$

where Θ_c, C_c and L_c are respectively the difficulty factor for cutting, the cutting parameter and the cutting length with values $\Theta_c = 3$, $C_c = 1.1388\text{x}10^{-3}$ and

$$L_c \approx 2R\pi n + 2(R - h_r)\pi n$$

for a ring radius R and ring height h_r.

(4) Weld n rings into the shell segment with double-sided GMAW-C fillet welds. ($2n$ fillet welds) :

$$K_{F4} = k_F\left(\Theta_W \sqrt{(n+1)\rho V_2} + 1.3x0.3394x10^{-3} a_W^2\, 4R\pi n\right) \tag{9.24}$$

The size of the weld for a ring of thickness t_r is $a_W = 0.5t_r$, but $a_{Wmin} = 3$ mm.
The volume of a shell part V_2 is given by

$$V_2 = 5V_1 + 2\left(R - \frac{h_r}{2}\right)\pi h_r t_r n \tag{9.25}$$

The total material cost for a shell part

$$K_M = k_M \rho V_2 \tag{9.26}$$

The cost of painting

$$K_P = k_P S_P, S_P = 4R\pi 1500 + 5x2x2\left(R - \frac{h_r}{2}\right)h_r \tag{9.27}$$

The total cost for a shell part thus is

$$K = K_M + 5(K_{F0} + K_{F1}) + K_{F2} + K_{F3} + K_{F4} + K_P. \tag{9.28}$$

The material cost factor is $k_M = 1$ \$/kg and the labour cost factor is $k_F = 1$ \$/min.

9.1.2.3 *Optimization and results*

The optimization can be carried out using any appropriate constrained optimization algorithm. Here it was performed using Rosenbrock's search algorithm (Farkas and Jármai 1997). The optimal values of the shell thickness (t) for $n = 5$, which comply with the design constraints and minimize the cost function, are given in Figure 9.1. The minimal masses and costs are summarized in Table 9.1.

Table 9.1. Summary of masses and costs

Shell part	mass [kg]	Cost without K_p [\$]	K_p [\$]	Total [\$]
top	5398	12096	6440	18536
middle	9472	19772	7603	27373
bottom	15648	30941	8778	39719
total	30518	62809	22821	85628

9.1.2.4 *Check for eigenfrequency*

For the approximate calculation of eigenfrequency a simple model is used: a beam of length L built in at end a free at other to which a concentrated mass m_1 is connected. The circular eigenfrequency for a beam without any concentrated mass at the end can be calculated as

$$\alpha = \frac{1.87^2}{L^2}\sqrt{\frac{EI_x}{m_0}} \tag{9.29}$$

For the average shell radius of R = 1350 mm, thickness t = 9 mm, cross-sectional area $A = 2R\pi t = 7.634\text{x}10^{-4}$ mm^2, moment of inertia $I_x = \pi R^3 t = 6.956\text{x}10^{10}$ mm^4, specific mass $m_0 = \rho A/g$, $g = 9.81\text{x}10^3$ mm/s^2 one obtains $\alpha = 8.45$/s or 1.34 Hz. This value should be modified considering the attached mass according to the value of $m_1/(m_0 L) = 950/305 = 3.1$ using the diagram in Prochnost' (1968) multiplying by $(1.2/1.87)^2 = 0.41$, i.e. $\alpha = 055$ Hz, which is larger than the rotor frequency 0.37 Hz, thus the tower satisfies the eigenfrequency requirement.

9.1.2.5 *Check for fatigue*

According to Eurocode 3 Part 1-9 (2002) the fatigue stress range for toe failure for $2\text{x}10^6$ cycles in the case of T-joints is 63-71 MPa depending on the diaphragm thickness. Dividing by a safety factor of 1.35 one obtains 47 MPa. Lavassas et al.

have given a load spectrum, which gives the reliable wind load for some numbers of cycles. E.g. for an average number of cycles $N = 10^5$ for a wind speed of 14 m/s M_W = 1280 kNm and F_W = 80 kN. For the given number of cycles the stress range is 171 MPa, the bending moment is 1280 + 45x80 = 4880 kNm and the stress $4880\text{x}10^6/(\pi R^2 t) = 38$ MPa < 171 MPa, the fatigue constraint is fulfilled.

9.1.3 Tubular truss structure

In the present study a 45 m high welded steel tubular truss tower is designed for a 1 MW turbine. The truss is statically determinate. The distance between parallel chords in the upper part of the tower is limited because of the rotating blades. In the lower part the chord distance can be linearly varied and the inclination angle can be optimized or a larger constant chord distance can be used (Fig.9.2).

Thus, in the optimization procedure the inclination angle or the larger constant chord distance and the member dimensions of the lower tower part are sought, which minimize the structural volume and fulfil the design constraints.

The constraints relate to the buckling strength of circular hollow section (CHS) members and to the local strength of welded tubular joints. Seismic behaviour is not treated. In the numerical problem the loads from wind acting on the turbine and from the nacelle mass are selected from the literature. Knowing the member forces an iterative suboptimization method is used for the calculation of compression member dimensions.

The cross-section of the truss can be quadratic or triangular. In the case of a triangular cross-section the whole horizontal load should be carried by a truss plane, since the horizontal load direction is variable. Therefore the quadratic cross-section is used. In this case only the half value of the horizontal load is acting on a truss plane.

9.1.3.1 *Suboptimization problem for the buckling design of a CHS compressed strut*

The overall buckling constraint for a strut of length L and loaded by a compressive force S according to Eurocode 3 is defined by

$$\frac{S}{A} \le \frac{\chi f_y}{\gamma_1}, \gamma_1 = 1.1 \tag{9.30}$$

where $A = \pi Dt = \pi D^2/\delta, \delta = D/t,$ (9.31)

f_y = 355 MPa is the yield stress, D is the mean diameter,

$$\chi = \frac{1}{\phi + \sqrt{\phi^2 - \bar{\lambda}^2}}, \phi = 0.5\left[1 + \alpha(\bar{\lambda} - 0.2) + \bar{\lambda}^2\right], \tag{9.32}$$

$$\bar{\lambda} = \lambda/\lambda_E, \lambda = KL/r, r = \sqrt{I/A} = D/\sqrt{8}, \tag{9.33}$$

$\lambda_E = \pi\sqrt{E/f_y}, \alpha = 0.34$ for cold formed CHS,

K is the end restraint factor, for chords $K = 0.9$, for braces $K = 0.75$ (Rondal et al. 1992), $E = 2.1\text{x}10^5$ MPa is the elastic modulus.

For given N, L, f_y, E and K the unknowns D and t should be determined, which fulfil the buckling constraint. Introducing symbols of

$$c_0 = 100K/\lambda_E, x = 10^4 N/L^2, y = 10^4 A/L^2, \tag{9.34}$$

Eq. (30) can be written as

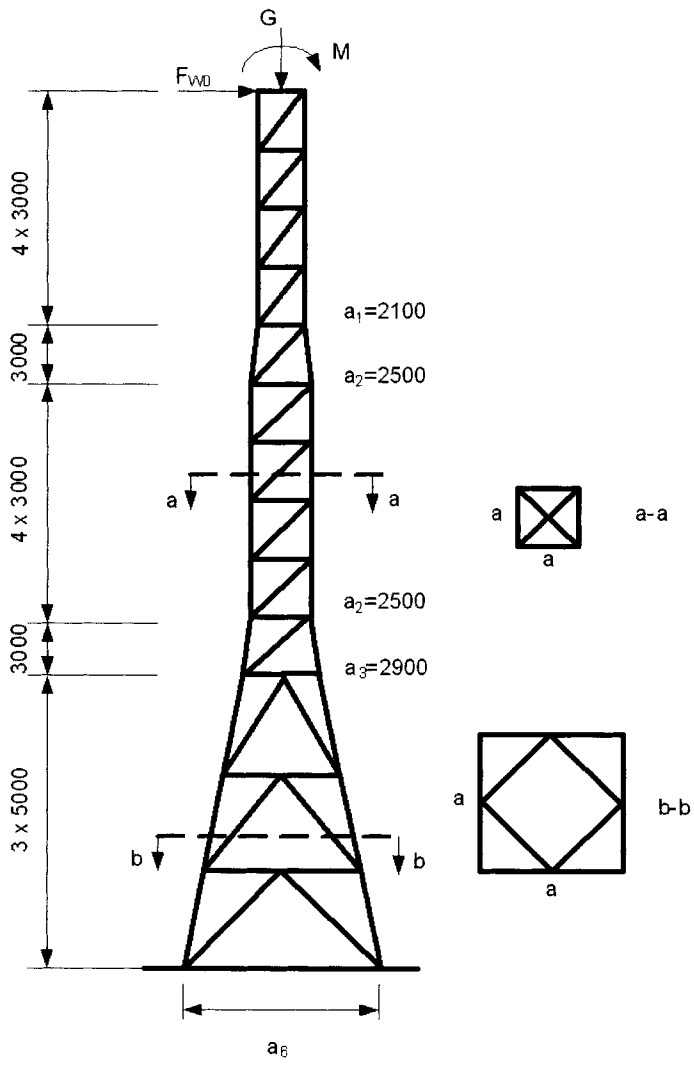

Figure 9.2 Truss structure of the tower with diaphragms

$$\frac{x}{f_y/1.1} \le \frac{y}{\phi + \sqrt{\phi^2 - c_0^2/(a^2 y)}}, \tag{9.35}$$

$$\phi = 0.5\left[1 + \alpha\left(\frac{c_0}{a\sqrt{y}} - 0.2\right) + \frac{c_0^2}{a^2 y}\right]. \tag{9.36}$$

Unfortunately, it is impossible to solve Eq (9.35) for y in closed form. Therefore a computer MathCad algorithm is used to calculate y for a given x, then

$$D = \frac{L}{100}\sqrt{\frac{y\delta}{\pi}}, t = \frac{D}{\delta}. \tag{9.37}$$

In the design we should use the maximum value of δ, but it is limited to 50 (Wardenier et al. 1991). In the case of available CHS profiles according to prEN 10210-2 (1996) δ is varied between 10-50. To obtain a realistic available profile, an iteration process should be used: δ is varied until D and t are in accordance of the available section.

In the case of very long struts with small compressive force, the limitation of the strut slenderness can be governing. From the limitation of

$$\lambda = KL/r \le \lambda_{\max}, \tag{9.38}$$

the required radius of gyration is

$$r \ge KL/\lambda_{\max}. \tag{9.39}$$

According to BS 5400 (1982) $\lambda_{\max} = 180$.

9.1.3.2 *Design of the upper and middle tower part*

The factored loads acting on the tower top according to Lavassas et al. (2003) are as follows: horizontal wind force F_{w0} = 282 kN, bending moment M = 997 kNm, the nacelle mass according to Spera (1995) G = 950 kN. It is sufficient to design one truss plan only, thus, the loads can be halved for it, $F_0 = F_{w0}/2$ = 141 kN, $M/2$ = 498.5 kNm and the two forces acting on each chord $G/4$ = 237.5 kN.

Wind forces acting on the middle of the tower parts (Figs 9.5, 9.6, 9.7): F_{W1} = 13.9, F_{W2} = 23.9 and F_{W3} = 19.25 kN.

9.1.3.3 *Optimum angle of the lower part*

The following analysis can help to understand the existence of an optimal angle in the case of such a combined loading. Three types of loads are acting on the tower as follows: horizontal force and bending moment from wind as well as vertical force from the nacelle mass. The effect of these loads should be analyzed separately.

In the structural volume the most significant part play the chords designed against buckling. Their dimensions are determined by the compression force and the rod length. It is sufficient to analyze the changing of the volume of chords in the function of the inclination angle. It has been shown that, in the case of a truss with parallel chords, an optimum height (distance between the chords) exists, which gives the minimum truss mass (Farkas and Jármai 1997).

Neglecting the branch, a simple numerical example shows that this statement is valid also for a cantilever truss with linearly varied height, loaded by a transverse force acting at the truss end. The case of a two-bar truss loaded by a horizontal force is shown in Fig. 9.3. The member force and length is

$$S = \frac{F}{2\sin\alpha}, L = \frac{H}{\cos\alpha} \tag{9.40}$$

When α increases, the member force S decreases and its length L increases, thus, an optimum inclination angle exists for the minimum structural volume.

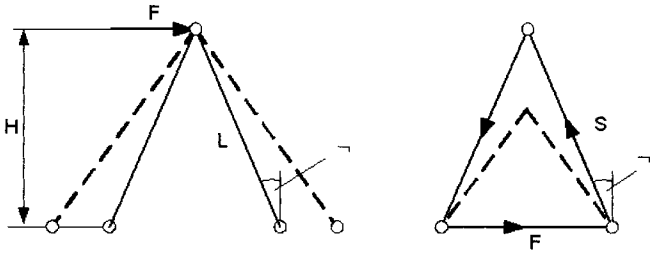

Figure 9.3 The member force and the bar length when the inclination angle changes in the case of a horizontal force

This fact can be verified by a numerical example for a truss with two bars of circular hollow section (CHS). Data are $F = 2\text{x}10^6$ [N], $H = 5$ m. The results of the calculation are given in Table 9.2.

Table 9.2. The volume of the truss shown in Fig. 9.3 as a function of the inclination angle

α	L [mm]	$S\,x10^{-3}$ [N]	D [mm]	t [mm]	A [mm^2]	$V=AL\text{x}10^{-7}$ [mm^3]
10	5077	5759	475.3	11.7	17050	8.66
20	5320	2924	333.0	9.4	9513	5.06
30	5773	2000	303.1	7.6	7034	4.06
40	6527	1556	283.9	7.1	6172	4.03
45	7071	1414	281.2	7.0	6055	4.28
50	7779	1305	282.8	7.1	6125	4.76
60	10000	1155	300.0	7.5	6893	6.89

It can be seen that the optimum angle is 40^0.

Another case is a simple 3-bar truss loaded by a pair of vertical forces (Fig.9.4). In this case

$$S = \frac{Q}{\cos\alpha}, L = \frac{H}{\cos\alpha} \tag{9.41}$$

When the angle increases, both the member force S and the length L increases. Thus, the optimum angle for the minimum structural volume is 0^0.

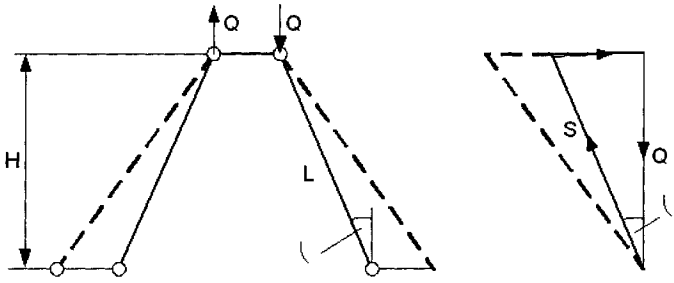

Figure 9.4. The member force and the bar length when the inclination angle changes in the case of a pair of vertical forces

From the above mentioned facts it can be concluded that, in the case of horizontal and vertical loads an optimal angle exists and it depends on the ratio of the magnitudes of the two load types. In the case of a high tower with a horizontal force on the top the bending moment is so large that the optimum inclination angle converges to zero. Detailed calculations show that this optimum angle is about 3^0, thus, it is more convenient for fabrication to use parallel chords. We use a bottom part with parallel chords with a distance of 2.9 m (Fig. 9.7).

9.1.3.4 *Design of circular hollow sections (CHS) for the three tower parts*

The suitable sections are obtained using the above described iterative method. The check of the sections is summarized in the following tables.

Table 9.3. Check of sections for the upper tower part (stresses in MPa)

Member	CHS	A [mm^2]	S [kN]	K	L [mm]	r [mm]	$\chi f_y/1.1$	$\sigma=S/A$
chords	244.5x8	5940	1320	0.9	3000	83.7	296	222
braces	114.3x5	1720	315	0.75	3662	38.7	207	180
columns	76.1x4	906	181	0.75	2100	25.5	232	200

Table 9.4. Check of sections for the middle tower part

Member	CHS	A [mm^2]	S [kN]	K	L [mm]	r [mm]	$\chi f_y/1.1$	$\sigma=S/A$
chords	323.9x10	9860	2348	0.9	3000	111	309	238
braces	114.3x5	1720	279	0.75	3905	38.7	191	162
columns	88.9x3.2	862	179	0.75	2500	30.3	232	207

Table 9.5. Check of sections for the bottom tower part

Member	CHS	A [mm^2]	S [kN]	K	L [mm]	r [mm]	$\chi f_y/1.1$	$\sigma=S/A$
chords	355.6x10	10900	3052	0.9	3000	122	312	280
braces	114.3x5	1720	285	0.75	4170	38.7	181	166
columns	88.9x4	1070	198	0.75	2900	30.0	203	185

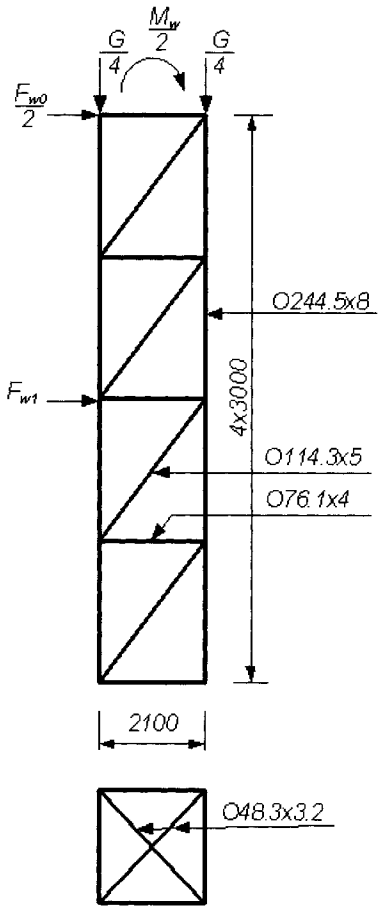

Figure 9.5. Truss of the top tower part

The struts of horizontal diaphragms are selected on the basis of the prescription of minimum rod slenderness

$$\lambda = \frac{KL}{r}, r \geq \frac{KL}{\lambda_{\min}} . \tag{9.42}$$

According to BS5400 $\lambda_{\min} = 180$. The selected CHS are shown in Table 9.6.

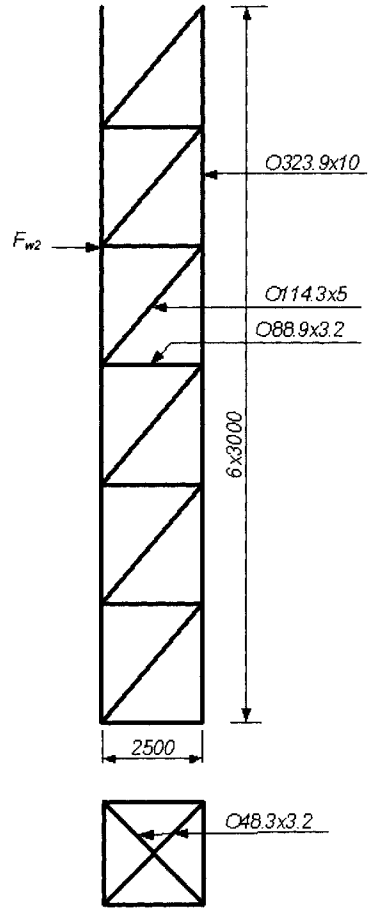

Figure 9.6. Truss of the middle tower part

Table 9.6. CHS for diaphragms

Part	L [mm]	r_{min} [mm]	CHS	r [mm]
Top	2970	12.4	48.3x3.2	16.0
Middle	3540	14.8	48.3x3.2	16.0
Bottom	4101	17.1	60.3x3.2	20.2

9.1.3.5 *Check of chord plastification in tubular joints*

According to Wardenier et al.(1991) the criterion for chord plastification is

$$S \le N^* = \frac{f_y t_1^2}{\sin\theta}\left(1.8 + 10.2\frac{d_2}{d_1}\right) f(\gamma, g') f(n'), \tag{9.43}$$

where with $\omega = a_i / 3000$

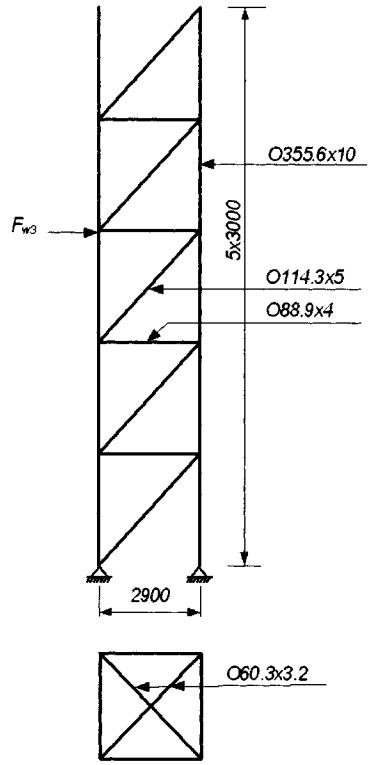

Figure 9.7. Truss of the bottom tower part

$$sin\theta = \frac{\omega}{(\omega^2+1)^{1/2}};$$

$$f(\gamma,g') = \gamma^{0.2}\left[1+\frac{0.024\gamma^{1.2}}{exp(0.5g'-1.33)+1}\right];\ \gamma = \frac{d_1}{2t_1};\ g' = \frac{0.1d_1}{t_1}; \qquad (9.44)$$

$$f(n') = 1+0.3n'(1-n');\qquad n' = -\frac{\sigma}{f_y}\ ,\ \text{(minus sign means compression);}$$

$$\sigma = S/A.$$

For multiplanar structures N^* should be multiplied by 0.9.

The calculations are summarized in Tables 9.7, 9.8, 9.9.

Table 9.7 Check of chord plastification in top tower part

Member	force S [kN]	CHS	A [mm^2]	σ [MPa]	f(n')	f(γ,g')	0.9N [kN]
chord	1320	244.5x8	5940	222	0.6947	2.4528	
brace	315	114.3x5					399
column	181	76.4x4					229

Table 9.8 Check of chord plastification in middle tower part

Member	force S [kN]	CHS	A [mm^2]	σ [MPa]	f(n')	f(γ,g')	0.9N [kN]
Chord	2348	323.9x10	9860	238	0.6638	2.57	
brace	315	114.3x5					460
column	179	88.9x3.2					294

Table 9.9 Check of chord plastification in bottom tower part

Member	force S [kN]	CHS	A [mm^2]	σ [MPa]	f(n')	f(γ,g')	0.9N [kN]
chord	3052	355.6x10	10900	280	0.5768	2.7175	
brace	285	114.3x5					365
column	198	88.9x4					254

9.1.3.6 *Check of joint eccentricity*

The eccentricity is defined by

$$e=\left(\frac{d_3}{2}+g\right)tan\theta+\frac{d_2}{2cos\theta}-\frac{d_1}{2}, \tag{9.45}$$

where $g = t_1$ is the gap and the requirement is

$$-0.55d_1 \le e \le 0.25d_1 . \tag{9.46}$$

The checks are shown in Table 9.10.

Table 9.10. Check of joint eccentricity, sizes in mm

Part	d_1	d_2	d_3	g	tanθ	cosθ	e	$0.55d_1$
Top	244.5	114.3	76.1	8	0.700	0.819	-20	134
Middle	323.9	114.3	88.9	10	0.768	0.768	-42	178
Bottom	355.6	114.3	88.9	10	0.967	0.719	-46	195

It can be seen that the requirement is in all cases fulfilled.

9.1.3.7 *Check of eigenfrequency*

The tower is calculated as a bent beam with a constant average moment of inertia of the middle part

$$I_x = 4\left(9910x10^4 + 9860x1250^2\right) = 6.20x10^{10}\ \text{mm}^4.$$

The eigenfrequency calculated with Eq (9.38) is

$$\alpha = \frac{1.87^2}{L^2}\sqrt{\frac{EI_x}{m_0}} = 11.2\ (1.78\ \text{Hz}).$$

This value should be modified considering the mass at the beam end m_1 = 950 kN. The tower mass is m_0L = 175 kN, thus the modifying coefficient for $m_1/(m_0L)$ = 5.4 is $(0.9/1.87)^2$ = 0.23, i.e. α = 0.41 Hz, which is larger than the rotor frequency 0.37 Hz, the tower fulfils the eigenfrequency requirement.

9.1.3.8 *Check of fatigue*

The chord members are connected to the base plate by fillet welds and these connections are reinforced by longitudinal attachments for the end of which the fatigue stress range according to Eurocode 3 Part 1-9 (2002) is for $2x10^6$ cycles 71 MPa. Using the wind load spectrum given by Lavassas et al. (2003) for an average number of cycles 10^6 the loads are F_W = 65 kN and M_W = 960 kNm, i.e. the bending moment 45x65 + 960 = 3885 kNm.

Compression force in a chord S = 3885/(2x2.9) = 670 kN and the stress 670x103/10.900 = 61 MPa. Fatigue stress range for 10^6 cycles is 89 MPa, the allowable stress range with a safety factor of 1.35 is 89/1.35 = 66 MPa, this is larger than 61 MPa, thus, the tubular tower is safe against fatigue. Note, that the hot spot stress method cannot be used according to Zhao et al. (2001), since the N-type CHS truss is not treated in it. For this joint also the stress range of 71 MPa is given.

9.1.3.9 *Cost calculation*

According to Price List (1995) the following profile prices are considered:

The structural mass is

$$G = \rho \sum_i A_i L_i \,. \tag{9.47}$$

Table 9.11. Material cost factors for available CHS diameters

d [mm]	k_M [$/kg]
48.3, 60.3, 76.4	1.0059
88.9, 101.6, 114.3	1.0553
139.7, 168.3, 177.8, 193.7	1.1294
219.1, 244.5, 273.0, 323.9	1.2922
355.6, 406.4	1.3642

and the material cost is calculated as

$$K_M = \rho \sum_i k_{Mi} A_i L_i \,. \tag{9.48}$$

Cost of cutting and grinding of the tubular member ends can be obtained by

$$K_{CG} = k_F \Theta_{dC} \sum_i \frac{2\pi d_i}{\sin\theta} \left(4.54 + 0.4229 t_i^2\right), \tag{9.49}$$

the difficulty (complexity) factor is Θ_{dC} = 3; d_i in m, t_i in mm.

Cost of assembly

$$K_A = k_F \Theta_{dA} (\kappa \rho V)^{1/2}; \quad \Theta_{dA} = 3, \tag{9.50}$$

Cost of welding

$$K_W = 1.3 k_F \Theta_{dW} \sum_i C_{Wi} a_{Wi}^n L_{Wi}; \quad \Theta_{dW} = 3.5, \tag{9.51}$$

for shielded metal arc welding (SMAW) $C_W = 0.7889\text{x}10^{-3}$; $a_{Wi} = t_i$ (mm) is the weld size, n=2; $L_{Wi} = \dfrac{2\pi d_i}{\sin\theta_i}$ is the weld length in mm.

Cost of painting

$$K_P = k_P \Theta_P A_P, \Theta_P = 2, \tag{9.52}$$

$k_P = 14.4\text{x}10^{-6}$ \$/mm^2.

the surface to be painted is

$$A_P = \sum_i d_i \pi L_i. \tag{9.53}$$

The details of the cost calculation are summarized in Table 9.12.

9.1.4 Conclusions

Two structural versions of a 45 m high 1 MW wind turbine tower are designed and compared to each other regarding the mass and cost. The stiffened shell structure should be designed with constraints on shell and stiffener buckling, eigenfrequency and fatigue. The shell consists of three slightly conical parts with variable diameters and thicknesses. The three parts are connected with bolted joints the cost of which is neglected. The cost is calculated according to the fabrication sequence, including the material, cutting of flat stiffeners from plates, assembly, welding and painting costs. The tubular truss structure consists also from three parts with different but constant width. The four truss planes are stiffened by horizontal diaphragms constructed from two struts. A suitable suboptimization method is used for the economic design of compressed CHS struts.

Table 9.12 Costs in \$ of the tubular tower, the surface A_P to be painted in mm^2

Part	G [kg]	K_M	K_{CG}	K_A	K_W	$A_P\text{x}10^{-6}$	K_P	K
top	3437	4139	1936	1180	2514	72.46	2087	11856
middle	7395	9096	2867	1965	3108	130.11	3747	20783
bottom	6701	8643	2551	1629	2353	116.17	3346	18522
total	17533	21878	7354	4774	7975	318.74	9180	51161

It is shown that, in the case of large bending moment from wind loads, the optimum inclination angle of the bottom truss part converges to zero. Therefore, the bottom part is also constructed with parallel chords. The tubular joints are checked for chord plastification and eccentricity. The truss is checked for eigenfrequency and fatigue.

The following costs are calculated: material, cutting and grinding of strut ends, assembly, welding and painting.

The comparison of the two structural versions shows that the tubular truss has smaller mass (17533 compared to 30518 kg), smaller surface to be painted and is much cheaper than the shell structure (51161 compared to 85628 $).

9.2 MINIMUM COST DESIGN OF A COLUMN-SUPPORTED OIL PIPELINE STRENGTHENED BY A TUBULAR TRUSS

9.2.1 Introduction

In the case, where the distance of supporting columns is in a special place larger than the other distances, is necessary to strengthen the pipe. This strengthening can be realized by prestressed cables or by an upper or lower truss welded to the main transporting pipe. It should be noted that it is assumed that the larger distance is not too large and a special supporting bridge is not needed.

The aim of our study is to design a lower strengthened tubular truss (Fig.9.8). This simple truss consists of two diagonals and a vertical column. The diagonals are loaded by tension and have the same cross-sectional area. The vertical column is loaded by compression and bending and is designed against overall buckling.

This complex structural system is statically indeterminate and the unknown force in the column is calculated by force method using a deflection equation. The symmetric truss geometry has an unknown, the height H. This unknown, as well as the dimensions of truss members, are calculated from the condition that the material and fabrication costs of the strengthening tubular truss should be minimum.

Constraint on local buckling of circular hollow section truss members, as well as the constraint on strength and geometry of the node, are also considered. The advanced cost function, used in our previous study (Farkas & Jármai 2001, 2003), includes the material and fabrication costs. The fabrication costs relate to the cutting of strut ends, assembly, welding and painting. For the constrained function minimization the efficient mathematical computer method is used based on the Rosenbrock's Hillclimb algorithm complemented by a discretization procedure to obtain available circular hollow sections. It can be mentioned, that the minimum volume design of pipeline bridges is treated by Orbán (1997).

9.2.2 Derivation of the column force

The structure of the strengthened pipe is statically indetermined. The unknown column force X_1 can be derived from a deflection equation. The deflection at midspan of simply supported pipe without strengthening from the distributed load p is (Fig.9.8)

$$w_p = \frac{5pL^4}{384EI_x}, \tag{9.54}$$

where L is the larger support distance, E is the elastic modulus, I_x is the moment of inertia of the original pipe. The deflection of the pipe without strengthening at the midspan from the column force X_1 is

$$w_1 = \frac{X_1 L^3}{48EI_x}. \tag{9.55}$$

The deflection caused by the axial deformation of the tubular truss is

$$w_2 = \sum_i \frac{S_i s_i L_i}{EA_i}, \tag{9.56}$$

where S_i is the normal force in the i-th strut caused by X_1, s_i is the normal force due to $X_1 = 1$, L_i is the strut length and A_i is the cross-sectional area of the strut.

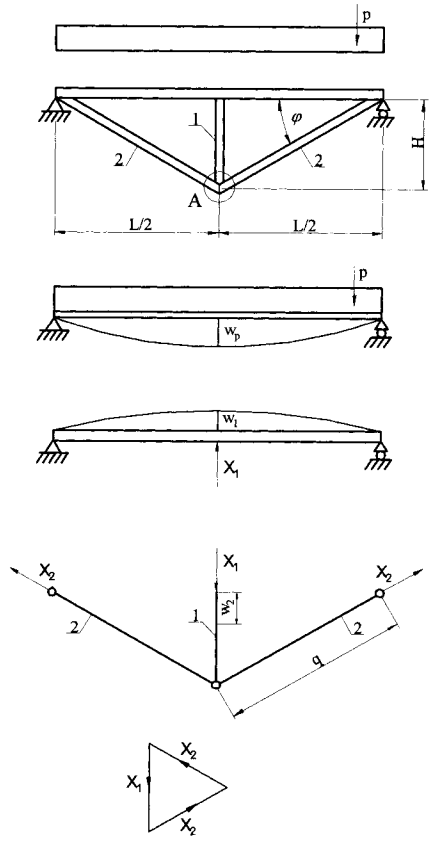

Figure 9.8. The simply supported pipe strengthened by a tubular truss. The deflections w_p, w_1 and w_2 are used to derive the unknown internal force X_1.

Introducing the length of diagonals as

$$q = \sqrt{\frac{L^2}{4} + H^2}\,, \tag{9.57}$$

the normal force in the diagonals is

$$X_2 = \frac{X_1 q}{2H}\,, \tag{9.58}$$

and

$$w_2 = \frac{X_1 H}{EA_1} + \frac{X_1 q^3}{2EA_2 H^2}\,. \tag{9.59}$$

From the deflection equation of

$$w_p - w_1 = w_2\,, \tag{9.60}$$

one obtains

$$X_1 = \frac{5pL^4}{384 I_x Q}, \tag{9.61}$$

$$Q = \frac{L^3}{48 I_x} + \frac{H}{A_1} + \frac{q^3}{2A_2 H^2}\,. \tag{9.62}$$

9.2.3 Design of the original pipe

Take the original pipe span length as L_0 = 12 m. Consider a simply supported pipe. Loads: self mass, oil in the pipe and internal pressure. We select for the original pipe according to DIN 2458 (1981) a profile of 219.1x6.3, self mass 33.06 kg/m. The cross-sectional area for the oil filling is $A_F = \pi 206.5^2 / 4 = 33491$ mm^2. Oil density is 0.8x10^{-6} kg/mm^3. According to the standard EN 1594 (2001) the partial safety factor for self mass is 1.5, for oil 1.39 and the yield strength should be multiplied by 0.72. The intensity of the factored uniformly distributed normal load is p = 1.5x33.06 + 1.39x0.8x33.491 = 86.83 kg/m = 0.8683 N/mm.

The maximum bending moment is:

$$M_{\max} = pL_0^2 / 8 = 15.63x10^6 \text{ Nmm.}$$

The section modulus is

$$W_x = \pi 212.8^2 x 6.3 / 4 = 224065 \text{ mm}^3\,.$$

and the maximum normal stress due to bending is

$$\sigma_{\max} = M_{\max} / W_x = 69.8 \text{ MPa.}$$

Stress due to an internal pressure of 64 bar = 6.4 MPa is

$$\sigma_P = p_P D/(2t) = 6.4x212.8/(2x6.3) = = 108.1 \text{ MPa},$$

the factored stress is 1.39x108.1 = 150.2 MPa, the reduced stress is

$$\sigma_{red} = \sqrt{\sigma_{\max}^2 + \sigma_P^2} = \sqrt{69.8^2 + 150.2^2} = = 165.6 < 0.72x235 = 169.2 \text{ MPa, OK.}$$

Take the larger span length of L = 17 m. For this span length a larger pipe is needed, we select the profile of 355.6x12.5 with a self mass of 106 kg/m. The section modulus is W_x = 1.117x10^6 mm^3 .The cross-sectional area for oil filling is A_F = 85841 mm^2 . The load intensity is p = 1.5x106 + 1.39x0.8x85.841 = 2.5445 N/mm. The bending moment is M = 91.92x10^6 Nmm. The bending stress is $\sigma_b = 82.29$ MPa. The factored stress from internal pressure is $1.39\sigma_p = 122.1$ MPa and the reduced stress is 147.2 < 169.2 MPa, OK. For the sake of comparison, we calculate the cost of this larger pipe according to Table 9.13: 1.3642x106x17 = 2458 $.

The cost of the original pipe for a larger span length is (Table 9.13) K_0 = 1.2922x17x33.06 = 726 $.

Now we calculate a strengthening for the original pipe in the case of span length L = 17 m. In the design of the strengthening we perform a minimum cost design procedure to achieve a maximum cost savings against the larger pipe without strengthening.

The unknown variables are as follows: outer diameters d_1, d_2, thicknesses t_1, t_2, geometric dimension H (Fig.9.8).

9.2.4 Optimization of the strengthening tubular truss

9.2.4.1 *Design constraints*

Stress constraint for the original pipe

$$\sqrt{\left(\frac{\frac{pL^2}{8} + \frac{X_1 L}{4}}{W_x}\right)^2 + 150.2^2} \le 169.2 \text{ MPa;} \tag{9.63}$$

W_x = 2.2406x10^5 mm^3; $\frac{pL^2}{8} = 31.37x10^6$ Nmm

Size limitation for tension members for fabrication reasons

$$d_2 \ge 1.08 d_1 . \tag{9.64}$$

Stress constraint for tension member

$$\frac{X_1 q / H}{A_2} \le 213 \text{ MPa}; \quad A_2 = \pi(d_2 - t_2)t_2; \tag{9.65}$$

Stress constraint for the column subject to compression and bending (cross section of class 3 according to EC3)

In order to avoid the column buckling in lateral direction, a lateral force F_u acting on the truss node should be considered. This force can be calculated using the formulae of the BS 5400 Part 3: 1982: for design of U-frames of bridges with unbraced compression chords.

$$F_u = \frac{P_C}{P_E - P_C} \cdot \frac{l_E}{667\delta}; \tag{9.66}$$

$$\delta = \frac{H^3}{3EI_{x1}}; \quad P_E = \frac{\pi^2 EI_{x2}}{l_E^2}; \tag{9.67}$$

$$I_{x2} = \frac{\pi(d_2 - t_2)^3 t_2}{8}; \quad P_C = X_1 q / H; \tag{9.68}$$

$$l_E = 2.5\left(EI_{x2}\delta L/2\right)^{0.25}. \tag{9.69}$$

This force causes bending of the column, thus it should be checked for compression and bending according to Eurocode 3 (2002).

$$\frac{X_1}{\chi A_1 f_y / \gamma_{M1}} + \frac{kF_u H}{W_{x1} f_y / \gamma_{M1}} \le 1; \tag{9.70}$$

$$A_1 = \pi(d_1 - t_1)t_1; \quad W_{x1} = \frac{\pi(d_1 - t_1)^2 t_1}{4}; \tag{9.71}$$

$$I_{x1} = \frac{\pi(d_1 - t_1)^3 t_1}{8}, \tag{9.72}$$

$$\chi = \frac{1}{\phi + \sqrt{\phi^2 - \bar{\lambda}^2}}; \tag{9.73}$$

$$\phi = 0.5\left[1 + 0.34\left(\bar{\lambda} - 0.2\right) + \bar{\lambda}^2\right]; \tag{9.74}$$

$$\bar{\lambda} = \frac{2H}{r_1 \lambda_E}; \quad r_1 = \sqrt{\frac{I_{x1}}{A_1}}; \tag{9.75}$$

$$\lambda_E = \pi\sqrt{\frac{E}{f_y}} = 93.91; \tag{9.76}$$

$$k = \frac{0.79 - 0.1188\dfrac{X_1}{A_1\chi f_y/\gamma_{M1}}}{1 - \dfrac{X_1}{A_1 f_y/\gamma_{M1}}}, \tag{9.77}$$

Constraint on local buckling of tubular members

$$\frac{d_i - t_i}{t_i} \le 50; i = 1,2\,. \tag{9.78}$$

Constraint on chord plastification at the joint (Fig.9.9)

According to Wardenier et al. (1991)

$$N_1^* = \frac{f_y t_2^2}{\sin\theta_1}\left[2.8 + 14.2\left(\frac{d_1}{d_2}\right)^2\right]\left(\frac{d_2}{2t_2}\right)^{0.2} \ge X_1,$$

$$\sin\theta_1 = \frac{L}{2q}. \tag{9.79}$$

Geometric constraint (range of validity) (Fig.9.8)

According to Wardenier et al. (1991)

$$\varphi \ge 30^0 \quad \text{i.e. } H \ge 4900 \text{ mm} \tag{9.80}$$

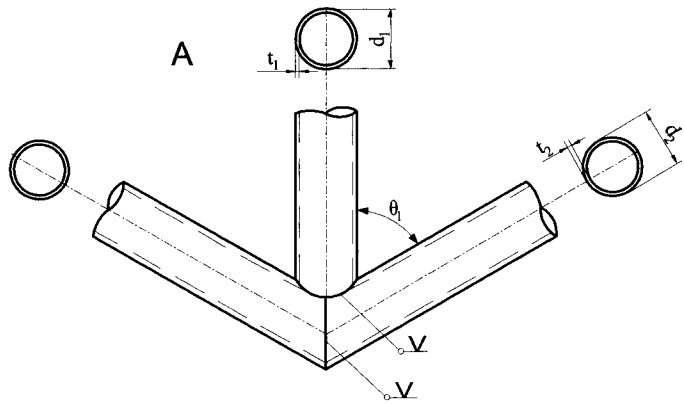

Figure 9.9. Details of the truss node A in Figure 9.8

9.2.4.2 *The cost function*

Material cost is calculated as

$$K_M = k_{M1}\rho A_1 H + 2k_{M2}A_2\rho q; \tag{9.81}$$

$\rho = 7850$ kg/m^3

The material cost factors are given in Table 9.13 in function of the outer diameter according to the Price list of the British Steel (1995).

The cost of cutting and grinding of strut ends (Jármai & Farkas 1999, Farkas & Jármai 2003) (Fig.9.9)

$$K_C = k_F\Theta_C\pi\left[\left(d_1 + \frac{d_1}{\cos\varphi}\right)\left(4.54 + 0.4229t_1^2\right)\right] +$$

$$+k_F\Theta_C\pi\left[\left(\frac{2d_2}{\sin\varphi} + \frac{2d_2}{\cos\varphi}\right)\left(4.54 + 0.4229t_2^2\right)\right],$$

$$\sin\varphi = \frac{H}{q}; \cos\varphi = \frac{L}{2q}, \tag{9.82}$$

fabrication cost factor $k_F = 0.667$ \$/min, $\Theta_C = 3$.

Cost of assembly of the original pipe with the strengthening:

Table 9.13. Material cost factors for circular hollow sections (CHS)

d [mm]	k_M [\$/kg]
88.9, 101.6, 114.3	1.0553
139.7, 168.3, 177.8, 193.7	1.1294
219.1, 244.5, 273.0, 323.9	1.2922
355.6, 406.4	1.3642
457.0, 508.0	1.4081

$$K_A = k_F\Theta_A\sqrt{\kappa\rho V}; \kappa = 4; \Theta_A = 3, \tag{9.83}$$

$$V = \pi DtL + H\pi\left(d_1 - t_1\right)t_1 +$$

$$+2q\pi\left(d_2 - t_2\right)t_2, \tag{9.84}$$

$\pi DtL = 60.6767x10^6$ mm^3

Cost of welding and additional works: SMAW butt and fillet welds

$$K_W = 1.3k_F\left[3.13x10^{-3}t_2\frac{\pi\left(d_2 - t_2\right)}{\cos\varphi}\right] +$$

$$+1.3k_F\left[2x0.7889x10^{-3}t_2^2\frac{\pi(d_2-t_2)}{\sin\varphi}\right]+$$

$$+1.3k_F\left[4x0.7889x10^{-3}t_1^2\pi(d_1-t_1)\right]. \tag{9.85}$$

The cost of painting is given by

$$K_P = k_P\left[H\pi d_1 + 2q\pi d_2\right] . \tag{9.86}$$

$k_P = 14.4\text{x}10^{-6}$ \$/mm^2.

The objective function to be minimized is

$$K = K_M + K_C + K_A + K_W + K_P . \tag{9.87}$$

9.2.4.3 *The optimization procedure and results*

In the optimization procedure the optimum values of H, d_1, t_1, d_2 and t_2 are sought, which fulfil the design constraints (Eqs 9.72, 9.73, 9.74, 9.79, 9.87 and 9.89) and minimize the cost function (Eq.9.96). For this purpose the Rosenbrock hillclimb algorithm is used. This is a direct search method (Farkas & Jármai 1997) which does not use derivatives and results in continuous optimum values. It is complemented by a discretization process to find the corresponding available CHS profiles.

The available CHS dimensions in mm according to DIN 2458 (1981) are as follows:
d: 88.9; 101.6; 114.3; 139.7; 168.3; 177.8; 193,7 (outer diameter)

t: 1.8; 2.0; 2.3; 2.6; 2.9; 3.2; 3.6; 4.0; 4.5; 5.0; 5.6; 6.3 (thickness).

The results are given in Table 9.14.

Table 9.14. Discretized optimization results for different values of H

H [mm]	d_1, t_1 [mm]	d_2, t_2 [mm]	K [\$]
4900	101.6x3.2	114.3x2.0	458
5000	108.0x2.0	127.0x2.6	505
5500	108.0x2.0	127.0x2.6	517
6000	114.3x2.6	127.0x2.6	542

It can be seen that the value of H = 4900 mm gives the minimum cost, thus the optimum solution is determined by the geometric constraint prescribing the minimum inclination angle of diagonals (Eq. 9.89).

Comparing the minimum cost of the original pipe and the strengthening tubular truss K_{min} = 726 + 458 = 1184 \$ with the cost of the larger pipe K = 2458 \$, it can be concluded that the strengthened pipe is much cheaper than the larger one.

9.2.5 Conclusions

The optimum dimensions of a welded tubular truss are determined, which strengthen a column-supported oil` pipeline for a larger (17 m) span length. The pipe is designed for an original span length (12 m). The truss column is designed for compression and bending. Bending is caused by a transverse force considered to avoid the lateral buckling. Since the strengthened structure is statically indetermined, the unknown force in the truss column is calculated from a deflection equation.

Design constraints relate to the member stresses as well as to strength and geometry of truss nodes. The cost function includes the costs of material, cutting and grinding of strut ends, assembly, welding and painting.
In the optimization process the unknowns are the truss height H and the diameter and thickness of truss members. The optimization shows that the optimal H is determined by the geometric constraint prescribing the minimum inclination angle of diagonals.

The cost comparison shows that the cost of the strengthened pipe is much lower than that of the larger pipe without strengthening.

10

Square Box Column Composed from Welded Cellular Plates

10.1 INTRODUCTION

Box beams and columns of large load-carrying capacity are widely applied in bridges, buildings, highway piers, pilons etc. Since the thickness required for an unstiffened box column can be too large, stiffened plate elements or cellular plates should be used.

Steinhardt (1975) has proposed a design method for box beams with stiffened flange plates using formulae for effective plate width. Nakai et al. (1985) have worked out empirical formulae for stiffened box stub-columns subject to combined actions of compression and bending.

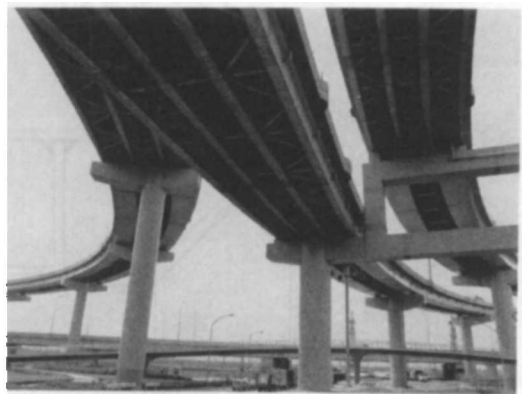

Ge et al. (2000) and Usami et al. (2000) have studied the cyclic behaviour and ductility of stiffened steel box columns used as bridge piers. Longitudinal flat plate stiffeners and diaphragms as well as constant compressive axial force and cyclic

lateral loading have been considered. Empirical formulae have been proposed for ultimate strength and ductility capacity.

Another papers about bridge piers can be found in conference proceedings as follows: Yamao,T. et al. (2004), Ohga,M. et al.(2004) and Hirota,T. et al. (2004).

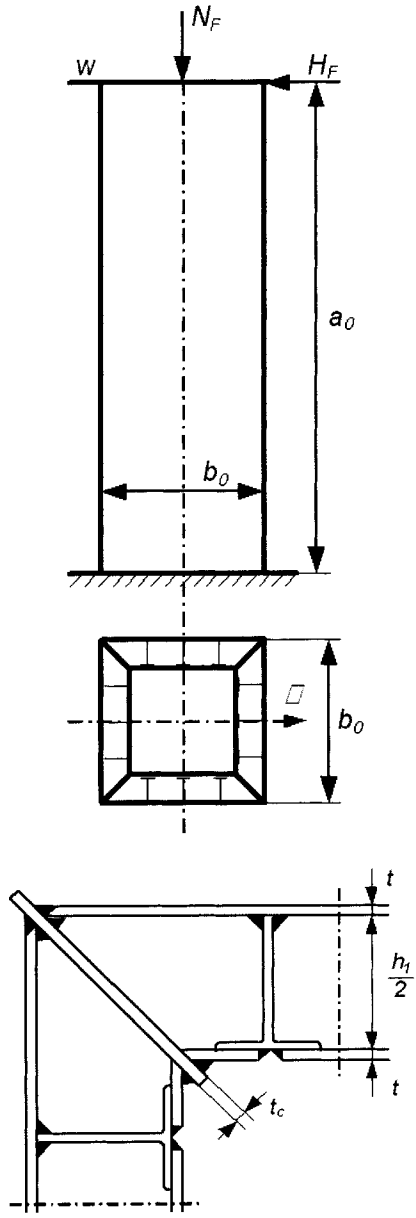

Figure 10.1. A cantilever stub-column of square box section with cellular side plates and the welded corner

In our previous studies it has been shown that, in the case of uniaxial compression, cellular plates is more economic than a longitudinally stiffened one (Farkas & Jármai 2006a). In a study we have elaborated a minimum cost design of a cellular plate subject to uniaxial compression (Farkas & Jármai 2006b).This method is used in present paper for a square box column constructed from four equal cellular plates.

A cantilever column is loaded by a compression force and a horizontal load, thus, it is subject to compression and bending. From this loading a compression force is calculated for two opposite plate elements, while the remaining plate elements are subject to compression and bending. Since this loading is not as dangerous for the buckling of the remaining side plate elements, it is sufficient to design only the two main plate elements. Halved rolled I-section stiffeners are used.

To show the necessity of stiffening, let us design an unstiffened square box column using the following data (Fig. 10.1): $L = a_0 = 15$ m, $N_F = 34000$ kN, $H_F = 0.1N_F$, the limit of the horizontal displacement on the column top $w_0 = L/1000 = 15$ mm, the steel yield stress $f_y = 355$ MPa, elastic modulus $E = 2.1\text{x}10^5$ MPa.

The limiting plate slenderness is expressed according to Eurocode 3 (2002)

$$b/t \le 1/\delta = 42\varepsilon, \varepsilon = \sqrt{235/f_y}, 1/\delta = 34, t \ge \delta b\,. \tag{10.1}$$

Taking the last inequality as equality, the cross section area, moment of inertia and section modulus are defined as

$$A = 4bt = 4\delta b^2, I_x = 2\delta b^4/3, W_x = 4\delta b^3/3\,. \tag{10.2}$$

The stress and displacement constraints are written as

$$\frac{N_F}{A} + \frac{H_F L}{W_x} \le \frac{f_y}{1.1}, \frac{H_F L^3}{3EI_x} \le w_0\,. \tag{10.3}$$

Since the displacement constraint is governing, the required box section width can be calculated as

$$b \ge \sqrt[4]{\frac{H_F L^3}{2\delta E w_0}} = 2805, t = 2805/34 = 82.5 \text{ mm}. \tag{10.4}$$

This thickness is unrealistically large, thus, stiffening is needed.

In the optimum design the following variables should be optimized: the column width b_0, the outer and inner plate thickness t, dimensions and number of stiffeners h, n. It is sufficient to determine the height h, since the other profile dimensions (b, t_w and t_f) can be calculated using approximate functions determined for a selected series of UB sections according to the Arcelor catalogue (Profil Arbed 2001).

The buckling constraints are formulated according to the Det Norske Veritas rules (1995).

10.2 CONSTRAINTS

10.2.1 Constraint on overall buckling of a cellular plate (Fig.10.2)

$$\sigma = \frac{N_F}{4A_e(n-1)} + \frac{0.1N_F a_0}{W_\xi} \le \sigma_{cr} = \frac{f_{y1}}{\sqrt{1+\lambda^4}}. \tag{10.5}$$

Effective cross-sectional area

$$A_e = \frac{h_1 t_w}{2} + b\ t_f + s_{ey} t, s_y = \frac{b_0}{n}. \tag{10.6}$$

Effective plate width

$$s_{ey} = s_y C\ , \tag{10.7}$$

$$C\ = \frac{1.8}{\beta} - \frac{0.8}{\beta^2}, \tag{10.8}$$

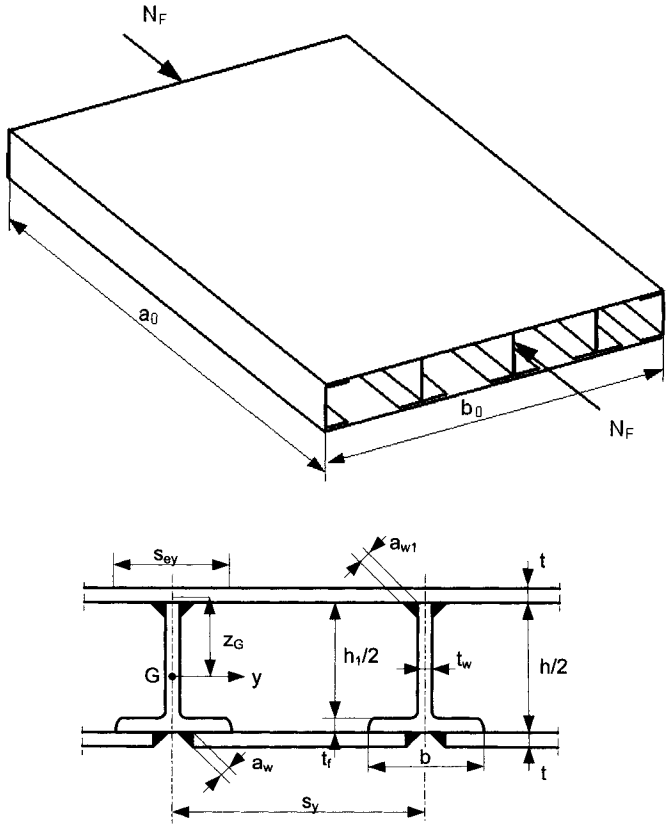

Figure 10.2. Cellular plate with longitudinal stiffeners

$$\beta = \frac{s_y}{t}\sqrt{\frac{f_y}{E}} \quad \text{if} \quad \beta \geq 1, \tag{10.9}$$

$$\beta = 1 \qquad \text{if} \quad \beta < 1.$$

The distance of the gravity centre G

$$z_G = \frac{1}{A_e}\left[\frac{h_1 t_w}{2}\left(\frac{h_1}{4}+\frac{t}{2}\right)+b\ t_i\left(\frac{h+t-t_f}{2}\right)+s_{ey}t\left(\frac{h}{2}+t\right)\right], \tag{10.10}$$

The moment of inertia

$$I_y = s_{ey}tz_G^2 + s_{ey}t\left(\frac{h}{2}+t-z_G\right)^2 + \frac{h_1^3 t_w}{96} + \frac{h_1 t_w}{2}\left(\frac{h_1}{4}+\frac{t}{2}-z_G\right)^2 + b\ t_f\left(\frac{h+t-t_f}{2}-z_G\right)^2$$

. (10.11)

The classic buckling force is derived from the Huber's differential equation for orthotropic plates

$$N_E = \frac{\pi^2}{b_0^2}\left(B_x\frac{b_0^2}{a_0^2}+2H+B_y\frac{a_0^2}{b_0^2}\right). \tag{10.12}$$

The bending and torsional stiffnesses

$$B_x = \frac{E_1 I_y}{s_y}; B_y = \frac{E_1 I_x}{s_x} = \frac{E_1 t(h+2t)^2}{8}, E_1 = \frac{E}{1-\nu^2}, \tag{10.13}$$

$$H = B_{xy} + B_{yx} + \frac{\nu}{2}\left(B_x + B_y\right), \tag{10.14}$$

$$B_{xy} = \frac{GI_y}{s_y}, B_{yx} = \frac{GI_x}{s_x}, G = \frac{E}{2(1+\nu)}. \tag{10.15}$$

Using Eqs (10.15), Eq (10.14) can be written in the form

$$H = \frac{B_x + B_y}{2}, \tag{10.16}$$

$$\sigma_E = \frac{N_E s_y}{A_e}, \tag{10.17}$$

$$\lambda = \sqrt{\frac{f_{y1}}{\sigma_E}}, \tag{10.18}$$

$$W_\xi = \frac{I_\xi}{\frac{b_0}{2} - z_G}, \tag{10.19}$$

$$I_\xi = 2\left\langle \left[I_y + A_e\left(\frac{b_0}{2} - z_G\right)^2 \right](n-1) + I_{\xi S} + \frac{b_0^3 t}{12} + \frac{b_1^3 t}{12} \right\rangle, \tag{10.20}$$

$$b_1 = b_0 - h - t.$$

If n is even

$$I_{\xi S} = \frac{b^3 t_f}{12}(n-1) + 2\left(bt_f + \frac{h_1 t_w}{2}\right)\sum_{i=1}^{\frac{n_y}{2}-1}\left(s_y^2 i^2\right), \tag{10.21a}$$

if n is odd

$$I_{\xi S} = \frac{b^3 t_f}{12}(n-1) + 2\left(bt_f + \frac{h_1 t_w}{2}\right)\sum_{i=1,3,5}^{n_y-2}\left[\left(\frac{s_y}{2}\right)^2 i^2\right]. \tag{10.21b}$$

10.2.2 Constraint on horizontal displacement of the column top

$$w_{\max} = \frac{H_F}{\gamma_M}\frac{L^3}{3EI_\xi} \le \frac{L}{\phi}, \gamma_M = 1.5, \phi = 300 - 1000. \tag{10.22}$$

10.2.3 Constraint on local buckling of face plates connecting the transverse stiffeners

$$t_C \ge \frac{\sqrt{2}h}{2x14\varepsilon}, \varepsilon = \sqrt{\frac{235}{\sigma}}. \tag{10.23}$$

10.3 NUMERICAL DATA (Fig. 1)

a_0 = 15000, N_x = 3x10^7 [N], steel yield stress f_y = 355 MPa, elastic modulus E = 2.1x10^5 MPa, shear modulus G = 0.81x10^5, density ρ = 7.85x10^{-6} kg/mm^3, Poisson ratio ν = 0.3, selected rolled I-sections UB profiles.

Ranges of unknowns: 4 < t < 20 mm, 152 < h < 1016 mm, 4<n<n_{max}, n_{max} are determined by the following fabrication constraints:

$$\frac{b_0}{n} - b_y \ge 300 \text{ mm}. \tag{10.24}$$

The other dimensions of a halved rolled I-section are given by approximate functions of h in Appendix.

$$h_1 = h - 2t_f \,. \tag{10.25}$$

The discrete values of h are as follows: 152.4, 177.8, 203.2, 257.2, 308.7, 353.4, 403.2, 454.6, 533.1, 607.6, 683.5, 762.2, 840.7, 910.4, 1016 mm.

10.4 COST FUNCTION

The cost function includes the cost of material, assembly, welding as well as painting and is formulated according to the fabrication sequence.

The cost of material

$$K_M = k_M \rho V_6 ; k_M = 1.0 \text{ \$/kg} \,. \tag{10.26}$$

Welding of the base plate with butt welds (SAW - submerged arc welding) (Farkas & Jármai 2003). A fabricated plate element has sizes of 6000x1500 mm or less.

The fabrication cost factor is taken as k_F = 1.0 \$/min, the factor of complexity of the assembly $\Theta_W = 2$:

$$K_{F0} = k_F \left[\Theta_W \; 3n\rho V_0 + 1.3 C_W t^{n_1} L_{W1} \right], \tag{10.27}$$

$$V_0 = a_0 b_0 t, \qquad L_{W1} = 2b_0 + a_0 (n-1), \tag{10.28}$$

$$\text{for } t < 11 \qquad C_W = 0.1346 x 10^{-3} ; n_1 = 2 \,, \tag{10.29a}$$

$$\text{for } t \geq 11 \qquad C_W = 0.1033 x 10^{-3} ; n_1 = 1.904 \,. \tag{10.29b}$$

Welding (n-1) stiffener webs to the base plate with double fillet welds (GMAW-C - gas metal arc welding with CO_2):

$$K_{F1} = k_F \left[\Theta \; \sqrt{n \; \rho V_1} + 1.3 x 0.3394 x 10^{-3} a_{w1}^2 \, 2a_0 (n \; -1) \right], \tag{10.30}$$

$a_{Wx} = 0.4 \; t_{wx}$ but $a_{wx.min} = 3$ mm,

$$V_1 = a_0 b_0 t + \left(\frac{h_1 t_w}{2} + b \; t_f \right) a_0 (n \; -1). \tag{10.31}$$

Welding of n-2 inner plate strips from 3 parts with butt welds

$$K_{F2} = k_F \left[\Theta \sqrt{3\rho V_2} + 1.3 C_W t^{n1} x 2 s_y \right] (n-2), \tag{10.32}$$

$$V_2 = a_0 s_y t$$

Welding of inner plate strips to the stiffener flanges with 2 fillet welds (excluding 2 side strips)

$$K_{F3} = k_F \left[\Theta \; \sqrt{(n-1)\rho V_3} + 1.3 x 0.3394 x 10^{-3} a_{w2}^2 \, 2a_0 (n \; -2) \right], \tag{10.33}$$

$a_{W2} = 0.7\,t$ but $a_{w2.min} = 3$ mm,

$V_3 = V_1 + V_2(n-2)$.

Welding of 4 outer plates of cellular plates to the corner plates with 4 fillet welds

$$K_{F4} = k_F\left[\Theta\sqrt{8\rho V_4} + 1.3x0.3394x10^{-3}\,a_{W2}^2 16a_0\right], \tag{10.34}$$

$$V_4 = V_3 + 4t_C a_0\left(\frac{h\sqrt{2}}{2} + 3t_C\right).$$

Welding of 8 inner side plate strips with 3 butt welds

$$K_{F5} = k_F\left[\Theta\sqrt{3\rho V_5} + 1.3C_W t^{n1} 2\left(s_y - \frac{h}{2}\right)\right]x8, \tag{10.35}$$

$$V_5 = a_0 t\left(s_y - \frac{h}{2}\right).$$

Welding of 8 inner side plate strips to the corner plates and side stiffener flanges with fillet welds

$$K_{F6} = k_F\left[\Theta\sqrt{9\rho V_6} + 1.3x0.3394x10^{-3}\,a_{W2}^2 16a_0\right], \tag{10.36}$$

$V_6 = V_4 + 8V_5$.

Painting cost is calculated as

$$K_P = k_P\Theta_P S_P, \tag{10.37}$$

$k_P = 14.4\text{x}10^{-6}$ \$/mm^2, $\Theta_P = 2$.

Surface to be painted

$$S_P = 4a_0(b_0 + b_1). \tag{10.38}$$

The total cost

$$K = K_M + 4(K_{F0} + K_{F1} + K_{F2} + K_{F3} + K_{F4}) + K_{F5} + K_{F6} + K_P. \tag{10.39}$$

10.5 OPTIMIZATION AND RESULTS

Table 10.1 shows optimal solutions for different h-values obtained by a systematic search using a Mathcad calculation.

Table 10.1 Optimal solutions for different h-values. The result is marked by bold letters. The allowable displacement is 15 mm

h [mm]	t [mm]	n	b_0 [mm]	$\sigma < \sigma_{cr}$ [MPa]	w [mm]	K [$]
152.4	6	13	5060	303<318	12.3	71060
257.2	5	13	5230	296<321	11.0	64130
353.4	5	10	5520	321<322	12.0	62610
454.6	5	8	5350	322<323	13.0	61400
533.1	**5**	**7**	**4700**	**294<323**	**15.0**	**60430**
607.6	5	7	4480	261<322	14.9	62730

It can be seen that the solution of h = 533.1 mm gives the minimum cost. For smaller h-s the stress constraint, for larger h-s the displacement constraint is active.

10.6 CONCLUSIONS

A cantilever stub column of a square box section is optimized. The column is subject to compression and bending and is constructed from four equal cellular side plates. The thickness and width of side plates as well as the dimensions and numbers of longitudinal stiffeners are calculated to fulfil the constraints and minimize the cost function.

The constraints on overall buckling are formulated according to the Det Norske Veritas design rules. The horizontal displacement of the column top is limited. The minimum distance between stiffeners is prescribed to ease the welding of stiffeners to the base plates.

Halved rolled I-profile stiffeners are used. Their height characterizes the whole profile, since the other dimensions can be expressed by height using approximate functions derived from the data of a profile series selected from available sections.

The cost function is formulated according to the fabrication sequence.

It is possible to compare the costs of three structural versions of the column with the same height, loads and constraints on stress and displacement as follows.

(1) The stringer-stiffened circular shell with an optimized radius of 2700 mm (see Chapter 8.6) has the minimum cost of K = 83309 (unstiffened K = 82177 $),

(2) the square box structure composed from orthogonally stiffened plates with an optimized width of b_0 = 4500 mm has the minimum cost of K = 76990 $ (see Farkas & Jármai 2008),

(3) the present cellular box structure with an optimized width of b_0 = 4700 mm has the minimum cost of K = 60430 $.

It can be concluded that the cellular box column is the most economic structural version.

Appendixes

Appendix A

Approximation of stresses in cover plate and stiffeners according to Schade (1941). The TableCurve2D (2003) is used finding the best curve-fitting function. (Sec.7.4)

$$x = \Theta_B = \frac{b_0}{a_0}\sqrt[4]{\frac{B_x}{B_y}}. \tag{A1}$$

Stress in the stiffener in x direction

$$c_{xs} = a + \frac{b}{x} + \frac{c}{x^2} + \frac{d}{x^3} + \frac{e}{x^4} + \frac{f}{x^5} + \frac{g}{x^6} + \frac{h}{x^7}, \tag{A2}$$

a = 0.4664267441239763
b = -4.624587383840012
c = 24.24565720683284
d = -63.81680636506682
e = 93.39987358860954
f = -76.71346352316542
g = 32.32002703712877
h = -5.198127750547869

Stress in the cover plate in x direction

$$c_x = a + \frac{b}{x} + \frac{c}{x^2} + \frac{d}{x^3} + \frac{e}{x^4} + \frac{f}{x^5} + \frac{g}{x^6} + \frac{h}{x^7}, \tag{A3}$$

a= 0.1955984693130098
b= -0.2897463241178856
c= -2.591464219165066

d= 22.85411176451855
e= -64.64101649616373
f= 87.66635206424669
g= -58.68763133158539
h= 15.60579575441681

Stress in the stiffener in y direction

$$c_{ys} = \frac{a + cx + ex^2 + gx^3 + ix^4 + kx^5}{1 + bx + dx^2 + fx^3 + hx^4 + jx^5}, \tag{A4}$$

a= 0.09335739292748108
b= -2.075188395008322
c= -0.1893111520991659
d= 1.793376862990908
e= 0.1463476326966368
f= -0.8378526877119945
g= -0.05338805456508658
h= 0.212909213858211
i= 0.009176903345325986
j= -0.02162297129304045
k= -0.0005962182063725342

Stress in the cover plate in y direction

$$c_y = \frac{a + cx + ex^2 + gx^3 + ix^4}{1 + bx + dx^2 + fx^3 + hx^4 + jx^5}, \tag{A5}$$

a= 0.03003781819502921D0
b= -2.042265097925914D0
c= -0.01097958991738318D0
d= 1.884628053759462D0
e= -0.001819275850703149D0
f= -0.8418981200681422D0
g= 0.0002355918865462362D0
h= 0.1725049205573912D0
i= 0.0001767942314140527D0
j= -0.01252238187246605D0

Deflection of the plate in the middle

$$c_w = a + bx + \frac{c}{x} + dx^2 + \frac{e}{x^2} + fx^3 + \frac{g}{x^3} + hx^4 + \frac{i}{x^4} + jx^5 + \frac{k}{x^5}, \tag{A6}$$

a= 19.3849502389358D0
b= -8.592520424643785D0
c= -28.03014210194325D0
d= 2.455088353738002D0
e= 25.02816526698025D0

f= -0.4373229820168736D0
g= -12.41706988320835D0
h= 0.04419737760687714D0
i= 2.482147546617202D0
j= -0.00193499443839704D0
k= 0.092741603399005D0

Appendix B

Approximate formulae for c_{fx} and c_{fy} for the local bending stresses of the base plate according to (Table Curve 2003) (Sec.7.4).

$$c_{fx} = a + bx + cx^2 + dx^3 + ex^4 + fx^5 \quad , \tag{B1}$$

$$x = \frac{s_{\max}}{s_{\min}} \quad , \qquad \text{(see Eqs. 7.149, 7.150)} \tag{B2}$$

a= -0.01714825171119342
b= -0.04225084511898836
c= 0.2808835957524557
d= -0.2454326924316682
e= 0.0864656177573734
f= -0.01121794872349564

$$x = \frac{s_{min}}{s_{max}}, \tag{B3}$$

$$c_{fy} = a + \frac{b}{x} + \frac{c}{x^2} + \frac{d}{x^3} + \frac{e}{x^4} + \frac{f}{x^5} \quad , \tag{B4}$$

a= 0.06984365541723147
b= -0.05101531212632416
c= 0.007438395232983666
d= 0.2053042707173005
e= -0.291931992763519
f= 0.1116609274910173

Appendix C

Characteristics of rolled UB profiles

Table C1. Characteristics of the selected rolled UB profiles (Sales program 2007 Commercial sections)

UB Profile	h [mm]	b [Mm]	t_w [mm]	t_f [mm]	A_S [mm^2]	I_y x10^{-4} [mm^4]
152x89x16	152.4	88.7	4.5	7.7	2032	834
178x102x19	177.8	101.2	4.8	7.9	2426	1356
203x133x25	203.2	133.2	5.7	7.8	3187	2340
254x102x25	257.2	101.9	6.0	8.4	3204	3415
305x102x28	308.7	101.8	6.0	8.8	3588	5366
356x127x39	353.4	126.0	6.6	10.7	4977	10172
406x140x46	403.2	142.2	6.8	11.2	5864	15685
457x152x60	454.6	152.9	8.1	13.3	7623	25500
533x210x92	533.1	209.3	10.1	15.6	11740	55230
610x229x113	607.6	228.2	11.1	17.3	14390	87320
686x254x140	683.5	253.7	12.4	19.0	17840	136300
762x267x173	762.2	266.7	14.3	21.6	22040	205300
838x292x194	840.7	292.4	14.7	21.7	24680	279200
914x305x224	910.4	304.1	15.9	23.9	28560	376400
1016x305x349	1008.1	302	21.1	40.0	44420	722300
1016x305x393	1016.0	303	24.4	43.9	50020	807700

Approximate formulae for the sizes of the universal beam UB according to the Arcelor catalogue (*Sales program* 2007 *Commercial sections*).

The other dimensions of a halved rolled I-section are expressed by the main height h according (*Sales program* 2007 *Commercial sections*) using curve-fitting calculations (Table Curve 2003) are as follows:

$$A_s = 1093.243940 + 0.033683995\, h_s^2 \tag{C1}$$

$$t_f = \sqrt{34.5525658 + 0.00065187579\, h_s^2} \tag{C2}$$

$$I_y = \exp\left[45.006178 - \frac{156.52880258}{\ln(h_s)}\right] \text{x}10^4 \tag{C3}$$

$$b = \sqrt{4676.099669 + 0.01115927 h_s^2} \tag{C4}$$

$$t_w = \sqrt{16.154183 + 4.228419\text{x}10^{-5}\, h_s^2 \ln(h_s)} \tag{C5}$$

$$h_1 = h_S - 2t_f \tag{C6}$$

Approximate formulae for UB profile dimensions

Calculation of b ($y = b$; $x = h$)

$$y = a+b\ln x+c/\ln x+d(\ln x)^2+e/(\ln x)^2+f(\ln x)^3+g/(\ln x)^3+h(\ln x)^4+i/(\ln x)^4 \tag{C7}$$

a = 4071797665.515043
b = -377581103.813262
c = -25351511152.9463
d = 17442666.41988002
e = 92925416774.55347
f = -155449.0539314809
g = -187087676930.7058
h = -10894.44641480538
i = 160167765716.8299

Calculation of t_f ($y = t_f$; $x = h$)

$$y = a+bx+cx^2+dx^3+ex^4+fx^5+gx^6+hx^7+ix^8 \quad \text{(C8)}$$

a = -26.93815960004096
b = 0.7030053163805572
c = -0.00569333794408951
d = $2.383106250400329\text{x}10^{-05}$
e = $-5.605511588090933\text{x}10^{-08}$
f = $7.662794270183799\text{x}10^{-11}$
g = $-5.902409057606285\text{x}10^{-14}$
h = $2.267417890058806\text{x}10^{-17}$
i = $-2.999371273581411\text{x}10^{-21}$

Calculation of t_w ($y = t_w$; $x = h$)

$$y = a+bx+cx^2+dx^3+ex^4+fx^5+gx^6+hx^7+ix^8 \quad \text{(C9)}$$

a = 4.598131596507252
b = -0.1667245080692302
c = 0.002662252638593643
d = $-1.662919423768273\text{x}10^{-05}$
e = $5.42570607199179\text{x}10^{-08}$
f = $-1.003562930723944\text{x}10^{-10}$
g = $1.063362616433473\text{x}10^{-13}$
h = $-6.028516559742138\text{x}10^{-17}$
i = $1.419727612597333\text{x}10^{-20}$

Another calculation of b

$$y = a+bx+c/x+dx^2+e/x^2+fx^3+g/x^3+hx^4+i/x^4+jx^5+k/x^5 \quad \text{(C10)}$$

a = -1108926.658794802
b = 2054.96457373585
c = 394347552.4221416
d = -2.475920494568994
e = -91315532919.66857
f = 0.001858445891156483
g = 13189053888762.85
h = $-7.856977790442618\text{x}10^{-07}$
i = -1073670362507492

$$j = 1.422535840934241 \times 10^{-10}$$
$$k = 3.744384150518803 \times 10^{16}$$

Appendix D

Table D1 Applied welding technologies

SMAW	Shielded Metal Arc Welding
SMAW HR	Shielded Metal Arc Welding High Recovery
GMAW-C	Gas Metal Arc Welding with CO_2
GMAW-M	Gas Metal Arc Welding with Mixed Gas
FCAW	Flux Cored Arc Welding
FCAW-MC	Metal Cored Arc Welding
SSFCAW (ISW)	Self Shielded Flux Cored Arc Welding
SAW	Submerged Arc Welding
GTAW	Gas Tungsten Arc Welding

Table D2 Welding times T_{w2} (min/mm) in the function of weld size a_w (mm) for longitudinal fillet welds, downhand position

Welding technology	a_w [mm]	$10^3 T_{w2} = 10^3 C_2 a_w^2$
SMAW	0-15	$0.7889a_w^2$
SMAW HR	0-15	$0.5390a_w^2$
GMAW-C	0-15	$0.3394a_w^2$
GMAW-M	0-15	$0.3258a_w^2$
FCAW	0-15	$0.2302a_w^2$
FCAW-MC	0-15	$0.4520a_w^2$
SSFCAW (ISW)	0-15	$0.2090a_w^2$
SAW	0-15	$0.2349a_w^2$

Table D3 Welding times T_{w2} (min/mm) in the function of weld size a_w (mm) for longitudinal 1/2 V and V butt welds downhand position

			1/2 V butt welds		V butt welds	
Welding technology	a_w [mm]		$10^3 T_{w2} = 10^3 C_2 a_w^2$		$10^3 T_{w2} = 10^3 C_2 a_w^2$	
SMAW	4-6	6-15	$3.13a_w$	$0.5214a_w^2$	$2.7a_w$	$0.45a_w^2$
SMAW HR	4-6	6-15	$2.14a_w$	$0.3567a_w^2$	$1.8462a_w$	$0.3077a_w^2$
GMAW-C	4-15		$0.2245a_w^2$		$0.1939a_w^2$	
GMAW-M	4-15		$0.2157a_w^2$		$0.1861a_w^2$	
FCAW	4-15		$0.1520a_w^2$		$0.1311a_w^2$	
FCAW-MC	4-15		$0.2993a_w^2$		$0.2582a_w^2$	
SSFCAW (ISW)	4-15		$0.1384a_w^2$		$0.1194a_w^2$	
SAW	4-15		$0.1559a_w^2$		$0.1346a_w^2$	

Table D4 Welding times T_{w2} (min/mm) in the function of weld size a_w (mm) for longitudinal K and X butt welds downhand position in the form $T_{w2} = \sum_i C_{2i} a_{wi}^n L_{wi}$

		K butt welds	X butt welds
Welding technology	a_w [mm]	$10^3 T_{w2} = 10^3 C_2 a_w^n$	$10^3 T_{w2} = 10^3 C_2 a_w^n$
SMAW	10-40	$0.3539 a_w^{1.93}$	$0.3451 a_w^{1.9}$
SMAW HR	10-40	$0.2419 a_w^{1.93}$	$0.2363 a_w^{1.9}$
GMAW-C	10-40	$0.1520 a_w^{1.94}$	$0.1496 a_w^{1.9}$
GMAW-M	10-40	$0.1462 a_w^{1.94}$	$0.1433 a_w^{1.9}$
FCAW	10-40	$0.1032 a_w^{1.94}$	$0.1013 a_w^{1.9}$
FCAW-MC	10-40	$0.2030 a_w^{1.94}$	$0.1987 a_w^{1.9}$
SSFCAW (ISW)	10-40	$0.0937 a_w^{1.94}$	$0.0924 a_w^{1.9}$
SAW	10-40	$0.1053 a_w^{1.94}$	$0.1033 a_w^{1.9}$

Table D5 Welding times T_{w2} (min/mm) in the function of weld size a_w (mm) for longitudinal T butt welds downhand position in the form $T_{w2} = \sum_i C_{2i} a_{wi}^n L_{wi}$

Welding technology	a_w [mm]	$10^3 T_{w2} = 10^3 C_2 a_w^n$
SMAW	2-8	$\left(0.1211 - 0.00473 a_w^{1.36}\right)^{-1}$
SMAW HR	2-8	$0.2155 a_w^2 + 2.1485$
GMAW-C	2-8	$0.2189 a_w^{1.84}$
GMAW-M	2-8	$0.2221 a_w^{1.82}$
FCAW	2-8	$0.1006 a_w^2 + 0.4247$
FCAW-MC	2-8	$0.2065 a_w^2 + 0.4405$
SSFCAW (ISW)	2-8	$0.0918 a_w^2 + 0.3791$
SAW	2-8	$0.01066 a_w^3 + 1.698$

Table D6 Welding times T_{w2} (min/mm) in the function of weld size a_w (mm) for longitudinal U and double U butt welds downhand position in the form $T_{w2} = \sum_i C_{2i} a_{wi}^n L_{wi}$

		U butt welds	double U butt welds
Welding technology	a_w [mm]	$10^3 T_{w2} = 10^3 C_2 a_w^n$	$10^3 T_{w2} = 10^3 C_2 a_w^n$
SMAW	20-40	$2.2326 a_w^{1.46}$	$1.8195 a_w^{1.37}$
SMAW HR	20-40	$1.5280 a_w^{1.46}$	$1.2461 a_w^{1.37}$
GMAW-C	20-40	$0.9642 a_w^{1.46}$	$0.7865 a_w^{1.37}$
GMAW-M	20-40	$1.6489 a_w^{1.46}$	$0.7526 a_w^{1.37}$
FCAW	20-40	$0.6514 a_w^{1.46}$	$0.5334 a_w^{1.37}$
FCAW-MC	20-40	$1.2833 a_w^{1.46}$	$1.0462 a_w^{1.37}$
SSFCAW (ISW)	20-40	$0.5962 a_w^{1.46}$	$0.4824 a_w^{1.37}$
SAW	20-40	$0.6702 a_w^{1.46}$	$0.5461 a_w^{1.37}$

Table D7 Welding times T_{w2} (min/mm) in the function of weld size a_w (mm) for longitudinal fillet welds in positional welding

Welding technology	a_w [mm]	$10^3 T_{w2} = 10^3 C_2 a_w^2$
SMAW	0-15	$1.6670 a_w^2$
GMAW-C	0-15	$0.4930 a_w^2$

Table D8 Welding times T_{w2} (min/mm) in the function of weld size a_w (mm) for longitudinal V butt welds in positional welding

Welding technology	a_w [mm]	$10^3 T_{w2} = 10^3 C_2 a_w^2$
SMAW	4-15	$0.9518 a_w^2$
GMAW-C	4-15	$0.2814 a_w^2$

Table D9 Time needed for different *PWT* techniques

Method	T_0 (min/m)
Grinding	60
TIG dressing	18
Hammer peening	4
UIT	15

Table D10 Cutting time of plates, T_{CP} (min/mm) in the function of weld size a_w (mm) for fillet for longitudinal fillet welds and T-, V-, 1/2 V butt welds

Cutting technology	Thickness t [mm]	$10^3 T_{CP} = 10^3 C_{CP} t^n$
Acetylene (normal speed)	2-15	$1.1388t^{0.25}$
Acetylene (high speed)	2-15	$0.9561t^{0.25}$
Stabilized gasmix (normal speed)	2-15	$1.1906t^{0.25}$
Stabilized gasmix (high speed)	2-15	$1.0858t^{0.23}$
Propane (normal speed)	2-15	$1.2941t^{0.24}$
Propane (high speed)	2-15	$1.1051t^{0.25}$

Table D11 Cutting time of plates for 1 mm length, T_{CP} (min/mm) in the function of weld size a_w (mm) for fillet for longitudinal X- and K butt welds

Cutting technology	Thickness t [mm]	$10^3 T_{CP} = 10^3 C_{CP} t^n$
Acetylene (normal speed)	10-40	$0.8529t^{0.36}$
Acetylene (high speed)	10-40	$0.6911t^{0.38}$
Stabilized gasmix (normal speed)	10-40	$0.8991t^{0.36}$
Stabilized gasmix (high speed)	10-40	$0.6415t^{0.44}$
Propane (normal speed)	10-40	$0.9565t^{0.36}$
Propane (high speed)	10-40	$0.7870t^{0.38}$

References

CHAPTER 1 Newer Mathematical Optimization Methods

Annamalai,N.(1970) *Cost optimization of welded plate girders*. Dissertation, Purdue Univ. Indianapolis, Ind.

Box,M.J. (1965) A new method of constrained optimization and a comparison with other methods. *Computer Journal*, **8** 42-52.

Dasgupta,D. (Editor), *Artificial Immune Systems and Their Applications*, Springer-Verlag, Inc. Berlin, January 1999, ISBN 3-540-64390-7

DeCastro,L. & Timmis,J. (2001) *Artificial Immune Systems: A New Computational Intelligence Approach*, ISBN 1-85233-594-7

Dorigo,M., Di Caro,G. & Gambardella, L.M. (1999) Ant algorithms for discrete optimization, *Artificial Life*, **5** No. 3, 137-172.

Fan,Y., Sarkar,S. & Lasdon,L. (1988) Experiments with successive quadratic programming algorithms, *J. Optim. Theory Appl.* **56** pp. 359--383.

Farkas,J. & Jármai,K. (1997) *Analysis and optimum design of metal structures*, Balkema Publishers, Rotterdam, Brookfield, 347 p. ISBN 90 5410 669 7.

Farkas,J. & Jármai,K. (2003) *Economic design of metal structures*, Millpress Science Publisher, Rotterdam, 340 p. ISBN 90 77017 99 2

Farkas,J., Simões,M.C. & Jármai,K. (2005) Minimum cost design of a welded stiffened square plate loaded by biaxial compression, *Structural and Multidisciplinary Optimization*, Springer Verlag, Wien-New York, **29** No. 4, 298-303.

Farkas,J., Jármai,K. & Snyman,J.A. (2007a) Global minimum cost design of a welded square stiffened plate supported at four corners. *7th World Congress on Structural and Multidisciplinary Optimization, WCSMO7,* May 21-May.25, 2007, COEX, Seoul, Korea, Proceedings on CD, A 0381, pp. 1057-1066.

Farkas,J., Jármai,K. & Kožuh,Z. (2007b) Cost minimization of an orthogonally stiffened welded steel plate subject to static and fatigue load. *Welding in the World*, **51** 2007, Special issue. pp. 357-366.

Farkas,J., Jármai,K. & Orbán,F. (2007c) Cost minimization of a ring-stiffened conical shell loaded by external pressure. *60th Annual Assembly of International Institute of Welding,* July 1 – July 8, 2007, Dubrovnik, Croatia, IIW-Doc. XV-1248-07, XV-F-80-07, 9 p.

Farmer,J.D., Packard N. & Perelson A., (1986) The immune system, adaptation and machine learning, *Physica D*, **2** 187-204.

Fiacco,A.V. & McCormick,G,P. (1968) *Nonlinear sequential unconstrained minimization technique.* John Wiley and Sons, Inc. New York.

Fourie,P.C. & Groenwold,A.A. (2000) Particle swarm in size and shape optimisation, International *Workshop on Multidisciplinary Design Optimization*, 7-10, Aug. 2000, Pretoria, South Africa, Proceedings 97-106.

Goldberg,D.E. (1989) *Genetic algorithms in search, optimization & machine learning*, Addison-Wesley Publ. Company, Inc.

Golomb,S.W. & Baumert,L.D. (1965) Backtrack programming, *J. Assoc. Computing Machinery*, **12** 516-524.

Groenwold,A.A. & Snyman,J.A. (2002) Global optimization using dynamic search trajectories. *J Global Optimiz*; **24** 51-60.

Himmelblau,D.M. (1971) *Applied nonlinear programming.* Mc Graw-Hill Book Co. New York.

Jármai,K. (1989a) Single- and multicriteria optimization as a tool of decision support system, *Computers in Industry,* Elsevier Applied Science Publishers, **11** No. 3. 249-266.

Jármai,K. (1989b) Application of decision support system on sandwich beams, verified by experiments, *Computers in Industry,* Elsevier Applied Science Publishers, **11** No. 3. 267-274.

Jármai,K. (2005) Particle swarm method as a new tool for structural optimization, *Journal of Computational and Applied Mechanics*, **6** No. 2. 207-226, Miskolc University Press

Kennedy,J. (1977) The particle swarm: social adaptation of knowledge, *Proceedings of the International Conference on Evolutionary Computation*, IEEE, Piscataway NJ, 303-308.

Kennedy,J. & Eberhart,R.C. (1995) Particle swarm optimization. Proc. *IEEE Int'l Conf. on Neural Networks*, **IV**, 1942-1948. IEEE service center, Piscataway, NJ, 1995. 1942-1948

Koski,J. (1994) *Multicriteria structural optimization*, Chapter 6 in Advances in design optimization, Ed. Adeli,H., Chapman and Hall, London,

Millonas,M.M. (1994) *Swarms, phase transitions, and collective intelligence.* In Langton,C.G. Ed., Artificial Life III. Addison Wesley, Reading, MA.

Mordecai,A. (2003) *Nonlinear Programming: Analysis and Methods.* Dover Publishing. ISBN 0-486-43227-0.

Osyczka,A. (1984) *Multicriterion Optimization in Engineering.* Ellis Horwood, Chichester.

Osyczka,A. (1992) *Computer aided multicriterion optimization system.* International Software Publishers. Krakow.

Pareto,V. (1896) *Cours d'economie politique.* Vols. I and II. Lausanne: F. Rouge

Rao,S.S. (1984) *Optimisation theory and applications.* Wiley Eastern Limited. New Delhi.

Rosenbrock,H.H. (1960) An automatic method for finding the greatest or least value of a function. *Computer Journal*, **3**, 175-184.

Rozvany,G.I.N (1997) Topology Optimization in Structural Mechanics, Springer Verlag, ISBN 3211829075

Siddall,J.N. (1982) *Optimal engineering design (Mechanical engineering)*, Marcell Dekker, 536 p. ISBN-13: 978-0824716332

Simões,L.M.C. & Negrão,J.H.J.O. (2000) Optimization of cable-stayed bridges with box-girder decks, Advances in Engineering Software, **31** No. 6, 417-423.

Snyman,J.A. (1982) A new and dynamic method for unconstrained minimization. *Applied Mathematical Modelling*; **6** 449-462.

Snyman,J.A. (1983) An improved version of the original leap-frog dynamic method for unconstrained minimization LFOP1(b). *Applied Mathematical Modelling*; **7** 216-218.

Snyman,J.A. & Fatti,L.P. (1987) A multi-start global minimization algorithm with dynamic search trajectories. *J Optimiz Theory Appl*; **54** 121-141.

Snyman,J.A. (2000) The LFOPC leap-frog method for constrained optimization. *Comp. Math. Applic.*, **40** 1085-1096.

Snyman,J.A. (2005) *Practical mathematical optimization, An introduction to basic optimization theory and classical and new gradient based algorithms*, Springer Verlag, Heidelberg, 257 p. ISBN-10: 0-387-29824-X

Snyman,J.A. & Kok,S. (2007) A strongly interacting dynamic particle swarm optimizational method. *Genetic and Evolutionary Computation Conference, GECCO 2007*, Proceedings, London, England, UK, July 7-11, 2007. ACM 2007, ISBN 978-1-59593-697-4: 183

Storn,R. (1995) Contrained optimization, *Dr. Dobb's Journal*, May, (1995), 119-123.

Storn,R. & Price,K. (1995) Differential evolution – simple and efficient adaptive scheme for global optimization over continuous spaces. *Technical Report* TR-95-012, ICSI.

Tímár,I., Horváth,P. & Borbély,T. (2003) Optimierung von profilierten Sandwichbalken, *Stahlbau*, **72** No. 2. 109-113.

Uys,P.E., Farkas,J., Jármai,K. & van Tonder,F.(2007) Optimisation of a wind turbine tower structure, *Journal of Engineering Structures,* **29** No. 7, July 2007, 1337-1342.

Zhou,J.L. & Tits,A.L. (1996) An SQP Algorithm for Finely Discretized Continuous Minimax Problems and Other Minimax Problems with Many Objective Functions, *SIAM J. on Optimization*, **6** No. 2, 461-487.

CHAPTER 2 Cost Calculations

Bodt,H.J.M. (1990) *The Global Approach to Welding Costs*. The Netherlands Institute of Welding, The Hague.

COSTCOMP (2002) *Programm zur Berechnung der Schweisskosten.* Deutscher Verlag für Schweisstechnik, Düsseldorf.

Farkas,J. & Jármai,K. (1997) *Analysis and Optimum Design of Metal Structures*. Balkema Publishers, Rotterdam, Brookfield,

Farkas J. & Jármai K. (2003) *Economic design of metal structures*, Millpress Science Publisher, Rotterdam, 340 p. ISBN 90 77017 99 2

Glijnis,P.C. (1999) Private communication.

Klansek,U. & Kravanja,S. (2006a) Cost estimation, optimization and competitiveness of different composite floor systems – Part 1. Self manufacturing cost estimation of composite and steel structures, *Journal of Constructional Steel Research*, **62** No. 5, pp. 434-448.

Klansek,U. & Kravanja,S. (2006b) Cost estimation, optimization and competitiveness of different composite floor systems – Part 2. Optimization based competitiveness between the composite I beams, channel-section and hollow-secsion, *Journal of Constructional Steel Research*, **62** No. 5, pp. 449-462.

Jalkanen,J. (2007) *Tubular truss optimization using heuristic algorithms*, PhD. Thesis, Tampere University of Technology, Finland. 104 p.

Jármai,K. & Farkas,J. (1999) Cost calculation and optimization of welded steel structures, *Journal of Constructional Steel Research*, Elsevier, **50** No. 2. 115-135.

Jármai,K., Farkas,J. & Uys,P. (2004) Optimum design and cost calculation of a simple frame with welded or bolted corner joints, *Welding in the World*, **48** No. 1-2. 42-49.

Ott,H.H. & Hubka,V. (1985) Vorausberechnung der Herstellkosten von Schweiss-konstruktionen (Fabrication cost calculation of welded structures). *Proc. Int. Conference on Engineering Design ICED*, 1985, Hamburg, 478-487. Heurista, Zürich.

Pahl,G. & Beelich,K.H. (1992) Kostenwachstumsgesetze nach Ähnlichkeits-beziehungen für Schweiss-verbindungen. *VDI-Bericht*, Nr. 457, 129-141, Düsseldorf.

Tizani,W.M.K., Yusuf,K.O., Davies,G. & Smith,N.J. (1996) A knowledge based system to support joint fabrication decision making at the design stage – Case studies for CHS trusses. *Tubular Structures* VII. Eds Farkas,J. & Jármai,K. Rotterdam-Brookfield, Balkema, 483-489.

CHAPTER 3 Seismic Resistant Design

Design of structures in seismic zones. (1995) Eurocode 8. Worked examples. Eds Lungu,D., Mazzolani,F. & Savidis,S. Tempus CME 001198/95 Project: Implementing of Structural Eurocodes in Romanian Civil Engineering Standards. Bridgeman Ltd, Timisoara, Romania.

Eurocode EN 1990 (2002) *Basis of structural design,* European Standard, Brussels, European Committee for Standardisation, CEN.

Eurocode 3 EN 1993-1-1 (2005) *Design of steel structures. Part 1-1: General structural rules*. European Standard, Brussels, European Committee for Standardisation, CEN.

Eurocode 8 Draft PrEN 1998-1-1 (1998) *Design provisions for earthquake resistance of structures*. Part 1- 1: General rules – Seismic actions and general requirements for structures. Part 1-2: General rules – General rules for buildings. Part 1-3: General rules – Specific rules for various materials and elements. Section 3: Specific rules for steel buildings. Brussels, CEN.

Eurocode 8 EN 1998-1-1 (2004) *Design of structures for earthquake resistance* - Part 1: General rules, seismic actions and rules for buildings, Final Draft, December, 215 p. Brussels, CEN.

Farkas,J. & Jármai,K. (2006) Seismic resistant optimum design of a welded steel frame supporting a pressure vessel. In *ICMS 2006. 11st Internat. Conf. Metal Structures* Rzeszów *Progress in Steel, Composite and Aluminium Structures.* Gizejowski,M.A. et al. eds. Proceedings. Taylor & Francis, London, etc. 2006. 328-329. CD-Rom. IIW-doc. XV-1226-06

Ifrim,M. (1984) *Dinamica structurilor si ingineria seismica.* Ed. 2. Editura didactica si pedagogica, Bucuresti

Jármai,K., Farkas,J. & Kurobane,Y. (2006) Optimum seismic design of a multi-storey steel frame. *Engineering Structures* **28** No. 7. 1038-1048.

CHAPTER 4 Fire Resistant Design

British Steel (1999) *The behaviour of multi-storey steel framed buildings in fire*, Swinden Technology Centre, Rotherham, U.K.

Cox G. (1999) Fire research in the 21st century, *Fire Safety Journal*, **32** 203-219.

Dutta,D. (1999) *Hohlprofil-Konstruktionen.* Ernst & Sohn, 532 p. ISBN 3-433-01310-1

BS EN 10210-2 (1997) *Hot finished structural hollow sections of non-alloy and fine grain structural steels. Tolerances, dimensions and sectional properties.* British Standard/European Standard 15-Dec-1997. ISBN 0 580 28914 1

BS EN 10219-2 (1997) *Cold formed welded structural sections of non-alloy and fine grain steels. Tolerances, dimensions and sectional properties.* British Standard/European Standard 15-Dec-1997. ISBN 0 580 28917 6

Buchanan,A.H. (2001) *Structural Design for Fire Safety*, Wiley and Sons.

Eurocode 1_1 (ENV 1991-1) (2002) *Basis of design and actions on structures – Part 1: Basis of design,* European Committee for Standardization (CEN), Brussels, Belgium.

Eurocode 1_2 (ENV 1991-1-2) (2002) *Basis of design and actions on structures – Part 2-2: Actions on structures - Actions on structures exposed to fire*, CEN, Brussels, Belgium.

Eurocode 3_1 (ENV 1993-1-1) (2005) *Design of Steel Structures, Part 1 – General Rules and Rules for Buildings*, CEN, Brussels, Belgium.

Eurocode 3_2 (ENV 1993-1-2) (2005) *Design of steel structures, Part 1.2: General rules - structural fire design*, (CEN), Brussels, Belgium.

ESAB (2003) *Cutting and consumption table.* Cutting speed according to DIN 2310.

ISO 834 (1975) *Fire resistance test – Elements of building construction*, International Standards Organisation, Genève, Switzerland.

Kay,T.R., Kirby,B.R. & Preston,R.R. (1996) Calculation of the heating rate of an unprotected steel member in a standard fire resistance test, *Fire Safety Journal,* **26**, 327-350.

Rodrigues,C.J.P., Neves,C.I., Valente,J.C. (2000) Experimental research on the critical temperature of compressed steel elements with restrained thermal elongation, *Fire Safety Journal*, **35** 77-98.

Sales program (2007) *Commercial sections*. Arcelor Mittal. Long Carbon Europe, http://www.arcelor.com/sections/upload/diglib/PDFs/190_en.pdf

CHAPTER 5 Large-span suspended roof members

Bin,M. (2003) *Analysis of suspension members of bending stiffness*. PhD. Thesis, Technical University of Kosice, (in Slovak)

Eurocode 3 EN 1993-1-1 (2005) *Design of steel structures*. Part 1-1: General structural rules. European Standard, Brussels, European Committee for Standardisation, CEN.

Farkas J. & Jármai K. (2003) *Economic design of metal structures*. Rotterdam, Millpress,

Kachurin,V.K. (1962) *Theory of suspension structures*. Gosstroyizdat, Moscow, 222 p. (in Russian).

Kmeť S., & Bin M.(2002) Experimental and theoretical behaviour analysis of non-linear suspended members of bending stiffness. *Inžinierske stavby,* **50** No. 2, 11-17. (in Slovak).

Kmeť,S., Farkas,J., Jármai,K. & Kanócz,J. (2006) *Optimization and reliability of large-span suspended members*, IABSE Symposium Budapest, September 13-15, Report pp. 92-93. Proceedings on CD A-0050.pdf 8 p.

Kmeť,S., Farkas,J., Jármai,K. & Kanócz,J. (2007) *Parametric evaluation of large-span suspended members*, 17th International Conference on Computer Methods in Mechanics CMM-2007 konferenciára, June 19-22, 2007, Łódź-Spała, Poland, Proceedings of abstract pp. 203-204, Full paper Proceedings on CD, papers/073071.pdf, 4 p.

Kvedaras,A.K. & Sharashkinas,V. (2003) *Behaviour of hollow concrete-filled steel members subjected to tension and bending*. In: Proceedings of the International Conference on Metal Structures, ICMS-03, Miskolc, pp. 105-110.

Moskalev,N.S. (1980) *Structures of suspension roofs*. Stroyizdat, Moscow, 264 p. (in Russian).

Sales program (2007) *Commercial sections*. Arcelor Mittal. Long Carbon Europe, http://www.arcelor.com/sections/upload/diglib/PDFs/190_en.pdf

Skladnev,N.N. & Shimanovsky,A.V. (1992) General calculation method for suspended structures of large-span buildings and constructions considering plastic properties of materials. In: Proceedings of IASS – CSCE International Congress "Innovative Large Span Structures", Vol. 2, Toronto, pp. 375-387.

Telojan,A.L. & Vedenikov,G.S. (1977) Non-linear computational method of cables with bending stiffness. *Strojiteľnaja mechanika i rasčet sooruženij*. Moscow, No. 6, 26-30. (in Russian).

CHAPTER 6 Frames

Al-Salloum,Y.A. & Almusallam,T.H. (1995) Optimality and safety of rigidly and flexibly jointed steel frames. *Journal of Constructional Steel Research,* **35** No. 2, 189-215.

Azuma, K., Kurobane, Y. & Makino, Y. (2000) Cyclic testing of beam-to-column connections with weld defects and assessment of safety of numerical modelled connections from brittle fracture, *Engineering Structures*, **22** No. 12, 1596-1608.

British Steel (1999) *The Behaviour of Multi-Storey Steel Framed Buildings in Fire*, Swinden Technology Centre, Rotherham, U.K.

BS EN 10219 (1997) *Cold formed square hollow sections of non-alloy and fine grain steels. Tolerances, dimensions and sectional properties.* British Standard/European Standard. 15-Dec-1997. ISBN 0 580 28917 6

BS EN 10210-2 (1997) *Hot finished structural hollow sections of non-alloy and fine grain structural steels. Tolerances, dimensions and sectional properties.* British Standard/European Standard 15-Dec-1997. ISBN 0 580 28914 1

BS EN 10219-2 (1997) *Cold formed welded structural sections of non-alloy and fine grain steels. Tolerances, dimensions and sectional properties.* British Standard/European Standard 15-Dec-1997. ISBN 0 580 28917 6

Buchanan,A.H. (2001) *Structural Design for Fire Safety*, Wiley and Sons.

Cox G. (1999) Fire research in the 21st century, *Fire Safety Journal*, **32** 203-219.

DASt Richtlinie 016 (1986) *Deutscher Ausschuss für Stahlbau.* Bemessung und konstruktive Gestaltung von Tragwerken aus dünnwandigen kaltgeformten Bauteilen.

Dutta,D. (1999) *Hohlprofil-Konstruktionen.* Ernst & Sohn, 532 p. ISBN 3-433-01310-1

Design of structures in seismic zones (1995). Eurocode 8. Worked examples. Eds Lungu,D., Mazzolani,F. & Savidis,S. Tempus CME 001198/95 Project: Implementing of Structural Eurocodes in Romanian Civil Engineering Standards. Bridgeman Ltd, Timisoara, Romania.

Eurocode 1 (ENV 1991-1) (2002) *Basis of Design and Actions on Structures – Part 1: Basis of Design,* European Committee for Standardization (CEN), Brussels, Belgium.

Eurocode 1 (ENV 1991-1-2) (2002) *Basis of Design and Actions on Structures – Part 2-2: Actions on Structures - Actions on Structures Exposed to Fire*, CEN, Brussels, Belgium. 60 p.

Eurocode 3 EN 1993-1-1 (2005) *Design of steel structures. Part 1-1: General structural rules.* European Standard, Brussels, European Committee for Standardisation, CEN.

Eurocode 3 EN 1993-1-2 (2005) *Design of Steel Structures, Part 1.2: General Rules - Structural Fire Design*, (CEN), Brussels, European Committee for Standardisation, CEN. 74 p.

Eurocode 4 Draft prEN 1994-1-2 (2003) *Design of composite steel and concrete structures. Part 1-2: General rules – Structural fire design*, Final Draft (stage 34), 7 May 2003, CEN, Brussels.

Eurocode 8 Draft PrEN 1998-1-1 (1998) *Design provisions for earthquake resistance of structures*. Part 1- 1: General rules – Seismic actions and general requirements for structures. Part 1-2: General rules – General rules for buildings. Part 1-3: General rules – Specific rules for various materials and elements. Section 3: Specific rules for steel buildings. Brussels, CEN.

Eurocode 8 prEN 1998-1-1 (2004) *Design of structures for earthquake resistance* - Part 1: General rules, seismic actions and rules for buildings, Final Draft, December, 215 p. Brussels, CEN.

ESAB (2003) *Cutting and consumption table*. Cutting speed according to DIN 2310.

Farkas,J. & Jármai,K. (1997) *Analysis and optimum design of metal structures*, Balkema Publishers, Rotterdam, Brookfield, 347 p. ISBN 90 5410 669 7.

Farkas,J.,Jármai,K.,Visser-Uys,P. (2002) Cost comparison of bolted and welded frame joints, *55th Annual Assembly of International Institute of Welding*, June 23-28, 2002, Copenhagen, XV-1101-02, XV-WG9-17-02, 13 p.

Farkas,J. & Jármai,K. (2003) *Economic design of metal structures*. Rotterdam, Millpress, 340 p. ISBN 90 77017 99 2

Fourie,P.C. & Groenwold,A.A. (2000) Particle swarm in size and shape optimisation, *International Workshop on Multidisciplinary Design Optimization, 7-10, Aug. 2000, Pretoria, South Africa*, Proceedings: 97-106.

Glushkov,G., Yegorov,I. & Yermolov,V. (1975) *Formulas for designing frames*, MIR Publishers, Moscow.

Ifrim,M. (1984) *Dinamica structurilor si ingineria seismica*. Ed. 2. Editura didactica si pedagogica, Bucuresti.

ISO 834 (1975) *Fire Resistance Test – Elements of Building Construction*, International Standards Organisation, Genève, Switzerland.

Iványi,M. (1999) *Structural steelwork, Eurocodes-Development of a Trans-National Approach*, Műegyetemi Kiadó, Budapest.

Kameshki,E.S. & Saka, M.P. (2003) Genetic algorithm based optimum design of nonlinear planar steel frames with various semi-rigid connections. *J. Constructional Steel Research* 59: 109-134.

Kay,T.R., Kirby,B.R. & Preston,R.R. (1996) Calculation of the heating rate of an unprotected steel member in a standard fire resistance test, *Fire Safety Journal*, **26** 327-350.

Kurobane,Y., Azuma,K. & Ogawa,K. (1997) *Brittle fracture in steel building frames* – Comparative study on Northridge and Kobe earthquake damage. IIW Doc. XV-946-97.

Kurobane,Y. (1998) *Improvement of I beam-to-RHS column moment connections for avoidance of brittle fracture.* Tubular Structures VIII. Proc. 8th International Symposium on Tubular Structures, Singapore. Eds Choo,Y.S & Van der Vegte, G.J., Balkema, Rotterdam-Brookfield. 3-17.

Kurobane, Y., Makino, Y., Miura, K., Tokutome, Y. and Tanaka, M. (2001) *Testing of new RHS column-to-beam connections with U-shaped welded joints*, Tubular Structures IX, R. Puthli and S. Herion eds, Balkema, Rotterdam, the Netherlands, pp. 493-502.

Kurobane, Y., Azuma, K. and Makino, Y. (2003) *Fully restrained beam-to-RHS column connections with improved details*, Proceedings, 10th International Symposium on Tubular Structures, Madrid, Spain, pp. 439-446.

Kurobane,Y., Packer,J.A., Wardenier,J. and Yeomans,N.F. (2004) *Design guide for structural hollow section column connections.* CIDECT Design Guide No. 9. Verlag TÜV Rheinland Köln, Germany, 211 p.

Miura, K., Makino, Y. Kurobane, Y., Tanaka, M., Tokutome, Y., and Vegte, van der, G.J. (2002) *Testing of beam-to-column connections without weld access holes.* Int. Journal of Offshore and Polar Engineering, **12** No. 3, pp.229-235.

Obukuro,Y., Makino,Y., Vegte,van der,G.J., Kurobane,Y., Azuma,K., & Shinde,H. (2002) *Testing of beam-to-RHS column field connections using F14T high strength bolts*, 7th Int. Conf. on Steel & Space Structures, Singapore, pp.351-358.

Ross, C.T.F. (1998) *Advanced applied finite element methods*, Horwood Publishers, Chichester, 470 p.

Rodrigues,J.P.C.; Neves,I.C. & Valente,J.C. (2000) Experimental research on the critical temperature of compressed steel elements with restrained thermal elongation, *Fire Safety Journal*, **35** 77-98.

Sales program (2007) *Commercial sections.* Arcelor Mittal. Long Carbon Europe, http://www.arcelor.com/sections/upload/diglib/PDFs/190_en.pdf

Shinde,H., Kurobane,Y, Azuma,K., Makino,Y. & Obukuro,Y. (2003) Additional full-scale testing of beam-to-column connections with improvements in welded joints, *Proceedings, 13th International Offshore and Polar Polar Engineering Conference, Honolulu, Hawaii, USA*: 243-249.

Shinde,H. (2004) *Experimental study into steel beam-to-column connections with improved details at beam ends*, M.S. Thesis, Sojo University, Kumamoto, Japan, Feb. (in Japanese).

Simões,L.M.C. (1996) Optimization of frames with semi-rigid connections. *Computers and Structures*, **60** No. 4. 531-539.

Steenhuis,M., Weynand,K. & Gresnigt,A.M. (1998) Strategies for economic design of unbraced steel frames. *J. Constructional Steel Research* 46: (1-3). Paper No.60. CD-ROM.

TableCurve 2D (2003) Users' manual, Systat Software Inc.

Weynand K., Jaspart J.-P. & Steenhuis M.(1998) *Economy Studies of Steel Building Frames with Semi-Rigid Joints,* Proceedings of the 2nd World Conference on Constructional steel Design, San Sebastian, Spain.

CHAPTER 7 Stiffened Plates

American Petroleum Institute (1987) *API Bulletin on design of flat plate structures.* Bul.2V.

Birchfield JR. (1981) Welded machines thrive on tough mining. *Welding Design and Fabrication* **54** No.4, 47-54.

Det Norske Veritas (DNV) (1985) Buckling strength analysis. Classification Notes No.30.1. Høvik, Norway

European Convention of Constructional Steelwork (ECCS) (1988) Recommendations for Steel Construction. Buckling of steel shells. No.56. Brussels

Eurocode 3. (1992) Design of steel structures. Part 1.1. General rules and rules for buildings. Brussels

Evans HR, Shanmugam NE. (1984) Simplified analysis for cellular structures. *J. Struct. Eng ASCE* **110** 531-543.

Farkas,J. (1974) Static investigations and optimum design of welded cell-type plates. (In Hungarian). *Gép* **26** 233-238

Farkas,J. (1976) Structural synthesis of welded cell-type plates. *Acta Techn. Acad. Sci. Hungaricae* **83** No.l-2, 117-131

Farkas,J. (1977) *Optimum design of metal structures.* Dissertation for academic degree of doctor of technical science (In Hungarian). Budapest

Farkas J.(1983) Metal structures. University textbook in Hungarian. 2nd ed. Budapest, Tankönyvkiadó

Farkas,J. (1984) *Optimum design of metal structures.* Budapest, Akadémiai Kiadó, Chichester, Ellis Horwood

Farkas,J. (1985) Discussion to the paper of Evans,R. & Shanmugam,N.E.: Simplified analysis for cellular structures. *J. Struct. Eng ASCE* **11** No.10, 2269-2271

Farkas,J. & Jármai,K. 1997: *Analysis and optimum design of metal structures.* Rotterdam-Brookfield: Balkema

Farkas J., Jármai K.: Analysis of some methods for reducing residual beam curvatures due to weld shrinkage, Welding in the World, 1998, Vol. 41, No.4, pp.385-398.

Farkas,J. & Jármai,K. (2000) Minimum cost design and comparison of uniaxially compressed plates with welded flat, L- and trapezoidal stiffeners. *Welding in the World,* **44** No.3, 47-51

Farkas,J. & Jármai,K. (2003) *Economic design of metal structures*. Millpress, Rotterdam

Farkas,J. & Jármai,K. (2005a) Optimum design of a welded stringer-stiffened steel cylindrical shell subject to axial compression and bending. *Welding in the World* **49** No.5-6, 85-89

Farkas,J.& Jármai,K. (2005b) Optimum design of a welded stringer-stiffened cylindrical steel shell loaded by bending. In: Hoffmeister,B. & Hechler,O.(Eds) *Proc. Eurosteel 2005. 4th Eurospean Conference on Steel and Composite Structures. Maastricht, The Netherlands* Aachen, Druck und Verlagshaus Mainz GmbH. Vol. A, pp. 1.3-15 – 1.3-22.

Farkas,J. & Jármai,K. (2006) Optimum design and cost comparison of a welded plate stiffened on one side and a cellular plate both loaded by uniaxial compression. *Welding in the World* **50** No.3-4, 45-51

Farkas,J., Jármai,K., Snyman,J.A. & Gondos,Gy. (2002) Minimum cost design of ring-stiffened welded steel cylindrical shells subject to external pressure. In: Lamas,A. & Simoes da Silva, L. (Eds) *Proc. 3rd European Conf. Steel Structures, Coimbra,* Universidade de Coimbra pp. 513-522

Farkas,J., Jármai,K. & Virág,Z. (2004) Optimum design of a belt-conveyor bridge constructed as a welded ring-stiffened cylindrical shell. *Welding in the World* **48** No.1-2, 37-41

Fujikubo M. & Yao T.(1999) Elastic local buckling strength of stiffened plate considering plate/stiffener interaction and welding residual stress, *Marine Structures* **12** 543-564

Grondin G.Y., Elwi A.E. & Cheng J.J.R. (1999) Buckling of stiffened steel plates – a parametric study, *J. Construct.Steel Research* **50** 151-175

Haroutel J. (1982) Soudage laser de structures sandwich métalliques du type Norsial. *Soudage et Techniques Connexes* Jan-Fevr., 25-31.

Jármai,K. & Farkas,J. (1999) Cost calculation and optimization of welded steel structures. *Journal of Constructional Steel Research* **50** 115-135

Jármai K. (2005) Particle swarm method as a new tool for structural optimization, Journal of Computational and Applied Mechanics, 2005, Vol. 6, No. 2. pp. 207-226, Miskolc University Press.

Jármai,K., Farkas,J. & Groenwold,A. (2006) Economic welded stiffening of a steel plate loaded by bending. IIW Regional Welding Congress, Stellenbosch, South Africa, CD-Rom.

Jármai,K., Snyman,J.A. & Farkas,J.(2006) Minimum cost design of a welded orthogonally stiffened cylindrical shell. *Computers and Structures* **84** No.12, 787-797

Kennedy J. & Eberhardt R. (1995) Particle swarm optimization. Proc. 1995 ICEC, Perth, Australia

Lee,S.L., Karashudi,P.,Zakeria,M. & Chan,K.S. (1971) Uniformly loaded orthotropic rectangular plate supported at the corners. *Civil Engineering Transactions Institution of Engineering Australia* **13** No.2, 101-106

Mikami,I & Niwa,K. (1996-97): Ultimate compressive strength of orthogonally stiffened steel plates. *J. Struct. Eng. ASCE,* **122** No.6, 674-682. Discussion and closure *J.Struct.Eng. ASCE*, **123** No.8, 1116-1119

Paik J.K., Thayamballi A.K. & Kim B.J. (2001) Large deflection orthotropic plate approach to develop ultimate strength formulations for stiffened panels under combined biaxial compression/tension and lateral pressure, *Thin-Walled Structures* **39** 215-24

Paik ,J.K. & Thayamballi, A.K. (2003) *Ultimate limit state design of steel-plated structures.* Wiley & Sons, Chichester, England

Pettersen E. (1979) *Analysis and design of cellular structures.* University of Trondheim, Norwegian Institute of Technology

Sales program (2007) *Commercial sections.* Arcelor Mittal. Long Carbon Europe, http://www.arcelor.com/sections/upload/diglib/PDFs/190_en.pdf

Sahmel P. (1978) Statische und konstruktive Probleme bei Hilfsvorrichtungen zum Transport schwerer Behälter. *Fördern und Heben* **28** 844-847

Schade H.A. (1941) Design curves for cross-stiffened plating under uniform bending load, *Trans.Soc.Nav.Arch. and Marine Engrs,* **49** 154-182

Shanmugam NE, Evans HR. (1984) A grillage analysis of the nonlinear and ultimate load behavior of cellular structures under bending loads. *Proc. Inst. Civ. Eng. Part 2.* **71** 705-719

Shanmugam NE, Balendra T. (1986) Free vibration of thin-walled multi-cell structures. *Thin-walled Struct.* **4**, 467-483

Simões, L.M.C. & Negrão, J.H.J.O. (1999) Optimization of cable-stayed bridges subjected to earthquakes with nonlinear behaviour. *Eng. Opt.* **31** 457-478

TableCurve 2D (2003) *Users' manual*, Systat Software Inc.

Timoshenko,S.P.& Woinowsky-Krieger,S. (1959) *Theory of plates and shells.* 2nd ed. McGraw Hill, New York

Timoshenko,S.P. & Gere,J.M. (1961) *Theory of elastic stability.* 2nd ed. New York-Toronto-London, McGraw Hill

Williams DG. (1969) *Analysis of doubly plated grillage under inplane and normal loading.* PhD Thesis. Imperial College, London, 1969.

CHAPTER 8 Welded Stiffened Cylindrical and Conical Shells

American Petroleum Institute (API) (2000) Bulletin 2U. *Bulletin on stability design of cylindrical shells.* 2nd ed. Washington

Box,M.J. (1965) A new method of constrained optimization and a comparison with other methods. *Computer Journal*, **8** 42-52.

Chryssanthopoulos,M.K., Poggi,C. & Spagnoli,A. (1998) Buckling design of conical shells based on validated numerical models. Thin-walled Struct. 31, No.1-3, 257-270.

Det Norske Veritas (DNV) (1995) *Buckling strength analysis.* Classification Notes No.30.1. Høvik, Norway

Det Norske Veritas (2002) Buckling strength of shells. Recommended Practice DNV-RP-C202. Høvik, Norway.

Dowling,P.J. & Harding,J.E.(1982) Research in Great Britain on the stability of circular tubes. In: *Behaviour of Offshore Structures. Proc. 3rd Int. Conference,* Vol.2. 1982. Hemisphere Publ. Corp. McGraw Hill, New York. pp.59-73

Ellinas,,C.P., Supple,W.J. & Walker,A.C. (1984) *Buckling of Offshore Structures.* Granada, London etc.

Eurocode 3 (2002). prEN 1993-1-1 *Design of steel structures.* Part 1-1: General structural rules. Brussels, CEN.

European Convention of Constructional Steelwork (ECCS) (1988) *Recommendations for Steel Construction. Buckling of steel shells.* No.56. Brussels

Farkas,J. (2002) Thickness design of axially compressed unstiffened cylindrical shells with circumferential welds. *Welding in the World* **46** No.11/12. 26-29

Farkas,J. & Jármai,K. (1997). *Analysis and optimum design of metal structures,* Rotterdam, Brookfield, Balkema

Farkas,J. & Jármai,K.(1998) Analysis of some methods for reducing residual beam curvatures due to weld shrinkage. *Welding in the World* **41** No.4. 385-398

Farkas J.& Jármai K. (2003). *Economic Design of Metal Structures*, Rotterdam: Millpress.

Farkas,J. & Jármai,K. (2005) Optimum design of a welded stringer-stiffened steel cylindrical shell subject to axial compression and bending. *Welding in the World* **49** No.5-6, 85-89

Farkas,J., Jármai,K., Snyman,J.A. & Gondos,Gy. (2002). Minimum cost design of ring-stiffened welded steel cylindrical shells subject to external pressure. In: *Proc. 3rd*

European Conf. Steel Structures, Coimbra, 2002, . Lamas,A. & Simoes da Silva, L. (Eds) Universidade de Coimbra, pp. 513-522

Farkas,J., Jármai,K. & Virág,Z. (2004) Optimum design of a belt-conveyor bridge constructed as a welded ring-stiffened cylindrical shell. *Welding in the World* **48** No.1-2, 37-41

Frieze,P.A., Cho,S. & Faulkner,D.(1984) Strength of ring-stiffened cylinders under combined loads. In: *Proc. 16th Annual Offshore Technology Conference*, 1984. Vol. 2." Paper OTC 4714. pp.39-48

Harding,J.E. (1981) Ring-stiffened cylinders under axial and external pressure loading. In: *Proc. Instn. Civ. Engrs*, Part 2, 71, 1981, Sept. pp. 863-878

Himmelblau,D.M. (1971) *Applied nonlinear programming*. Mc Graw-Hill Book Co. New York.

Jármai, K. (1998) *Topology optimization of tubular structures.* In: *Mechanics and Design of Tubular Structures*, Springer Verlag, Jármai,K. & Farkas, J. (Eds) 1998. pp.225-284

Jármai,K. & Farkas,J.(1999) Cost calçulation and optimization of welded steel structures. *Journal of Constructional Steel Research* **50**. 115-135

Jármai,K., Farkas,J.& Virág,Z. (2003) Minimum cost design of ring-stiffened cylindrical shells subject to axial compression and external pressure. In: *5th World Congress of Structural and Multidisciplinary Optimization,* Short papers. Italian Polytechnic Press, Milano, 2003. pp. 63-64

Kennedy,J. (1977) The particle swarm: social adaptation of knowledge. In: *Proceedings of the International Conference on Evolutionary Computation, IEEE, Piscataway NJ,* pp. 303-308

Kennedy J & Eberhardt R. (1995) Particle swarm optimization. In: *Proc. Int. Conf. on Neural Networks, Piscataway, NJ, USA,* pp. 1942-1948

Klöppel,K. & Motzel,E. (1976) Traglastversuche an stählernen, unversteiften und ringversteiften Kegelstumpfschalen. Teil 1. Versuchsbericht. Stahlbau 45, No.10. 289-301.

Liszkai,T. & Farkas,J. (1999) Minimum cost design of ring and stringer stiffened cylindrical shells. *Computer Assisted Mechanics and Engineering Sciences* **6** 425-437

Profil Arbed (2001) Structural shapes.

Rao,S.S. (1984) *Optimisation theory and applications*. Wiley Eastern Limited. New Delhi.

Rao,S.S. & Reddy,E.S. (1981) Optimum design of stiffened conical shells with natural frequency constraints. Computers & Structures 14, No.1-2, 103-110.

Rosenbrock, H.H. (1960) An automatic method for finding the greatest or least value of a function. *Computer Journal* **3** No.3, 175-184

Ross,C.T.F. (1984) Finite element programs for axisymmetric problems in engineering, Ellis Horwood, Chichester.

Shen Hui-shen, Zhou Pin & Chen Tien-yun (1993) Postbuckling analysis of stiffened cylindrical shells under combined external pressure and axial compression. *Thin-Walled Struct.* **15** 43-63

Siddall,J.N. (1982) *Optimal engineering design (Mechanical engineering)*, Marcell Dekker, 536 p. ISBN-13: 978-0824716332

Singer,J., Arbocz,J. & Weller,T. (2002) Buckling experiments: experimental methods in buckling of thin-walled structures. Vol.2. Shells, built-up structures, composites and additional topics. New York, Wiley & Sons.

Snyman J A. (1982) A new and dynamic method for unconstrained minimization. *Applied Mathematical Modelling* **6** 449-462

Snyman J A. (1983) An improved version of the original leap-frog dynamic method for unconstrained minimization LFOP1(b). *Applied Mathematical Modelling* **7** 216-218

Snyman J A. (2000) The LFOPC leap-frog method for constrained optimization. *Computers Math. Applic.* **40** 1085-1096

Snyman J A, Stander N & Roux W J. (1994) A dynamic penalty function method for the solution of structural optimization problems. *Applied Mathematical Modelling* **18** 453-460

Snyman J A: A gradient-only line search method for the conjugate gradient method applied to constrained optimization problems with severe noise in the objective function. To appear in the *International Journal for Numerical Methods in Engineering*, 2004.

Snyman J A, Heyns P S & Vermeulen P J. (1995) Vibration isolation of a mounted engine through optimization. *Mechanism and Machine Theory* **30** 109-118

Snyman J A & Berner D F. (1999) The design of a planar robotic manipulator for optimum performance of prescribed tasks. *Structural and Multidisciplinary Optimization* **18** 95-106

Snyman J A. (1985) Unconstrained minimization by combining the dynamic and conjugate gradient methods. *Quaestiones Mathematicae* **8** 33-42

Spagnoli,A. (1997) Buckling behaviour and design of stiffened conical shells under axial compression. PhD thesis, University of London, London.

Spagnoli,A. & Chryssanthopoulos,M.K. (1999a) Buckling design of stringer-stiffened conical shells in compression. J. Struct. Eng. ASCE 125, No.1. 40-48.

Spagnoli,A. & Chryssanthopoulos,M.K. (1999b) Elastic buckling and postbuckling behaviour of widely-stiffened conical shells under axial compression. Eng. Struct. 21, No.9. 845-855.

Spagnoli,A. (2001) Different buckling modes in axially stiffened conical shells. Eng. Struct. 23, No.8. 957-965.

TableCurve 2D. (2003) *Users' manual*, Systat Software Inc.

Tian,J., Wang,C.M. & Swaddiwudhipong,S. (1999) Elastic buckling analysis of ring-stiffened cylindrical shells under general pressure loading via the Ritz method. *Thin-Walled Struct.* **35** 1-24

Timoshenko,S.P.& Gere,J.M.(1961) *Theory of elastic stability.* 2nd ed. New York, Toronto, London, McGraw Hill

Wilke,D.N., Schutte,J.F. & Groenwold,A.A. (2003) Constrained particle swarm searches in the optimal sizing design of truss structures. In: *International Conference on Metal Structures, Miskolc,* 2003. Jármai K. & Farkas J.(Eds), Rotterdam, Millpress, pp. 301-308

CHAPTER 9. Tubular Structures

American Petroleum Institute (API).(2000). Bulletin 2U. *Bulletin on stability design of cylindrical shells.* 2nd ed. Washington.

Bazeos,N.,Hatzigeorgiou,G.D.,Hondros,I.D.,Karamaneas,H.,Karabalis,D.L.&Besko s,D.E. (2002). Static, seismic and stability analyses of a prototype wind turbine steel tower. *Eng. Struct.* **24** 1015-1025.

British Steel (1995). *Price list 20. Steel tubes, pipes and hollow sections. Part 1b. Structural hollow sections.* British Steel, Corby, UK.

BS 5400:Part 3: (1982). Steel, concrete and composite bridges. Code of practice for design of steel bridges. BSI,London.

Det Norske Veritas (DNV).(1995).*Buckling strength analysis.* Classification Notes No.30.1. Hovik, Norway.

DIN 2458: (1981). *Geschweisste Stahlrohre. Masse.* Berlin, Deutsches Institut für Normung.

EN 1594: (2001). *Gas supply systems. Pipelines for maximum operating pressure over 16 bar. Functional requirements.* CEN Brussels.

Eurocode 1:1999a. (1995) Basis of design and actions on structures. Part 2-1. Actions on structures. Densities, self-weight and imposed loads. ENV 1991-2-1

Eurocode 1. 1999b. Part 2-4.(1999) Wind loads. ENV 1991-2-4

Eurocode 3. (2002). Design of steel structures. Part 1-1. General structural rules. PrEN 1993-1-1

Eurocode 3. Part 1-9. (2002). Design of steel structures. Fatigue strength of steel structures. CEN, Brussels.

Farkas,J. & Jármai,K. (1997). *Analysis and design of metal structures.* Rotterdam, Balkema.

Farkas,J. & Jármai,K. (1998). Analysis of some methods for reducing residual beam curvatures due to wekd shrinkage. *Welding in the World* **41** No.4, 385-398

Farkas,J., Jármai,K. (2001). Height optimization of a triangular CHS truss using an improved cost function. In: *Tubular Structures IX.* Proceedings of the 9th International Symposium on Tubular Structures, Düsseldorf, 2001. Balkema, Lisse etc. 2001. 429-435.

Farkas,J. (2002). Thickness design of axially compressed unstiffened cylindrical shells with circumferential welds. *Welding in the World* **46** No.11/12, 26-29

Farkas,J., Jármai,K., Snyman,J.A.. & Gondos,Gy. (2002). Minimum cost design of ring-stiffened welded steel cylindrical shells subject to external pressure. *Proc. 3rd European Conf. Steel Structures,* Coimbra, 2002, eds. Lamas,A. & Simoes da Silva, L. Universidade de Coimbra, 513-522

Farkas,J. & Jármai,K. (2003). *Economic design of metal structures.* Rotterdam, Millpress.

Farkas,J., Jármai,K. & Virág,Z. (2004). Optimum design of a belt-conveyor bridge constructed as a welded ring-stiffened cylindrical shell.. *Welding in the World* **48** No.1-2. 37-41

Farkas,J., Jármai,K. (2006) Cost comparison of a tubular truss and a ring-stiffened shell structure for a wind turbine tower. In: *Tubular Structures XI.* Proc. 11th Int. Symposium and IIW Int. Conf. on Tubular Structures, Québec City, Canada, 2006. Eds Packer,J.A. & Willibald,S. Taylor & Francis, London etc. pp. 341-349.

Jármai,K., Farkas,J.(1999). Cost calculation and optimization of welded steel structures. *Journal of Constructional Steel Research* **50** 115-135

Jármai,K., Farkas,J. & Virág,Z. (2003). Minimum cost design of ring-stiffened cylindrical shells subject to axial compression and external pressure. In: *5th World Congress of Structural and Multidisciplinary Optimization,* Short papers. Italian Polytechnic Press, Milano, 63-64.

Horváth,G., Tóth,L. (2001). New methods in wind turbine tower design. *Wind Engineering* **25** No.3.171-178

Koumousis,V.K., Dimou,C.K. (1995). Optimal design of wind mill towers. In: *Steel Structures – Eurosteel '95.* Ed. Kounadis. Rotterdam, Balkema. 443-450.

Lavassas,I., Nikolaidis,G., Zervas,P., Efthimiou,E., Doudoumis,I.N. & Baniotopoulos,C.C. (2003). Analysis and design of the prototype of a steel 1-MW wind turbine tower. *Eng. Struct.* **25** 1097-1106.

Orbán,F. (1997) Minimum volume design of pipeline bridges, In *International Symposium on Design of Metal Structures*, University of Miskolc, Hungary. Publications of the University of Miskolc, Series C, Mechanical Engineering, Edited by K. Jármai, **47** 111-122.

Price List 20. (1995). Steel tubes, pipes and hollow sections. Part 1b. *Structural hollow sections.* British Steel Tubes and Pipes.

Prochnost', ustoichivost', kolebaniya. (1968). Moskva, Mashinostroenie. (Strength, stability, vibration. In Russian.)

Rondal,J., Würker,K.-G., Dutta,D., Wardenier,J. & Yeomans,N. (1992). *Structural stability of hollows sections*. Köln, Verlag TÜV Rheinland.

Spera,D.A. ed. (1994). *Wind turbine technology*. New York, ASME Press.

Timoshenko,S.P. & Gere,J.M. (1961). *Theory of elastic stability*. 2nd ed. New York, Toronto, London, McGraw Hill.

Wardenier,J., Kurobane,Y., Packer,J.A., Dutta,D. & Yeomans,N. (1991). *Design guide for circular hollow section (CHS) joints under predominantly static loading*. Köln: Verlag TÜV Rheinland.

Zhao,X.L. et al. (2001). *Design Guide for Circular and Rectangular Hollow Section Welded Joints under Fatigue Loading*. TÜV-Verlag, Köln.

CHAPTER 10 Box column constructed from cellular plates

Det Norske Veritas (DNV) (1995): *Buckling strength analysis*. Classification Notes No.30.1. Høvik, Norway.

Eurocode 3. Steel structures. Part 1-1. (2002).

Farkas J. & Jármai K.(2003) *Economic design of metal structures,* Rotterdam, Millpress.

Farkas J. & Jármai K. (2006a) Optimum design and cost comparison of a welded plate stiffened on one side and a cellular plate both loaded by uniaxial compression, *Welding in the World* **50** No.3-4. 45-51.

Farkas,J. & Jármai,K. (2007) Economic orthogonally welded stiffening of a uniaxially compressed steel plate. *Welding in the World* **51** No.7-8. 74-78.

Farkas,J. & Jármai,K. (2008) Minimum cost design of a square box column composed from orthogonally stiffened welded steel plates. Proc. DFE 2008 Miskolc.

Ge,H., Gao,Sh. & Usami,Ts. (2000) Stiffened steel box columns. Part 1. Cyclic behaviour. *Earthquake Engineering and Structural Dynamics* **29** 1691-1706.

Hirota,T., Sakimoto,T.,Yamao,T., Watanabe,H. (2004): Experimental study on hysteretic behaviour of inverted L-shaped steel bridge piers filled with concrete. In *Thin-walled Structures.* Proc. 4th Int. Conf. on Thin-walled Structures, Loughborough,UK. 2004. Ed. J. Loughlan. Institute of Physics Publ., Bristol & Philadelphia, pp. 373-380.

Nakai,H., Kitada,T. & Miki,T. (1985) An experimental study on ultimate strength of thin-walled box stub-columns with stiffeners subjected to compression and bending. *Proc. JSCE Structural Eng./Earthquake Eng.* **2** No.2. 87-97.

Ohga,M.,Takemura,Sh.,Imamura,S. (2004): Nonlinear behaviours of round corner steel box-section piers. In *Thin-walled Structures.* Proc. 4th Int. Conf. on Thin-walled Structures, Loughborough,UK. 2004. Ed. J. Loughlan. Institute of Physics Publ., Bristol & Philadelphia, pp. 365-372.

Sales program (2007) *Commercial sections*. Arcelor Mittal. Long Carbon Europe, http://www.arcelor.com/sections/upload/diglib/PDFs/190_en.pdf

Steinhardt,O. (1975) *Berechnungsmodelle für ausgesteifte Kastenträger. In Beiträge zum Beulproblem bei Kastenträgerbrücken.* Deutscher Ausschuss für Stahlbau. Berichtsheft 3. 27-35.

Usami,Ts., Gao,Sh. & Ge,H. (2000) Stiffened steel box columns. Part 2. Ductility evaluation. *Earthquake Eng. and Structural Dynamics* **29** 1707-1722.

Yamao,T.,Matsumara,S.,Hirayae,M.,Iwatsubo,K. (2004): Steel tubular bridge piers stiffened with inner cruciform plates under cyclic loading. In *Thin-walled Structures*. Proc. 4th Int. Conf. on Thin-walled Structures, Loughborough,UK. 2004. Ed. J. Loughlan. Institute of Physics Publ., Bristol & Philadelphia, pp. 357-364.

Subject index